

Flavour Symmetries in Pati-Salam Grand Unifying Theories

DISSERTATION
zur Erlangung des Grades eines Doktors
der Naturwissenschaften

vorgelegt von
M.Sc. Florian Hartmann

eingereicht bei der Naturwissenschaftlich-Technischen Fakultät
der Universität Siegen
Siegen 2015

Gutachter:

- Prof. Dr. Wolfgang Kilian
- Prof. Dr. Thorsten Feldmann

Datum der mündlichen Prüfung: 15.06.2015

Prüfer:

- Prof. Dr. Otfried Gühne
- Prof. Dr. Ivor Fleck
- Prof. Dr. Thorsten Feldmann
- Prof. Dr. Wolfgang Kilian (Vorsitz der Prüfungskommission)

Abstract

The theoretical description of the Standard Model of Particle Physics (SM) is based on a product of three symmetry group factors, $SU(3) \times SU(2) \times U(1)$, corresponding to three of the four fundamental interactions. These are the weak, the strong and the electromagnetic interactions. Gravity is not included in the SM. In addition, it describes the elementary fermionic matter in terms of five different representations of that group. For large energies, it can be embedded in a single group with fewer representations for the SM particles in the context of Grand Unified Theories (GUT) like $SO(10)$. Moreover, in the SM the five fermion representations each come in three flavours which differ only by their masses. These as well as the mixing between the different flavours are parametrised by the Yukawa matrices.

In this thesis we present models based on a Pati-Salam (PS) symmetric GUT which generate the Yukawa matrices dynamically. The PS group is only a semi-simple group and thus it does not achieve complete unification. Still, it can be embedded in $SO(10)$. The breaking of PS down to the SM allows for multiple intermediate symmetries at various scales.

In the first class of models, we assume complete unification of all three gauge couplings at the GUT scale. Moreover, we restrict ourselves to a setup where all additional fields can be embedded in small representations of $SO(10)$. Finally, we allow all of these fields to appear in three copies similar to the SM fermions. We then study the possible ranges for the intermediate scales.

In the second class of models we focus on the flavour aspects and present two approaches to generate the Yukawa matrices dynamically. In both cases we consider gauged flavour symmetries which are broken by vacuum expectation values of additional scalar “flavon” fields.

In the first approach, the Yukawa matrices are generated using non-renormalisable terms, i.e. allowing for multiple insertions of these flavons. Here, we consider the special case that the SM Higgs field exists in three generations and transforms similarly to the SM fermions under the flavour gauge group. This motivates us to consider also flavon representations being larger than the commonly used fundamental one. We present particular models containing flavons which transform solely in the decuplet or triplet representation, respectively.

In the second approach we introduce additional fermionic fields that communicate the breaking of the flavour symmetry to the SM fermions. These extra fermions violate fundamental properties of the SM such as the pure left-chiral couplings of the weak gauge bosons. We study how large such effects can be and to what extent they may be observable in current or future experiments.

Zusammenfassung

Die theoretische Beschreibung des Standardmodells der Teilchenphysik (SM) basiert auf einem Produkt von drei Symmetriegruppen, $SU(3) \times SU(2) \times U(1)$, die drei der vier fundamentalen Wechselwirkungen entsprechen. Diese sind die starke, die schwache und die elektromagnetische Wechselwirkung. Die Gravitation wird im SM nicht betrachtet. Zusätzlich beschreibt das SM die elementaren fermionischen Teilchen basierend auf fünf unterschiedlichen Darstellungen dieser Gruppe. In sogenannten „Großen Vereinheitlichten Theorien“ (GUT) kann das SM bei hohen Energien in einer einfachen Symmetriegruppe, wie beispielsweise der $SO(10)$, mit einer einzigen Darstellung der Fermionen eingebettet werden. Des Weiteren kommen alle Darstellungen der Fermionen des Standardmodells in drei Generationen vor, den sogenannten „Flavours“, die sich lediglich durch ihre Massen unterscheiden. Diese Massen sowie die Mischung zwischen den unterschiedlichen Flavours werden im Standardmodell über die Yukawa-Matrizen parametrisiert.

In dieser Arbeit werden Modelle auf Basis einer Pati-Salam (PS) symmetrischen GUT betrachtet, die die Yukawa-Matrizen dynamisch erzeugen. Die PS-Gruppe ist lediglich eine halbeinfache Gruppe und erreicht somit selbst keine vollständige Vereinheitlichung. Allerdings erlaubt PS eine weitere Einbettung in eine $SO(10)$ -Theorie. Zusätzlich besitzt PS die Möglichkeit mehrerer intermediärer Symmetrien bei der Reduktion auf die Symmetriegruppe des Standardmodells.

In der ersten Klasse von Modellen wird eine vollständige Vereinheitlichung aller drei Eichkopplungen an der GUT-Skala angenommen. Außerdem beschränkt sich der Ansatz auf zusätzliche Felder, die eine weitere Einbettung in die $SO(10)$ ermöglichen. Schließlich wird all diesen Feldern erlaubt, in drei Generationen im Niederenergiespektrum vorhanden zu sein. Unter diesen Annahmen werden die möglichen Energiebereiche der intermediären Skalen betrachtet.

Die zweite Klasse an Modellen konzentriert sich auf den Flavour-Sektor und präsentiert zwei Ansätze zur expliziten Realisierung der Yukawa-Matrizen. In beiden Fällen wird die Flavour-Symmetrie als geeicht betrachtet und von Vakuumerwartungswerten von zusätzlichen skalaren Feldern, den sogenannten Flavonen, gebrochen.

Im ersten Ansatz wird die Yukawa-Matrix mittels nicht renormierbarer Terme erzeugt. Hier betrachten wir den speziellen Fall, dass auch das SM Higgs-Boson in drei Generationen vorkommt und sich ähnlich der Fermionen unter der Flavour-Symmetrie transformiert. Ein solcher Ansatz legt eine Betrachtung von größeren Darstellungen als der üblicherweise betrachteten fundamentalen Darstellung für die Flavonen nahe. Es werden zwei spezielle Modelle präsentiert, welche einerseits lediglich die fundamentale Triplet-Darstellung sowie andererseits ausschließlich die Dekuplett-Darstellung verwenden.

Im zweiten Ansatz wird die Brechung der Flavour-Symmetrie über zusätzlich eingeführte fermionische Partner vermittelt. Diese zusätzlichen Fermionen verletzen grundlegende Eigenschaften des Standardmodells, wie zum Beispiel die Tatsache, dass die schwachen Eichbosonen nur an linkshändige Fermionen koppeln. In diesem Modell wird betrachtet, wie groß solche Verletzungen sein können und in welchem Ausmaß diese in aktuellen oder zukünftigen Experimenten beobachtbar sind.

Contents

Introduction	1
I. General Overview & Theoretical Background	3
1. Grand Unified Theories	5
1.1. Selected Aspects of the Standard Model	5
1.2. Reasons for going Beyond the SM	7
1.3. Supersymmetry	9
1.4. Roadmap to Unification	11
1.4.1. SU(5) à la Georgi and Glashow	12
1.4.2. Complete Unification in SO(10)	14
1.4.3. Pati-Salam: an Alternative Route	15
1.4.4. Larger Groups	17
2. Flavour Symmetries; SM and Beyond	19
2.1. The Concept of Flavour	19
2.1.1. Flavour Symmetries	20
2.1.2. Yukawa Sector	21
2.2. Structure of Masses and Mixing in the SM	23
2.3. Theory of Neutrino Masses	25
2.3.1. See-Saw Mechanism	25
2.3.2. Double See-Saw	26
2.3.3. Sequential Right-Handed Neutrino Dominance	28
2.4. Flavour in GUTs	29
2.4.1. Flavour in Pati-Salam	30
II. Explicit Models of Flavour in Pati-Salam	33
3. PS-Breaking and Gauge Coupling Unification	35
3.1. Intermediate Symmetries and Scales	36
3.2. Particle Content and VEV Structure	38
3.3. Superpotential and Higgs Mechanism	41

3.4.	Spectra and Phenomenology	43
3.4.1.	Mass Matrix	43
3.4.2.	The MSSM Higgs	47
3.4.3.	The Multiplet F	48
3.4.4.	Matter Couplings	48
3.5.	Unification Conditions	49
3.6.	Unification within Supersymmetry	52
3.6.1.	General Overview	53
3.6.2.	Class E	56
3.6.3.	Class F	59
3.6.4.	Classes A to D	61
3.7.	Unification Without Supersymmetry	62
3.7.1.	Class E	65
3.7.2.	Class F	66
3.7.3.	Class A to D	66
3.8.	Summary	69
4.	Effective Theory of Flavour	71
4.1.	Model Framework	71
4.2.	A Triplet-Flavon Model	74
4.2.1.	Setup of the Model	74
4.2.2.	Operator Analysis	76
4.3.	Larger Flavon Representations	78
4.4.	Flavon Decuplet Model	79
4.4.1.	Setup of the Model	80
4.4.2.	Operator Analysis	81
4.4.3.	Possible Variations	82
4.5.	Summary	83
5.	Gauged Flavour Symmetry	85
5.1.	Motivation	86
5.2.	Model Setup	86
5.3.	Quark Flavour Sector	91
5.3.1.	Approximate Flavour Structure	91
5.3.2.	Diagonalising the Mass Matrix	92
5.3.3.	Gauge Kinetic Terms	96
5.3.4.	Higgs Coupling	100
5.4.	Lepton Sector	101
5.4.1.	Effective Ansatz	101
5.4.2.	Single Scalar extension	103
5.4.3.	GRV-like extension	103
5.4.4.	Resulting Lepton Sector	106
5.5.	Phenomenology of the Quark Sector	107
5.5.1.	Setup of the Scan	107

5.5.2. Effects on the Flavour Parameter	109
5.6. Comments on a Supersymmetric Extension	116
5.7. Summary	117
6. Conclusions & Outlook	119
Appendix	122
A. Unification Model	125
A.1. Model Naming Scheme	125
A.2. Mass Matrices	126
A.3. Vacuum Expectation Values and Mass Scales	129
A.4. Beta-Function Coefficients	129
B. Low-Energy Flavour Model	133
B.1. Tensor Products of $SU(3)$	133
B.2. From $U(1)$ to $Z(N)$	134
C. Low-Energy Flavour Symmetry Breaking	137
C.1. Gauge Anomalies	137
C.2. Calculation of S and T	139
C.3. Scan over Flavour Parameter	140
Bibliography	143
Danksagung	153
List of publications	155

Introduction

The Standard Model of particle physics (SM) developed in the late 60's has been proven to be a very predictive theory. Measurements have shown that it is also an extremely precise description of particle physics. Nonetheless, already since its formulation there have been efforts to find a unification of the independent SM interactions to a Grand Unified Theory (GUT). This is mainly theoretically motivated as it may simplify the structure and solve some theoretical issues of the SM like neutrino masses and charge quantisation. The first ideas of such a unification were proposed by Georgi and Glashow [1] as well as Fritzsche and Minkowski [2] in the early 70's. Such GUTs provide a description of particle physics by only a single basic interaction at high energies. Back then, people assumed only a single new energy scale (the GUT scale) to be present where all interactions should unify. This was motivated by the fact that the energy dependent gauge couplings approach each other with increasing energy and seemed to meet at roughly 10^{16} GeV. Additionally, it kept the theory predictive as intermediate scales would introduce additional parameters which are not constrained by experimental data. However, this assumption becomes more and more questionable as hints for intermediate scales have appeared; moreover single scale unification has issues on its own. One of these hints is the right-handed neutrino scale usually introduced to explain the smallness of the SM neutrino masses which have been experimentally suggested in the late 70's and were established until 2002 [3–5]. The flavour structure, which is often not considered in unified theories, may also introduce various additional scales in a GUT framework.

One aim of this thesis is to address the question of multiple scales, especially in the context of embedding flavour, in GUTs. Since a theory of flavour depends significantly on the chosen GUT we limit ourselves to the Pati-Salam symmetry (PS) [6, 7]. The PS symmetry itself does not achieve full unification but qualifies as an intermediate theory which is complex enough to feature a great variety of interesting aspects while still not being completely arbitrary. A second question we intend to address in this thesis is the general embedding of flavour in GUTs based on the PS symmetry.

Throughout this thesis, we are mainly interested in depicting possible routes of going beyond the SM. Thus, we are not limited by the loss of predictive power we encounter when giving up the concept of a single unification scale. We do not aim for explaining *specific* measurements or finding *the* theory of everything. Rather we want to shed some light on potential implications arising when combining flavour and GUT physics. Thus we deliberately keep the presented models rather unconstrained to not exclude interesting effects right from the beginning.

We are often working in a supersymmetric framework as GUT physics suggest to introduce Supersymmetry (SUSY) [8–10]. In addition, it usually simplifies the model building process which is another reason to consider SUSY. Nevertheless, we also study non-supersymmetric realisations of our models. In the last model we give up the concept of SUSY to explicitly deduce flavour effects.

Organisation of the thesis

We have divided this thesis into two parts. The first part gives a general overview of the topic of GUTs (Chapter 1) and presents the different aspects of flavour (Chapter 2). We also provide some basic theoretical tools here, needed later on in this thesis. In the second part we study explicit models realising the embedding of flavour in Pati-Salam GUTs. This part is split into three chapters, corresponding to the different aspects and models. The essential results thereof have been published in [A-C].

In Chapter 3 we consider how to generally break the Pati-Salam symmetry to the SM via intermediate scales. Basing our model on simple assumptions, we set up a framework achieving such a breaking while guaranteeing gauge coupling unification (GCU). As we stick to a simple construction principle, we are able to deduce general features present in various explicit realisations. Here, we perform a detailed discussion in the framework of SUSY from which we deduce a non-supersymmetric case. Having constructed a fundamental framework, we take a look at the realisation of flavour in such a model. This we do using two different approaches.

In the first setup (Chapter 4), we consider a single $SU(3)$ flavour symmetry, broken by scalar fields (flavons) acquiring vacuum expectation values (vevs) at a high scale. The Yukawa structure is realised by higher dimensional operators, containing multiple insertions of the flavon vevs. This we do considering different representations for the flavon fields. Motivated by matter-Higgs unification we demand the SM Higgs boson to appear in three generations, transforming identically to the SM fermions under the flavour gauge group. As we only consider the model at a very high energy scale, we restrict ourselves to the supersymmetric realisation.

In the second ansatz presented in Chapter 5 we generate the Yukawa matrices at rather low energies by means of a renormalisable potential. This setup is an adaption of an idea by Grinstein, Redi, Villadoro [11] to the framework of Pati-Salam GUTs. Here, the Yukawa structure is generated by integrating out fermionic messenger fields which couple the flavons to the SM fermions, thereby mediating the flavour symmetry breaking. We consider the model in a non-supersymmetric framework, as we intend to explore possible flavour effects of the model without specifying a SUSY breaking sector. Nevertheless, we also comment on how to supersymmetrise the setup.

We conclude the thesis with a short general summary and give an outlook on further ideas in Chapter 6. A few appendices give some details on the calculation and basic concepts used. We again split this appendix into three different parts, corresponding to the chapters of the main part of the thesis.

Part I.

General Overview & Theoretical Background

Chapter 1

Grand Unified Theories

In this chapter we introduce the concept of Grand Unified Theories (GUTs). Since these constitute an extension of the Standard Model of Particle Physics (SM), we first give a basic overview of the SM. Afterwards, we briefly comment on especially theoretical issues of the SM which motivate to consider GUTs. As GUTs are usually considered within the framework of Supersymmetry (SUSY), we present a short overview of its features relevant for this thesis. Having set the stage, we give a historically motivated introduction to GUTs.

1.1. Selected Aspects of the Standard Model

The SM describes the particle interaction based on only a few simple symmetry principles. The framework behind is a quantum field theory in which the fundamental interactions are represented by gauge symmetries and the force carriers are the corresponding gauge bosons [12]. The particles are described by fields transforming non-trivially under these symmetries. The SM includes three of the four fundamental forces which are the electromagnetic, the weak and the strong force; there is so far no theory of gravity compatible with a gauged quantum field theory. A detailed review on theoretical aspects and the experimental status of the SM can be found in References [13–15] and references therein.

Gauge Symmetry

The gauge symmetry of the SM is a direct product of gauge groups associated with the strong and the electroweak interactions.

The strong interaction is responsible for the formation of hadrons. It is represented by an unbroken colour gauge group $SU(3)_c$. The mediators of the strong interaction are the gluons G^a which are embedded in the adjoint (octet) representation of $SU(3)_c$. So far only particles invariant under the $SU(3)_c$ symmetry (colour singlets) have been directly measured in experiments. This fact is described by the concept of confinement and related to the observation that for large scales (small energies) the coupling is non-perturbative (see e.g. [16, 17]).

The second part of the SM are the electroweak interactions which are a combination of the electromagnetic and the weak interactions. The weak interactions are responsible for weak decays, e.g. the β -decay. The electroweak interactions are represented by a direct product of the group $SU(2)_w$ of the weak interactions and the hypercharge $U(1)_Y$, resulting

1. Grand Unified Theories

quarks				leptons			
$(\mathbf{3}, \mathbf{2})_{1/6}$	$\begin{pmatrix} u \\ d \end{pmatrix}_L$	$\begin{pmatrix} c \\ s \end{pmatrix}_L$	$\begin{pmatrix} t \\ b \end{pmatrix}_L$	$(\mathbf{1}, \mathbf{2})_{-1/2}$	$\begin{pmatrix} \nu_e \\ e \end{pmatrix}_L$	$\begin{pmatrix} \nu_\mu \\ \mu \end{pmatrix}_L$	$\begin{pmatrix} \nu_\tau \\ \tau \end{pmatrix}_L$
$(\mathbf{3}, \mathbf{1})_{2/3}$	u_R	c_R	t_R				
$(\mathbf{3}, \mathbf{1})_{-1/3}$	d_R	s_R	b_R	$(\mathbf{1}, \mathbf{1})_{-1}$	e_R	μ_R	τ_R

Table 1.1.: Fermion content of the SM. The first column shows the representations under the SM gauge group which is given in the standard way as $(SU(3)_c, SU(2)_w)_{U(1)_Y}$.

in the gauge group $SU(2)_w \times U(1)_Y$. This group gets spontaneously broken within the SM to the electromagnetic $U(1)_{\text{em}}$ by the Higgs mechanism. The mediators of the electroweak interactions are before symmetry breaking the three $SU(2)$ gauge bosons W^a and the hypercharge boson B . In the broken phase they are redefined to the massive charged W^\pm as well as the neutral Z^0 bosons and the massless photon γ .

Summing up, the full gauge group of the SM is given by

$$G_{\text{SM}} = SU(3)_c \times SU(2)_w \times U(1)_Y. \quad (1.1)$$

Particle Content

In the SM, the fermions are embedded in the fundamental representations of the gauge group factors discussed above. They can be separated in two classes, the quarks and the leptons. Quarks transform in the triplet representation under the strong interactions whereas leptons are colour singlets. The charged leptons and quarks come in pairs of left- and right-handed fermions. The neutral leptons, the neutrinos, are purely left-handed. All left-handed fields are combined in doublets of the weak interaction. We note that we do not consider right-handed neutrinos as part of the SM.

The fermion content of the SM including their transformation properties under G_{SM} are given in Table 1.1. We note that there are two different ways of defining the hypercharge in the literature that differ by a factor of 2, as a $U(1)$ -charge is only defined up to a general rescaling. In the following, we will label the left-handed doublet by Q_L (L_L), which may be any quark (lepton) of the first row as well as the singlets by U_R , D_R and E_R , which correspond to the up-, down-type quarks and leptons of the second and third row of Table 1.1, respectively.

The SM Lagrangian

The SM Lagrangian can be divided in three parts and is given by

$$\mathcal{L}_{\text{SM}} = \mathcal{L}_{\text{kin}} + \mathcal{L}_{\text{Yuk}} + V_{\text{scalar}}, \quad (1.2)$$

where \mathcal{L}_{kin} is the kinetic part, \mathcal{L}_{Yuk} contains the Yukawa interactions and V_{scalar} is the scalar potential. The first two of them are essential for the concept of flavour and will be discussed

in more detail in the next chapter. The scalar potential is briefly discussed below. For completeness, we state all parts of the SM Lagrangian in shorthand notation here;

$$\mathcal{L}_{\text{kin}} = \sum \bar{\Psi}_{L,R} \not{D} \Psi_{L,R} + \frac{1}{4} \sum F_{\mu\nu}^a F^{a\mu\nu} + |\not{D}\phi|^2, \quad (1.2a)$$

$$\mathcal{L}_{\text{Yuk}} = \sum Y_{\Psi} \bar{\Psi}_L \phi \Psi_R, \quad (1.2b)$$

$$V_{\text{scalar}} = \mu^2 \phi^\dagger \phi + \lambda (\phi^\dagger \phi)^2, \quad (1.2c)$$

where the covariant derivative \not{D} and the field strength tensor $F_{\mu\nu}^a$ are given by

$$\not{D} = \gamma^\mu D_\mu = \gamma^\mu \left(i\partial_\mu - \sum_{a=1}^{12} \mathfrak{g}^a t^a A_\mu^a \right), \quad (1.3a)$$

$$F_{\mu\nu}^a = \partial_\mu A_\nu^a - \partial_\nu A_\mu^a + \mathfrak{g}^a f^{abc} A_\mu^b A_\nu^c, \quad (1.3b)$$

and a, b, c run from 1 to 12. Here, Ψ_L (Ψ_R) may be any of the left- (right-)handed fermion fields Q_L, L_L (U_R, D_R, E_R) and ϕ is the scalar Higgs field. A_μ denotes the vector containing the gauge fields (G_μ^a, W_μ^a, B_μ), \mathfrak{g} consists of the coupling constants (g_s, g, g') and t^a is the vector of the generators (T^a, τ^a, Y).

Higgs Mechanism

The Higgs mechanism of the SM is responsible for the symmetry breaking and the masses of the gauge bosons [18–20].

The scalar potential V_{scalar} is invariant under the product group $SU(2)_w \times U(1)_Y$, however, its ground state is not. The vacuum expectations value (vev) of the scalar field ϕ can be calculated to $v = \sqrt{-\mu^2/\lambda}$, where the parameter μ^2 must be negative. Moreover, the scalar potential is still invariant under a change of the complex phase of the scalar field ϕ . Thus, the ground state spontaneously breaks the symmetry down to $U(1)_{\text{em}}$ which is still a good symmetry of the ground state.

The Higgs mechanism results in mass terms for the gauge boson from the kinetic Lagrangian due to this breaking. The Goldstone bosons of the broken symmetry become the longitudinal modes of the massive gauge bosons. Thus, only a single neutral scalar field, the Higgs boson, is a physical particle. It has been observed quite recently by the ATLAS and CMS experiment at the LHC at CERN [21, 22]. In addition, the Higgs boson generates masses for the fermions due to the Yukawa part of the Lagrangian.

1.2. Reasons for going Beyond the SM

Although the SM is a very predictive and accurate theory (see e.g. [23]), there are in particular theoretical reasons to consider models beyond the Standard Model (BSM). In the following, we briefly discuss some of these issues. A more detailed discussion, especially on how to solve the shortcomings discussed below, can be found in [24–26] and will be addressed throughout this thesis.

1. Grand Unified Theories

Neutrino Masses

The SM itself does not contain right-handed neutrinos which results in exactly massless neutrinos. However, recent measurements have shown that neutrinos mix and thus at least two of them have to have non-vanishing masses (cf. Section 2.2). Therefore, some mechanism to generate these masses has to be introduced. A detailed discussion on such mechanisms is given in Section 2.3.

Gauge Coupling Unification

The gauge couplings themselves are not constant but rather change with energy. This change in energy is explained in the framework of renormalisation [27, 28]. It can be calculated in good approximation from knowing solely the fermion content of the theory. Considering the behaviour of the three gauge couplings of the SM, we find that they approach each other with increasing energy. They nearly meet close to the Planck scale which motivates to unify the gauge symmetries at this scale. In the minimal supersymmetric extension of the SM they actually meet within uncertainties at the so-called GUT scale $M_{\text{GUT}} \approx 10^{16}$ GeV (see e.g. [29, 30]). The unification of the gauge couplings will be discussed within an explicit model in Chapter 3.

Origin of Flavour

The SM contains three generations of quarks and leptons that differ solely by their masses. The relations between these are parametrised by the Yukawa matrices but not explained. The Yukawa matrices feature 13 of the 19 free parameters of the SM without neutrino masses and mixing. Including these adds another 7 or 9 Yukawa parameter, depending on whether neutrinos are Dirac or Majorana particles. To reduce these parameters one might consider BSM theories to find a guiding principle based on symmetry arguments. The framework of unification reduces the Yukawa sector but does not address this subject in general. However, it gives room for interesting flavour models as discussed in the main part of this thesis.

Charge Quantisation

An important feature of nature is the equality of the absolute value of the electron and proton charge, i.e. neutral atoms. The charge of the electron is historically defined by the elementary charge $Q_e = -e$. As the proton (uud) and the (neutral) neutron (udd) are composite particles of up- and down-type quarks, this equality leads to fractional charges $Q_d = -1/3 e$ and $Q_u = +2/3 e$ for the quarks.

This charge assignment is not determined from first principles in the SM. It can be traced back to the fact that the hypercharge of the fermions cannot be completely fixed. However, most GUTs do provide an explanation for this issue as they embed the $U(1)_Y$ into a non-abelian group. In these GUTs, all gauge transformations and charges of the fermions are completely fixed.

Hierarchy Problems

In gauge theories, the mass m of a scalar particle is not protected by any symmetry. Thus, there is no natural scale for the mass parameter m_0^2 of the theory. In the SM, this problem

affects the electroweak symmetry breaking Higgs since it is the only scalar in the theory. Calculating radiative corrections to the Higgs mass, we get a quadratic divergence which can be renormalised by an ultraviolet cutoff parameter Λ . Hence, the renormalised mass is given by

$$m^2 = m_0^2 + a\Lambda^2 + \dots, \quad (1.4)$$

where a is a calculable value. Here, m is the experimentally observable mass of the scalar which is physical and has to be independent under renormalisation. However, since m_0 and Λ are both unphysical parameters we can choose them such that we get the measured value for m . Thus, if there is no new physics and gravity is turned off at any high scale, there is no problem at all. However, if we introduce a new physics scale such as a GUT scale or consider gravity which introduces the Planck scale, Λ becomes a physical parameter. Thus, we have a fine-tuning problem as the scales of m and Λ differ by many orders of magnitude ($m \ll \Lambda$). The level of fine-tuning needed to cancel the scale of Λ by m_0 is often called naturalness. Thus, this problem of the SM including higher scale physics is often referred to as naturalness problem.

In the literature one sometimes finds another hierarchy problem, namely in the Yukawa sector of the SM. As there are large hierarchies between the masses (cf. Section 2.2), also the Yukawa couplings have to feature these hierarchies. These are given by the mass ratios and are as large as 10^6 .

There are additional aspects that are not explained by the SM. Examples are dark matter, dark energy, baryon-asymmetry, gravitation, inflation and many more which are not relevant for this thesis and will not be discussed here.

1.3. Supersymmetry

Most GUTs are constructed within the framework of Supersymmetry. The main reason for that is the naturalness problem which we encounter when introducing additional scales to the SM (cf. discussions above). SUSY provides a solution to this problem as we outline below. Another motivation for SUSY is the fact that it is the only possible extension of the Poincaré algebra in four dimensions which the SM, as well as all other quantum field theories, are based on. As such, it is an extension of the space-time symmetry that relates bosons and fermions.

In the following, we take a look at the main features of SUSY. We will not give an introduction or complete discussion of SUSY here but only discuss aspects relevant for this work. The main aspects of SUSY are nowadays textbook knowledge and can be found in e.g. [31–34].

Solution to the Naturalness Problem

Supersymmetry introduces a scalar field for each of the SM fermions and *vice versa* which are the so-called superpartners. In exact SUSY, the SM fields and their superpartners have

1. Grand Unified Theories

equal mass and cancel the contribution of the fermions to the running of the SM Higgs mass parameter. Thus, additional fermions with masses above the SUSY scale do not contribute to the naturalness problem.

Due to the large top Yukawa coupling, the contribution of the top quark to the naturalness problem is the most important one in the SM. This contribution gets not cancelled exactly by the superpartner of the top as it has not been found yet ¹. Hence, we still encounter a logarithmic divergence which sometimes is called the “little hierarchy problem”.

Superpotential

An additional advantage of supersymmetry is the superfield formalism which includes the superpotential W . The scalar potential of the theory can be derived from a superpotential with mass dimension up to three. Hence, the number of allowed terms and their invariant structures is limited compared to the non-SUSY case².

The scalar potential of the theory is given by

$$\mathcal{L} = |F^i|^2 + \frac{1}{2} |D^a|^2, \quad (1.5)$$

where the F-terms follow from the superpotential W and the D-terms are determined purely from the gauge symmetry and the contained superfield content ϕ_i . They are given by

$$D^a = g_a \sum_i \phi_i^* T^a \phi_i \quad \text{and} \quad F^i = - \left(\frac{\partial W}{\partial \phi_i} \right)^*. \quad (1.6)$$

(Accidental) SUSY Breaking

Supersymmetry is spontaneously broken if one of the F- or D-terms has a non-vanishing ground state. In order to ensure the validity of SUSY down to some low scale, we have to verify this for any GUT breaking vev of the high scale. Otherwise SUSY would be broken accidentally.

In addition, SUSY can be broken softly, i.e. by so-called soft-breaking terms which are introduced in the effective Lagrangian by hand [35]. This is often realised by breaking SUSY spontaneously in a hidden sector. However, the mechanism of SUSY breaking and the mass structure of the superpartner is not relevant for this work. Hence, we will not discuss the SUSY-breaking any further.

Two Higgs Doublets

As the superpotential has to be holomorphic, we are not allowed to use the complex conjugate Higgs field to generate masses for the up-quark sector (cf. Section 2.1.2). Hence, we have to introduce an additional Higgs field which results in a two Higgs doublet model of Type II (cf. e.g. [36, 37]). In general, the two doublets get different vevs v_u and v_d . Nevertheless, the Higgs sector has to reproduce the masses of the electroweak gauge bosons. From the kinetic terms of the two Higgs fields one can read off that both vevs contribute

¹Neither have any other superpartner been observed (see “Problems of SUSY”).

²However, the soft sector needed to break SUSY introduces a lot of additional terms and structures.

quadratically to the gauge boson masses. Thus, they have to add up quadratically to the square of the SM vev v . The ratio of these two vevs is commonly denoted by $\tan \beta$,

$$\tan \beta = \frac{v_u}{v_d} \quad \text{with} \quad v_u^2 + v_d^2 = v^2. \quad (1.7)$$

Nonrenormalisation Theorem

The nonrenormalisation theorem states that the parameters of the superpotential do not receive renormalisation corrections [8, 38]. It is a consequence of the condition that the superpotential is holomorphic. This theorem is of particular interest for couplings with positive mass dimension as they may encounter a naturalness problem. However, this does not imply that SUSY needs not be renormalised at all, as field renormalisation is still present.

Problems of SUSY

One of the main issues of SUSY is the fact that despite extensive searches no superpartner has been observed so far. The most recent lower bounds on the SUSY scale come from the LHC and are in the range of a few TeV (e.g. [15, 39–41]). However, these searches are all based on simplifying conditions and specific models. Thus, the general bound is lower. Nevertheless, due to the large number of free parameters in the soft breaking sector, SUSY cannot be excluded easily and for special parameter points even much lower SUSY scales are still conceivable.

An additional shortcoming is the so-called μ problem. The μ parameter is the residual mass parameter of the electroweak symmetry breaking Higgs. Although it does not receive renormalisation corrections its size still lacks in motivation. As it is the only scale in the theory one would expect it to be near the Planck scale rather than in the electroweak regime. This is however a purely theoretical problem and may or may not be seen as such.

1.4. Roadmap to Unification

As we have discussed in Section 1.1, the SM combines two interactions to a more fundamental one and thus links phenomena that for a long time seemed to be unrelated. Hence, it seems to be natural to search for a unification principle of the SM interactions to correlate the different gauge sectors of the SM. Another motivation comes from the fact that the gauge couplings (strong, weak and hypercharge) approach each other at large energies. In the simplest of the supersymmetric extensions, the Minimal Supersymmetric SM (MSSM) (see e.g. [33, 34]), all three gauge couplings unify at roughly $M_{\text{GUT}} \approx 10^{16}$ GeV which is not far below the Planck scale³.

Since the SM is extremely successful in predicting low energy data up to several TeV [23], it should be the low energy effective theory of the unified model. Thus, a unifying gauge group has to have the SM as a subgroup, $G_{\text{GUT}} \supset G_{\text{SM}}$. The number of good quantum numbers of the theory corresponds to the number of diagonal generators which is the rank of a group. The SM gauge group G_{SM} has rank 4 and thus, the unifying group has to

³We use $M_{\text{Planck}} = 10^{18.2}$ GeV $\approx 1.6 \cdot 10^{18}$ GeV.

1. Grand Unified Theories

have $\text{rank}(G_{\text{GUT}}) \geq 4$. There are only a few groups fulfilling these constraints which are not merely trivial extensions, i.e. additional group factors multiplied to G_{SM} . The only possible rank 4 group is $SU(5)$. At rank 5 the groups mainly considered are $SO(10)$ and $SU(4) \times SU(2) \times SU(2)$. At rank 6 and 8, there are the exceptional groups E_6 and E_8 which are usually discussed as GUT, especial in the context of string theory. In this context, also even larger groups such as $SO(32)$ are discussed. One can consider different or larger groups but for multiple reasons (especially simplicity) they have not been discussed extensively so far. Most of the groups mentioned before will be outlined in the following, especially $SU(5)$ as it may be seen as prototype. In the presentation of the GUTs we follow the historical development. A review on GUTs can be found in e.g. [42, 43]

1.4.1. $SU(5)$ à la Georgi and Glashow

The smallest group unifying all SM gauge factors is $SU(5)$. It was first discussed by Georgi and Glashow in 1974 [1]. The embedding of the SM gauge group in $SU(5)$ can easily be seen when constructing the generators of $SU(5)$ explicitly. Therefore, we choose the basis such that the first generators can be represented as direct product of the $SU(3)_c$ and $SU(2)_w$ generators,

$$\left(SU(5) \right) \hat{=} \left(\begin{array}{cc} SU(3)_c & 0 \\ 0 & SU(2)_w \end{array} \right). \quad (1.8)$$

By this construction principle we can identify 11 of the 24 generators L_i of $SU(5)$ with the SM ones ($T^{1\dots 8}$ and $\tau^{1\dots 3}$),

$$L_{1\dots 8} = \left(\begin{array}{cc} T^{1\dots 8} & 0 \\ 0 & 0_{2 \times 2} \end{array} \right) \quad \text{and} \quad L_{9\dots 11} = \left(\begin{array}{cc} 0_{3 \times 3} & 0 \\ 0 & \tau^{1\dots 3} \end{array} \right), \quad (1.9)$$

where we have used a shorthand notation to display the 5×5 matrices L . The hypercharge has to be diagonal in this basis as it is the fourth good quantum number. As the rank of $SU(5)$ is four it is (up to normalisation) fixed to match

$$Y \sim L_{12} = \frac{1}{\sqrt{15}} \text{diag}(-2, -2, -2, 3, 3). \quad (1.10)$$

The remaining 12 generators are the off-diagonal generators X and Y ,

$$L_{13\dots 18} = \left(\begin{array}{ccc} 0_{3 \times 3} & X & 0 \\ X^\dagger & 0 & 0 \\ 0 & 0 & 0 \end{array} \right) \quad \text{and} \quad L_{19\dots 24} = \left(\begin{array}{ccc} 0_{3 \times 3} & 0 & Y \\ 0 & 0 & 0 \\ Y^\dagger & 0 & 0 \end{array} \right). \quad (1.11)$$

These gauge bosons transform non trivially under both $SU(3)_c$ and $SU(2)_w$, and thus mediate new transitions like proton decay. These will be discussed later in this section.

Unifying the Fermions

In order to combine different fermion representations we have to ensure equal chirality for them. We know that a charged conjugated right-handed fermion transforms left-handed and vice versa,

$$(f_R)^c \sim \bar{f}_L, \quad (1.12)$$

where f represents any fermionic field. Hence, we can write the complete SM fermion content as left-handed fermions. Next, we consider the branching rules of $SU(5)$ to the SM gauge group [42]. The smallest representations containing all of the SM representations are $\bar{\mathbf{5}}$ and $\mathbf{10}$,

$$\bar{\mathbf{5}} \rightarrow (\bar{\mathbf{3}}, \mathbf{1})_{1/3} + (\mathbf{1}, \mathbf{2})_{-1/2} \quad \text{and} \quad \mathbf{10} \rightarrow (\mathbf{3}, \mathbf{2})_{1/6} + (\bar{\mathbf{3}}, \mathbf{1})_{-2/3} + (\mathbf{1}, \mathbf{1})_1. \quad (1.13)$$

Hence, we can combine the lepton doublet with the charge conjugated down quark singlet to an anti-fundamental representation. The charge conjugated up quark singlet, the quark doublet and the charge conjugated lepton singlet fit together into a decuplet representation of $SU(5)$. This defines the embedding of the SM quarks which we give for the first generation for explicitness,

$$\bar{\psi} = ((d_R^1)^c, (d_R^2)^c, (d_R^3)^c, \nu_L, e_L), \quad (1.14a)$$

$$\chi = \begin{pmatrix} 0 & (u_R^3)^c & -(u_R^2)^c & -u_L^1 & -d_L^1 \\ -(u_R^3)^c & 0 & (u_R^1)^c & -u_L^2 & -d_L^2 \\ (u_R^2)^c & -(u_R^1)^c & 0 & -u_L^3 & -d_L^3 \\ u_L^1 & u_L^2 & u_L^3 & 0 & -e_R^c \\ d_L^1 & d_L^2 & d_L^3 & e_R^c & 0 \end{pmatrix}, \quad (1.14b)$$

where the superscript on the quarks are colour indices.

After the breaking of $SU(5)$ down to the SM, the generator L_{12} corresponds to an unbroken $U(1)$ which is identified with the hypercharge. Thus, the $U(1)$ charges of the SM fermions are fixed by L_{12} . However, these charges do not match the hypercharges historically considered in the SM. Thus, a factor of $5/3$ is introduced to match the SM hypercharge. The charge operator for the electric charge can be calculated following the Gell-Mann-Nishijima formula to

$$Q = T_3 + Y = \frac{1}{2} L_{11} + \frac{1}{2} \sqrt{\frac{5}{3}} L_{12} = \text{diag} \left(-\frac{1}{3}, -\frac{1}{3}, -\frac{1}{3}, 1, 0 \right). \quad (1.15)$$

We note that the charge operator is defined for the fundamental representation and its $SU(2)$ components have to be multiplied by an epsilon tensor when applying it to the $\bar{\mathbf{5}}$.

Higgs Embedding & $SU(5)$ Breaking

The electroweak symmetry breaking Higgs has to be embedded in $SU(5)$, i.e. we need a representation that couples to the Yukawa terms $\bar{\Psi} \bar{\Psi}$, $\bar{\Psi} \chi$ and/or $\chi \chi$. Thus, it has to be part of the product $\mathbf{5} \times \mathbf{5}$, $\mathbf{5} \times \bar{\mathbf{10}}$ or $\bar{\mathbf{10}} \times \bar{\mathbf{10}}$. The decomposition of these tensor products

1. Grand Unified Theories

can be found in [42]. The smallest representation which is able to provide an electroweak breaking Higgs doublet is the fundamental quintuplet $\mathbf{5}$. To be compatible with SUSY, we in addition have to introduce the conjugate representation $\bar{\mathbf{5}}$. These are the Higgs fields originally considered by Georgi and Glashow. Alternatively, it is possible to embed the Higgs doublet in a pair of $\mathbf{45}$ and $\bar{\mathbf{45}}$. The up- (down-)type Higgs H^u (H^d) is contained in the $\mathbf{5}$ and $\mathbf{45}$ ($\bar{\mathbf{5}}$ and $\bar{\mathbf{45}}$). In any case, the Yukawa interaction is given by⁴

$$\mathcal{L}_{\text{Yuk}} = Y^D \bar{\psi} H^d \chi + Y^U \chi H^u \chi + \text{h.c.} . \quad (1.16)$$

In addition to the embedding of the electroweak Higgs we have to introduce Higgs fields breaking $SU(5)$ down to the SM in the first place. For this, we have to assign a vev to the SM singlet component of an $SU(5)$ representation. A common way to achieve a breaking of $SU(5)$ is to use the adjoint $\mathbf{24}$ representation. The next larger possible representation is the $\mathbf{75}$.

The $SU(5)$ model constructed so far treats each generation of fermions separately, similar to the SM. The role of flavour symmetries in GUTs will be discussed in the next chapter.

Problems of $SU(5)$

There are two unsolved issues in the simplest $SU(5)$ model presented here, both related to proton decay. First of all, the additional gauge bosons X and Y introduce proton decay in the theory. Naturally one would assume masses of the order of the GUT scale for those. Naively calculating the proton decay rate using this assumption, one starts to get in tension with the current bound on proton lifetime from Super-Kamiokande which is 8.2×10^{33} years [44, 45].

The second and more severe problem is the doublet-triplet splitting problem. The fundamental representation containing the electroweak symmetry breaking Higgs decomposes into the Higgs doublet and an additional triplet. These triplets again allow for rapid proton decay if they couple to the SM fermions and have masses around the electroweak scale. The doublet however has to be light as it plays the role of the electroweak Higgs. Thus, we are left with the problem of splitting up the masses and/or couplings of different components of the fundamental representation over several orders of magnitude.

1.4.2. Complete Unification in $SO(10)$

One of the most common symmetries unifying the gauge sector of the SM is $SO(10)$. It was first discussed by Fritzsche and Minkowski in 1974 [2]. Its attractiveness lies in the fact that it is the smallest group unifying both gauge interactions and fermion spectrum. Its rank is 5 and thus larger than that of the SM or $SU(5)$. Thus, it contains $SU(5) \times U(1)$ as a subgroup. All fermions fit into the $\mathbf{16}$ which is the fundamental representation of $SO(10)$. Its branching to $SU(5)$ and further to the SM is given by

$$\mathbf{16} \xrightarrow{SU(5)} \mathbf{10}_{-1} + \bar{\mathbf{5}}_3 + \mathbf{1}_{-5} \quad (1.17a)$$

$$\xrightarrow{\text{SM}} (\mathbf{3}, \mathbf{2})_{1/6} + (\bar{\mathbf{3}}, \mathbf{1})_{1/3} + (\bar{\mathbf{3}}, \mathbf{1})_{-2/3} + (\mathbf{1}, \mathbf{2})_{-1/2} + (\mathbf{1}, \mathbf{1})_1 + (\mathbf{1}, \mathbf{1})_0 . \quad (1.17b)$$

⁴Note that the invariant structure and the resulting low energy Yukawa terms clearly depend on the choice of Higgs representation.

In addition to the SM fermions it contains a singlet under the complete SM gauge group $(\mathbf{1}, \mathbf{1})_0$. This singlet is a good candidate for a right-handed neutrino.

The electroweak symmetry breaking Higgs is contained in a $\mathbf{10}$ which splits up into $\mathbf{5} + \bar{\mathbf{5}}$ under $SU(5)$. Again, the larger representation for the electroweak Higgs leads to coloured scalars which have to be made artificially massive. Another possibility to include the electroweak Higgs in $SO(10)$ is to embed it in a $\mathbf{120}$ or $\mathbf{126}$. These are all the possibilities for a standard Higgs since we want to construct a renormalisable gauge invariant Yukawa term.

Taking a look at the breaking of $SO(10)$ we recognise directly that one possibility is to first break it to $SU(5)$, as it is a subgroup that contains the SM. Such a breaking can be realised by assigning a vev to the adjoint $\mathbf{45}$ representation which contains an $SU(5)$ singlet. Moreover, the $\mathbf{45}$ contains a $\mathbf{24}$ under $SU(5)$ which can be used to break $SU(5)$. This further breaking can be realised at the same scale as the $SO(10)$ breaking or at a lower scale, depending on whether the Higgs potential splits up these two vevs. Another way of breaking $SU(5)$ itself can be achieved by a vev of the singlet component of $\mathbf{16}$ or $\mathbf{126}$. These representations can also break $SO(10)$ directly down to the SM gauge group. An orthogonal way of breaking $SO(10)$ is to assign a vev to a $\mathbf{54}$ which breaks $SO(10)$ to $SO(6) \times SO(4)$ [42]. This is the relevant breaking path for this work which therefore is discussed in more detail in the next section.

1.4.3. Pati-Salam: an Alternative Route

For discussing unification nowadays one often considers $SO(10)$ to be broken down to the SM through $SU(5)$. However, there is an additional possibility to break $SO(10)$ to $SO(6) \times SO(4)$ which is clearly also a subgroup. It is not trivial to see, that this group also contains the SM. Thus, it is more common to consider the product group $SU(4) \times SU(2) \times SU(2)$ which is locally isomorphic (i.e. has the same algebra) to $SO(6) \times SO(4)$ as can be seen from the corresponding Dynkin diagram [42]. Using these groups, it is easy to see that $SU(3)_c$ is contained in $SU(4)$ and one of the two $SU(2)$ factors may serve as $SU(2)_w$. The $U(1)_Y$ is embedded in a combination of the diagonal generators of $SU(4)$ and the remaining $SU(2)$, which we from now on label by $SU(2)'$. As there is no overlap between the two possible breaking paths, they can be considered orthogonal.

Independent from the breaking of $SO(10)$ this symmetry group was first considered as an extension of the SM by Pati and Salam in 1974 in a bottom-up approach [6, 7]. In their model they took lepton number to be a fourth colour which unifies quarks and leptons to $SU(4)$. In addition, they considered the model to be a left-right symmetric extension of the SM and included the additional $SU(2)'$. To ensure left-right symmetry and reduce the number of individual gauge couplings they considered an additional Z_2 symmetry. Such a Z_2 factor is also present in the breaking of $SO(10)$. Unlike in this thesis, it is not always considered to be part of the PS symmetry.

To sum up, the gauge symmetry of Pati-Salam (PS) models is given by

$$G_{\text{PS}} = SU(4) \times SU(2) \times SU(2)' \times Z_2. \quad (1.18)$$

Different Labelling of PS

The product groups of the PS symmetry are often labelled with the indices L, R and C ;

$$\tilde{G}_{\text{PS}} = SU(4)_C \times SU(2)_L \times SU(2)_R \times Z_{LR}, \quad (1.19)$$

where the subscripts denote colour and left- and right-chirality. This is often used as the left-(right-)handed SM fermions transform solely under $SU(2)_{L(R)}$. However, for this thesis such a labelling is ambiguous as we discuss a model in which left- (right-)handed fermions transform non trivially under $SU(2)_{R(L)}$, respectively, in Chapter 5. On the other hand, we consider the Z_2 to be exact at the PS scale. It interchanges the $SU(2)$ and $SU(2)'$ representations as well as conjugates the $SU(4)$. Thus, the Z_2 guarantees the equality of left- and right-handed isospin as long as it is unbroken and may be seen as explicit left-right symmetry. Therefore it is often labelled as Z_{LR} . Nevertheless, throughout the rest of this work we will consider the PS symmetry as defined in (1.18).

Fermion Representation

The embedding of the fermions in PS follows directly from the fermion embedding of $SO(10)$. There, we have embedded the fermions in the **16** which decomposes to PS and further to the SM like

$$\mathbf{16} \xrightarrow{\text{PS}} (\mathbf{4}, \mathbf{2}, \mathbf{1}) + (\bar{\mathbf{4}}, \mathbf{1}, \mathbf{2}) \quad (1.20a)$$

$$\xrightarrow{\text{SM}} (\mathbf{3}, \mathbf{2})_{1/6} + (\mathbf{1}, \mathbf{2})_{-1/2} + (\bar{\mathbf{3}}, \mathbf{1})_{1/3} + (\bar{\mathbf{3}}, \mathbf{1})_{-2/3} + (\mathbf{1}, \mathbf{1})_1 + (\mathbf{1}, \mathbf{1})_0. \quad (1.20b)$$

As we consider lepton number as fourth colour, we combine the $SU(2)$ quark and fermion doublets into a $(\mathbf{4}, \mathbf{2}, \mathbf{1})$, denoted by Ψ_L . Again, we consider only the left-handed fields to be in line with SUSY. The remaining fields, the charge conjugated quarks together with the charge conjugated electron and a right-handed anti-neutrino, are unified to Ψ_R , transforming as $(\bar{\mathbf{4}}, \mathbf{1}, \mathbf{2})$. Summing up, the fermions are embedded in PS as

$$\Psi_L = \begin{pmatrix} u_L^1 & u_L^2 & u_L^3 & \nu_L \\ d_L^1 & d_L^2 & d_L^3 & e_L \end{pmatrix} \quad \text{and} \quad \Psi_R = \begin{pmatrix} u_R^1 & u_R^2 & u_R^3 & \nu_R \\ d_R^1 & d_R^2 & d_R^3 & e_R \end{pmatrix}^c, \quad (1.21)$$

where 1, 2, 3 are again colour indices and we show the first generation for definiteness.

Depending on the explicit realisation of the Z_2 symmetry, these two multiplets can be considered as a single reducible representation $\Psi_L \oplus \Psi_R$. This Z_2 is naturally realised in a model motivated by $SO(10)$ as each $SO(10)$ representation decomposes in a Z_2 symmetric sum.

So far we can conclude that PS is in some sense opposite to $SU(5)$ as it combines all fermions in a single multiplet but merely reduces the gauge symmetry to a product group with two independent gauge couplings. As such, it is natural to consider it as intermediate step, similar to $SU(5)$. Since the breaking of PS (Chapter 3) as well as the Yukawa sector of the theory (Chapter 4 and Chapter 5) are the main part of this thesis, we discuss these in detail later on.

1.4.4. Larger Groups

An even larger group as the already unifying gauge group $SO(10)$ is the exceptional Lie group E_6 . It has rank 6 and contains $SO(10) \times U(1)$ and therefore also all groups discussed above as a subgroup. A different breaking path to the SM is via the so-called trinification $SU(3) \times SU(3) \times SU(3)$. The fundamental representation of E_6 is **27**. Its branching rule to $SO(10)$ is given by $\mathbf{27} \rightarrow \mathbf{16} + \mathbf{10} + \mathbf{1}$. The **16** may contain the SM fermions as discussed above. In addition, the **10** contains a pair of electroweak Higgs doublets. Thus, the fundamental representation can contain all SM fermions as well as the MSSM Higgs fields if we are in a supersymmetric framework. This is usually referred to as matter-Higgs unification. Moreover, it contains a right-handed neutrino candidate and an additional electroweak singlet. Thus, it has generated quite some interest in the late 80's. Another reason why one started to discuss E_6 models was the arise of string theory. Here, some versions of $N = 8$ supergravity in five dimensions lead to a Planck scale E_6 local gauge symmetry [46–48].

String theory and supergravity also motivated the consideration of the groups $SO(32)$ and the exceptional group E_8 . $E_8 \times E_8$ is one of the two emerging gauge groups from heterotic string models while the other is $SO(32)$ [49]. Moreover, E_8 contains $E_6 \times SU(3)$ as a subgroup. However, models based on E_8 have the significant problem that E_8 contains solely self-conjugate representations and thus features only vector-like theories. Hence, they need to be uplifted to an at least five dimensional theory in order to break it in such a way that the low energy effective theory has the chiral fermions we observe in nature. Because of its $E_6 \times SU(3)$ subgroup one has also tried to connect the $SU(3)$ with a flavour symmetry [42, 50].

Nowadays there is only little interest in the exceptional groups in particle physics apart from string theory. Nevertheless, we will take the fact that E_6 combines the MSSM Higgs scalar with the fermions as motivation to consider three generations of the MSSM Higgs in Chapter 3 and 4. In such models, the MSSM Higgs may be subject to flavour similar to the SM fermions. An example of this kind is considered in Chapter 4.

Flavour Symmetries

Standard Model and Beyond

As mentioned in the last chapter, the concept of flavour is an important part of the SM and flavour symmetries provide a good starting point when going beyond. In this chapter we introduce the different aspects of flavour in the SM and how to implement them in Grand Unified Theories. We discuss quark and lepton flavour as there is plenty of space for relating both sectors in GUTs.

To start with, we comment on the different notions of flavour in the SM and give a brief introduction on the flavour sector and flavour symmetries of the SM. Moreover, we discuss the differences between quark and lepton flavour symmetries. In the second part we consider the issues of flavour in GUTs and give a short overview on how to correlate quark and lepton flavour. More details can be found in References [51, 52] and references therein.

2.1. The Concept of Flavour

The notion of flavour usually summarises all effects dealing with masses and mixing of quarks and leptons in the SM and beyond. In the SM, all these effects are parametrised by the Yukawa matrices and thus the flavour sector is synonymous to the Yukawa sector. However, there is no unique definition of flavour. Depending on the fields it may solely refer to a “sub-sector” (e.g. quarks, leptons, generations) of the one stated above.

Historically, Gell-Mann and Fritzsche introduced the notion of flavour to organise the “particle-zoo” observed by experiments in the mid-20th century [15, 53]. Gell-Mann introduced an additional flavour (strangeness) to the already known concept of isospin (up and down flavour) and grouped the mesons and baryons in representations of $SU(3)$, forming the so-called “eightfold-way” [54–56]. This work paved the way for the introduction of the quark model. Such a definition of flavour in the quark sector can be easily extended to the six quark flavours (up, down, strange, charm, bottom and top flavour). However, a combination of all quarks into a single representations of a flavour group (such as $SU(6)$) is not reasonable.

In the lepton sector, a definition of flavour similar to the quark sector is possible. As neutrinos and charged leptons differ vastly in their masses one often distinguishes between charged-lepton and neutrino flavour.

For the purposes of GUT model building it is convenient to define flavour as the generation index of quarks and leptons, often referred to as “family”. This provides an orthogonal way

2. Flavour Symmetries; SM and Beyond

of correlating the SM fermion content. In the context of BSM physics, flavour symmetries are commonly called horizontal whereas GUT symmetries are vertical, in line with the usual visualisation of the SM fermion content (cf. Table 1.1). Throughout this thesis, the flavour sector will denote the whole sector of fermion masses and mixing whereas flavour symmetries always act on the three generations of fermions.

2.1.1. Flavour Symmetries

Similar to the meaning of flavour there is no unique definition of flavour symmetries in particle physics. In the SM, the flavour symmetry is often defined as the symmetry of the Lagrangian without the Yukawa interactions. It is a symmetry orthogonal to the gauge symmetry. Therefore we consider the kinetic sector of the fermions in the SM which is given by

$$\mathcal{L}_{\text{kin}} = i \bar{Q}_L^i \not{D} Q_L^i + i \bar{U}_R^i \not{D} U_R^i + i \bar{D}_R^i \not{D} D_R^i + i \bar{L}_L^i \not{D} L_L^i + i \bar{E}_R^i \not{D} E_R^i, \quad (2.1)$$

where \not{D} is the covariant derivative and contains the gauge fields and the superscripts $i = 1, 2, 3$ denotes the three generations of fermions (cf. (1.2a) and following discussions). These terms provide the coupling of the fermions to the gauge bosons. Considering the symmetries of these terms, we can easily deduce that an $SU(3)$ rotation as well as a phase shift, which corresponds to a $U(1)$ symmetry, on each of the SM building blocks (Q_L , U_R , D_R , L_L and E_R) leaves the kinetic Lagrangian invariant. Thus, we end up with a flavour symmetry of the SM given by¹

$$G_F^{\text{SM}} = U(3)_{Q_L} \times U(3)_{D_R} \times U(3)_{U_R} \times U(3)_{L_L} \times U(3)_{E_R}, \quad (2.2)$$

which is the maximal symmetry of the kinetic Lagrangian. However, often a smaller symmetry than this is considered to be the flavour symmetry of the SM; the flavour symmetry as defined above is split up in a ‘‘pure’’ flavour part which is broken by the Yukawa interactions and an accidental part which is still a good symmetry of the full Lagrangian. Examples of such accidental symmetries are $U(1)_B$, $U(1)_{L_e} \times U(1)_{L_\mu} \times U(1)_{L_\tau}$ or $U(1)_{B-L}$. As flavour symmetry is often considered either in the quark or the lepton sector, we discuss both sectors separately.

Quark Sector

Considering only the part of the kinetic Lagrangian (1.2a) containing the quarks, the maximal flavour symmetry is given by $U(3)_{Q_L} \times U(3)_{D_R} \times U(3)_{U_R}$. The quarks all have a non-vanishing mass and mix with each other. The only symmetry preserved by the Yukawa matrices is the baryon number $U(1)_B$. It is a diagonal $U(1)$ that can be factored out of any of the three $U(3)$ factors. Thus, the resulting pure flavour symmetry of the quark sector is given by

$$G_F^Q = SU(3) \times U(3) \times U(3). \quad (2.3)$$

¹Note that $U(3) = SU(3) \times U(1)$.

Lepton Sector

In the lepton sector the situation is different. Here, individual lepton number is a good quantum number up to high energies. However, it is broken by the masses and mixing of the neutrinos. Depending on the nature of neutrino masses (Dirac or Majorana) even total lepton number may not be a good symmetry of the Lagrangian. Considering the SM without neutrino mass and mixing, the maximal flavour symmetry is $U(3)_{L_L} \times U(3)_{E_R}$. After inserting Yukawa couplings, the remaining symmetry is individual lepton number $U(1)_{L_e} \times U(1)_{L_\mu} \times U(1)_{L_\tau}$. One of the $U(1)$ factors corresponding to the total lepton number can be factored out but not the whole accidental symmetry, as $U(1) \times U(1) \times U(1)$ is not a normal subgroup of $U(3) \times U(3)$. Thus, the Yukawa couplings break the lepton flavour symmetry to

$$G_{\text{F}}^L = SU(3) \times U(3) \xrightarrow{Y_L} U(1) \times U(1). \quad (2.4)$$

As a consequence one cannot gauge the lepton flavour symmetry G_{F}^L , as this would result in at least two massless gauge bosons which are phenomenologically excluded.

However, since the discovery of neutrino mixing, massless neutrinos are phenomenologically excluded [5, 15]. Thus, we have to add either right-handed partners or a Majorana mass term for the left-handed SM neutrinos. Right-handed neutrinos introduce an additional $U(3)_{N_R}$ to the lepton flavour symmetry when they are included in the SM fermion content. If neutrinos are pure Dirac particles, individual lepton number is no longer an accidental symmetry of the Lagrangian as neutrinos mix. Hence, the situation is similar to the quark sector. If neutrinos are Majorana fermions, they violate lepton number and there is no symmetry left in the lepton sector. Therefore, the resulting pure flavour symmetry of the lepton sector depends strongly on the implementation of neutrino masses.

GUTs

The definition of the flavour symmetry may also vary in each explicit BSM model. If one considers a unification of the fermions, the maximal flavour symmetry can change as additional relations may exist. An explicit choice of symmetry often depends on the aim of the model. Different realisations of the flavour sector in a PS symmetric GUT will be discussed in this thesis. In Chapter 4 we take the flavour symmetry to be $SU(3)$ whereas we use the maximally possible flavour symmetry $SU(3) \times SU(3)$ in Chapter 5.

2.1.2. Yukawa Sector

In the SM, the pure flavour symmetry is broken completely by the Yukawa couplings. These introduce masses for the fermions and allow for a mixing among the different generations. In addition, we include a mass term for the SM neutrinos without specifying it further as it is needed for neutrino mixing. We discuss possible ways of generating such a term and the experimental evidence for neutrino mixing in Section 2.3.1. Here, we start with a detailed discussion of the quark Yukawa sector and afterwards comment on lepton mixing.

The SM quark Yukawa sector is given by

$$\mathcal{L}_{\text{Yuk}} = Y_u^{ij} \bar{Q}_L^i \tilde{\phi} U_R^j + Y_d^{ij} \bar{Q}_L^i \phi D_R^j + \text{h.c.}, \quad (2.5)$$

2. Flavour Symmetries; SM and Beyond

where Y_u and Y_d are arbitrary 3×3 matrices (cf. (1.2b) and following discussions). They can be diagonalised by a bi-unitary transformation which we parametrise as²

$$\hat{Y}_u = \mathcal{V}_u Y_u \mathcal{U}_u^\dagger \quad \text{and} \quad \hat{Y}_d = \mathcal{V}_d Y_d \mathcal{U}_d^\dagger. \quad (2.6)$$

Inserting these transformations in the Yukawa Lagrangian (2.5), we use the freedom of rotating the fermion fields in any basis to write the Lagrangian in a diagonal basis. After this rotation we are in the mass-basis where each of the so defined fermion fields has a distinct mass. If we redefine our fermion fields, we have to do this consistently in all parts of the Lagrangian, especially in the gauge kinetic term given in (2.1). This we have to consider after the $SU(2)$ symmetry breaking since the masses are generated by inserting the Higgs vev that breaks $SU(2) \times U(1)_Y \rightarrow U(1)_{\text{em}}$. In the broken phase, the first term of (2.1) leads to

$$\mathcal{L}_{\text{kin}} \supset i \bar{Q}_L \not{D} Q_L \quad (2.7a)$$

$$\supset g \left(\bar{U}_L \not{W}^+ D_L + \bar{D}_L \not{W}^- U_L + \bar{U}_L \not{W}^0 U_L + \bar{D}_L \not{W}^0 D_L \right) \quad (2.7b)$$

$$= g \left(\bar{U}'_L \not{W}^+ \underbrace{\mathcal{V}_u \mathcal{V}_d^\dagger}_{\equiv V_{\text{CKM}}} D'_L + \bar{D}'_L \not{W}^- \underbrace{\mathcal{V}_d \mathcal{V}_u^\dagger}_{\equiv V_{\text{CKM}}^\dagger} D'_L + \bar{U}'_L \not{W}^0 U'_L + \bar{D}'_L \not{W}^0 D'_L \right), \quad (2.7c)$$

where we have defined $V_{\text{CKM}} = \mathcal{V}_u \mathcal{V}_d^\dagger$ and the (un)primed quarks denote the (flavour) mass basis. The other parts of the kinetic Lagrangian are left unchanged by these transformations. We find, that changing the basis from the flavour eigenbasis, i.e. diagonal coupling to the gauge bosons, to the mass eigenbasis, i.e. diagonal mass matrix, induces a mixing matrix among the different generations, i.e. among the different flavour. This mixing is parametrised by the Cabibbo-Kobayashi-Maskawa matrix V_{CKM} [57, 58]. We note that the rotations of the right-handed quarks $\mathcal{U}_{u,d}$ are unphysical in the SM framework. This may not be the case in unified theories as they allow for right-handed gauge bosons. In such a setup, a generally non-trivial mixing matrix $U_{\text{CKM}} = \mathcal{U}_u^\dagger \mathcal{U}_d$ is present (cf. Chapter 5).

A similar result can be found in the lepton sector if and only if one includes a mass term for the neutrinos. The mixing matrix in the lepton sector is the Pontecorvo-Maki-Nakagawa-Sakata matrix³ U_{PMNS} [59–61]

Representation of the Mixing Matrices

The CKM matrix is often given in terms of the so-called Wolfenstein parameters [62] which are historically motivated but are of no further importance for this thesis. The global fit to the CKM matrix in the SM framework is performed with respect to these parameters [63, 64]. Still, there are multiple ways to represent both the quark and neutrino mixing matrix in literature. Throughout this thesis, we parametrise all mixing matrices by three mixing angles and one Dirac phase, defined by

$$V(\theta_{12}, \theta_{23}, \theta_{13}, \delta_{13}) = \begin{pmatrix} c_{12}c_{13} & s_{12}c_{13} & s_{13}e^{-i\delta_{13}} \\ -s_{12}c_{23} - c_{12}s_{23}s_{13}e^{i\delta_{13}} & c_{12}c_{23} - s_{12}s_{23}s_{13}e^{i\delta_{13}} & s_{23}c_{13} \\ s_{12}s_{23} - c_{12}c_{23}s_{13}e^{i\delta_{13}} & -c_{12}s_{23} - s_{12}c_{23}s_{13}e^{i\delta_{13}} & c_{23}c_{13} \end{pmatrix}, \quad (2.8)$$

²Throughout the thesis, hatted quantities denote diagonal matrices.

³We note that the PMNS matrix is defined analogue to the CKM matrix. The difference in notation (V_{CKM} and U_{PMNS}) is for historical reasons only.

where $c_{\alpha\beta} = \cos(\theta_{\alpha\beta})$ and $s_{\alpha\beta} = \sin(\theta_{\alpha\beta})$. In general, if right handed neutrinos are Majorana fermions, the PMNS matrix can also contain Majorana phases (see e.g. [51]), which will not be discussed here.

2.2. Structure of Masses and Mixing in the SM

We know from experiment that the quark and lepton mixing and mass patterns are very different [15]. In the quark sector, there is a strong hierarchy among the different generations (e.g. $m_t/m_u \sim 7 \times 10^5$) but only a weak hierarchy regarding the up- and down-type quarks of the same generation (e.g. $m_t/m_b \sim 40$). This is different in the lepton sector. Here, we again find a strong hierarchy in the charged lepton sector (e.g. $m_\tau/m_e \sim 3.7 \times 10^4$), whereas the mass pattern of the neutrinos is still not completely determined. Nonetheless, there exists an upper limit on neutrino masses from cosmology which is in the eV range [65] and thus there is a very large hierarchy between neutrino masses and all other fermion masses (e.g. $m_\nu/m_t < 10^{-11}$), in particular charged leptons.

Neutrino Sector

First hints on neutrino masses came already from the Homestake experiment, which measured only one third of the expected neutrinos coming from the sun [3, 66]. An explanation for this deficit was given by the theory of neutrino oscillations developed by Pontecorvo in 1957 and later on independently by Maki, Nakagawa and Sakata in 1962 [59–61, 67, 68]. Additional experiments such as (Super-)Kamiokande (SK) [4, 69], SAGE [70, 71], or GALLEX [72] were set up and measured a similar deficit. The first experiment able to observe the appearance of μ neutrinos was SNO in 2002 [5, 73], which confirmed the theory of neutrino oscillations. These experiments have measured the so-called solar angle θ_{12} . In addition, experiments to determine the atmospheric angle θ_{23} and the reactor angle θ_{13} were built. The atmospheric angle was already observed by SK in 1998 [74]. The reactor angle was for a long time believed to be zero in line with the favoured description of the PMNS matrix by a tri-bimaximal mixing pattern. However, it has been measured quite recently (2012) to be non-zero by the experiments Daya Bay, Reno and Double Chooz [75–77].

Besides the mixing angles also the mass-squared differences Δm_{12}^2 and $|\Delta m_{23}|^2$ have been measured. However, the ordering of m_2 and m_3 as well as the absolute mass scale are yet undetermined. This leaves two different orderings; normal ($m_2 < m_3$) and inverted ($m_3 > m_2$). On the other hand, the absolute mass scale of neutrinos is yet unknown. Thus, also the quasi degenerate case is possible, if $m_1, m_2, m_3 \gg \Delta m_{12}^2, |\Delta m_{23}|^2$. The current upper bound on the sum of the three neutrino masses, which is roughly of the order of eV, comes from astrophysical considerations. On the other hand, there are experiments trying to determine neutrino masses from neutrinoless double-beta decay [78–81] or by measuring the endpoint of the beta decay spectrum [82]. Both give bounds on a specific combination of mass eigenstates and PMNS elements.

The current best fit values for the quark and lepton masses as well as for the neutrino mass differences are shown in Table 2.1.

2. Flavour Symmetries; SM and Beyond

Fermion Masses					
up-type			down-type		
m_u [MeV]	m_c [GeV]	m_t [GeV]	m_d [MeV]	m_s [MeV]	m_b [GeV]
$2.3^{+0.7}_{-0.5}$	1.275 ± 0.025	160^{+5}_{-4}	$4.8^{+0.5}_{-0.3}$	95 ± 5	4.18 ± 0.03
leptons			neutrinos		
e [MeV]	μ [MeV]	τ [GeV]	$\sum_{i=1}^3 \nu_i$ [eV]	Δm_{21}^2 [10^{-5} eV]	$ \Delta m_{23}^2 $ [10^{-3} eV]
0.511	150.7	1.886	< 2	$7.54^{+0.26}_{-0.22}$	$2.43^{+0.06}_{-0.10}$

Table 2.1.: Masses of the SM fermions as given in [15]. For the leptons we do not state an uncertainty as they are known very precisely.

Mixing Matrices

By looking at the measured values for the mixing matrices one finds a nearly diagonal matrix in the quark sector with small off-diagonal elements [63, 64] whereas the neutrino mixing matrix is in first approximation democratic [83–85], i.e. all elements are of equal size. Because of the large mass differences in the charged and neutral sector, flavour transitions between the charged leptons have not been observed so far. The different structures of the quark and lepton mixing are so far not understood. Two approaches on how to generate both sectors in a coherent framework will be discussed in Chapter 4 and Chapter 5.

Structure of U_{PMNS}

The structure of the PMNS matrix is, although measured experimentally, so far not understood theoretically⁴. There are different approaches on explaining the PMNS matrix, starting from special matrices related to underlying symmetries. The most famous of these is the tri-bimaximal mixing matrix⁵

$$U_{\text{TBM}} = \begin{pmatrix} \sqrt{\frac{2}{3}} & \sqrt{\frac{1}{3}} & 0 \\ -\sqrt{\frac{1}{6}} & \sqrt{\frac{1}{3}} & \sqrt{\frac{1}{2}} \\ \sqrt{\frac{1}{6}} & -\sqrt{\frac{1}{3}} & \sqrt{\frac{1}{2}} \end{pmatrix}, \quad (2.9)$$

predicting $\sin^2(\theta_{12}) = 1/3$, $\sin^2(\theta_{23}) = 1/2$ and $\theta_{13} = 0$. Other structures which are often used are bi-maximal, bi-trimaximal or golden-ratio. An overview on the theory of neutrino masses and mixing as well as the (current) experimental status is given in e.g. [51, 86, 87].

The current best fit values for the quark and lepton mixing are shown in Table 2.2.

⁴The same is also true for the CKM matrix.

⁵Although exact tri-bimaximal mixing is nowadays experimentally excluded it provides a good first ansatz for lepton mixing.

Mixing Parameters				
quarks	$\sin \theta_{12}$	$\sin \theta_{23}$	$\sin \theta_{13}$	δ_{13} [°]
	0.2255 ± 0.0005	0.0417 ± 0.0006	0.00363 ± 0.00012	69.4 ± 3.4
leptons	$\sin^2 \theta_{12}$	$\sin^2 \theta_{23}$	$\sin^2 \theta_{13}$	δ_{13} [°]
	0.304 ± 0.012	(NO) 0.451 ± 0.001 (IO) $0.577^{+0.027}_{-0.035}$	$0.0219^{+0.0010}_{-0.0011}$	251^{+67}_{-59}

Table 2.2.: Quark and lepton mixing parameters. The CKM parameters are taken from UTfit [63], the PMNS parameters are shown for normal (NO) and inverse ordering (IO) as given by ν fit [83].

2.3. Theory of Neutrino Masses

The SM was developed for massless neutrinos and thus without an implementation of a mechanism for generating neutrino masses. In the SM neutrinos are purely left-handed as they have been introduced to cure the problem of a continuous spectrum in the beta decay, which is a weak decay. As right-handed neutrinos are strictly speaking not part of the SM, no renormalisable neutrino mass term is possible. However, they are often considered to be a trivial extension, as they are not observable by present experiments anyway. As discussed above, there is experimental evidence that at least two of those have a small but non-vanishing mass. Thus, a mechanism for generating neutrino masses has to be implemented in the SM and theories beyond.

One possible way of implementing the masses is simply to introduce right-handed neutrinos and write down a Yukawa coupling term. These Yukawa matrices must have extremely small eigenvalues, which is why this setup appears disfavoured. However, it may suffice to introduce right-handed neutrinos as they are singlets under the complete SM gauge group. As such, they may be their own anti-particles and allow for a Majorana mass term. Together with the Dirac mass, this Majorana mass introduces a see-saw mechanism which is described in the following. In addition to the standard see-saw mechanism (see-saw Type I), we consider the double see-saw and a see-saw with single right-handed neutrino dominance in order to generate a phenomenologically valid flavour structure for the SM neutrinos.

2.3.1. See-Saw Mechanism

The see-saw mechanism provides an explanation for light masses of neutral fields. It was first introduced in the late 70's [88–90] and is mainly discussed in the context of neutrinos. There are three commonly used realisations for SM neutrinos (Type I to III) leading to similar results. Here, we explain the Type I and only comment on Type II and III.

The basic principle of the see-saw mechanism is to introduce some heavy partners for the SM neutrino which through their coupling effectively generate a light mass for the latter. In

2. Flavour Symmetries; SM and Beyond

Type I, the heavy partner is the right-handed neutrino N_R ⁶, which features a Dirac mass term together with the SM neutrinos via the Higgs mechanism, similar to the other fermions. In addition, the right-handed neutrino is allowed to have a Majorana mass M . The Lagrangian of the see-saw mechanism is given by

$$\mathcal{L}_{\text{see-saw}} = Y_\nu \phi \bar{\nu}_L N_R + M N_R N_R + \text{h.c.} . \quad (2.10)$$

After inserting the Higgs vev which is of the order of the electroweak scale, we can write $m = Y_\nu v$. Since the Majorana mass M is not protected by any symmetry it may be much larger than the electroweak scale, $m \gg M$. In fact, the natural scale for M would be the scale where this term can be generated dynamically or the largest allowed scale in the theory which usually is of the order of M_{Planck} .

The mass matrix of the neutrino components following from (2.10) takes the form

$$M_\nu = \begin{pmatrix} 0 & m \\ m^T & M \end{pmatrix} . \quad (2.11)$$

In the case of large hierarchies $m \ll M$, the mass matrix can be diagonalised to leading order in m/M ,

$$\hat{M}_\nu \approx \begin{pmatrix} -m M^{-1} m^T & 0 \\ 0 & M \end{pmatrix} . \quad (2.12)$$

This mass matrix now features a light left-handed Majorana neutrino and its heavy right-handed partner. The diagonalisation of the mass matrix is equivalent to integrating out the heavy right-handed neutrinos.

Taking the Yukawa coupling to be of order one, the Majorana scale M has to be roughly $M \sim 10^{14}$ GeV to generate neutrinos in the eV range. Nevertheless, this scale is not fixed as neither the masses of the SM neutrinos are known nor do the Yukawa couplings have to be of order one⁷. The number of right-handed partners is in principle arbitrary but we have to include more than one as we have to generate at least two massive SM neutrinos. Thus, a mass matrix with rank 2 or larger is required. Most GUTs favour three generations as they are unified with the SM particle content, e.g. form $SU(2)'$ doublets with E_R .

The Type II and Type III see-saw are similar to the one described above. Yet, the heavy partner is either a scalar (Type II) or a fermionic (Type III) triplet under $SU(2)$. Diagrammatically, all three types of see-saw are shown in Figure 2.1. As mentioned before we restrict ourselves to the Type I see-saw in this thesis and will not give more details on the other Types.

2.3.2. Double See-Saw

In the previous section we considered a way of generating light neutrino masses by integrating out heavy right-handed partners. This mechanism together with the Majorana

⁶We denote the right-handed neutrino by N_R rather than ν_R to indicate that it is a heavy fermion.

⁷The top Yukawa is the only Yukawa coupling of order one in the SM.

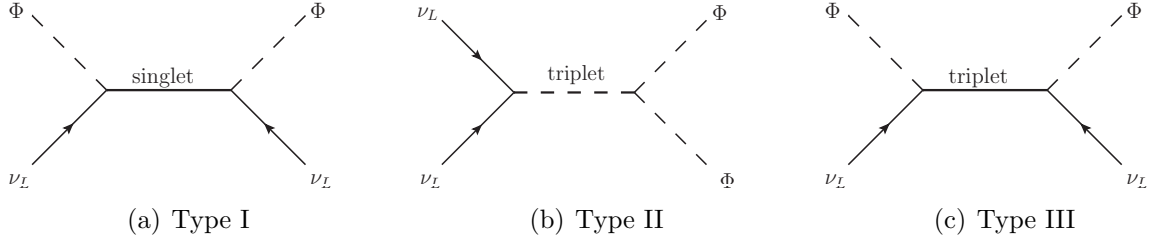


Figure 2.1.: Diagrammatic representation of the three (main) types of the see-saw mechanism.

mass matrix provides an additional flavour structure. Nevertheless, if the neutrino Dirac matrix features large hierarchies, the Majorana matrix has to compensate it as neutrinos maximally feature a small hierarchy. This is the case in many GUTs where the Dirac matrix of the neutrinos is proportional to the up-type quarks. From (2.12) we can read off that the Majorana matrix is multiplied by m^2 and thus must feature twice the hierarchy present in the Dirac matrix. In the GUT case, its smallest eigenvalue is of order of 10^{-12} and thus of similar size as a potential pure Dirac neutrino Yukawa coupling. Hence, such a setup is disfavoured as well.

A solution of this problem is to introduce a double see-saw as discussed in e.g. [91, 92]. In this setup, the Majorana mass matrix M itself is generated by a see-saw mechanism. It can be realised if the right-handed neutrinos have no Majorana mass term but couple to a set of singlets \mathcal{S} with a massive coupling M_{NS} . These singlets then possess a large Majorana mass M_S . The corresponding Lagrangian is

$$\mathcal{L}_{\text{double}} = Y_\nu \phi \bar{\nu}_L N_R + M_{NS} N_R \mathcal{S} + M_S \mathcal{S} \mathcal{S} + \text{h.c.}, \quad (2.13)$$

and the resulting mass matrix is given by

$$M_\nu = \begin{pmatrix} 0 & m & 0 \\ m^T & 0 & M_{NS} \\ 0 & M_{NS}^T & M_S \end{pmatrix}. \quad (2.14)$$

If we assume $M_S \gg M_{NS}$, we can integrate out the heavy singlets resulting in an effective Majorana mass for the right-handed neutrinos of the form

$$M \sim M_{NS} M_S^{-1} M_{NS}^T, \quad (2.15)$$

where M_{NS} and M_S are allowed to be matrices in flavour space and M should still be larger than the Dirac mass m . At this stage, we are left with a see-saw mechanism similar to the one discussed above. After performing the second see-saw, i.e. integrating out the right-handed neutrinos N_R , the effective SM neutrino mass matrix can be written as

$$M_\nu = m M_{NS}^T{}^{-1} M_S M_{NS}^{-1} m^T. \quad (2.16)$$

In such a setup, M_{NS} may at least partially cancel the hierarchy present in m . As a special case one could assume a symmetry that enforces $m \equiv M_{NS}$. The complete neutrino mass

2. Flavour Symmetries; SM and Beyond

and mixing is then encoded in M_S , as m and M_{NS} exactly cancel each other. We note that the mixing may still be affected by the lepton Yukawa matrix.

In many GUTs a different motivation for a double see-saw is present as N_R is no longer a singlet under all symmetries and one needs to generate the Majorana mass term M dynamically. This is often done similar to the double see-saw mechanism. One example will be presented in Chapter 5.

Looking at the scales needed to realise a double see-saw we find one particularly interesting case, using only scales present in most GUTs; the additional singlets \mathcal{S} get masses of the order of the Planck scale while the Dirac mass M_{NS} is of order of the GUT scale ($M_{\text{GUT}} \sim 10^{16}$ GeV). Such a setup results in an effective right-handed neutrino scale in the favoured region of $M_{N_R} \sim 10^{14}$ GeV.

2.3.3. Sequential Right-Handed Neutrino Dominance

Another ansatz to reproduce phenomenological valid neutrino structures is the mechanism of Sequential Right-Handed Neutrino Dominance (SRHND) [93–97]. In this setup, the flavour structure is generated sequentially by integrating out hierarchical right-handed neutrinos. The easiest formulation of the mechanism is in a basis where the right-handed neutrinos are diagonal. In this basis, we can write the matrices defined in (2.11) as

$$M \equiv \begin{pmatrix} Y & 0 & 0 \\ 0 & X & 0 \\ 0 & 0 & X' \end{pmatrix} \quad \text{and} \quad m \equiv \begin{pmatrix} 0 & a & a' \\ e & b & b' \\ f & c & c' \end{pmatrix}, \quad (2.17)$$

where we only consider the special case of a vanishing $(1, 1)$ entry in m . After integrating out the right-handed neutrinos we get a sequential dominance in the resulting light neutrino mass matrix if the conditions

$$\frac{e^2, f^2, |ef|}{Y} \gg \frac{|xy|}{X} \gg \frac{|x'y'|}{X'} \quad (2.18)$$

are fulfilled, where $x, y \in a, b, c$ and $x', y' \in a', b', c'$. Each light neutrino mass is determined by a single right-handed neutrino and the dominant contribution to the structure of the neutrino matrix comes from the lightest neutrino Y . The resulting light mass matrix is given by

$$m_\nu \approx \begin{pmatrix} \frac{a^2}{X} & \frac{ab}{X} & \frac{ac}{X} \\ * & \frac{b^2}{X} + \frac{e^2}{Y} & \frac{bc}{X} + \frac{ef}{Y} \\ * & * & \frac{c^2}{X} + \frac{f^2}{Y} \end{pmatrix}. \quad (2.19)$$

The resulting mass eigenvalues are

$$m_1 \sim \mathcal{O}\left(\frac{x'y'}{X'}\right), \quad m_2 \approx \frac{a^2}{X s_{12}^2}, \quad m_3 \approx \frac{e^2 + f^2}{Y}, \quad (2.20)$$

where $s_{12} = \sin(\theta_{12})$ is defined by the mixing angles which can be calculated to leading order in m_2/m_3 to

$$\tan(\theta_{23}) \approx \frac{e}{f}, \quad \tan(\theta_{12}) \approx \frac{a}{b c_{23} - c s_{23}}, \quad \tan(\theta_{13}) \approx \frac{a(e b + f c) Y}{(e^2 + f^2)^{3/2} X}. \quad (2.21)$$

We note that we have assumed the Yukawa matrix to be real. The complete calculation for complex Yukawa matrices as well as different realisations of SRHND are discussed in [93–97].

2.4. Flavour in GUTs

In the earliest GUTs flavour was discussed similar to the SM case by just a triplication of the particle content. Not much has changed since then, yet people started to consider the flavour symmetry as additional orthogonal symmetry. It can be realised by many different discrete as well as continuous groups like A_4 , S_3 , $\Delta(96)$, $PSL_2(7)$, $SO(3)$ or $SU(3)$ just to name some of them. A recent review of different choices can be found in e.g. [98]. There have also been efforts to further unify the flavour and the gauge symmetry, for example in E_8 or $SO(32)$ (see e.g. [42, 50]) or by certain string theories and the compactification of multiple dimensions. A review on string theory is given in e.g. [99–101].

Anyhow, GUTs have a large impact on flavour physics independent on whether flavour symmetry is unified with the gauge couplings or not. They relate different sectors of the SM like quarks and leptons and may thus reduce the maximal flavour symmetry of the kinetic Lagrangian. Moreover, GUTs relate the Yukawa structure of the SM among themselves and the three (or counting neutrinos four) independent Yukawa matrices may be reduced. This is however only true for a minimal setup. In the SM the representation of the Higgs is unambiguously assigned by the fermion representations. As the representations for the fermions are larger in GUTs, additional Higgs structures are allowed. These are usually not aligned and thus disentangle the Yukawa matrices again. Hence, the explicit flavour structure of a GUT is strictly model-dependent.

Another way to discuss the flavour structure in GUTs is to consider a bottom up approach. As a consequence of quantum field theory, the Yukawa couplings are energy-dependent. Therefore, the corresponding renormalisation group equation has to be solved in order to deduce the Yukawa matrices at the GUT scale (see e.g. [102, 103]). One can then attempt to approximate the resulting mass ratio at the GUT scale by group theoretical factors arising for different Higgs representations. This is based on the assumption that the next relevant scale for flavour physics is the GUT scale and thus the SM running is valid at all scales. Although this assumption may be questionable it provides at least some predictive power and generates mass relations at the GUT scale. The most prominent example for such a mass relation is the approximation

$$3m_e \approx m_d, \quad m_\mu \approx 3m_s, \quad m_\tau \approx m_b, \quad (2.22)$$

identified and implemented in $SU(5)$ by Georgi and Jarlskog [104]. As it is a bottom up approach, it is nevertheless applicable to any GUT. A similar relation for the up-sector is not reasonable as neutrino masses are of different scale and not fully determined yet.

2. Flavour Symmetries; SM and Beyond

In the following, we give a brief overview of the flavour structure of PS-GUTs in general. More details can be found in Chapter 4 and Chapter 5 where we explicitly construct a possible flavour sector within a PS framework.

2.4.1. Flavour in Pati-Salam

In PS symmetric models, the maximal flavour symmetry of the kinetic Lagrangian is reduced since the fermions are unified into the representations $\bar{\Psi}_L$ and Ψ_R . Hence, the maximal flavour symmetry of the gauge kinetic terms is $U(3) \times U(3)$. Since $U(1)_{B-L}$ is included in $SU(4)$ it does not contribute to the starting $U(3) \times U(3)$ symmetry and thus must not to be removed when defining the “pure” flavour symmetry. However, as long as we do not include a Majorana mass term for the right handed neutrinos we still encounter one $U(1)$ factor that is unbroken by the Yukawa matrices. This can be regarded as fermion number and is a generalisation of baryon and lepton number. Therefore, the maximal “pure” flavour symmetry of PS is

$$G_F^{\text{PS}} = SU(3) \times SU(3) \times U(1). \quad (2.23)$$

Another unification happens in the Yukawa sector. As we are left with only two multiplets we have in general only a single Yukawa matrix. Nevertheless, if the $SU(2)'$ is broken at some large scale, the running of the Yukawa couplings for the up and down sector may separate the Yukawa couplings at the electroweak scale. The same may be true for the quark and lepton sector below the scale where $SU(4)$ is broken. In a non-minimal setup, additional Higgs representations may introduce variations in the different Yukawa sectors. Such a setup is explicitly given in Chapter 5. Nevertheless, we are confronted with a strongly hierarchical Dirac mass structure for the neutrinos as it is related to the quark sector. How we can account for such a structure by introducing double see-saw or SRHND was discussed in the previous section.

Moreover, the misalignment U_{CKM} in the right-handed fermions is physical in a PS symmetric setup. Such a mixing is similar to the one we have encountered in the SM (cf. Section 2.1.2) but only relevant here as the right-handed quarks couple to the charged $SU(2)'$ gauge bosons. The same arguments apply in the lepton sector.

One Feasible Flavour Structure

Finally we give an example of an explicit implementation of a double see-saw in PS. It was shown, that a tri-bimaximal mixing matrix in the neutrino sector fits current neutrino data quite well if corrections from the charged lepton sector proportional to V_{CKM} are present [105, 106]. This may be the case in PS if the basis is chosen such that the complete quark mixing is encoded in the down type Yukawa matrix. Hence also the charged lepton sector features a CKM-like rotation of the mass eigenstates. Here, we follow the ansatz of a tri-bimaximal Majorana matrix. In addition, PS relates the neutrinos and the up-type quarks. Thus, the Dirac matrices for the complete lepton sector is fixed in PS symmetric theories up to overall coefficients. Now we have the problem, that the neutrino Yukawa matrix is hierarchic and thus does not commute with U_{TBM} . This can be solved by a double see-saw.

Hence, if we assume the Yukawa structure as

$$Y_l = Y_d = V_{\text{CKM}} \hat{Y}_l \quad , \quad Y_\nu = Y_u \equiv M_{NS} \quad \text{and} \quad S_\nu = U_{TBM} \hat{M} \quad , \quad (2.24)$$

we end up with a good first approximation of the flavour sector.

Having outlined the basic principles of the SM and Grand Unified Theories as well as the concept of flavour, we now present explicit models addressing the aspect of implementing flavour in a PS-symmetric GUT framework.

Part II.

Explicit Models of Flavour in Pati-Salam

Chapter 3

Pati-Salam Symmetry Breaking and Gauge Coupling Unification

Starting from a Pati-Salam symmetric setup, we study in this chapter the possibility for complete Gauge Coupling Unification (GCU) where all the SM gauge couplings coincide at some large energy scale. Following the arguments of unification we put a completely unified theory near or even at the Planck scale. In addition, we allow for multiple intermediate scales which may be useful when considering flavour structures in Grand Unified Theories. This we study for supersymmetric as well as non-supersymmetric setups. We will be mainly concerned with the SUSY setup as it simplifies the model and is strongly motivated in the context of GUTs (see Section 3.6). We assume SUSY to be realised above a few TeV. To start with, we consider the various breaking paths from PS down to the SM. The breaking should be achieved by a Higgs mechanism already seeded at the scale of exact PS symmetry, i.e. generated by a PS symmetric superpotential. Depending on the hierarchies between the symmetry breaking vevs, the breaking features different intermediate scales. According to these hierarchies we construct classes of models which realise these different breaking paths.

For this purpose we study an explicit realisation for a conceivable supersymmetric scalar sector including all symmetry breaking Higgs fields. From this superpotential we construct the mass matrix of the additional superfields and discuss the resulting mass structure. Making use of the latter we assign the superfields to the different intermediate breaking scales. Adopting these assignments we briefly discuss the various intermediate unification conditions before actually performing the GCU analysis. This we do by a semi-analytic scan over the discrete set of configurations possible in the model classes constructed before. Afterwards, we also consider the non-supersymmetric GCU, keeping the assumptions derived in the supersymmetric case. We conclude the chapter with a summary of our findings.

The main results of this chapter have already been published in Reference [A].

3.1. Intermediate Symmetries and Scales

The PS symmetry is an interesting intermediate symmetry *en route* to complete GCU. It may be valid up to the Planck scale where gravitation is strong and thus a perturbative quantum field theory is unlikely to be an appropriate description. Thus, we do not specify the final GUT symmetry or the mechanism of breaking it any further. Rather we start with a PS symmetry which we assume to be valid up to the scale of GCU.

Multiple Subgroups

In addition, PS need not be broken to the SM in a single step but can exhibit a variety of breaking paths with multiple intermediate scales. In the setup discussed here, the symmetry breaking is generated by a Higgs mechanism similar to the SM. More explicitly, we introduce scalar fields \mathcal{S} transforming in a PS representation that features a singlet component in its branching to the unbroken subgroup. We assign a vev to these fields denoted by $\langle \mathcal{S} \rangle$ which is assumed to be aligned along the distinct direction invariant under the unbroken symmetry. Within a simple such setup, we consider all of these paths of breaking PS to its continuous subgroups.

As discussed in Section 1.4.3, the $SU(4)$ part of PS unifies quarks and leptons. Thus, it obviously contains the colour $SU(3)_c$ of the SM. Moreover, it contains $U(1)_{B-L}$ with charges corresponding to the difference between baryon number B and lepton number L . The $SU(2)'$ of PS is an analogue of the weak $SU(2)_w$ of the SM which groups together U_R and D_R as well as N_R and E_R (cf. Section 1.4.3). It can be broken to $U(1)'$ which may be seen as right-handed isospin. A subgroup of the product $U(1)_{B-L} \times U(1)'$ is the SM hypercharge $U(1)_Y$.

In order to generate a breaking to these subgroups we need three different vevs which we will specify later on. These are sufficient to realise all possible breaking paths of the PS symmetry to subgroups being or containing factors of the SM gauge group. The resulting partial breaking structures are,

$$SU(4) \xrightarrow{\langle \Sigma \rangle} SU(3)_c \times U(1)_{B-L}, \quad (3.1a)$$

$$SU(2)' \xrightarrow{\langle T' \rangle} U(1)', \quad (3.1b)$$

$$SU(4) \times SU(2)' \xrightarrow{\langle \Phi' \rangle} SU(3)_c \times U(1)_Y, \quad (3.1c)$$

$$SU(4) \times U(1)' \xrightarrow{\langle \Phi' \rangle} SU(3)_c \times U(1)_Y, \quad (3.1d)$$

$$U(1)_{B-L} \times SU(2)' \xrightarrow{\langle \Phi' \rangle} U(1)_Y, \quad (3.1e)$$

$$U(1)_{B-L} \times U(1)' \xrightarrow{\langle \Phi' \rangle} U(1)_Y, \quad (3.1f)$$

$$SU(2) \times U(1)_Y \xrightarrow{\langle h \rangle} U(1)_{em}, \quad (3.1g)$$

where we have also listed the electroweak symmetry breaking for completeness.

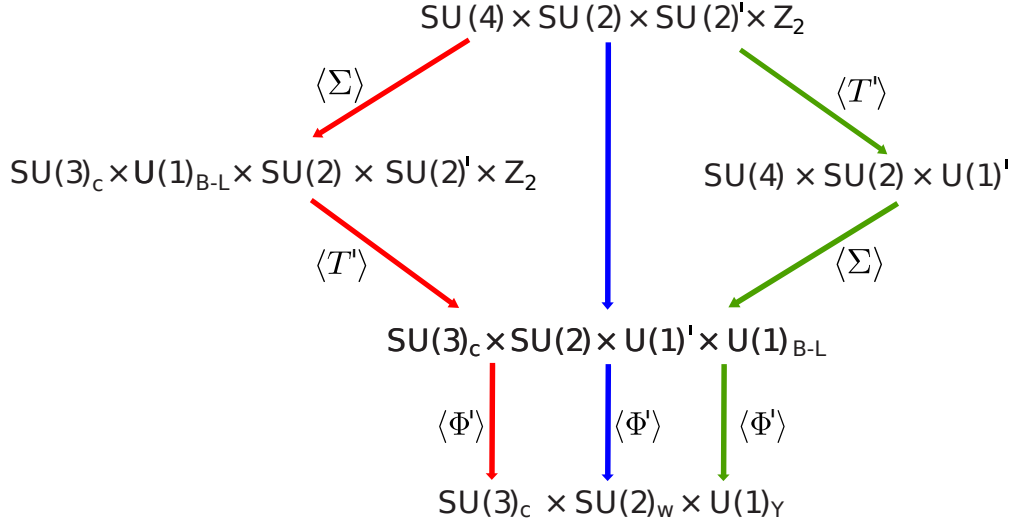


Figure 3.1.: Graphical illustration of the different breaking paths depending on the different classes. Class B is shown in red, C in green and D in blue. For clarity, the other classes are not explicitly shown but can easily be constructed.

In this setup, $\langle \Sigma \rangle$ and $\langle T' \rangle$ break only one part ($SU(4)$ or $SU(2)'$ respectively), while $\langle \Phi' \rangle$ is able to break PS directly to the SM. Thus, we can either use solely $\langle \Phi' \rangle$ or a combination of two or more of these vevs. As we are interested in multi-step breaking and for reasons that are discussed when considering the explicit superpotential, we discard the breaking with only $\langle \Phi' \rangle$.

Various Breaking Paths

As we are interested in a multi-step breaking of the PS symmetry, we include more than one of these vevs in our model. If these are of a similar scale, we break the symmetry by different vevs but effectively still generate only a single-scale breaking. Allowing for hierarchies between these vevs results in a multi-scale breaking of the PS symmetry in which the scales are defined by the vevs. Depending on the ordering of these vevs we generate all possible breaking paths which we depict in Figure 3.1.

Here, the scale $\langle \Phi' \rangle$ must always be smaller than or equal to the other (two) scales since it breaks PS completely. Thus, we can construct six classes of PS models differentiated by their hierarchy patterns. We denote them as follows:

- class A:** $\langle \Phi' \rangle \sim \langle T' \rangle \sim \langle \Sigma \rangle$ (one scale),
- class B:** $\langle \Phi' \rangle \ll \langle T' \rangle \ll \langle \Sigma \rangle$ (three scales),
- class C:** $\langle \Phi' \rangle \ll \langle \Sigma \rangle \ll \langle T' \rangle$ (three scales),
- class D:** $\langle \Phi' \rangle \ll \langle T' \rangle \sim \langle \Sigma \rangle$ (two scales),
- class E:** $\langle \Phi' \rangle \ll \langle \Sigma \rangle$ and $\langle T' \rangle = 0$ (two scales),
- class F:** $\langle \Phi' \rangle \ll \langle T' \rangle$ and $\langle \Sigma \rangle = 0$ (two scales).

3. PS-Breaking and Gauge Coupling Unification

Again, class A is of minor interest as it features only a single scale. However, we include it as a limiting case. Class D also represents a limiting case which we will not discuss in detail. The symmetry breaking chains associated to these classes are shown in Figure 3.1 (see also [107]). The intermediate scales corresponding to these breaking steps, will be constrained by the condition of GCU later in this chapter.

The vevs $\langle\Phi'\rangle$ and $\langle T'\rangle$ are of particular interest for flavor physics as they break the $SU(2)'$ symmetry. As long as the right-handed SM fermions are paired up in $SU(2)'$ doublets, there are no terms that distinguish right-handed up- from down-type quarks, which however is required for the presence of mixing (cf. Section 2.1.2). Therefore, the maximal energy scale below which flavour mixing appears in the renormalisable part of the effective theory is given by either $\langle\Phi'\rangle$ or $\langle T'\rangle$. On the other hand, both $\langle\Sigma\rangle$ and $\langle\Phi'\rangle$ separate quarks from leptons. We only expect a direct relation between quark and lepton flavour mixing in classes where $SU(2)'$ is broken above the breaking of $SU(4)$, i.e. in classes C and F where $\langle\Sigma\rangle < \langle T'\rangle$.

In this chapter we mainly consider a supersymmetric setup. This introduces an additional scale in our model, the SUSY breaking scale M_{SUSY} . We assume SUSY to be broken softly by terms in the TeV range. As we are only interested in the high energy behaviour of the model, we do not consider this breaking any further.

3.2. Particle Content and VEV Structure

Getting our motivation from complete GCU we confine ourselves to a set of Higgs fields compatible with a unifying theory. The smallest possibility containing PS is $SO(10)$, which is why we choose only Higgs fields fitting in the lowest dimensional representations of $SO(10)$. We find that these can be even further combined to the fundamental and adjoint representation of E_6 if we allow for additional singlets. The maximal particle content considered in this chapter is shown in Table 3.1.

Multiplicity of the Particles

In an E_6 GUT, the SM fermions are contained in the fundamental $\mathbf{27}$ representation. As discussed in Section 1.4, this representation additionally contains two SM doublets that qualify for the MSSM Higgs fields. However, in a non-supersymmetric setup they cannot be combined as they have a different spin, 0 for the scalars and 1/2 for the fermions. In a supersymmetric theory both scalars and fermions are contained in chiral superfields which allows for matter-Higgs unification. Such a situation would imply that some scalars occur in three copies just like the SM fermions. In particular the electroweak breaking Higgs field is one of these scalars. To be inclusive, we allow all fields considered in this chapter to come in three generations. We do this independently of their grouping in E_6 representations as some of them may get GUT-scale masses by the breaking of the unified group which we do not consider. As we are interested in a renormalisable effective theory realised below the GUT scale, such fields are effectively not present. Therefore, we allow all fields to appear once, as three copies or not at all. In general, other multiplicities of fields are feasible. However, these are less motivated and including only the mentioned multiplicities already results in a rich variety of intermediate scales. Moreover, achieving GCU becomes more constrained if we include more fields in the theory as the gauge couplings approach the non-perturbative regime for lower energies (cf. Section 3.5 and discussions in Section 3.6 and Section 3.7).

Field	$(SU(4), SU(2), SU(2)')$	$SO(10)$	E_6
Σ	$(\mathbf{15}, \mathbf{1}, \mathbf{1})$	} 45	} 78
$T \oplus T'$	$(\mathbf{1}, \mathbf{3}, \mathbf{1}) \oplus (\mathbf{1}, \mathbf{1}, \mathbf{3})$		
E	$(\mathbf{6}, \mathbf{2}, \mathbf{2})$		
$\Phi \oplus \bar{\Phi}'$	$(\mathbf{4}, \mathbf{2}, \mathbf{1}) \oplus (\bar{\mathbf{4}}, \mathbf{1}, \mathbf{2})$	16	
$\bar{\Phi} \oplus \Phi'$	$(\bar{\mathbf{4}}, \mathbf{2}, \mathbf{1}) \oplus (\mathbf{4}, \mathbf{1}, \mathbf{2})$	$\bar{16}$	
S_{78}	$(\mathbf{1}, \mathbf{1}, \mathbf{1})$	1	
$\Psi_L \oplus \Psi_R$	$(\mathbf{4}, \mathbf{2}, \mathbf{1}) \oplus (\bar{\mathbf{4}}, \mathbf{1}, \mathbf{2})$	16	
h	$(\mathbf{1}, \mathbf{2}, \mathbf{2})$	} 10	} 27
F	$(\mathbf{6}, \mathbf{1}, \mathbf{1})$		
S_{27}	$(\mathbf{1}, \mathbf{1}, \mathbf{1})$		

Table 3.1.: Chiral superfield multiplets of the PS models considered in this model. The fields are classified by their gauge-group quantum numbers; the discrete Z_2 symmetry renders the multiplets left-right symmetric and thus irreducible. Conjugated quantities are additional degrees of freedom. All fields listed above may come in three generations, except for $\Psi_{L/R}$ which is always present in three generations.

Due to the ambiguity in the multiplicity of the fields, we may further categorise models constructed along these lines. Each model type may fit into any of the above classes. It contains the three generations of MSSM matter¹ superfields $\Psi_{L/R}$ together with the following extra superfields;

Type m (Minimal Model): Within a given class, the minimal model is the one with minimal field content that realises the corresponding symmetry-breaking chain. In classes A to D, this model contains a single copy of each of the multiplets Φ , Σ and T . In classes E (F) the multiplet T (Σ) is omitted. We do not include the multiplet h in the spectrum as the pair of MSSM Higgs doublets may be contained in Φ (see Section 3.4).

Type s (SO(10)-like Model): In this model type, the PS multiplets can be unified in complete $SO(10)$ representations. All multiplets listed in Table 3.1 are present as a single copy except for the matter multiplets $\Psi_{L/R}$.

Type e (E₆-like Model): In this type of model all fields of Table 3.1 are present. The multiplets h , F and S_{27} appear in three copies since they combine with the matter multiplets. For the other multiplets we set the multiplicity to one.

Type g (Generic Model): Here we classify all models that do not qualify as either of the above three types. We will denote these models by their class and a unique number. The numbering scheme is outlined in Appendix A.1.

¹Containing all of the SM fermions, we consider only Ψ_L and Ψ_R as matter superfields.

3. PS-Breaking and Gauge Coupling Unification

VEV Structure

With this Higgs content we can accomplish all of the breaking paths given in (3.1). We first take a look at the scalar fields that ought to get a vev. As the adjoint representation of $SU(N)$ is able to break $SU(N) \rightarrow SU(N-1) \times U(1)$, we choose Σ and T to lie in the adjoint of $SU(4)$ and $SU(2)'$, respectively, while transforming trivially under all other gauge group factors. They get a vev in the τ^3 and T^{15} direction, respectively, where we use the common basis for $SU(2)$ and $SU(4)$ constructed by generalising the Gell-Mann matrices (cf. [108]). On the other hand, the fundamental representation of both $SU(4)$ and $SU(2)'$ will lead to a similar breaking but without maintaining the $U(1)$ factor. Yet, a $U(1)$ corresponding to the hypercharge can be conserved if we consider a bifundamental representation (fundamental in both, $SU(4)$ and $SU(2)'$). Therefore, Φ' and $\bar{\Phi}'$ transform (anti-) fundamental under $SU(4)$ and $SU(2)'$ simultaneously. They receive vevs in the right-handed neutrino directions and are thus able to break the complete PS symmetry down to the SM. Nevertheless, it is not sufficient to consider vevs for only Φ' and $\bar{\Phi}'$ if we want to break the symmetry at the renormalisable level (see (3.6) and discussions below). The vevs are assigned in the following way, where we only display the relevant subspaces:

$$\langle \Phi' \rangle = \begin{pmatrix} 0 & 0 & 0 & v_\Phi \\ 0 & 0 & 0 & 0 \end{pmatrix}^T, \quad \langle \bar{\Phi}' \rangle = \begin{pmatrix} 0 & 0 & 0 & v_{\bar{\Phi}} \\ 0 & 0 & 0 & 0 \end{pmatrix}, \quad (3.2a)$$

$$\langle T' \rangle = \begin{pmatrix} v_T & 0 \\ 0 & -v_T \end{pmatrix}, \quad (3.2b)$$

$$\langle \Sigma \rangle = 2\sqrt{6} \begin{pmatrix} v_\Sigma & 0 & 0 & 0 \\ 0 & v_\Sigma & 0 & 0 \\ 0 & 0 & v_\Sigma & 0 \\ 0 & 0 & 0 & -3v_\Sigma \end{pmatrix}. \quad (3.2c)$$

Discussion of the Particle Content

In addition to these Higgs fields which are needed to break PS, we now introduce further fields which complete our field content. The matter fields of the SM (or rather of the MSSM) are contained in the multiplets $\Psi_{L/R}$ (cf. Section 1.4.3). There are three copies of this representation to account for the three SM generations, each one including a right-handed neutrino superfield. The other supermultiplets contain the MSSM Higgs bidoublet, various new Higgs superfields and extra ‘‘exotic’’ matter. We now take a closer look at these superfields:

1. h directly qualifies as MSSM Higgs bidoublet as it decomposes into two doublets with hypercharge $\pm 1/2$.
2. Σ and $T^{(\prime)}$ are chiral multiplets in the adjoint representation. They have the same quantum numbers as the vector (gauge) superfields of $SU(4)$ and $SU(2)^{(\prime)}$, respectively. As such, they feature colour octet and weak triplet states.
3. $\Phi^{(\prime)}$ and $\bar{\Phi}^{(\prime)}$ are extra multiplets with matter quantum numbers and their charge-conjugated images, respectively. Therefore, they decompose in quark-like ($|B-L| = 1/3$) and lepton-like ($|B-L| = 1$) superfields.

4. All fields contained in E and F are coloured. They decompose into triplets and anti-triplets under $SU(3)_c$. Hence, they can be viewed as vector-like quarks and their scalar superpartners. Depending on their couplings, they may behave as leptoquarks or diquarks as they have B–L charge $\pm 2/3$. The multiplet F has both leptoquark and diquark couplings and thus can violate baryon number (cf. Section 3.4.3). For the multiplet E this is not possible. The superfield Σ also provides vector-like quark and antiquark superfields but with B–L charge $\pm 4/3$. They feature merely leptoquark couplings to the MSSM matter fields at the renormalisable level and hence conserve baryon number.
5. The singlet fields S_{78} and S_{27} (and any further singlet fields that originate from $SO(10)$ or E_6 singlets) can couple to any gauge-invariant quadratic polynomial. In addition, the superfields Σ , $\bar{\Phi}'$, Φ' and T' contain singlet components with respect to the SM gauge group, which we use to break the symmetry as mentioned above.

3.3. Superpotential and Higgs Mechanism

From the field content given in Table 3.1 we can now construct the most general renormalisable superpotential. In order to realise the different breaking paths we may set some of the vevs or couplings to zero. We split up the superpotential in several parts which allows us to include subsets of the fields present in the model;

$$W = W_{\Phi/\Sigma/T} + W_{h/F} + W_E + W_S + W_{\text{Yukawa}}. \quad (3.3)$$

The main part, including all fields needed to break PS, is given within $W_{\Phi/\Sigma/T}$. It generates the Higgs potential for all steps in the staged Higgs mechanism. It consists of fields that are allowed to get a vev only. We may set some terms to zero in order to obtain a minimal superpotential in the classes E and F where not all of these fields should get a vev.

The superpotential $W_{h/F}$ is present in the models that contain the fields h and/or F . Similarly, the field E comes with the terms W_E . The potential W_S contains all interactions of the singlets with the other Higgs fields. In each term, S indicates an arbitrary linear combination of all PS singlets present in the model.

If the superfields h and/or F are present, the superpotential W_{Yukawa} is possible. This part, which is the only renormalisable superpotential involving two matter superfields, implicitly contains generation indices. Analogously, generation indices are implied for all superfields that occur in more than one copy. We note that the Yukawa coupling Y is symmetric and universal across leptons, neutrinos, up- and down-type quarks. We will comment on the flavour sector in Section 3.4.4.

$$\begin{aligned} W_{\Phi/\Sigma/T} = & -m_\Phi \left(\bar{\Phi} \Phi + \bar{\Phi}' \Phi' \right) \\ & - \frac{1}{2} m_\Sigma \Sigma^2 + \frac{1}{3} l_\Sigma \Sigma^3 + l_{\Sigma\Phi} \left(\bar{\Phi} \Sigma \Phi + \bar{\Phi}' \Sigma \Phi' \right) \\ & - \frac{1}{2} m_T \left(T^2 + T'^2 \right) + l_{T\Phi} \left(\bar{\Phi} T \Phi + \bar{\Phi}' T' \Phi' \right) \end{aligned} \quad (3.4a)$$

3. PS-Breaking and Gauge Coupling Unification

$$\begin{aligned}
W_{h/F} = & -\frac{1}{2}m_h h^2 - \frac{1}{2}m_F F^2 + l_{h\Phi} h \left(\Phi \Phi' + \bar{\Phi}' \bar{\Phi} \right) \\
& + l_{F\Phi} F \left(\Phi \Phi + \Phi' \Phi' \right) + l_{F\bar{\Phi}} F \left(\bar{\Phi} \bar{\Phi} + \bar{\Phi}' \bar{\Phi}' \right) \\
& + l_{\Sigma F} F \Sigma F + l_{Th} h \left(T + T' \right) h
\end{aligned} \tag{3.4b}$$

$$\begin{aligned}
W_E = & -\frac{1}{2}m_E E^2 + l_{TE} E \left(T + T' \right) E \\
& + l_{\Sigma E} E \Sigma E + l_{FEh} F E h
\end{aligned} \tag{3.4c}$$

$$\begin{aligned}
W_S = & -\frac{1}{2}m_S S^2 + \frac{1}{3}l_S S^3 \\
& + s_\Phi S \left(\bar{\Phi} \Phi + \bar{\Phi}' \Phi' \right) + s_T S \left(T^2 + T'^2 \right) + s_\Sigma S \Sigma^2 \\
& + s_h S h^2 + s_F S F^2 + s_E S E^2
\end{aligned} \tag{3.4d}$$

$$W_{\text{Yukawa}} = Y \Psi_L h \Psi_R + Y_F F \left(\Psi_L \Psi_L + \Psi_R \Psi_R \right) \tag{3.4e}$$

From this superpotential we now calculate the F-terms of SUSY. In addition, we need to construct the D-terms for the spectrum given in Table 3.1. Having both, we can deduce the complete renormalisable scalar potential of our model (cf. Section 1.3). We have explicitly done this for the case of each field being present once and omitting the Yukawa-Lagrangian \mathcal{L}_{Yuk} . In general, we may also calculate non-renormalisable contributions to the superpotential and thus also to the scalar potential. However, as the renormalisable part suffices to generate the various breaking paths discussed above, we do not include them at this point. Nonetheless, they may become relevant in particular when considering the flavour sector of a given model (cf. Chapter 4).

We stated before, that the fields Σ , T' and $\Phi' \oplus \bar{\Phi}'$ qualify as Higgs fields breaking PS stepwise. Thus, we have to show, that the scalar potential has a local minimum for the vev structure given in (3.2). In addition, we have to guarantee that supersymmetry is maintained at each breaking step (see Section 1.3). Therefore, we have to verify that all F- and D-terms vanish [31, 32] after inserting the vevs.

The ground-state values of the D-terms are zero if and only if the vevs of mutually conjugate fields exist simultaneously and coincide in value. For T and Σ the D-terms automatically vanish since their generators are traceless. Therefore, we must have $\langle \Phi' \rangle = \langle \bar{\Phi}' \rangle$:

$$v_\Phi \equiv v_{\bar{\Phi}}. \tag{3.5}$$

Having verified the vanishing of the D-term, we now scrutinise the F-terms. Inserting the vevs, we obtain the necessary and sufficient conditions

$$0 = F_{\Phi_4} = v_\Phi \left(m_\Phi - 3 l_{\Sigma\Phi} v_\Sigma - l_{T\Phi} v_T \right), \tag{3.6a}$$

$$0 = 6F_{\Sigma_{15}} = \sqrt{\frac{3}{8}} \left(8 v_\Sigma \left(m_\Sigma - 4 l_\Sigma v_\Sigma \right) - l_{\Sigma\Phi} v_\Phi^2 \right), \tag{3.6b}$$

$$0 = F_{T'_3} = m_T v_T - l_{T\Phi} v_\Phi^2, \tag{3.6c}$$

$$0 = F_S = s_\Phi v_\Phi^2 + s_\Sigma v_\Sigma^2 + s_T v_T^2. \tag{3.6d}$$

We choose to solve these equations with respect to the mass parameters of Φ , T and Σ as well as for one of the singlet couplings. This is simpler than solving for the vevs as those appear quadratically. It is nevertheless equivalent since we do not know the mass parameters which would determine the vevs in a top-down approach. We obtain

$$m_\Phi = l_{\Sigma\Phi} v_\Sigma + l_{T\Phi} v_T, \quad (3.7a)$$

$$m_T = \frac{l_{T\Phi} v_\Phi^2}{v_T}, \quad (3.7b)$$

$$m_\Sigma = \frac{l_{\Sigma\Phi} v_\Phi^2}{8 v_\Sigma} + 4 l_\Sigma v_\Sigma, \quad (3.7c)$$

$$s_\Phi = -\frac{s_\Sigma v_\Sigma^2 + s_T v_T^2}{v_\Phi^2}. \quad (3.7d)$$

Inserting those relations in the superpotential and setting the fields to their ground-state values, we have verified that these vev configurations minimise the scalar potential while maintaining supersymmetry. Thus, depending on their mutual hierarchy they realise the symmetry-breaking chains of the model classes A to D.

For the model classes E and F, we assume a vanishing vev of T or Σ , respectively. Nevertheless, PS symmetry is broken completely down to the SM gauge symmetry. We find, that for a vanishing vev the corresponding multiplet must not couple to Φ' or $\overline{\Phi}'$. Otherwise SUSY is accidentally broken, as either $F_{T'}$ or F_Σ does not vanish. This can be realised by entirely omitting the multiplet or by setting $l_{\Sigma\Phi}$ ($l_{T\Phi}$) to zero, which may be realised by additional symmetries.

For the renormalisable superpotential discussed here it is not allowed to set v_Σ and v_T to zero simultaneously. Looking at (3.6a) we find that in this case the solution of the minimisation condition would be $v_\Phi \equiv 0$ and we would generate no breaking at all. In addition, it is not possible to set $v_\Phi = 0$ as in this case (3.6c) would demand $v_T \equiv 0$ and thus $SU(2)'$ would remain unbroken. This is not true for v_Σ as the superpotential contains a trilinear term for Σ . Such a term is not possible for T' as $SU(2)$ has no cubic invariant. Moreover, Φ' has to participate in the breaking as it is the only field breaking $U(1)' \times U(1)_{B-L}$ down to hypercharge in our setup.

3.4. Spectra and Phenomenology

The setup described above introduces a great variety of spectra for PS models. In this work, we are not aiming to set up benchmark models but rather to explore the main characteristics. Thus, a qualitative understanding of the spectra will be sufficient for our purposes. We focus on the different scales of the model and assign different types of fields and physics to those. In addition, the setup provides interesting phenomenological consequences which will be discussed afterwards.

3.4.1. Mass Matrix

Having verified that SUSY remains unbroken down to the TeV scale where soft-breaking terms appear, we have determined the mass matrix of the scalar fields in the PS broken

3. PS-Breaking and Gauge Coupling Unification

phase, i.e. inserting the minimisation conditions and vevs. We have then calculated the corresponding mass eigenvalues, neglecting all remaining bilinear mass terms m_i . The calculation is analogue to the mass calculation in Reference [D], where we only considered a subset of the full superpotential given in (3.4). The full mass matrices in the broken phase are given in Appendix A.2. As mentioned before, we do not intend to derive quantitative results here. From the mass matrices given in Appendix A.2 we may obtain such quantitative results by fixing the parameters contained in the superpotential (3.4). However, as we are mainly interested in the running of the gauge couplings, where these parameters enter only logarithmically, we do not gain anything of such a specification of the model. Instead of calculating the masses explicitly, we assign mass scales to the individual unbroken (i.e. SM) multiplets which we parametrise by the vevs and their hierarchy. In Table 3.2, we list the results for all fields and the interesting model classes B, C, E and F. The classes A and D are limiting cases and are therefore not listed separately. They can be deduced from the other cases by setting all three vevs to a single vev v_{PS} (class A) or by setting $v_T = v_\Sigma = v_{\text{PS}}$ (class D).

We should keep in mind that Table 3.2 refers only to the mass contributions that result from symmetry breaking. All superfields may carry an individual PS-symmetric bilinear superpotential term m_i , except for the matter multiplets which are chiral fields. These mass terms are either completely arbitrary or fixed by the conditions that determine the vacuum expectation values (see (3.7)). As we include supersymmetry, they may be light without causing naturalness problems [8, 38]. Furthermore, a vev in any PS singlet field may contribute a similar term, again unrestricted by symmetries. To get a handle on these scales we implicitly assume that the sum of all these mass terms is either negligible or of the order of the GUT scale, which is the largest scale in the setup. With respect to GCU, the second possibility is equivalent to omitting the field completely.

On the other hand, given only the renormalisable Lagrangian terms of (3.4) there exist classes for which some of the fields E , Σ and T do not receive a mass from PS and subsequent symmetry breaking. For these fields, either the bilinear mass term or effective masses induced by higher-dimensional operators play an important role and must be included as independent parameters. From a phenomenological point of view we are mainly interested in the lowest possible mass for each of those fields. We discuss this issue at the beginning of Section 3.6.

Additional Intermediate Mass Scale

While most multiplets acquire masses proportional to either one of the symmetry-breaking scales v_T, v_Σ, v_Φ , there are various cases where the mass becomes proportional to a ratio of v_Φ and one or both of the vevs v_Σ and v_T . For large hierarchies, these masses can be significantly smaller than v_Φ . In other words, there is an extra see-saw effect, unrelated to the well-known neutrino see-saw [109–111]. We denote this induced mass scale by M_{IND} in order to distinguish it from the right-handed see-saw scale. It is located below the scale where PS is completely broken and we limit it for practical reason to be above or at the SUSY scale. Such an intermediate scale appears naturally in models with multiple scales where the trilinear coupling of the symmetry breaking field is absent [109]. A generic expression is

$$M_{\text{IND}} \sim \frac{v_\Phi^2}{v_\Sigma + v_T}. \quad (3.8)$$

field	$(SU(3)_c, SU(2)_L)_Y$	class B $v_T \ll v_\Sigma$	class C $v_\Sigma \ll v_T$	class E $v_T = 0$	class F $\Sigma = 0$
Σ	$(\mathbf{8}, \mathbf{1})_0$	v_Σ	v_Σ	v_Σ	—
E	$(\mathbf{3}/\bar{\mathbf{3}}, \mathbf{2})_{\pm 5/6}$	—	—	—	—
E	$(\mathbf{3}/\bar{\mathbf{3}}, \mathbf{2})_{\pm 1/6}$	—	—	—	—
$\Phi/\bar{\Phi}$	$(\mathbf{3}/\bar{\mathbf{3}}, \mathbf{2})_{\pm 1/6}$	v_Σ	v_T	v_Σ	v_T
$\Phi'/\bar{\Phi}'$	$(\mathbf{3}/\bar{\mathbf{3}}, \mathbf{1})_{\pm 2/3}$	v_Σ	v_Σ	v_Σ	v_Φ
Σ	$(\mathbf{3}/\bar{\mathbf{3}}, \mathbf{1})_{\pm 2/3}$	v_Σ	v_Σ	v_Σ	—
$\Phi'/\bar{\Phi}'$	$(\mathbf{3}/\bar{\mathbf{3}}, \mathbf{1})_{\pm 1/3}$	v_Σ	v_T	v_Σ	v_T
F	$(\mathbf{3}/\bar{\mathbf{3}}, \mathbf{1})_{\pm 1/3}$	$\frac{v_\Phi^2}{v_\Sigma}$	$\frac{v_\Phi^2}{v_T}$	$\frac{v_\Phi^2}{v_\Sigma}$	$\frac{v_\Phi^2}{v_T}$
T	$(\mathbf{1}, \mathbf{3})_0$	$\frac{v_\Phi^2}{v_T}$	$\frac{v_\Phi^2}{v_T}$	—	$\frac{v_\Phi^2}{v_T}$
$\Phi/\bar{\Phi}$	$(\mathbf{1}, \mathbf{2})_{\pm 1/2}$	v_T	v_T	v_Φ	v_T
h	$(\mathbf{1}, \mathbf{2})_{\pm 1/2}$	$\frac{v_\Phi^2}{v_T}$	$\frac{v_\Phi^2}{v_T}$	v_Φ	$\frac{v_\Phi^2}{v_T}$
$\Phi'/\bar{\Phi}'$	$(\mathbf{1}, \mathbf{1})_{\pm 1}$	v_T	v_T	v_Φ	v_T
T'	$(\mathbf{1}, \mathbf{1})_{\pm 1}$	v_T	v_T	—	v_T
T'	$(\mathbf{1}, \mathbf{1})_0$	v_Φ	v_T	—	v_Φ
Σ	$(\mathbf{1}, \mathbf{1})_0$	v_Σ	v_T	v_Σ	—
$\Phi'/\bar{\Phi}'$	$(\mathbf{1}, \mathbf{1})_0$	v_Φ	v_Σ	v_Φ	$\frac{v_\Phi^2}{v_T}$
S_{27}/S_{78}	$(\mathbf{1}, \mathbf{1})_0$	$\frac{v_\Sigma^2}{v_T}$	$\frac{v_\Sigma^3}{v_T^2}$	—	—
S_{27}/S_{78}	$(\mathbf{1}, \mathbf{1})_0$	$\frac{v_\Sigma^2}{v_T}$	$\frac{v_\Sigma^3}{v_T^2}$	v_Φ	$\frac{v_\Phi^2}{v_T}$

Table 3.2.: Mass hierarchy of the scalar fields in the different classes of the complete model. If none is shown, there is no contribution from the vev and the hierarchy is undefined. Classes A and D are limiting cases of B and C. Class A can be reached if one sets all vevs equal to a single vev v_{PS} and class D if one just sets $v_\Sigma = v_T = v_{\text{PS}}$. The fields are ordered such that those which mix are grouped together. Thus, the mass eigenstates are a linear combination of the listed fields. Massless components which are the Goldstone bosons are not considered here explicitly.

3. PS-Breaking and Gauge Coupling Unification

Depending on the model class, some of the multiplets F , h , or T become associated with M_{IND} . In class F this applies also to the singlet part of T' (cf. Table 3.2). We thus get “light” supermultiplets consisting of scalars and fermions which may be coloured, charged or neutral, and acquire a mass that does not coincide with any of the symmetry-breaking scales. If the hierarchy between the vevs is strong, M_{IND} may be sufficiently low to become relevant for collider phenomenology. In model classes B, C and F, it provides a μ term for h and may thus be related to electroweak symmetry breaking. In any case, the threshold M_{IND} must be taken into account in the renormalisation-group running of the gauge couplings.

Goldstone Bosons

Not all of the scalar fields are physical; since the broken symmetries are gauged, nine of the scalar fields are Goldstone bosons that provide the longitudinal modes of the massive PS gauge bosons that are integrated out in the breaking to the SM gauge group. Six of them ($GB_{1..6}$) are related to $SU(4) \rightarrow SU(3)_c \times U(1)_{B-L}$, two additional ones ($GB_{7,8}$) implement $SU(2)' \rightarrow U(1)'$ and the last one (GB_9) comes from the breaking of the $U(1)$ subgroups $U(1)_{B-L} \otimes U(1)' \rightarrow U(1)_Y$. We identify these Goldstone bosons as

$$GB_{1,2,3} = -i \frac{\sqrt{3} v_\Phi}{2 v_\Sigma} \Phi'_3 - i \frac{\sqrt{3} v_\Phi}{2 v_\Sigma} \overline{\Phi}'_3 + \Sigma_3 + \Sigma^*_3, \quad (3.9a)$$

$$GB_{4,5,6} = i \frac{\sqrt{3} v_\Phi}{2 v_\Sigma} \Phi'^*_3 + i \frac{\sqrt{3} v_\Phi}{2 v_\Sigma} \overline{\Phi}'_3 + \Sigma_{\bar{3}} + \Sigma^*_{\bar{3}}, \quad (3.9b)$$

$$GB_7 = T'_{1_1} + T'^*_{1_1} - \frac{i}{\sqrt{2}} \frac{v_\Phi}{v_T} \overline{\Phi}'_{1_1} - \frac{i}{\sqrt{2}} \frac{v_\Phi}{v_T} \Phi'^*_{1_1}, \quad (3.9c)$$

$$GB_8 = T'_{1_{-1}} + T'^*_{1_{-1}} + \frac{i}{\sqrt{2}} \frac{v_\Phi}{v_T} \Phi'_{1_{-1}} + \frac{i}{\sqrt{2}} \frac{v_\Phi}{v_T} \overline{\Phi}'^*_{1_{-1}}, \quad (3.9d)$$

$$GB_9 = \text{Im}(\Phi'_{1_0}) - \text{Im}(\overline{\Phi}'_{1_0}). \quad (3.9e)$$

Here, 3 and $\bar{3}$ are the $(\mathbf{3}, \mathbf{1})_{2/3}$ and $(\overline{\mathbf{3}}, \mathbf{1})_{-2/3}$ components of the Higgs fields Φ' , $\overline{\Phi}'$ and Σ , respectively. For vanishing vevs, the corresponding fields do not mix into the Goldstone bosons. Thus, if $v_\Sigma = 0$ ($v_T = 0$), the Goldstone bosons $GB_{1..6}$ ($GB_{7,8}$) are only mixtures of the field Φ' and $\overline{\Phi}'$.

SM Singlets

The most complicated mass matrix belongs to the SM singlets that are contained in the various PS multiplets. Even if we do not consider PS singlets there are still five SM singlets which mix non-trivially. Generally, their masses cannot be calculated in closed analytical form. To get a handle on these particles, we computed the dependence on the different scales numerically. Starting with one of the patterns of hierarchical scales introduced in the different classes above, we find additional scales and new hierarchy patterns which do not coincide with M_{IND} . These may have interesting consequences for flavor and Higgs physics. However, as singlets do not contribute to the running of the gauge couplings at leading-logarithmic level, we do not attempt a detailed discussion of the singlet sector in this work.

3.4.2. The MSSM Higgs

Apart from the matter fields and Goldstone bosons, the spectrum must provide the Higgs bidoublet of the MSSM that is responsible for electroweak symmetry breaking. This multiplet should either be massless or have a suppressed mass compared to the scales of the model which may coincide with M_{SUSY} . Mass terms are provided by soft-SUSY breaking parameters and the μ term which mixes both doublets. We note that the μ term may result from the vev of one of the electroweak singlets in the model, i.e. the model may implement a NMSSM-type solution for the μ problem [112, 113].

The obvious candidate for the MSSM Higgs bidoublet is the superfield h as mentioned while introducing the particle content. A further candidate for the pair of electroweak symmetry breaking doublets is provided by the multiplets Φ and $\bar{\Phi}$, each containing one doublet. With respect to the SM gauge symmetry they have the same quantum numbers as h . We note that they do not couple to $\Psi_L \Psi_R$ at the renormalisable level. Although they are not in a bidoublet representation of PS, we will group and denote them collectively as h_Φ in the following. They are of particular interest as they are physical scalar fields while their Z_2 partners, the right-handed doublets in Φ' and $\bar{\Phi}'$, serve as Goldstone bosons and are thus unphysical. Therefore, they are protected against a mass term down to the scale where the Z_2 symmetry is broken, which coincides with the $SU(2)'$ breaking in our setup. Their squared mass matrix can be calculated to be

$$\mathcal{M}_{(1,2)}^2 = \begin{pmatrix} m_h^2 + l_{h\Phi}^2 v_\Phi^2 & (l_{T\Phi} v_T - m_h) l_{h\Phi} v_\Phi \\ (l_{T\Phi} v_T - m_h) l_{h\Phi} v_\Phi & l_{h\Phi}^2 v_\Phi^2 + l_{T\Phi}^2 v_T^2 \end{pmatrix}. \quad (3.10)$$

This fields h_Φ are of special interest in class E where v_Φ is the only $SU(2)'$ breaking vev as $v_T = 0$. In this case, both bidoublets get masses and a mixing term only proportional to the coupling $l_{h\Phi}$. By forbidding the coupling of Φ and h , the bidoublets h_Φ are massless while h still gets a mass from its bilinear m_h . Hence both fields are maximally split. With this coupling present, the situation becomes more complicated. Now, both fields get a contribution to their mass of the order $l_{h\Phi} v_\Phi$. For $m_h = 0$ we reach the other limit, where both mass eigenvalues are degenerate and of order v_Φ .

In each of the other classes, h_Φ gets a mass term proportional to v_T and mixes with h proportional to v_Φ . Thus, the diagonalisation of the mass matrix results in a see-saw like mass pattern where the lighter bidoublet gets a mass proportional to the induced see-saw scale M_{IND} . In the limit $v_\Phi \ll v_T$, we obtain the approximate eigenvalue structure

$$\mu \approx m_h + \frac{l_{h\Phi}^2 v_\Phi^2}{l_{T\Phi} v_T} \quad \text{and} \quad m'_{h_\Phi} \approx l_{T\Phi} v_T, \quad (3.11a)$$

where we allow for the bilinear m_h as an independent contribution to the μ term, not directly related to PS breaking. Both contributions to the μ term may be as low as the TeV scale where soft-breaking terms come into play. In these setups, the electroweak hierarchy may be generated at least partly by a high-energy hierarchy in the PS symmetry-breaking chain.

In short, in various classes of PS models the MSSM Higgs bidoublet may be naturally light or actually originate from the superfields Φ , which reduces the minimal set of scalars. This

3. PS-Breaking and Gauge Coupling Unification

scenario would also lead to a model where the both $SU(2)'$ as well as $SU(2)$ are broken by a single GUT field². In other words, the MSSM Higgs bidoublet (in particular, the Higgs boson that has been observed) may belong to either h or h_Φ , or be a mixture of both.

3.4.3. The Multiplet F

The mass of the multiplet F is generically see-saw suppressed and thus comparatively light. This appears as a common feature of all model classes with more than one scale. It can couple to the matter fields via W_{Yukawa} . This leads to an effective superpotential of the form

$$W_{\text{eff}} \sim F_{\mathbf{3}} (Q_L Q_L + U_R^c R_R^c + D_R^c N_R^c) + F_{\bar{\mathbf{3}}} (Q_L L_L + U_R^c D_R^c). \quad (3.12)$$

As we easily see from this superpotential, the possible Yukawa couplings provide both diquark and leptoquark couplings, explicitly breaking baryon number in the low-energy theory. In fact, F is the analogue of the coloured Higgs field which in $SU(5)$ GUT models induces rapid proton decay unless it is very heavy (see Section 1.4.1 and 1.4.2).

However, in PS models the Yukawa matrices Y_F and Y are not related. Hence there is no doublet-triplet splitting problem [114, 115]. By omitting the coupling of F to Ψ , proton decay is not present in our setup up to the unification scale. Here, it might again be possible, e.g. in $SO(10)$. The coupling may be forbidden for instance by a flavor symmetry or by an appropriate discrete quantum number.

If the F multiplet is sufficiently light, it may provide detectable new particles at colliders. Without the Yukawa coupling Y_F there is no immediate decay to MSSM matter fields but other terms in the Lagrangian provide indirect decay channels. In this situation, the particles (colour-triplet scalars and fermionic superpartners) may be long-lived and become rather narrow as resonances.

3.4.4. Matter Couplings

In this part of the thesis we are not aiming at describing the flavour sector. Nevertheless, we will give a short motivation for possible realisations of the flavour sector in this model without going into details. For a detailed analysis of the flavour sector in PS models we refer to later chapters.

The renormalisable superpotential contains terms that couple h to matter fields Ψ . Thus, after electroweak symmetry breaking, matter fields can get masses via the vev of h . However, PS allows only for a single Yukawa coupling as discussed in Section 2.4.1. This gives strict constraints on the flavour structure of our model. Nevertheless, there is no reason for flavor physics to originate solely from the renormalisable superpotential. In particular, if h_Φ turns out to be the MSSM Higgs, flavour physics has to arise purely from non-renormalisable operators.

In Chapter 4 we will give explicit examples of such a realisation from higher dimensional operators in a similar framework. Also adding additional fermionic degrees of freedom may strongly affect the flavour sector. One realisation of such a setup will be presented in Chapter 5.

²Remember, Φ and Φ' are related due to the Z_2 symmetry at the GUT scale.

As long as we stay within the framework described above, we may still consider non-renormalisable operators to parametrise the flavour structure. The generated terms are suppressed by a scale Λ which may coincide with one of the scales in our model. For instance, if we consider dimension-four terms in the superpotential, we identify the following interactions that can affect matter-Higgs Yukawa couplings in the low-energy effective theory,

$$W_{\text{Yukawa}}^{\text{NLO}} = \frac{Y_{h\Sigma}}{\Lambda} \Psi_L \mathbf{h} \Sigma \Psi_R + \frac{Y_{\Phi}}{\Lambda} \Psi_L \left(\Phi \Phi' + \overline{\Phi} \overline{\Phi}' \right) \Psi_R + \frac{Y_{EF}}{\Lambda} \Psi_L E F \Psi_R. \quad (3.13)$$

There are additional couplings to gauge singlets which may also be flavour dependent. Overall there is great freedom in assigning masses and generating hierarchies in the mass and mixing parameters.

Neutrino Mass

As a left-right-symmetric extension of the SM, the model presented here contains right-handed neutrinos. Moreover, it generates a neutrino Yukawa coupling related to the up-type quarks. Hence, the model features Dirac mass terms for the neutrinos which are however not consistent with the neutrino phenomenology. Furthermore, the extra fields that are present in our setup are able to induce any of the three neutrino see-saw mechanisms [90, 116] which may account for the neutrino mass and mixing structure as explained in Section 2.3.1. The field Φ' provides a vev that can couple to right-handed neutrinos generating a Majorana mass term proportional to v_{Φ} . However, such a mass term requires the introduction of non-renormalisable operators which is beyond the scope of this thesis. Combined with the Dirac mass this results in a type I see-saw. The field T contains $SU(2)$ -triplet scalars and their fermionic superpartner and may thus induce a type II or type III see-saw mechanism. Again, we refer to later chapters for a more detailed study on neutrino masses and mixing.

3.5. Unification Conditions

Within the framework of multi-scale breaking of the PS symmetry (class A-F), we impose unification conditions on the gauge couplings to constrain the scales present in the model. As stated above, we require complete unification of all gauge couplings at the unification scale M_{GUT} . This is equivalent to require a complete unification to a gauge group containing $SO(10)$. The unification scale itself is not fixed but depends on the spectrum and the intermediate scales. For each of the intermediate scales we state the corresponding matching conditions. At these scales the spectrum generally changes, i.e. particles are integrated out. We work to leading-logarithmic level only, where matching conditions depend solely on the spectra. At next-to-leading order, the superpotential parameters enter the running. However, given the great freedom in choosing a model in the first place, there is little to be gained from including such effects in our framework.

3. PS-Breaking and Gauge Coupling Unification

Running of the Couplings

Abelian gauge couplings do exhibit discontinuous behaviour as an artefact of different normalisation conventions in the various energy regimes. Non-abelian gauge couplings are always continuous. The running of a gauge coupling between fixed scales μ_1 and μ_2 is given to leading-logarithmic order by

$$\frac{1}{\alpha_i(\mu_2)} = \frac{1}{\alpha_i(\mu_1)} - \frac{b_i}{2\pi} \ln\left(\frac{\mu_2}{\mu_1}\right). \quad (3.14)$$

Here, the b_i are group theoretical factors that can be calculated from the representations of the “active” particles³ [117]. Hence, we have to consider the evolution of the gauge couplings iteratively, starting from M_Z where the gauge couplings are measured all the way up to the GUT scale. Inserting the intermediate mass scales, the complete running is a sum of multiple terms. For instance in class B we have

$$\begin{aligned} \frac{1}{\alpha_i(M_{\text{GUT}})} = \frac{1}{\alpha_i(M_Z)} &- \frac{b_i^{(1)}}{2\pi} \ln\left(\frac{M_{\text{SUSY}}}{M_Z}\right) - \frac{b_i^{(2)}}{2\pi} \ln\left(\frac{M_{\text{IND}}}{M_{\text{SUSY}}}\right) - \frac{b_i^{(3)}}{2\pi} \ln\left(\frac{v_\Phi}{M_{\text{IND}}}\right) \\ &- \frac{b_i^{(4)}}{2\pi} \ln\left(\frac{v_T}{v_\Phi}\right) - \frac{b_i^{(5)}}{2\pi} \ln\left(\frac{v_\Sigma}{v_T}\right) - \frac{b_i^{(6)}}{2\pi} \ln\left(\frac{M_{\text{GUT}}}{v_\Sigma}\right). \end{aligned} \quad (3.15)$$

Here, M_{IND} denotes the additional see-saw induces scale introduced in (3.8). As this scale depends on the numerical values of superpotential parameters which we do not fix, we treat it as a free parameter. We show later that this assumption does not influence the results significantly. Distinguishing different model classes with their corresponding hierarchy patterns, we have to appropriately adapt the ordering of scales and the definition of the $b_i^{(n)}$.

The calculation of the coefficients in this formula is straightforward and can be found in Appendix A.4. We note that the running of the couplings in (3.15) does not depend on the assumption of SUSY. The supersymmetric and non-supersymmetric frameworks differ only by their particle content which in the SUSY case simplifies the form of the β -function (cf. (A.20) and (A.21)).

For simplicity, we always assume that all masses of the particles coincide with one of the scales mentioned above. This is a legitimate assumption as order-one prefactors in the mass terms would only enter logarithmically in the running of the couplings (3.15), which is a minor uncertainty. It is based on the assumption that no further hierarchies from couplings become relevant here and all additional fields are integrated out at their “natural” mass scale which we have determined in the previous section (cf. Table 3.2). As we have no information on possible hierarchies in the couplings, considering those would only lead to a wider range of possibilities. Thus, we do not investigate this any further.

Matching Conditions

Regarding $U(1)$ couplings with their normalisation ambiguity, we have to explicitly consider the unification condition for

$$U(1)' \otimes U(1)_{B-L} \xrightarrow{\langle\Phi\rangle} U(1)_Y. \quad (3.16)$$

³“Active” refers to particles which have a mass smaller than the energy scale considered and thus may be generated as real particles.

To define the strength of the hypercharge gauge coupling, we explicitly calculate the unbroken direction and identify the charges Q' and Q_{B-L} in $SU(2)'$ and $SU(4)$, respectively. This results in a relation between the group generators and therefore between charges and couplings. From the usual definition for the hypercharge⁴

$$Y = \frac{B-L}{2} + \tau'_3, \quad (3.17)$$

we obtain⁵

$$\alpha_Y^{-1}(v_\Phi) = \frac{2}{3} \alpha_{B-L}^{-1}(v_\Phi) + \alpha_{1'}^{-1}(v_\Phi). \quad (3.18)$$

The charges $Q_{U(1)'}$ and Q_{B-L} are fixed by their embedding in the non-abelian groups.

For the non-abelian symmetry breaking steps, the unification conditions just depend on the breaking pattern, i.e.

$$\text{GUT} \xrightarrow{\langle X \rangle} SU(4) \otimes SU(2) \otimes SU(2)', \quad (3.19a)$$

$$SU(4) \xrightarrow{\langle \Sigma \rangle} SU(3)_c \otimes U(1)_{B-L}, \quad (3.19b)$$

$$SU(2)' \xrightarrow{\langle T' \rangle} U(1)', \quad (3.19c)$$

where the GUT group may be any group containing $SO(10)$. These three breaking patterns result in the matching conditions

$$\alpha_4^{-1}(M_{\text{GUT}}) = \alpha_2^{-1}(M_{\text{GUT}}) = \alpha_{2'}^{-1}(M_{\text{GUT}}) \equiv \alpha_{\text{GUT}}^{-1}(M_{\text{GUT}}), \quad (3.20a)$$

$$\alpha_3^{-1}(v_\Sigma) = \alpha_{B-L}^{-1}(v_\Sigma) \equiv \alpha_4^{-1}(v_\Sigma), \quad (3.20b)$$

$$\alpha_{1'}^{-1}(v_T) = \alpha_{2'}^{-1}(v_T) = \alpha_2^{-1}(v_T), \quad (3.20c)$$

respectively. In the classes where one of the breaking steps is absent, the corresponding conditions apply at the next lower scale. In class E and F, we have to substitute $\alpha_{B-L} = \alpha_4$ or $\alpha_{1'} = \alpha'_2$ in (3.18), respectively.

Next to the unification and matching conditions we have the additional constraint that the mass scales are properly ordered. For class B we have:

$$M_{\text{SUSY}} \leq M_{\text{IND}} \leq v_\Phi \leq v_T \leq v_\Sigma \leq M_{\text{GUT}} \lesssim M_{\text{Planck}}. \quad (3.21)$$

Furthermore, the coupling strengths α_i have to be sufficiently small and positive at all mass scales as we want to stay within the perturbative regime.

Counting the number of conditions and free parameters (scales), we observe that the models are still under-constrained. Hence, we can derive constraints for the mass scales and exclude particular models but not fix all scales completely. Nevertheless, imposing unification does restrict the model parameter space significantly as we will show in the following sections.

⁴We do not rescale $U(1)$ in order to match the $SU(5)$ normalisation, as is often done in the literature.

⁵We label the gauge coupling by a subscript corresponding uniquely to the gauge factor (e.g. α_3) instead of the usual SM notation (e.g. α_s).

3.6. Unification within Supersymmetry

In this section, we explicitly study the unification properties of the model classes defined in Section 3.1. Therefore, we define for each relevant class (B, C, E and F) a set of configurations. This set is constructed following the three basic assumptions:

1. The number of superfield generations (0,1,3) is independently varied for each of the fields h , F , $\Phi^{(\prime)} \oplus \bar{\Phi}^{(\prime)}$, Σ , E , $T \oplus T'$. Remember, that Φ and $\bar{\Phi}$ cannot be varied independently as both are needed for the PS breaking.
2. Each field is associated to its “natural” mass scale as discussed in Section 3.4. Alternatively, we can set the masses of the fields to the GUT scale which is equivalent to omitting them.
3. Each configuration has to have at least one pair of “light” MSSM Higgs candidates (see Section 3.4.2).

Following this construction principle we end up with a set of 828 distinct configurations. These are not equally distributed among the four classes as by construction in some classes more fields have to be present; e.g. class B requires at least one generation of Σ and T while one of them may be absent in class E and F, respectively. Additionally, class E allows for configurations in which the MSSM Higgs bidoublet is contained in Φ instead of h as we will discuss below. Thus, class E features 324 configurations whereas class F features only 216 and class B and C 144 each. We assign a discrete label to each of these configurations following the naming convention given in Appendix A.1.

For each of these so constructed configurations, we numerically calculate the allowed range of mass scales where the GCU conditions (3.18), (3.20) and (3.21) can be fulfilled. As we are not able to fix all scales, we do this by varying two of the scales independently and solving the complete set of equations and inequalities for the remaining scales. If we find no solution for a particular configuration, we do not consider it any further. For the remaining configurations, we obtain model-specific relations between the mass scales. As a result, we can express those scales as functions of one or two independent mass parameters that we have chosen as input.

For all numerical results, we fix the common soft SUSY-breaking scale at

$$M_{\text{SUSY}} = 2.5 \text{ TeV} \approx 10^{3.4} \text{ GeV} . \quad (3.22)$$

We have also considered a lower SUSY-breaking scale of $M_{\text{SUSY}} = 250 \text{ GeV}$ which is disfavoured by LHC data [15, 40, 41]; it turns out, that the unification conditions are generically easier to satisfy for larger values of the soft SUSY-breaking scale.

With these conventions in mind, our scan will be exhaustive as we scan over a discrete set of configurations. At this point, we change our notation from vevs to mass scales (see Appendix A.3) since we are now dealing with mass scales rather than vev structures or specific mass eigenvalues.

Extra Mass Parameters

Considering the second construction principle stated above, we find that in some classes the fields E , Σ and T do not obtain a mass term from symmetry breaking. Thus, we have to

assign their masses which are generally free parameter to one of the scales by hand. To get a handle on these masses, we have considered all possibilities for assigning the mass scales of these superfields to the mass scales in our framework. This we have done by imposing GCU with those fields assigned to any of the scales and determining their lowest possible numerical value. As a result, we can exclude the possibility that these extra scales are at the lower end of the spectrum. More specifically, in all model classes we find a lower bound for the coloured multiplet E of about $m_E \gtrsim 10^8$ GeV. Similar results apply to Σ and T , if we do not consider lowering the GUT scale below about 10^{16} GeV. For definiteness, we fix their mass scales whenever they are undetermined at M_{PS} for the scan over the configurations.

As stated in point three, we need to provide at least one candidate pair of electroweak Higgs bosons. These have to be effectively massless in our setup, i.e. have masses dominated by soft SUSY breaking terms at or below the SUSY scale. Possible candidates and their masses have been discussed in Section 3.4.2. For the scan, we consider the SM running of the gauge couplings up to the SUSY scale, i.e. including only a single Higgs doublet in the spectrum, and add the additional “massless” doublets at M_{SUSY} . This we motivate by the non-observation of additional Higgs bosons by the LHC (see e.g. [37, 118]) and our ignorance on the soft-SUSY breaking sector.

In addition, we have checked to what extent h_Φ may serve as low energy MSSM-like Higgs. Therefore, we have considered whether their mass scale given in Table 3.2 may coincide with the SUSY scale. This is only possible in class E where $v_T = 0$, as otherwise $SU(2)'$ would remain unbroken down to the electroweak scale. Thus, we must include at least one generation of h in classes B, C and F.

3.6.1. General Overview

Before discussing the various classes of models in more detail we summarise some generic features and specific observations gained by studying all 828 configurations. A statistical summary of the following discussions is given in Table 3.3.

Successful GCU

Successful GCU is possible in roughly half of the models. Except for class E, all such configurations allow for a unification scale of $M_{\text{GUT}} > 10^{16}$ GeV and are thus favoured by the non-observation of proton decay. In class E this is true for half of them.

In contrast to classes C, E and F, the allowed ranges in class B are rather constrained. This allows us to fix the scales for at least some of the configurations in a semi-quantitative way. In classes C, E and F such a fixing is only possible if we constrain one more scale by hand.

New Light Particles

An important aspect of the models is the possibility of light (multi TeV) new scalars and fermions. Such particles may be within the reach of future collider experiments. Therefore, we have to study the bounds on the lowest scale of the model which is by definition M_{IND} . On the other hand, we demand complete unification near the Planck scale in order to be not ruled out by the bound on the proton life time (cf. Section 1.4). We find 114 configurations

3. PS-Breaking and Gauge Coupling Unification

	class B	class C	class E	class F	Σ
scanned	144	144	324	216	828
GCU	18	57	254	29	358
$M_{\text{GUT}} > 10^{16}$ GeV	18	57	131	29	235
$M_{\text{IND}} < 10$ TeV & $M_{\text{GUT}} > 10^{16}$ GeV	8	34	72	0	114
multiple light Higgs	1	18	225	0	239
$M_{\text{LR}} < 100$ TeV	0	0	108	0	108
10^{12} GeV < $M_{N_R} < 10^{14}$ GeV	16	42	123	3	184
$M_{\text{IND}} \in [0.1, 10] \frac{v_\Phi^2}{v_\Sigma + v_T}$	14	20	203	26	263

Table 3.3.: The Number of configurations fulfilling certain conditions within the SUSY framework.

that satisfy these conditions of which most (72) are categorised as class E. As such, they contain only light colour triplets F . In the other classes, also the $SU(2)$ triplets T may get masses in the TeV-range. However, these are quite constrained by the requirement of GCU. 34 of the aforementioned models are categorised as class C and support only one light generation of T . In class B only a few models fulfil these conditions, again with only one generation of T , and none of them belongs to class F. We may generalise this observation to the statement that $SU(2)$ triplets T , if present in the intermediate range, rarely get low mass and tend to be associated with lower GUT scales.

Light colour triplets F are on the contrary a quite common feature of the models. In class E they are actually allowed over a large mass range for the GUT scale. In classes B and C, we may have colour triplets around some 100 TeV as long as there is only one generation of light $SU(2)$ triplets. In class F, the lowest mass scale and thus also the colour triplets are generically heavier (cf. Section 3.6.3).

We illustrate the possibility of light particles in Figure 3.2, where we show the lowest possible scale with respect to their multiplicity⁶. The figure displays a considerable fraction of configurations where new matter is possible at the lowest scales (green squares), so we should be prepared to observe exotic particles or at least their trace in precision observables at collider experiments.

Multiple Light Higgs

One key feature of our setup is the possibility of having up to six $SU(2)$ scalar bidoublets (h and h_Φ) massless at the SUSY scale. For 239 configurations we find more than one Higgs bidoublet near the electroweak scale most of which fall in class E. Also in class C we find a handful of configurations with multiple Higgs. In class B is a single configuration possible and none in class F. It is interesting to note that in class E most successful configurations have

⁶Keep in mind that the $SU(2)$ triplets T are not light in class E (cf. Table 3.2).

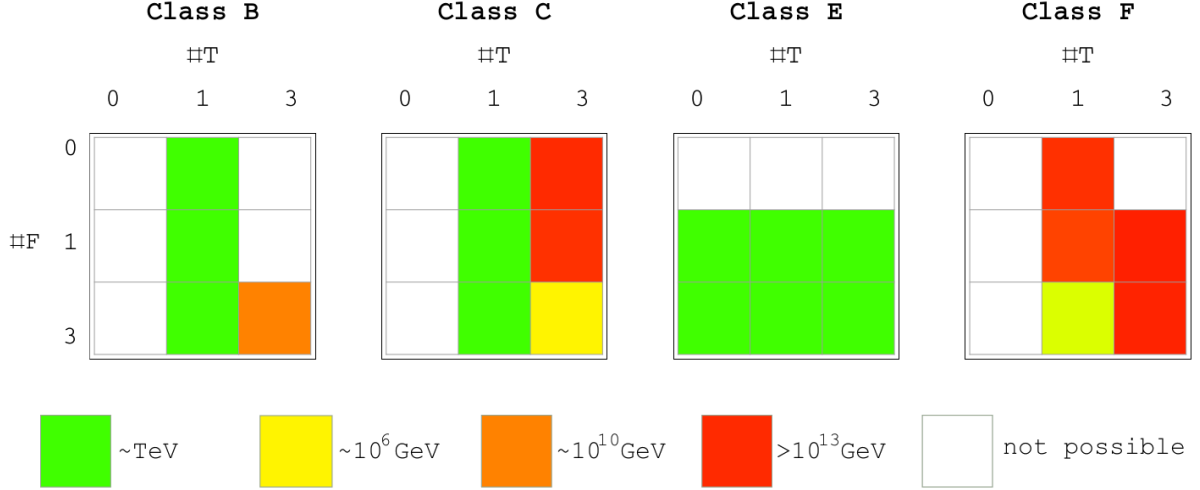


Figure 3.2.: Graphical illustration of the lowest new mass scale, depending on the multiplicity in the low-energy spectrum. We vary the number of low-lying $SU(2)$ triplets T (x axis) and low-lying colour triplets F (y axis), independently⁶. The colours indicate the lowest mass scale, ranging from green (SUSY scale) to red (Planck scale). White squares correspond to configurations not leading to GCU or which are inconsistent with the class definitions.

more than one light bidoublet. This is because h and h_Φ are taken as degenerate in mass. A more detailed discussion will follow when we look explicitly at class E (cf. Section 3.6.2).

Left-Right Symmetry Scale

Our setup allows for rather light left-right symmetry-breaking scales. In class E, this scale is directly related to $\langle \Phi' \rangle$ as it is the only $SU(2)'$ breaking vev present. Thus, such a light LR scale may lead to an imprint on flavour precision observables due to right handed W' and Z' gauge bosons. We find 108 configurations with $M_{LR} < 10^5 \text{ GeV}$ in class E.

In class F, the LR-breaking scale is bounded from below by $M_{PS} > 10^{16.4} \text{ GeV}$. This is due to the fact that the left-right symmetry is already broken by the vev of the field T' which is the largest vev in this class. Similar arguments apply for class C. However, here the lower bound is reduced to $M_{PS} > 10^{10.6} \text{ GeV}$. Nevertheless, the corresponding LR gauge bosons are still beyond the reach of current and future collider experiments. The bound is even lower in class B, as the vev of T' is no longer the largest of the vevs. Still, the LR scale cannot be below the limit of $M_{LR} > 10^{6.2} \text{ GeV}$ and thus there is little hope of seeing effects of the corresponding gauge bosons in future experiments.

Right- Handed Neutrino Scale

Another observable of interest is the preferred mass range for right-handed neutrinos. Many see-saw models favour it to be in the range of $M_{N_R} \sim 10^{14} \text{ GeV}$, well below the GUT scale (cf. Section 2.3). In our setup, the Majorana mass parameter is not fixed at the GUT scale but should rather be of the order $\langle \Phi' \rangle$ where all symmetries that protect this

3. PS-Breaking and Gauge Coupling Unification

term are broken. Scanning all configurations with respect to this scale, we find 184 with $10^{12} \text{ GeV} \lesssim M_{N_R} \lesssim 10^{14} \text{ GeV}$. Actually, in classes B and C three-quarters and in class E still half of all successful models fall in this category. Only in class F this scale is typically higher; only 10 percent of the models allow for a neutrino scale in this range.

Scales Fixed by GCU

Although the constraints on the mass scales from GCU are in general quite weak, they pin down all scales to a narrow range for a few configurations. The most obvious case is the standard $SO(10)$ coupling unification at the GUT scale, i.e. all vevs are located at M_{GUT} . This well-studied model is contained in our scan as a limiting case. We reproduce the observation that for this case the only light multiplet is the MSSM Higgs h . However, we also find a few configurations where the scales are essentially fixed but the spectrum and unification pattern is different. Those are all classified as class E and will be discussed later.

Correlated M_{IND}

So far, we always considered M_{IND} to be a free parameter. To be more restrictive on this scale, which is not a fundamental one, we impose the bound

$$M_{\text{IND}} \in [0.1, 10] \frac{v_{\Phi}^2}{v_{\Sigma} + v_T}. \quad (3.23)$$

While this does not significantly reduce the number of allowed models it drastically reduces the configurations with TeV-scale new particles. Most of the models still allowing TeV-scale new particles belong to class E. In this class, still one quarters of all models allow for coloured triplets below about 10 TeV.

It also affects the preferred neutrino scale. In class B and E the number is reduced to three-quarters of those allowing for $10^{12} \text{ GeV} \lesssim M_{N_R} \lesssim 10^{14} \text{ GeV}$ in the general case. In class C this is even reduced to 30 percent and class F now features no more configuration with such a preferred neutrino scale.

Moreover, the number of configurations with multiple generations of MSSM Higgs bosons is reduced by 20 percent in class E. With this constrained, there are only four configurations with more than one generation not belonging to class E; one in class B and three belonging to class C.

From these considerations we may conclude that taking M_{IND} as free parameter is reasonable and does not drastically change our results.

3.6.2. Class E: $v_T = 0$ and $v_{\Sigma} \neq 0$

From the general overview presented so far we can conclude that class E contains the largest set of configurations with phenomenologically interesting features. In this class, the ordering of new thresholds is in ascending order: the scale of soft SUSY breaking M_{SUSY} , the see-saw induced scale M_{IND} , the left-right unification scale M_{LR} , the scale where PS symmetry emerges M_{PS} and the scale of complete gauge-coupling unification M_{GUT} .

$$E : M_{\text{SUSY}} \leq M_{\text{IND}} \leq M_{\text{LR}} \leq M_{\text{PS}} \leq M_{\text{GUT}} \quad (3.24)$$

Two of these scales can be regarded as free parameters; we take the lowest (M_{IND}) and highest (M_{GUT}) free scale for that purpose. The other scales are then fixed by the matching and unification conditions if they can be satisfied at all.

Our basic setup features 324 configurations in class E. For 254 of these it is possible to implement GCU of which 131 allow for a scale $M_{\text{GUT}} > 10^{16}$ GeV and 76 are able to produce GCU at the Planck scale.

As discussed before, in class E the superfield h is not necessarily contained in the spectrum (cf. end of Section 3.6), as we take h_ϕ to be massless. We find 77 configurations leading to GCU in which the MSSM-like Higgs is h_ϕ . As mentioned above, most of the configurations have more than one bidoublet massless at the SUSY scale. Only 29 feature exactly one. There are roughly 50 configurations with two, three or six bidoublets each and 81 with 4. Zero or five are generally excluded by our setup. We also find that a larger number of light bidoublets is correlated with a lower GUT scale. Especially in the case of six bidoublets we find that the maximal value for the GUT scale is limited to $M_{\text{GUT}} < 10^{16}$ GeV.

We note that in some configurations of class E the see-saw scale M_{IND} is of no phenomenological relevance as they do not contain the coloured superfield F (cf. Table 3.2). Thus, we should break down the model space according to the multiplicity of the F multiplet: zero on the one hand (no see-saw scale), one or three on the other hand.

If there is no field F , the lowest-lying threshold above the SUSY scale is the scale of left-right unification M_{LR} . It turns out that for some configurations this scale can be as low as the SUSY scale. At the other end of the spectrum, the complete unification scale M_{GUT} can vary in the range between 10^9 GeV and 10^{19} GeV. It is not constrained by the low LR scales mentioned above.

In the cases of one or three generations of F , the induced see-saw scale M_{IND} can be as low as the soft SUSY-breaking scale, independent of the GUT scale. The upper bound for the see-saw scale is only fixed by the requirement that it is the lowest-lying scale and is approximately $M_{\text{IND}} \lesssim 10^{16}$ GeV. Thus, many models feature a nearly degenerate unification near the Planck scale.

As mentioned before, there are configurations fixing all scales. These possess three generations of h , Φ , T and one generation of Σ . The multiplicity of E is not fixed. For three generations of E also one or zero generations of T are possible. In these configurations the LR scale is fixed at $M_{\text{LR}} = 7 \times 10^3$ GeV and the PS scale at $M_{\text{PS}} = 10^9$ GeV, which is also approximately the GUT scale.

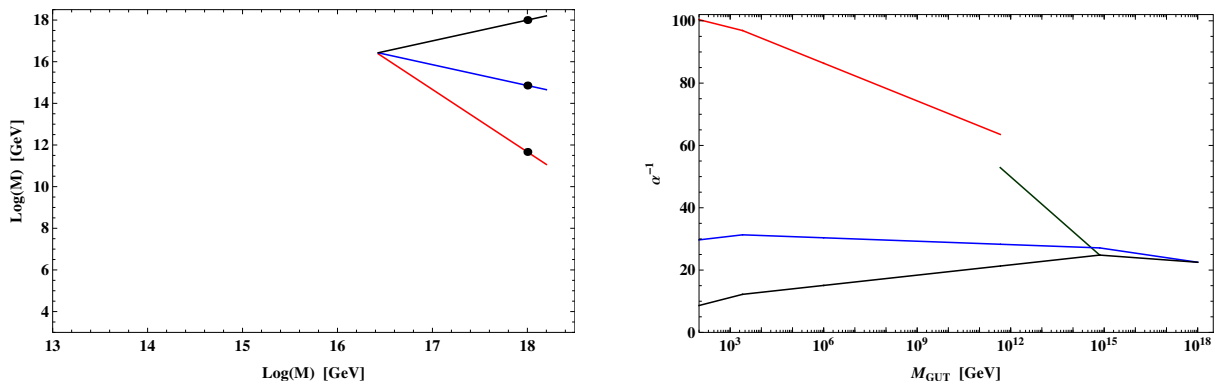
We now consider in somewhat more detail the three particular model types described in Section 3.2.

Type Em: Minimal Model

In class E, the minimal model is the standard MSSM without Higgs⁷, supplemented only by the additional fields Φ and Σ above their respective thresholds. Looking at Table 3.2, we see that this setup does not provide an induced see-saw scale. Hence, the sub-unification scales depend only on one free parameter which we take to be M_{GUT} . Figure 3.3(a) shows the variation of the two other scales, and for comparison M_{GUT} itself, as a function of M_{GUT} .

⁷The electroweak breaking Higgs is contained in Φ .

3. PS-Breaking and Gauge Coupling Unification



(a) Possible variation of scales leading to GCU. The GUT scale is shown in black, the PS scale in blue and the LR scale in red. An induced scale is not present in this type. The black dots indicate the scales for the exemplary plot shown in (b).

(b) Exemplary running of the gauge couplings for complete unification at $M_{\text{GUT}} = 10^{18}$ GeV. The kink in the running corresponds to the SUSY scale. The hypercharge coupling is shown in red, the B-L coupling in green, the weak coupling in blue and the strong coupling in black.

Figure 3.3.: Variation of the unification scales and exemplary running of the gauge couplings for the type Em.

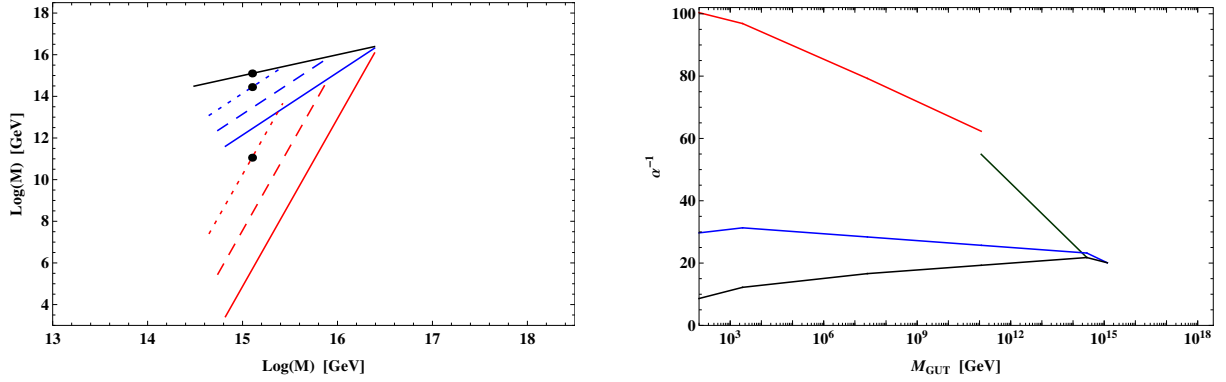
For the value of $M_{\text{GUT}} \approx 3 \times 10^{16}$ GeV all scales approximately coincide. This is the minimal M_{GUT} value for which GCU is possible in this setup. For this particular parameter point, the GUT symmetry (e.g., $SO(10)$) directly breaks down to the MSSM by virtue of $v_{\Sigma} = v_{\Phi}$, so this is actually the standard $SO(10)$ scenario. If we request a larger GUT scale, the PS scale decreases but never drops below $M_{\text{PS}} \gtrsim 10^{14}$ GeV. The left-right unification scale can vary in the range of 10^{11} GeV $\lesssim M_{\text{LR}} \lesssim 10^{16}$ GeV. This includes the favoured mass range for right-handed neutrinos. A sample unification plot is given in Figure 3.3(b).

Type Es: $SO(10)$ -like Models

We now turn to a model with complete $SO(10)$ representations below the GUT scale. With this spectrum we can vary independently M_{IND} and M_{GUT} within a certain range.

It turns out that M_{GUT} cannot reach the Planck scale in this type of model. The maximally allowed value for M_{GUT} depends on M_{IND} and decreases with increasing M_{IND} . The value of M_{IND} , and thus the mass of the colour-triplet fields F , can be as low as the soft SUSY-breaking scale.

Another important difference is that the scales approach each other with increasing M_{GUT} . In Figure 3.4(a) we plot the variation of the sub-unification scales as function of M_{GUT} for three fixed values of M_{IND} (solid $M_{\text{IND}} = 10^{3.4}$ GeV, dashed $M_{\text{IND}} = 10^{5.4}$ GeV and dotted $M_{\text{IND}} = 10^{7.4}$ GeV). Furthermore, we again shown an exemplary unification plot in Figure 3.4(b). The black lines corresponding to M_{GUT} lay on top of each other, as the different choices for M_{IND} solely change the allowed range where M_{GUT} may be varied. For the lowest value of M_{IND} it is possible to have GCU without any sub-unification at $M_{\text{GUT}} \approx 10^{16.4}$ GeV. For larger M_{IND} we see a gap opening between M_{LR} and M_{PS} . However, it is still possible to achieve $M_{\text{PS}} = M_{\text{GUT}}$.



(a) Possible variation of scales leading to GCU. The GUT scale is shown in black, the PS scale in blue and the LR scale in red. The variation in the IND scale is illustrated for discrete choices of M_{IND} : $10^{3.4}$ GeV (solid), $10^{5.4}$ GeV (dashed) and $10^{7.4}$ GeV (dotted). The black dots indicate the scales for the exemplary plot shown in (b)

(b) Exemplary running of the gauge couplings for complete unification at $M_{\text{GUT}} = 10^{15.1}$ GeV. The hypercharge coupling is shown in red, the B-L coupling in green, the weak coupling in blue and, the strong coupling in black.

Figure 3.4.: Variation of the unification scales and exemplary running of the gauge couplings for the type Es.

Type Ee: E_6 -inspired Models

In model of type Ee, we demand three generations of the ‘‘MSSM-like’’ Higgs field h and the coloured field F . Thus, we are able to combine those with the matter fields to a complete **27** representation under E_6 for each generation. In this scenario, GCU is possible over a wide range of mass scales.

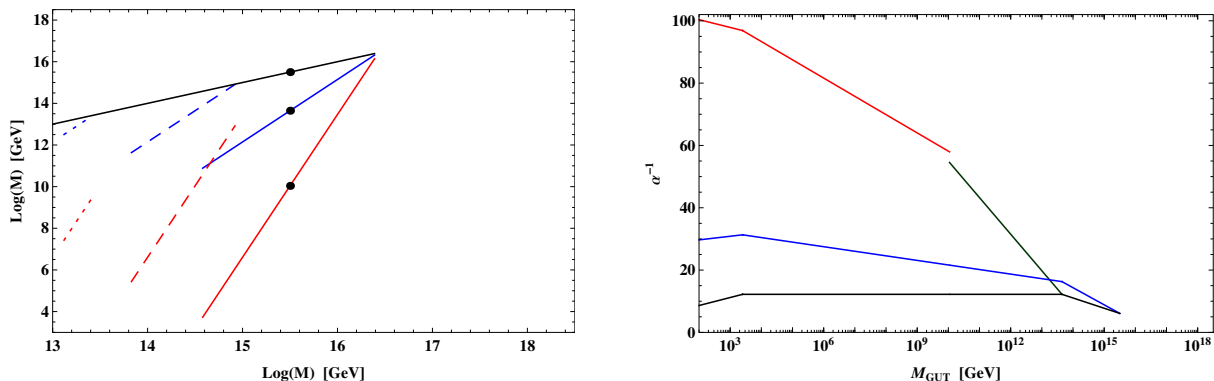
Like in the $SO(10)$ inspired type Es discussed above, the separation between the sub-unification scales decreases with increasing scale M_{GUT} . Over the whole range of M_{IND} it is possible to have PS unification coincide with the complete GCU ($M_{\text{PS}} = M_{\text{GUT}}$). Complete unification at a single scale is possible for $M_{\text{GUT}} \approx 10^{16.4}$ GeV if the scale of light triplets is equal to the soft SUSY-breaking scale, $M_{\text{F}} = M_{\text{SUSY}} = 2.5 \times 10^3$ GeV. This is the well known $SU(5)$ limiting case since all fields of the low energy spectrum can be grouped to complete $SU(5)$ representations.

Compared to the previous two model types, the gauge coupling at the unification point α_{GUT}^{-1} is significantly lower and in some cases approaches the non-perturbative regime. In Figure 3.5 we show the variation of scales and an exemplary unification plot.

3.6.3. Class F: $\mathbf{v}_{\text{T}} \neq \mathbf{0}$ and $\mathbf{v}_{\Sigma} = \mathbf{0}$

This class has a more restricted phenomenology than the other classes. Nevertheless, it contains some models that exhibit GCU. In class-F models, $SU(2)'$ and thus the LR symmetry is broken above the scale where $SU(4)$ reduces to colour. We therefore might expect tighter relations between lepton- and quark-flavour mixing. The relevant scales of this class are, in ascending order: the see-saw induced scale M_{IND} , the quark-lepton unification

3. PS-Breaking and Gauge Coupling Unification



(a) Possible variation of scales leading to GCU. The GUT scale is shown in black, the PS scale in blue and the LR scale in red. The variation in the IND scale is illustrated for discrete choices of M_{IND} : $10^{7.4}$ GeV (solid), $10^{5.4}$ GeV (dashed) and $10^{7.4}$ GeV (dotted). The black dots indicate the scales for the exemplary plot shown in (b).

(b) Exemplary running of the gauge couplings for complete unification at $M_{GUT} = 10^{15.1}$ GeV. The hypercharge coupling is shown in red, the B-L coupling in green, the weak coupling in blue and the strong coupling in black.

Figure 3.5.: Variation of the unification scales and exemplary running of the gauge couplings for the type Ee.

scale M_{QL} , the PS scale M_{PS} and the unification scale M_{GUT} .

$$F : M_{SUSY} \leq M_{IND} \leq M_{QL} \leq M_{PS} \leq M_{GUT} \quad (3.25)$$

Again, we take M_{IND} and M_{GUT} as free scales and vary these. Table 3.2 indicates that all models in this class do have the additional see-saw scale M_{IND} as T' and thus T is always included. The intermediate scales tend to be higher than in class E.

Out of the 216 configurations of class F only 29 configurations are consistent with GCU. In all cases, M_{GUT} can be as large as the Planck scale.

As discussed in the general overview, light degrees of freedom are not possible in this class. The minimal value of M_{IND} is strongly dependent on the number of $SU(2)$ triplets. In the case of three triplets it is strictly larger than 10^{16} GeV. Thus, we look at the configurations with only one generation of T . In these configurations, M_{IND} has to be larger than $M_{IND} \gtrsim 10^6$ GeV. The lower bound is realised for three generations of F and rises if a fewer number of fields F are included.

We conclude that in class F the extra fields may play a role for flavor physics in an intermediate energy range but are unlikely to be observable at collider experiments. We now again take a look at the predefined models stated in Section 3.2.

Type Fm: Minimal Model

The minimal model of class F contains the superfields Φ and $T^{(\prime)}$ in addition to the MSSM matter spectrum.

In models of this type, the lowest possible see-saw mass value is $M_{IND} \approx 10^{12}$ GeV and the LR scale is bounded from below by $M_{LR} \gtrsim 10^{15}$ GeV. Thus these are ruled out, since the

mass of the electroweak symmetry breaking Higgs h_Φ is associated to the LR scale. As it does not include a light Higgs candidate, it is not contained in the scan and the general overview. A next to minimal setup explicitly including one generation of h is not able to produce GCU.

Type Fs/Fe

A model of type Fs is not consistent with GCU. This is because α_3^{-1} grows too fast and overshoots α_2^{-1} before the condition (3.17) for a possible QL scale can be fulfilled. Likewise, a model of type Fe consistent with GCU is not possible.

Model F189: Flavour-Symmetry Inspired Model

In the absence of the previous types we take a look at a configuration which might be viewed as E_6 -inspired. However, instead of the three generations of h we include only a single and assume that the other two bidoublets get GUT scale masses by some unspecified mechanism. Such a setup is realised in model F189⁸. For this setup, unification is possible over a wide range of mass scales. There is a strong correlation of M_{IND} and M_{GUT} . Thus, we can choose the only relevant free parameter to be M_{IND} . It can vary between 10^7 GeV $\lesssim M_{\text{IND}} \lesssim 10^{16}$ GeV. For its largest allowed value all scales are approximately equal which is the $SO(10)$ limiting case. Conversely, the lowest possible M_{IND} value corresponds to GUT unification near the Planck scale. In any case, the QL, the PS and the GUT scales are nearly degenerate. Thus, we do not show a plot of the variation of the scales or a sample unification plot.

As mentioned above, there is no possible configuration leading to GCU with three generations of the field h .

3.6.4. Classes A to D: $\mathbf{v}_T \neq 0$ and $\mathbf{v}_\Sigma \neq 0$

In the classes A to D, we effectively combine model classes E and F. There are five different scales in class B and C, two of which are fixed by requiring GCU. For concreteness, we also fix $M_{\text{GUT}} = 10^{18.2}$ GeV, i.e. we assume complete unification at the Planck scale. Still, we can choose two parameters independently and obtain allowed and forbidden regions but no one-to-one correspondences. In addition to M_{IND} , we chose (for technical reasons) M_{QL} as free scale in class C although it is not the largest free scale. In class B we vary M_{IND} and M_{PS} in line with the former setups. As mentioned earlier, class A and D represent limiting cases and are thus not discussed in detail. The ordering of scales in the other two scenarios is

$$B : M_{\text{SUSY}} \leq M_{\text{IND}} \leq M_{\text{U1}} \leq M_{\text{LR}} \leq M_{\text{PS}} \leq M_{\text{GUT}} \equiv M_{\text{Planck}}, \quad (3.26)$$

$$C : M_{\text{SUSY}} \leq M_{\text{IND}} \leq M_{\text{U1}} \leq M_{\text{QL}} \leq M_{\text{PS}} \leq M_{\text{GUT}} \equiv M_{\text{Planck}}, \quad (3.27)$$

where M_{U1} indicates the mass scale where the extra $U(1)$ groups break down to hypercharge. This is the natural scale for a Majorana mass term of the right-handed neutrinos as such a term breaks both $B - L$ and right-handed isospin. Further below this scale is the induced see-saw scale M_{IND} which we again constrain to be above the soft SUSY breaking scale M_{SUSY} . The labels LR and QL refer to $SU(2)'$ (left-right) and $SU(4)$ (quark-lepton) symmetry breaking, respectively.

⁸For the meaning of the label numbering the models we refer to Appendix A.1.

3. PS-Breaking and Gauge Coupling Unification

Of the 144 configurations in classes B and C, 18 (B) and 57 (C) are consistent with GCU. We again observe that the number of T generations has a strong impact on the lowest mass scale. If there is only one generation of T , the value of M_{IND} can approach the SUSY scale independently of the number of F in both classes. The situation differs drastically when considering three generations of T . Here, the minimal value for M_{IND} additionally depends crucial on the number of generations of the field F . In class C, it ranges from $M_{\text{IND}} \gtrsim 10^{15}$ GeV (no F) down to $M_{\text{IND}} \gtrsim 10^6$ GeV (three F generations). In class B the situation is even worse. Here GCU is not possible with less than three generations of the field F . Even in this case its lowest value $M_{\text{IND}} \gtrsim 10^{10}$ GeV is above the corresponding one of class C.

Type Bm/Cm: Minimal Model

In the minimal model, there is a single generation of each of the fields Φ , $T^{(i)}$ and Σ . For both Bm and Cm GCU is possible. However, the lowest scale is limited to rather high values of $M_{\text{IND}} \gtrsim 10^{13}$ GeV (type Bm) and $M_{\text{IND}} \gtrsim 10^{10}$ GeV (type Cm), respectively. Since we again do not explicitly add an electroweak symmetry breaking Higgs, both minimal setups are ruled out. Again, they are not in the scan and overview as they do not feature a light Higgs candidate. Moreover, if we explicitly include one generation of h , GCU can no longer be achieved.

Types Bs/Cs and Be/Ce

Again, these setups do not allow for GCU.

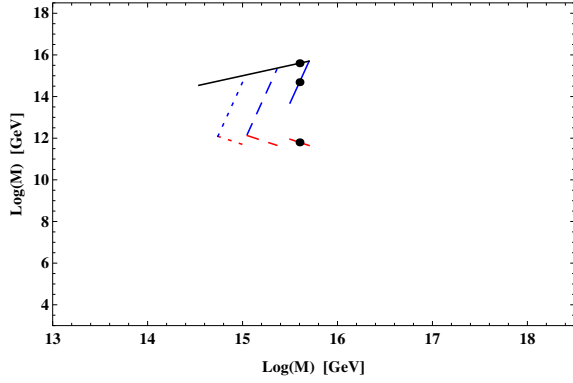
Class-B/C Models with $M_{\text{IND}} < 10$ TeV

We may ask for configurations which results in setups where the see-saw scale is sufficiently low (say $M_{\text{IND}} < 10$ TeV) so that the new particles can have an impact on collider phenomenology. We find 8 (34) models where this is possible within class B (C). One configuration within class B is model B199, where we consider three copies of h , F and Σ , one generation of Φ and T and no multiplet E . In class C there is a similar model C211, which has the same spectrum, but three copies of Φ . The corresponding plots are shown in Figures 3.6, 3.7.

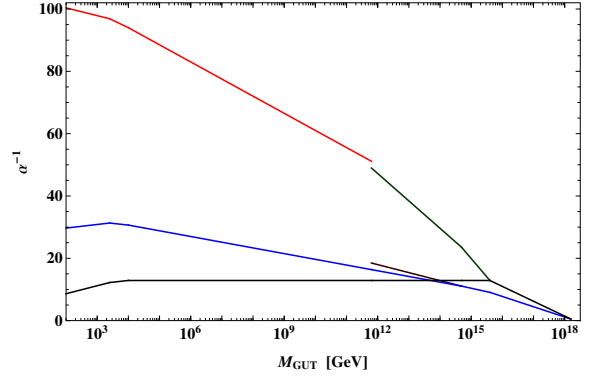
3.7. Unification Without Supersymmetry

We now turn to scenarios without supersymmetry. Here, the same classes of models as in the supersymmetric case are considered, omitting the fermionic superpartners of the additional multiplets. The same is done with the fermionic superpartners of matter and gauge fields. Here, it is not our aim to present a detailed analysis, as we have done in the SUSY case, but rather to provide an insight into the GCU of non-supersymmetric PS models. Hence, we do not construct a scalar potential for the fields given in Table 3.1, which would contain more free parameters and terms, and derive the corresponding masses for the scalar fields from it here. Instead, we assume that the masses of all scalar fields coincide with those of the corresponding superfields as mentioned in Section 3.4. Also we do not discuss

3.7. Unification Without Supersymmetry

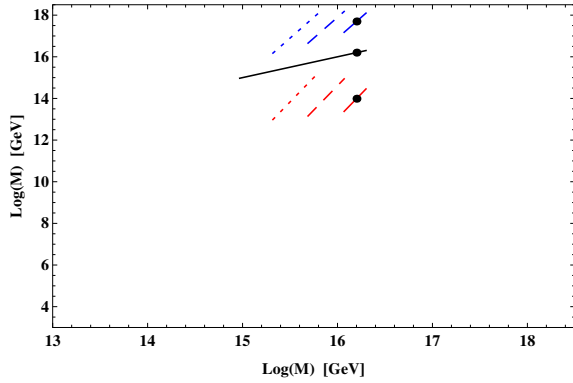


(a) Possible variation of scales leading to GCU. The PS scale is shown in black, the LR scale in blue and the MSSM scale in red. The variation in the IND scale is illustrated for discrete choices of M_{IND} : 10^4 GeV (solid), 10^7 GeV (dashed) and 10^{10} GeV (dotted). The black dots indicate the scales for the exemplary plot shown in (b).

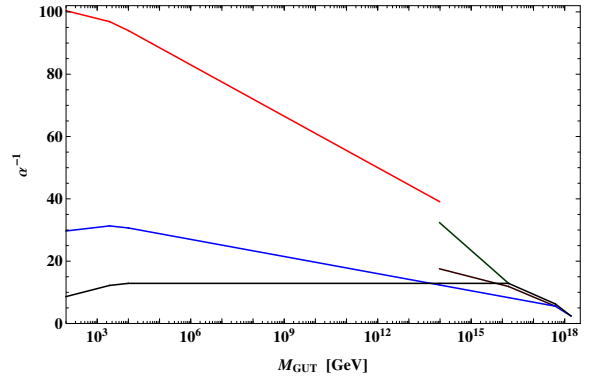


(b) Exemplary running of the gauge couplings for complete unification at $M_{\text{GUT}} = 10^{18.2}$ GeV. The hypercharge coupling is shown in red, the $U(1)'$ coupling in brown, the B-L coupling in green, the weak coupling in blue and the strong coupling in black.

Figure 3.6.: Variation of the unification scales and exemplary running of the gauge couplings for the type B199.



(a) Possible variation of scales leading to GCU. The QL scale is shown in black, the PS scale in blue and the MSSM scale in red. The variation in the IND scale is illustrated for discrete choices of M_{IND} : 10^4 GeV (solid), 10^7 GeV (dashed) and 10^{10} GeV (dotted). The black dots indicate the scales for the exemplary plot shown in (b).



(b) Exemplary running of the gauge couplings for complete unification at $M_{\text{GUT}} = 10^{18.2}$ GeV. The hypercharge coupling is shown in red, the $U(1)'$ in brown, the B-L in green, the weak in blue and the strong coupling in black.

Figure 3.7.: Variation of the unification scales and exemplary running of the gauge couplings for the type C211.

3. PS-Breaking and Gauge Coupling Unification

any aspects of naturalness inevitably appearing when multiple scalar fields have masses at different scales. Furthermore, the meaning of scales and symmetry breaking patterns do not need be changed as they do not depend on the assumption of SUSY. Similarly, the unification conditions themselves are equal in both cases. Only the coefficients of the running couplings are adapted to the non-supersymmetric case as explained in Appendix A.4. The aforementioned assumptions may be *ad hoc* but allow us to compare supersymmetric and non-supersymmetric models in a meaningful way.

Next to the adjustments mentioned so far we have to adopt the GUT-scale fixing of the classes B and C. The value of $M_{\text{GUT}} = 10^{18.2}$ GeV which we used to fix an additional scale in the SUSY classes B and C allows only for one configuration (class C) that satisfies GCU in the non-SUSY case. Thus, we lower the GUT-scale fixing to $M_{\text{GUT}} \equiv 10^{16}$ GeV as we generally find lower mass thresholds than in the supersymmetric case. Lowering this scale further would allow for GCU in even more configurations but is disfavoured by the proton lifetime.

Successful GCU

We study the same set of 828 configurations constructed in the previous section with the assumptions stated above. Again, more than half of the configurations allow for GCU. As in the SUSY case, most of them belong to class E. Classes B and C are still disfavoured but not excluded. However, now also most configurations of class F satisfy the condition of GCU. In any case lower GUT scales tend to be favoured.

New Light Scalar Particles

In the non-SUSY setup the possible light $SU(2)$ or colour triplets are pure scalar fields. These may be stable, if we do not assume any additional couplings to the SM fermions.

Similar to the SUSY case, we find quite a range for light colour triplets F in the TeV-range, most of which belong to class E. There is also quite some range for light colour triplets accompanied by one generation of light T in class F. However, this lowers the maximally allowed GUT scale to $M_{\text{GUT}} \lesssim 10^{16}$ GeV in most of the cases. In class E three generations of F are preferred while class F has an equal number of configurations with one and three generations.

Moreover, we find that three generations of light (TeV-range) $SU(2)$ triplets T are excluded. In particular, in class F the lower bound for those is $M_T \gtrsim 10^8$ GeV. In class C, the bound becomes 10^{11} GeV and in class B there is no GCU at all.

Multiple Light Higgs

In models of class E we find roughly one third of configurations in which the MSSM Higgs is not part of h but rather of the multiplet h_Φ (see Section 3.4.2). Similar to the SUSY case it is very unlikely or even impossible to find more than one generation of light bidoublets in class C or B, respectively. Also for class E we find similar result as in the SUSY case. Again, most configurations prefer four generations, one, two and three are equally likely and six are disfavoured. In contrast to the previous considerations there are now plenty of configurations of class F with three generations of bidoublets h . However, one is still favoured here. Again we observe that increasing the multiplicity of bidoublets lowers the maximal unification scale.

Right-Handed Neutrino Scale

Similar to the SUSY models we observe a LR symmetry breaking scale roughly around $M_{\text{LR}} \sim 10^{13}$ GeV in a large fraction of the successful configurations. To be precise, most of the configurations in class B, C and E feature such a neutrino scale. In class F still 60 percent allow for neutrinos in the range 10^{12} GeV $< M_{N_R} < 10^{14}$ GeV. Nevertheless, there are configurations where this scale can be much lower and even reaches down to below 100 TeV in some cases.

Correlated M_{IND}

Again, we find that constraining the induced scale M_{IND} does not change the results very much. Thus, we see our assumptions justified to include this scale as a free parameter in our scans.

Scales Fixed by GCU

In the non-supersymmetric case we again find in all classes some configurations in which all mass scales are “exactly” fixed. This usually corresponds to degenerate mass scales. A common scale for such classes is $M_{\text{GUT}} \approx 10^{14}$ GeV.

Gauge Coupling at M_{GUT}

A general feature of non-SUSY spectra is the fact that the high-energy effective values of the gauge couplings are larger than in the SUSY case. This is due to the lower number of fields that contribute to the running of the gauge-couplings.

An overview of the non-supersymmetric statistics can be found in Table 3.4. We now consider the classes separately. However, we will not repeat a discussion as detailed as the one in the SUSY section but only give a short specific overview for each class. In addition we present for each class one selected configuration that we find denotative.

3.7.1. Class E

Again, class E features most allowed configurations which is why we start our discussion with it. For class E it is possible to implement GCU in 230 configurations, of which only 23 provide a complete unification near the Planck scale. Similar to the supersymmetric case, we find 88 configurations where the electroweak symmetry breaking Higgs is provided by Φ . On the other hand, an interesting possibility is the existence of three generations of h (type Ee) although there is no direct relation to E_6 unification without SUSY. Such configurations are allowed by the constraint of GCU whereby the GUT scale can vary between 10^{14} GeV $\lesssim M_{\text{GUT}} \lesssim 10^{17}$ GeV. One possible configuration exhibits three generations of F , one of Σ and Φ each and no fields E or T . For this special configuration the variation of the scales and a unification plot is shown in Figure 3.8. We find, that the variation of the LR scale strongly depends on the GUT scale. The PS scale varies only weakly and is always close to the GUT scale.

3. PS-Breaking and Gauge Coupling Unification

	class B	class C	class E	class F	Σ
scanned	144	144	324	216	828
GCU	10	30	230	201	471
$M_{\text{GUT}} > 10^{16}$ GeV	10	30	111	16	167
$M_{\text{IND}} < 10$ TeV & $M_{\text{GUT}} > 10^{16}$ GeV	1	8	110	16	135
multiple light Higgs	0	3	171	67	241
$M_{\text{LR}} < 100$ TeV	0	0	136	0	136
10^{12} GeV $< M_{N_R} < 10^{14}$ GeV	9	30	211	126	376
$M_{\text{IND}} \in [0.1, 10] \frac{v_\Phi^2}{v_\Sigma + v_T}$	10	12	201	93	342

Table 3.4.: The Number of configurations fulfilling certain conditions within the non-SUSY framework.

3.7.2. Class F

In class F there are now plenty of configurations leading to successful GCU. In general we find that there is not much room for scale variation. The GUT scale can be as large as $M_{\text{GUT}} \approx 10^{17}$ GeV. The scales M_{QL} , M_{PS} and M_{GUT} are close to each other since the lightest of these scales is fixed to be larger than $M_{\text{QL}} \gtrsim 10^{13}$ GeV. However, the induced see-saw scale can be as light as the SUSY scale. There are also configurations with GCU where all scales are essentially fixed and not far from the GUT scale. Those lead to $M_{\text{GUT}} \approx 2 \times 10^{14}$ GeV which is rather low.

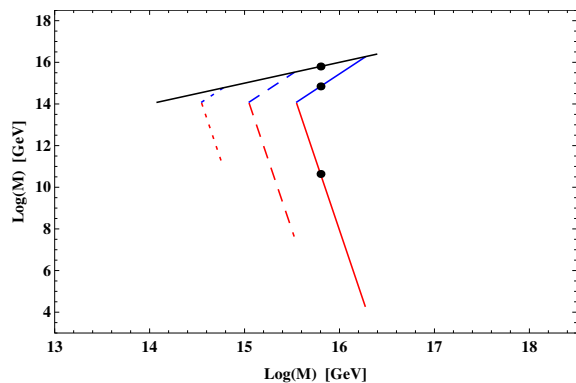
One exemplary configuration leading to GCU above 10^{16} GeV is model F213. Here, we have three generations of F and one of T . These scalar particles can be rather light, potentially as low as the SUSY scale. In addition, this model contains three generations of the fields Φ and Σ and one generation of E . We show the possible scale variation and a sample unification plot for this model in Figure 3.9.

3.7.3. Class A to D

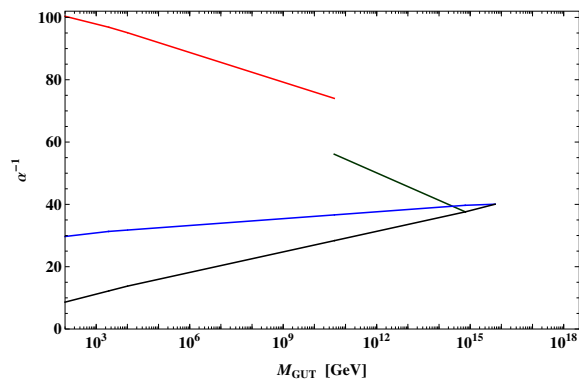
The classes A to D are still disfavoured. Nevertheless, we find 30 (10) configurations allowing for GCU in class C (B). However, this requires to lower the scale of complete unification which we fix in these classes to $M_{\text{GUT}} = 10^{16}$ GeV. In class C, the QL scale emerges typically close the PS scale. Likewise, the PS scale can become as large as the GUT scale such that the energy range with pure PS symmetry may vanish.

Looking at the possibility of three Higgs generations, we do not find any configurations in class B and only a few in class C. On the other hand, these model classes favour three generations of Φ .

3.7. Unification Without Supersymmetry

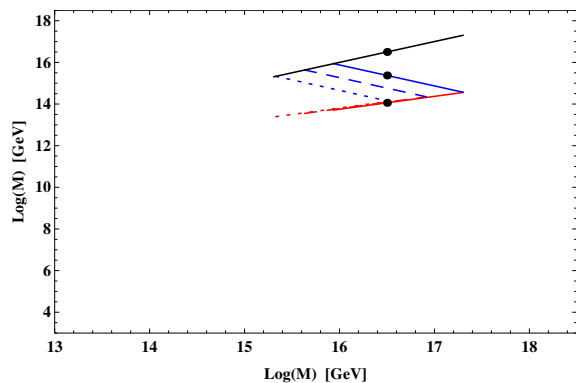


(a) Possible variation of scales leading to GCU. The GUT scale is shown in black, the PS scale in blue and the LR scale in red. The variation in the IND scale is illustrated for discrete choices of M_{IND} : 10^4 GeV (solid), 10^7 GeV (dashed) and 10^{10} GeV (dotted). The black dots indicate the scales for the exemplary plot shown in (b).

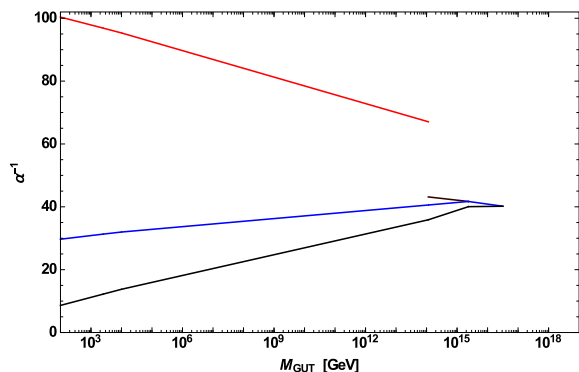


(b) Exemplary running of the gauge couplings for complete unification at $M_{\text{GUT}} = 10^{15.8}$ GeV. The hypercharge coupling is shown in red, the B-L coupling in green, the weak coupling in blue and the strong coupling in black.

Figure 3.8.: Variation of the unification scales and exemplary running of the gauge couplings for the non-SUSY type Ee.



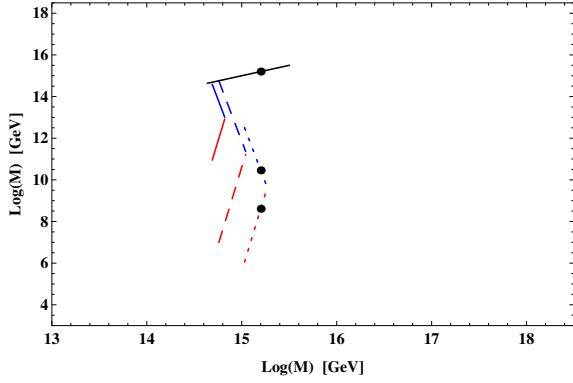
(a) Possible variation of scales leading to GCU. The GUT scale is shown in black, the PS scale in blue and the QL scale in red. The variation in the IND scale is illustrated for discrete choices of M_{IND} : 10^4 GeV (solid), $10^{8.5}$ GeV (dashed) and 10^{13} GeV (dotted). The black dots indicate the scales for the exemplary plot shown in (b).



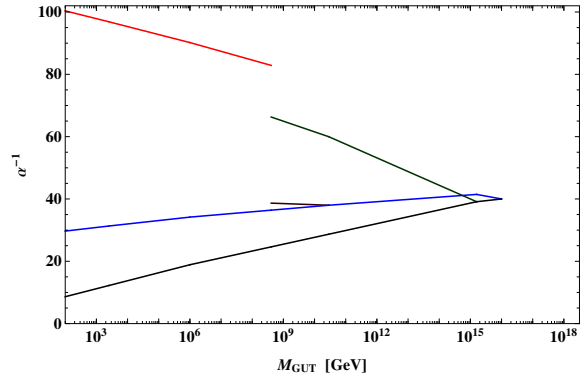
(b) Exemplary running of the gauge couplings for complete unification at $M_{\text{GUT}} = 10^{16.5}$ GeV. The hypercharge coupling is shown in red, the $U(1)'$ coupling in brown, the weak coupling in blue and the strong coupling in black.

Figure 3.9.: Variation of the unification scales and exemplary running of the gauge couplings for the type non-SUSY F213.

3. PS-Breaking and Gauge Coupling Unification

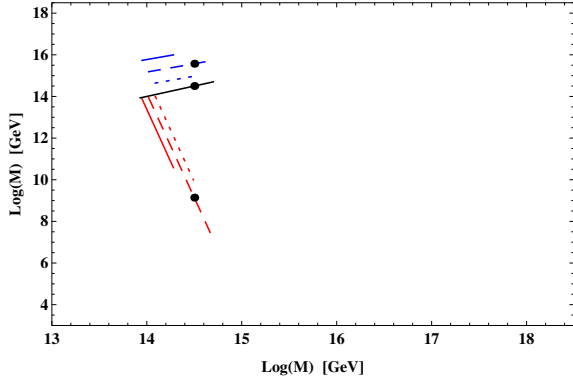


(a) Possible variation of scales leading to GCU. The PS scale is shown in black, the LR scale in blue and the MSSM scale in red. The variation in the IND scale is illustrated for discrete choices of M_{IND} : 10^4 GeV (solid), 10^5 GeV (dashed) and 10^6 GeV (dotted). The black dots indicate the scales for the exemplary plot shown in (b).

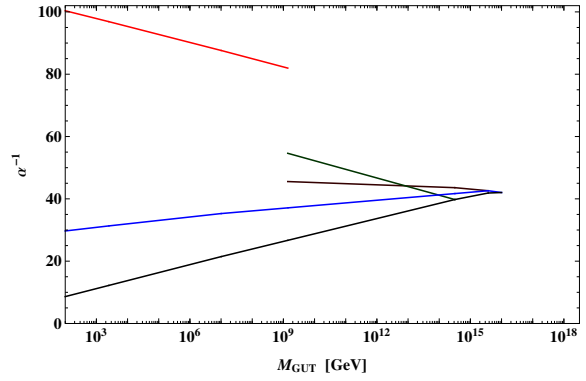


(b) Exemplary running of the gauge couplings for complete unification at $M_{\text{GUT}} = 10^{16}$ GeV. The hypercharge coupling is shown in red, the $U(1)'$ coupling in brown, the B-L coupling in green, the weak coupling in blue and the strong coupling in black.

Figure 3.10.: Variation of the unification scales and exemplary running of the gauge couplings for the non-SUSY type B53.



(a) Possible variation of scales leading to GCU. The QL scale is shown in black, the PS scale in blue and the MSSM scale in red. The variation in the IND scale is illustrated for discrete choices of M_{IND} : 10^4 GeV (solid), 10^7 GeV (dashed) and 10^{10} GeV (dotted). The black dots indicate the scales for the exemplary plot shown in (b).



(b) Exemplary running of the gauge couplings for complete unification at $M_{\text{GUT}} = 10^{16}$ GeV. The hypercharge coupling is shown in red, the $U(1)$ coupling in brown, the B-L coupling in green, the weak coupling in blue and the strong coupling in black.

Figure 3.11.: Variation of the unification scales and exemplary running of the gauge couplings for the non-SUSY type C45.

In Figure 3.10 and Figure 3.11, we display the scale relations and gauge-coupling unification for two distinct models; B53 and C45. The former contains three generations of F which can be as light as a few TeV. In addition it contains three generations of E and one generation of all other fields. We find quite some range for scale variation here. For the largest value of the PS scale ($M_{\text{PS}} \approx 10^{15}$) we find a degeneracy of all lower scales. Model C45 also features new particles at the TeV scale. Here we include three generations of Φ and Σ and one generation of all other fields. We again find quite some space to vary the scales.

3.8. Summary

In this chapter we have presented a survey of models with respect to gauge coupling unification that contains multiple intermediate scales. These correspond to left-right symmetry, quark-lepton unification, Pati-Salam symmetry and complete gauge coupling unification (e.g. $SO(10)$) as well as an additional induced scale. The order of these scales depends on the hierarchy of the PS breaking vevs, where we have identified four interesting classes. We have studied supersymmetric models in detail and also considered non-supersymmetric models which we have deduced from the former ones.

We have obtained our set of configurations following simple construction principles which allow for only a small set of PS multiplets consistent with unification *à la* $SO(10)$ or E_6 . For these we have limited ourselves to the smallest representations. Moreover, we did not demand all fields to be present in the low-energy theory. On the other hand, we have allowed all of them to appear in three generations similar to the fermion fields. We have allowed for multiple breaking paths (classes) leading to different intermediate scales with varying interpretations.

The constraints imposed from gauge coupling unification are not sufficient to fix all scales to numerical predictions. Instead, we have deduced characteristic patterns of scales in the models and correlated them to specific choices for the particle content and classes.

For a large fraction of these configurations we find the possibility for gauge coupling unification with additional intermediate scales. In general, the supersymmetric setup allows for larger variations of the scales, especially when asking for a complete unification above $M_{\text{GUT}} > 10^{16}$ GeV. Nevertheless, the non-supersymmetric setup allows for more configurations. In particular, the possibility of breaking the left-right symmetry above the quark-lepton symmetry opens up. This breaking path is strongly constrained in the SUSY setup.

In a wide range of supersymmetric models complete gauge coupling unification can be pushed up to the Planck scale. This fact, together with the properties of PS symmetry, significantly reduces the tension that the non-observation of proton decay can put on GUT model building. In the non-supersymmetric case we are way more constrained but still find quite a range of models with GUT scales above 10^{16} GeV.

We focused on models with intermediate scales which are well below the GUT scale and can be associated to quark-lepton or left-right symmetry breaking. As such, they are important for the generation of the flavour sector and decouple the issues of flavour from gauge coupling unification. Although we have not discussed the flavour sector in this chapter, this fact may

3. *PS-Breaking and Gauge Coupling Unification*

be useful for models where we construct the flavour sector explicitly. We will come back to this issue in the following chapters.

As an extra feature, the different stages of gauge symmetry breaking can yield the generation of a small see-saw like suppressed mass scale. The masses of certain particles, including SM-like Higgs doublets and new exotic (s)quarks, are determined by this scale and may thus be accessible at colliders. On the other hand, $SU(2)'$ triplets tend to raise the left-right-symmetry scale above the scale of quark-lepton unification and may thus enforce a direct relation between quark and lepton flavour physics.

Another generic property of the models under consideration is that the scale of left-right symmetry breaking, naturally associated with the generation of neutrino masses, is within an intermediate mass range. A neutrino mass scale significantly below the GUT scale is favoured by numerical estimates of see-saw mechanisms that explain the smallness of the observed neutrino masses. We will make use of this option in the following chapters.

In addition, we encounter configurations which allow for a multi-Higgs doublet model at the low scale. Furthermore, the observable Higgs doublet need not be a member of a $(\mathbf{1}, \mathbf{2}, \mathbf{2})$ representation as often assumed, but can also originate from a $(\mathbf{4}, \mathbf{2}, \mathbf{1}) + \text{c.c.}$ representation, i.e. behave as a scalar lepton. The effective μ term, which sets the scale for low-energy Higgs physics, can be naturally suppressed due to the newly introduced see-saw like mass scale. The possibility of three generations of h will be discussed explicitly in the next chapter when we construct a realisation of flavour through non-renormalisable terms.

Effective Theory of Flavour

High-Energy Yukawa Generation

In this chapter we discuss one possible way of including a theory of flavour in a Pati-Salam symmetric Grand Unified Theory. Within this framework we introduce a gauged flavour symmetry which is spontaneously broken at a high scale by vacuum expectation values of scalar fields, the so-called flavons. The flavons couple to the SM Yukawa sector through non-renormalisable operators. The SM flavour hierarchies are generated by multiple insertions of the flavons. Thus, we do not restrict ourselves to renormalisable operators like we did in the previous chapter.

Such a setup was first discussed by Froggatt and Nielsen in 1979 [119], where the flavour symmetry was a simple $U(1)_{\text{FN}}$. Since then this concept has been extended to non-abelian flavour symmetries and has been widely discussed in the literature. In this chapter we consider a single $SU(3)_F$ flavour symmetry. Similar models have already been studied for example in [51, 120–125]. However, the key feature of our model is that we consider three Higgs generations transforming non-trivially under the flavour symmetry. Such a model is in line with a further unification of all low energy representations à la E_6 as discussed in the previous chapter.

We start the chapter by setting the stage for the model. Then, we discuss an explicit realisation with triplet flavons. Afterwards we consider larger representations for the flavons to see if the setup can be simplified. As a result, we study a realisation with decuplet flavons. We conclude the chapter with a short summary and address several aspects of the model which we find relevant to discuss further in future studies.

The main results of this chapter have already been published in Reference [B].

4.1. Model Framework

As discussed above, the complete gauge symmetry we start with is

$$SU(4) \times SU(2) \times SU(2)' \times Z_2 \times SU(3)_F. \quad (4.1)$$

Here, we consider solely a supersymmetric setup, as SUSY provides many simplifying features when considering GUT models (cf. Section 1.3).

We study the particular case of three Higgs generations [126–128] which can be associated with a flavour symmetry [129–131]. This structure may arise in a supersymmetric GUT where

4. Effective Theory of Flavour

electroweak Higgs and matter fields are unified in a single representation [48, 132]. The three generations of Higgs bidoublets transform as fundamental triplet under the gauged $SU(3)_F$ symmetry similar to the matter fields. Next to the MSSM particle content with enlarged Higgs sector, we introduce new scalar fields transforming solely under the flavour symmetry. These acquire vevs at some high scale thereby breaking the flavour symmetry completely.

Relation to the Model Scan

The models presented in this chapter are an extension for a subset of models considered in Chapter 3 that explicitly construct a phenomenologically viable flavour sector. Here, we study the special case of three generations of the MSSM Higgs bidoublet h transforming in the fundamental representation of the flavour symmetry. Such an assumption is supported by the scan where we found plenty of such configurations consistent with complete gauge coupling unification. Moreover, we include only additional superfields that transform trivially under the PS symmetry and therefore do not spoil the unification properties. As we use only a part of the particle content introduced in Table 3.1, we assume the remaining fields not to couple to the flavour sector. This can be achieved for example by introducing an additional (discrete) symmetry.

We consider the PS symmetry to be valid at an arbitrary but large GUT scale, which is (at least partially) broken in the large energy region. In this chapter we do not construct such a breaking explicitly but refer to the considerations of the previous chapter. As already discussed there, a renormalisable setup may not be sufficient to generate the observed flavour structure in PS models (cf. Section 3.4.4). Therefore, we drop the assumption of renormalisability in this chapter and particularly make use of non-renormalisable terms. In Chapter 5, we again constrain ourselves to renormalisable terms and show that a viable flavour sector can be generated when introducing additional fermionic fields.

General Flavour Structure

The model is an effective theory expanded in some large but unspecified mass scale M . Hence, we have to additionally take into account all non-renormalisable terms which are not forbidden by symmetry or by explicit constraints on the low-energy effective theory. This allows in general mass terms for those components of the flavon superfields that are not absorbed as Goldstone bosons into massive flavour-gauge bosons. Generically, we denote the ratio of any flavon vev $\langle\phi\rangle$ and the expansion scale M by ϵ ;

$$\epsilon = \frac{\langle\phi\rangle}{M}. \quad (4.2)$$

We assume that ϵ distinguishes the up- from the down sector ($\epsilon_d \neq \epsilon_u$) and also allow for a third distinct expansion parameter ϵ_ν in the neutrino sector. Such differences are expected in the effective superpotential as a consequence of the breaking of the PS gauge symmetry, in particular from the left-right symmetry breaking. Here, we do not consider this breaking any further. General considerations on PS breaking can be found in the previous chapter.

The aim of this setup is to generate the hierarchies of the Yukawa matrices in powers of ϵ and thus from multiple insertions of flavons ϕ . The vev of a single flavon should not contain

an inner hierarchy, i.e. the components of the vev should either be zero or of similar size. However, in contrast to the simplest ansatz of Froggatt and Nielsen, the different flavons may have hierarchical vevs, i.e. $\langle \phi' \rangle \gg \langle \phi \rangle$. Such hierarchies are necessary to generate a successive breaking of the flavour symmetry. In addition, they simplify the structure of the model as lower dimensional operators suffice to generate the hierarchical pattern.

A qualitative picture of the scales in the model is shown in Figure 4.1 where explicit values are for illustrative purpose only and should not be taken at face value.

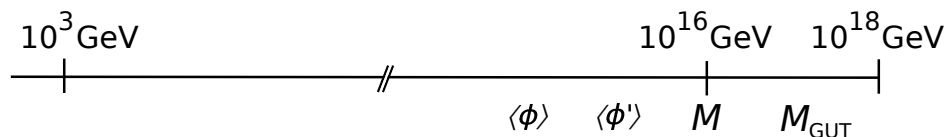


Figure 4.1.: Visualisation of the scales of the model (Numerical values for illustrative purposes only).

With these basic building blocks at hand we intend to reproduce the low-energy flavour structure of the SM. Here, we are interested in the general structure of the Yukawa matrices rather than their explicit values. Effective Yukawa matrices exhibiting the hierarchical structure

$$Y_{u,d} \approx \begin{pmatrix} 0 & O(\epsilon_{u,d}^3) & O(\epsilon_{u,d}^3) \\ O(\epsilon_{u,d}^3) & O(\epsilon_{u,d}^2) & O(\epsilon_{u,d}^2) \\ O(\epsilon_{u,d}^3) & O(\epsilon_{u,d}^2) & O(1) \end{pmatrix} y_{t,b}, \quad (4.3)$$

with $\epsilon_u \approx 0.05$ and $\epsilon_d \approx 0.15$ can accommodate the observed CKM matrix and the quark-mass hierarchies [133]. This structure of the Yukawa matrices should hold at the unification scale and hence, we may generate it by the vevs of the flavon fields. In order to compare (4.3) with the SM Yukawa matrices we have to calculate their evolution with energy corresponding to the renormalisation group equations from the GUT scale down to the electroweak scale. Such a discussion is beyond the scope of this work as we are only interested in approximate structures. More details on the energy behaviour of the Yukawa couplings can be found in e.g. [102, 103].

As discussed in Section 2.3, the structure of the lepton mixing matrix U_{PMNS} is strongly affected by right-handed neutrinos due to the see-saw mechanism. Therefore, one possibility to account for the neutrino sector is to generate a Majorana mass matrix for the right-handed neutrinos. For the Yukawa structure given above, sequential right-handed neutrino dominance (SRHND) [95] is able to implement a phenomenologically viable PMNS mixing matrix and mass hierarchy in the neutrino sector [51]. A short introduction in this mechanism and conditions of applicability can be found in Section 2.3.3. The main concept is that a single right-handed neutrino gives the main contribution to the 23 block, while a second right-handed neutrino is required to give subdominant contributions to generate the full effective neutrino mass matrix.

Trivial Yukawa Structure

Before considering explicit realisations of such a model, we discuss one particularly important operator occurring generically in any such construction. The appearance of this

4. Effective Theory of Flavour

operator is a direct consequence of the fact that we consider the Higgs bidoublet to transform as flavour triplet. It will be relevant for later discussions as it is one major reason to study non-fundamental flavon representations.

Starting with the gauge symmetry (including flavour) of (4.1), we identify a single renormalisable dimension 3 Yukawa term in the superpotential¹,

$$Y_0 = \varepsilon^{ijk} \Psi_{L,i} \Psi_{R,j} h_k, \quad (4.4)$$

where ε^{ijk} is the three dimensional Levi-Civita-Tensor. This term is special in the sense that no insertion of a flavon vev is needed. It is similar to the usual MSSM Yukawa term but with an anti-symmetric Yukawa matrix. Thus, it generates a coupling that is non-diagonal among the lepton and quark generations. This results in a Yukawa structure with one vanishing and two degenerate entries. It cannot be the dominant contribution to the Yukawa matrix as phenomenologically the top mass is dominating. Taking a look at (4.3), we find that in our setup it has to be suppressed at least by a factor ϵ^3 with respect to the top Yukawa coupling.

Such a problematic operator has already been noticed in setups with flavour singlet Higgs fields where the flavour symmetry is $SO(3)$ and $h\Psi_L\Psi_R$ itself may form an invariant operator. This effect has encouraged many authors to consider the larger group $SU(3)$ where such a term is no longer invariant. For general reviews on such models for different discrete and continuous symmetries see [51, 87, 98, 134]. Avoiding this difficulty in an analogue manner is not possible as $SU(3)$ is the largest group with triplet representations². Hence we take a different ansatz and consider larger flavon representations which may reflect the structure of the effective Yukawa term. In any such case, we still have to forbid the operator Y_0 but may potentially suppress or even forbid its reoccurrence at higher orders.

4.2. A Triplet-Flavon Model

To start with, we first consider the simplest non-trivial flavour embedding of the flavons ϕ , the (anti-)triplet representations. Thus, the flavons transform similar to the matter and Higgs multiplets Ψ and h . A similar setup has been discussed e.g. in [120–122], however, there the Higgs bidoublet was $SU(3)_F$ blind.

4.2.1. Setup of the Model

Particle Content

In this chapter we break the flavour symmetry successively and thus introduce two flavons ϕ_3 and ϕ_{23} . As these flavons should get vevs at some high energy scale we have to ensure that they do not accidentally break SUSY (cf. Section 1.3). Concerning the vanishing of the D-terms, which is also-called D-term flatness, the simplest way of achieving this is to introduce their conjugate partners and assign equal vevs to them. A discussion on the vanishing of the F-terms is postponed to later studies concerning the scalar potential as we do not consider

¹We count the dimension in terms of the superpotential, where a dimension 3 term is renormalisable and terms with mass dimension 4 and higher are non-renormalisable.

²Although a fourth generation is not finally excluded there is no evidence for such a scenario

Field	$SU(3)_F$	PS	$U(1)$	Z_3	Z_2^{MP}
Ψ_L	$\mathbf{3}$	$(4, 2, 1)$	1	0	–
Ψ_R	$\mathbf{3}$	$(\bar{4}, 1, 2)$	1	0	–
h	$\mathbf{3}$	$(1, 2, 2)$	1	0	+
ϕ_3	$\mathbf{3}$	$(1, 1, 1)$	–3	–1	+
$\bar{\phi}_3$	$\bar{\mathbf{3}}$	$(1, 1, 1)$	–1	0	+
ϕ_{23}	$\mathbf{3}$	$(1, 1, 1)$	0	1	+
$\bar{\phi}_{23}$	$\bar{\mathbf{3}}$	$(1, 1, 1)$	–1	1	+
Φ'	$\mathbf{1}$	$(4, 1, 2)$	6	0	+

Table 4.1.: Transformation properties of the matter, Higgs and flavon superfields responsible for the flavour structure in the flavon triplet model.

the potential generating the flavon vevs here. In order to generate Majorana mass terms for the right-handed neutrinos we enlarge the spectrum by a PS-breaking multiplet Φ' as introduced in the previous chapter. We list the fields and quantum numbers that are relevant for the present discussion in Table 4.1.

The spectrum is completed by further superfields which restore the Z_2 left-right symmetry, cancel the $SU(4)$ gauge anomaly and implement symmetry breaking down to the MSSM. This can be done in a similar manner as discussed in the general PS-breaking model of Chapter 3. Since these superfields do not affect the flavour structure we do not list them explicitly.

Furthermore, we observe that the particle content of Table 4.1, including all PS breaking fields, exhibits a $SU(3)_F$ gauge anomaly. This anomaly can be cancelled by additional fields that do not contribute to the matter flavour structure. For instance, these can be the fields $\bar{\phi}_{10}$ and ϕ_6 which transform as $\bar{\mathbf{10}}$ and $\mathbf{6}$, respectively, and are PS-singlets. We expect such or similar fields to be introduced in the context of vacuum alignment of the flavon vevs [135]. However, we do not consider the scalar potential here but just state the vev structure we use.

Additional Symmetries

The setup discussed so far still allows for Yukawa terms which are inconsistent with the observed structure of masses and mixing. Therefore, we supplement the gauge symmetry by a $U(1) \times Z_3$ symmetry and assign specific charges to the fields, such that unwanted terms are forbidden³. The corresponding quantum numbers are also given in Table 4.1. Furthermore, we impose a Z_2^{MP} symmetry similar to matter parity.

VEV Structure

In our setup, the flavour symmetry is broken in two steps. First, we break $SU(3)_F$ down to $SU(2)_F$ by a vev of the flavon field ϕ_3 . Then, the field ϕ_{23} further breaks the remaining

³To avoid an extra Goldstone boson, the $U(1)$ may be considered to be gauged. Alternatively we may reduce it to a discrete Z_N sub-symmetry as described in Appendix B.2.

4. Effective Theory of Flavour

flavour symmetry. The flavons ϕ_i are labelled by the directions in flavour space in which their vevs are aligned. The mutually conjugated fields have to have equal vevs in order to guarantee exact D-term flatness (cf. Section 1.3). For the sake of simplicity, we align the ‘‘MSSM-Higgs’’ vev along the third component in flavour space. Collecting all flavour-breaking Higgs fields, we assume the vacuum structure

$$\langle \phi_3 \rangle \sim \langle \bar{\phi}_3 \rangle \sim M (0, 0, \sqrt[3]{\epsilon}), \quad (4.5a)$$

$$\langle \phi_{23} \rangle \sim \langle \bar{\phi}_{23} \rangle \sim M (0, \epsilon, \epsilon), \quad (4.5b)$$

$$\langle \Phi' \rangle \sim M_\nu, \quad (4.5c)$$

$$\langle h \rangle = (0, 0, 1) v_{\text{MSSM}}. \quad (4.5d)$$

4.2.2. Operator Analysis

We now generate all possible interactions of matter with Higgs and flavon fields that yield contributions to the low-energy flavour sector. These operators are constructed in the PS symmetric phase, i.e. they are invariant under the complete gauge symmetry as well as the extra $U(1) \times Z_3$ symmetry. They are not limited by the condition of renormalisability as we consider an effective theory. After the breaking of the PS and flavour symmetry, these operators effectively generate the low-energy Yukawa matrices obtained in the MSSM framework. Here, we are going to reproduce the structure of (4.3) and a Majorana matrix consistent with SRHND (cf. Section 2.3.3).

Before considering the allowed operators we take a look at the lower dimensional ones which have to be forbidden. As already mentioned in the discussion of the general framework of the model we find the operator Y_0 which is generically present in any setup. We choose to eliminate this term by the extra $U(1)$ symmetry introduced above. At dimension 4, there is no $SU(3)_F$ invariant that can generate a Yukawa operator. At dimension 5 we find that all potential operators are proportional to Y_0 . They take the form

$$\frac{\bar{\phi} \phi}{M^2} Y_0, \quad (4.6)$$

which, after symmetry breaking, would re-introduce Y_0 with a parametric suppression less than or equal to ϵ^2 . We forbid all of them using the extra symmetry stated above.

Yukawa Structure

We finally identify an operator⁴ that should give the dominant contribution to the Yukawa matrices at dimension 6;

$$W_{\text{lead}} = \frac{1}{M^3} (h \bar{\phi}_3) (\Psi_L \bar{\phi}_3) (\Psi_R \bar{\phi}_3). \quad (4.7)$$

This term generates the Yukawa coupling for the third generation only. However, at the same order a second operator,

$$W_{(23)} = \frac{1}{M^3} (h \bar{\phi}_{23}) (\Psi_L \bar{\phi}_{23}) (\Psi_R \bar{\phi}_{23}), \quad (4.8)$$

⁴The notation is such, that a pair of fields should be contracted with a δ_i^j and likewise a triple with ε_{ijk} .

is able to generate the 2-3-block of the Yukawa matrix. It is important to note that as long as there are only two distinct flavon fields involved the universal term Y_0 is not generated at this order. Such terms vanishes by antisymmetry; e.g.

$$(\bar{\phi}_{23} \bar{\phi}_{23} \bar{\phi}_{23}) Y_0 = (\bar{\phi}_3 \bar{\phi}_3 \bar{\phi}_{23}) Y_0 \equiv 0. \quad (4.9)$$

The coupling and mixing of the first generation is derived from even higher order operators. This is consistent with the hierarchy pattern of the Yukawa matrices. In our setup, operators of dimension 7 and 8 are excluded as consequence of the extra symmetry. Therefore, all sub-leading operators are at least of dimension 9. The corresponding superpotential reads:

$$\begin{aligned} W_{\text{sub}} = \frac{1}{M^6} & \left[(\phi_{23} \bar{\phi}_{23})^2 (h \bar{\phi}_{23}) (\phi_{23} \Psi_L \Psi_R) + (\phi_{23} \bar{\phi}_3)^2 (h \bar{\phi}_3) (\phi_{23} \Psi_L \Psi_R) \right. \\ & + (\phi_{23} \bar{\phi}_{23})^3 (h \Psi_L \Psi_R) + (\phi_{23} \bar{\phi}_3)^3 (h \Psi_L \Psi_R) \\ & + (\phi_{23} \bar{\phi}_3)^2 (\Psi_L \bar{\phi}_3) (h \phi_{23} \Psi_R) + (\phi_{23} \bar{\phi}_{23})^2 (\Psi_L \bar{\phi}_{23}) (h \phi_{23} \Psi_R) \\ & \left. + (\phi_{23} \bar{\phi}_{23})^2 (\Psi_R \bar{\phi}_{23}) (h \phi_{23} \Psi_L) + (\phi_{23} \bar{\phi}_3)^2 (\Psi_R \bar{\phi}_3) (h \phi_{23} \Psi_L) \right]. \quad (4.10) \end{aligned}$$

In summary, we obtain the following hierarchical structure of the low-energy effective Yukawa matrices, given at first relevant order in ϵ and neglecting all factors of order one:

$$Y_{u/\nu} \approx \begin{pmatrix} 0 & \epsilon_u^3 & \epsilon_u^3 \\ \epsilon_u^3 & \epsilon_u^2 & \epsilon_u^2 \\ \epsilon_u^3 & \epsilon_u^2 & 1 \end{pmatrix} \epsilon_u, \quad Y_{d/l} \approx \begin{pmatrix} 0 & \epsilon_d^3 & \epsilon_d^3 \\ \epsilon_d^3 & \epsilon_d^2 & \epsilon_d^2 \\ \epsilon_d^3 & \epsilon_d^2 & 1 \end{pmatrix} \epsilon_d. \quad (4.11)$$

Higher dimensional operators contribute at most at similar or even higher order. These contributions can be neglected as we do not consider order one coefficients anyway. For the (1, 1)-element we have tested that it is equal to zero up to corrections of order $\mathcal{O}(\epsilon^7)$.

Majorana Sector

We now turn to the neutrino sector and the PMNS matrix. The interplay between the Yukawa and Majorana mass matrices is capable of producing a non-hierarchical pattern in the neutrino sector as discussed above.

From the field content and the assignment of quantum numbers given in Table 4.1 we infer all allowed operators that generate a right-handed neutrino Majorana mass up to dimension 12;

$$\begin{aligned} W_{\text{Maj}} = \frac{1}{M^9} \Phi'^2 & \left[(\phi_3 \bar{\phi}_{23})^3 (\Psi_R \bar{\phi}_3)^2 + (\phi_3 \bar{\phi}_{23}) (\phi_3 \bar{\phi}_3)^2 (\Psi_R \bar{\phi}_{23})^2 + (\phi_3 \bar{\phi}_3)^3 (\Psi_R \bar{\phi}_3)^2 \right. \\ & \left. + (\phi_3 \bar{\phi}_3) (\phi_3 \bar{\phi}_{23})^2 (\Psi_R \bar{\phi}_3) (\Psi_R \bar{\phi}_{23}) + (\phi_3 \bar{\phi}_{23})^2 (\phi_{23} \phi_3 \Psi_R)^2 \right]. \quad (4.12) \end{aligned}$$

Inserting the vacuum alignment given in (4.5), the effective Majorana mass matrix takes the form

$$M_{RR} = \begin{pmatrix} \sqrt[3]{\epsilon_\nu^8} & 0 & 0 \\ 0 & \epsilon_\nu^2 & \epsilon_\nu^2 \\ 0 & \epsilon_\nu^2 & 1 \end{pmatrix} \sqrt[3]{\epsilon_\nu^8} \frac{\langle \Phi' \rangle^2}{M}. \quad (4.13)$$

4. Effective Theory of Flavour

This Majorana mass matrix is diagonal up to corrections of order ϵ_ν^2 . Furthermore, the right-handed neutrino mass eigenstates are hierarchical ($\epsilon_\nu^3 : \epsilon_\nu^2 : 1$). If we allow for a new expansion parameter $\epsilon_\nu \lesssim \epsilon_u^2$, we fulfil the requirements for SRHND (cf. Section 2.3.3) and the effective PMNS matrix exhibits large mixing angles. For special choices of the order-one coefficients specific mixing patterns, e.g. tri-bimaximal and golden-ratio, are possible. We have checked numerically that realistic neutrino mixing parameters as well as masses can be obtained.

To conclude, we have shown that a model with flavons and Higgs fields transforming as flavour triplets together with the extra symmetries listed in Table 4.1 is able to qualitatively explain the observed SM flavour structure.

4.3. Larger Flavon Representations

As we have seen in the previous section it is possible to set up a model with triplet flavons that qualitatively reproduces the correct structure of the fermion mass matrices. However, to achieve this we had to eliminate formally leading order terms in the superpotential which would have generated an unwanted flavour structure. Hence, the leading contribution to the effective Yukawa matrices is given by dimension 6 operators, i.e. by terms containing three flavon fields. Although such a scenario is perfectly possible, the assignment of extra quantum numbers may be considered ad-hoc and unnatural.

This issue can be traced back to the appearance of the operator Y_0 (cf. (4.4)). As discussed above, this motivates us to consider larger flavon representations. In the effective theory, a generic Yukawa coupling takes the form $\tilde{Y} h \Psi_L \Psi_R$. The prefactor \tilde{Y} has to transform according to one of the terms in the reduction of the tensor product

$$\mathbf{3} \otimes \mathbf{3} \otimes \mathbf{3} = \mathbf{1} \oplus \mathbf{8} \oplus \mathbf{8}' \oplus \mathbf{10}. \quad (4.14)$$

The simplest possibility for \tilde{Y} is the vev of a single flavon field which transforms according to either the singlet, octet or anti-decuplet representations of $SU(3)_F$. However, this will only be a viable assumption for the leading contribution. Additional corrections need not involve a single flavon but may also adopt products of flavons. This is also true for further representations that are not contained in the reduction.

The singlet representation is of no interest since it generates only the unwanted structure of the operator Y_0 . The triplet representation has been discussed above. We now turn to the next larger representations.

The Sextet Representation

The sextet is a symmetric two index tensor in $SU(3)_F$. It can be constructed as the symmetric part of two fundamental triplets, $\mathbf{6}_{ij} = (\mathbf{3}_i \otimes \mathbf{3}_j)_{\text{sym}}$. As it does not appear in the decomposition of the product (4.14), the leading Yukawa operator has to have at least dimension 5. It contains a pair of sextet and anti-sextet coupled to a singlet and is thus proportional to Y_0 . This operator has to be suppressed by extra quantum

numbers. A second invariant at this order (combination via **8**) does not help either. A hierarchical $SU(3)_F \rightarrow SU(2)_F$ breaking chain can be generated by dimension 6 operators and perturbations are introduced at higher order. In essence, a model of this kind is similar to the triplet model, so we do not develop it any further.

The Octet Representation

The octet is the adjoint representation of $SU(3)_F$ and as such real. It can be coupled to the product of three triplets in two different ways as there are two octets in the corresponding reduction (cf. (4.14)). Both operators do not produce a pattern which can be expressed as single dominant entry responsible for the mass of the third generation.

There exist further insertions of octet flavons at each order as the product of two octets contains a singlet as well as an octet. Each dimension which allows for an even number of octets in the product contains the invariant operator Y_0 . These terms have to be suppressed. On the other hand, there are no terms that generate a phenomenologically viable pattern directly. Therefore such a flavon representation can be added to generate corrections to a leading structure but does not constitute a useful ansatz by itself.

The Decuplet Representation

The decuplet representation of $SU(3)_F$ is much more promising. It is a natural choice since it is the symmetric product of three triplets, $\mathbf{10}_{ijk} = (\mathbf{3}_i \otimes \mathbf{3}_j \otimes \mathbf{3}_k)_{\text{sym}}$. As such, it has the same structure as the leading contribution of the triplet model. By assuming a vev in a component with maximum weight we generate a leading Yukawa term for just the third generation at dimension 4. Corrections proportional to Y_0 occur in the expansion of higher-dimensional operators where they can easily be further suppressed by imposing additional symmetries. In the following section, we build a model based on this representation which results in a viable phenomenology.

Larger Representations

We may consider also larger $SU(3)_F$ representations such as **15** and **15'**. However, all higher-dimensional multiplets can only occur combined to a lower-dimensional representation in order to couple to the Yukawa operator as they are not part of the reduction given in (4.14). As we have already found a promising representation that may generate the dominant contributions at leading order, we do not follow this path any further.

4.4. Flavon Decuplet Model

In this section, we present a model based on decuplet flavons which should be seen as a proof of principle. Similar to the triplet case we keep the discussion at a qualitative level and consider only possible hierarchical patterns of the model. Our guiding principle is simplicity. Thus, we allow only for decuplet flavons and require the Yukawa and Majorana mass matrix to be determined solely by operators proportional to the SM Yukawa operator or the simplest Majorana mass term, respectively. Many variations of the details (like vev directions, (discrete) global symmetries or charges) are possible. We briefly comment on

4. Effective Theory of Flavour

Field	$SU(3)_F$	PS	Z_4	Z_2^{MP}
Ψ_L	$\mathbf{3}$	$(4, 2, 1)$	1	–
Ψ_R	$\mathbf{3}$	$(\bar{4}, 1, 2)$	1	–
h	$\mathbf{3}$	$(1, 2, 2)$	1	+
ϕ_3	$\bar{\mathbf{10}}$	$(1, 1, 1)$	1	+
ϕ_2	$\bar{\mathbf{10}}$	$(1, 1, 1)$	1	+
$\bar{\phi}_3$	$\mathbf{10}$	$(1, 1, 1)$	3	+
$\bar{\phi}_2$	$\mathbf{10}$	$(1, 1, 1)$	0	+
Φ'	$\bar{\mathbf{3}}$	$(4, 1, 2)$	1	+

Table 4.2.: Transformation properties of the matter, Higgs and flavon superfields in the flavon decuplet model.

this issue at the end of this section. Such variations may be useful or even necessary when studying the potential of the flavons or performing actual fits to flavour observables. Such considerations are however beyond the scope of this work.

4.4.1. Setup of the Model

Particle Content

Similar to the triplet model we assign matter and Higgs fields to the triplet representation of $SU(3)_F$. The flavour breaking flavons $\phi_{i=2,3}$ are now considered to be in the (anti-)decuplet representation. For each field ϕ_i we introduce a conjugate field $\bar{\phi}_i$ which receives an equal vev to achieve exact D-term flatness. The PS-breaking multiplet Φ' which gives rise to Majorana masses for the right-handed neutrinos transforms also in the flavour triplet representation. The field content relevant for the flavour structure together with its transformations is given in Table 4.2. Similar to the triplet model we do not discuss the precise dynamics of PS and flavour-symmetry breaking and omit extra fields that restore left-right symmetry and cancel gauge anomaly contributions.

Additional Symmetries

By construction we encounter Yukawa operators that are not consistent with the measured flavour structure. The most prominent one is Y_0 . These are excluded by introducing the additional discrete global Z_4 symmetry. Moreover, we impose a Z_2^{MP} symmetry which is similar to matter parity.

VEV Structure

The flavour symmetry is again broken in two steps by hierarchical vevs for ϕ_3 and ϕ_2 . First, ϕ_3 breaks $SU(3)_F$ to $SU(2)_F$ giving rise to masses for the third generation. In a second step, ϕ_2 will break $SU(2)_F$. This generates masses for the second generation and introduces a mixing between both. In contrast to the triplet case it is not trivial to see whether a rotation

of the second vev in the $(2, 2, 2)$ -component only is possible here. Thus, we allow for vevs in each tensor-component whose indices are all larger than one. A further study of the flavon potential may give a conclusive answer on possible vev alignments. The masses of the first generation and the large Cabibbo angle are generated by higher order corrections. We align the electroweak breaking Higgs vev along the flavour diagonal direction. In summary, the vev structure is given by:

$$\langle \phi_3 \rangle_{333} = \langle \bar{\phi}_3 \rangle_{333} \sim \epsilon, \quad (4.15a)$$

$$\langle \phi_2 \rangle_{ijk} = \langle \bar{\phi}_2 \rangle_{ijk} \sim \epsilon^3 \quad \text{with } i, j, k \geq 2, \quad (4.15b)$$

$$\langle h \rangle = (1, 1, 1) v_{\text{MSSM}}, \quad (4.15c)$$

$$\langle \Phi' \rangle = (0, 0, 1) v_{\Phi}. \quad (4.15d)$$

4.4.2. Operator Analysis

We now explicitly construct the operators generating the Yukawa and Majorana mass matrices. Again, we are aiming at hierarchical structures rather than fits to flavour observables. Therefore, we confine ourselves on generating the Yukawa structure given in (4.3) and a hierarchical Majorana mass matrix compatible with SRHND.

Yukawa Structure

Looking at the Yukawa potential, we find that Y_0 is forbidden by the Z_4 symmetry. The leading terms that do contribute have dimension 4. They take the simple form (suppressing all flavour indices):

$$W_{\text{lead}} \sim \frac{1}{M} \phi_3 \Psi_L \Psi_R h + \frac{1}{M} \phi_2 \Psi_L \Psi_R h. \quad (4.16)$$

The invariant structure for the dimension 4 operator is trivial. For operators of multiple insertion of decuplet flavons the contractions are non-trivial and can no longer be expressed in a short-hand notation as it was possible in the triplet case. We comment on this issue in the Appendix B.1 where we introduce the formalism to generate the $SU(3)_F$ invariants used here. Neglecting these issues we can write the sub-leading terms of dimension 5 without flavour indices as

$$W_{\text{dim5}} = \frac{1}{M^2} [h \phi_3 \bar{\phi}_2 \Psi_L \Psi_R + h \phi_2 \bar{\phi}_2 \Psi_L \Psi_R]. \quad (4.17)$$

Already at this level we are able to generate a Yukawa matrix consistent with the one given in (4.3). As mentioned above, ϵ should differ in the up and down sector. We obtain

$$Y_{u/\nu} \sim \begin{pmatrix} 0 & \epsilon_u^3 & \epsilon_u^3 \\ \epsilon_u^3 & \epsilon_u^2 & \epsilon_u^2 \\ \epsilon_u^3 & \epsilon_u^2 & 1 \end{pmatrix} \epsilon_u \quad \text{and} \quad Y_{d/l} \sim \begin{pmatrix} 0 & \epsilon_d^3 & \epsilon_d^3 \\ \epsilon_d^3 & \epsilon_d^2 & \epsilon_d^2 \\ \epsilon_d^3 & \epsilon_d^2 & 1 \end{pmatrix} \epsilon_d. \quad (4.18)$$

For completeness we list also the next order in the expansion, namely the dimension 6 operators

$$W_{\text{dim6}} = \frac{h \Psi_L \Psi_R}{M^3} [\bar{\phi}_3 \bar{\phi}_3 \bar{\phi}_3 + \phi_3 \phi_3 \bar{\phi}_3 + \phi_2 \phi_3 \bar{\phi}_3 + \phi_2 \phi_2 \bar{\phi}_3 + \phi_3 \bar{\phi}_2 \bar{\phi}_2 + \phi_2 \bar{\phi}_2 \bar{\phi}_2]. \quad (4.19)$$

4. Effective Theory of Flavour

These terms would yield a subdominant contribution of the order of

$$Y_{\text{sub}}^f \sim \begin{pmatrix} \epsilon^6 & \epsilon^8 & \epsilon^6 \\ \epsilon^8 & \epsilon^6 & \epsilon^6 \\ \epsilon^6 & \epsilon^6 & \epsilon^2 \end{pmatrix} \epsilon. \quad (4.20)$$

With suitable order-one coefficients inserted in (4.18), we obtain a phenomenologically viable flavour structure in the quark and charged lepton sector.

Majorana Sector

After constructing the Yukawa sector we have to show that the setup can generate a Majorana mass matrix for the right-handed neutrinos capable of implementing sequential dominance (cf. [121] and Section 2.3.3). With the field content given in Table 4.2 we can construct the following superpotential where we consider terms up to dimension 7,

$$W_{\text{Maj}} \sim \frac{1}{M} (\Psi_R \Phi')^2 \left[1 + \frac{1}{M^2} (\phi_3 \bar{\phi}_3 + \phi_2 \bar{\phi}_3 + \bar{\phi}_2 \bar{\phi}_2) + \frac{1}{M^3} (\phi_3 \bar{\phi}_2 \bar{\phi}_3 + \phi_2 \bar{\phi}_3 \bar{\phi}_2) \right]. \quad (4.21)$$

From this superpotential we obtain a Majorana mass matrix for the right-handed neutrinos which takes the form

$$M_{\text{Maj}} \sim \begin{pmatrix} \epsilon_\nu^6 & \epsilon_\nu^7 & \epsilon_\nu^5 \\ \epsilon_\nu^7 & \epsilon_\nu^4 & \epsilon_\nu^4 \\ \epsilon_\nu^5 & \epsilon_\nu^4 & 1 \end{pmatrix} M_{N_R}. \quad (4.22)$$

This matrix is diagonal up to small corrections and exhibits a hierarchical pattern with eigenvalues of order $\epsilon_\nu^6 : \epsilon_\nu^4 : 1$. Looking at the conditions for sequential dominance (2.18) we find that in contrast to the triplet model we only need a mild hierarchy in the expansion parameters; $\epsilon_\nu < \epsilon_u$. Inserting order-one coefficients and allowing for CP-violating phases it is possible to fit neutrino observables. We have verified this by (naively) scanning a small part of the parameter space where we have already found allowed regions. However, we do not provide explicit results here as the model is too unconstrained to allow for predictive conclusions. In addition, we have not included effects such as running and threshold corrections in our considerations.

To summarise, we may state that the general ansatz for a decuplet model looks very simple and appealing. However, the complications may be hidden in the more complicated flavon potential of the model which we assume to generate the vev structure discussed above. Hence, we briefly comment on some variations which could be relevant if one wants to be more specific.

4.4.3. Possible Variations

We now give a short overview of possible variations that we have identified while constructing the model. We have chosen the vevs for the flavons such that they look particularly simple. This may however not be the best configuration when considering an explicit potential for the flavons.

As mentioned above, we have numerically checked whether the proposed neutrino structure of the model is qualitatively able to generate the measured neutrino masses and mixing structure. We found that the special configuration

$$\langle\phi_2\rangle_{222} = -2\epsilon^3, \quad \langle\phi_2\rangle_{322} = \epsilon^3, \quad \langle\phi_2\rangle_{332} = 0, \quad \langle\phi_2\rangle_{333} = \epsilon^3, \quad (4.23)$$

results in a fine-tuning among the elements of the Yukawa matrices which improves the scan in the neutrino parameter performed in order to test the Yukawa structure.

Also the alignment of the electroweak breaking Higgs vev appears somewhat unmotivated at first sight. However, we have chosen it such that it simplifies the generation of the mass for the first generation and the Cabibbo angle. Nevertheless, it is also possible to align the vev along a single direction in flavour space while extending the field content and/or the additional symmetry.

For reasons of unification it would be appealing to have Φ' transforming as a singlet under the flavour symmetry. However, this is not possible if we stick to our simple ansatz and do not include flavons transforming in different representations. This can be understood by noticing that there exist no invariant product of two triplets together with any number of (anti-) decuplets.

4.5. Summary

In this chapter we have presented a model that implements flavour in a Pati-Salam symmetric Grand Unified Theory through vevs of flavour breaking flavons. We have worked in a framework with a MSSM Higgs bidoublet which transforms non-trivially under the flavour gauge group. We have assumed a gauged $SU(3)_F$ flavour symmetry that is broken spontaneously at some high scale below the unification scale. The flavour sector has been expanded in powers of these hierarchical vevs resulting in the observed SM hierarchies.

The simplest such setup adopts flavons which transform in the fundamental (triplet) representation of $SU(3)_F$. We have explicitly constructed such a model to show that it is possible to reproduce the low energy flavour structure. However, we have focused on hierarchical structures only. Thus, our work should be seen as proof of principle rather than as concrete model of flavour.

Due to the general structure of the setup the MSSM Yukawa operator forms a flavour invariant by itself. This leads to some complications in constructing a model based on triplet flavons. Thus we have investigated if larger representations of $SU(3)_F$ may reduce these complications and adopt for the particular structure of the Yukawa operator containing three triplets. Here, we have found the decuplet as the natural candidate.

Thus, we have additionally constructed an explicit realisation with solely decuplet flavons. Again, we kept our discussions at the level of a “proof on principle model”. Nevertheless we have briefly commented on variations of our “simplest” setup. As the successful construction with decuplet flavons requires less terms and a smaller additional symmetry, we consider this solution to be more attractive.

A generic feature of the models discussed here is the occurrence of additional MSSM Higgs fields with flavour quantum numbers. Such a configuration is consistent with gauge coupling

4. *Effective Theory of Flavour*

unification as shown in Chapter 3. Thus, dedicated collider searches as well as an extended study of multi Higgs doublet models are definitely worth pursuing. Moreover, it would be interesting to study the Higgs potential and the impact of multiple Higgs generations and their mixing on flavour data.

As a further step it would be very interesting to study which vev-patterns can be achieved by scalar potentials involving representations larger than the fundamental one. This can be done in a general study or explicitly for the setup described above. With this knowledge, one can study if non-fundamental representations are also useful in other flavour setups, e.g. other GUTs or flavour symmetries. A possible next step would be to generate benchmark models following the setups presented here to compare with flavour observables.

Chapter 5

Gauged Flavour Symmetry

Low-Energy Yukawa Generation

In this chapter we consider a different method of implementing flavour in a Pati-Salam symmetric Grand Unified Theory. The ansatz is based on a work of Grinstein, Redi and Villadoro (GRV) from 2010 [11]. Similar to the model constructed in the previous chapter we consider a gauged flavour symmetry which we extend to $SU(3)_I \times SU(3)_{II}$. However, in this setup we allow only for renormalisable operators in the Lagrangian and communicate the flavour symmetry breaking through additional fermionic fields. As we intend to study effects on the low energy observables without considering a soft-SUSY breaking sector, we focus on a non-supersymmetric setup. We note that we do not follow the ansatz of Minimal Flavour Violation (MFV) [136–138] in this model although we find that the flavour violating effects are in some sense minimal.

We start our discussion with a short motivation of the model where we briefly sketch the idea of Grinstein et al. Afterwards, we present the basic setup of the model and highlight the differences with respect to their work. We then focus on the quark sector of the model as this results in the most stringent constraints. Here, we discuss the approximate flavour structure which follows from integrating out the fermionic partners. As this generates large deviations for the parameters related to the third generation, we analytically calculate the basis transformations leading to the mass eigenstates. This transformation we calculate up to quadratic order in the introduced flavour scale M . Thus, we are able to determine additional flavour effects which we scrutinise subsequently. Afterwards, we briefly discuss possible realisations of flavour in the lepton sector and their importance for gauge anomaly cancellation.

To be able to quantitatively probe the low energy flavour effects we then perform a systematical, yet not exhaustive scan over the model parameter space. Based on this scan we illustrate the effects on several flavour observables. Finally, we briefly comment on how to supersymmetrise the model. We conclude this chapter with a short summary and an outlook on further aspects of the model which are left for further studies.

The main results of this chapter are published in Reference [C].

5.1. Motivation

In 2010, Grinstein, Redi and Villadoro presented a way of gauging flavour by introducing a minimal set of additional fermionic fields [11]. In their work, they considered the maximal quark flavour symmetry of the gauge kinetic term in the SM, $G_F = SU(3)_{Q_L} \times SU(3)_{U_R} \times SU(3)_{D_R}$ (cf. Section 2.1.1). The symmetry is broken by two flavons S_u and S_d which transform as bitriplet under $SU(3)_{Q_L} \times SU(3)_{U_R}$ and $SU(3)_{Q_L} \times SU(3)_{D_R}$, respectively. Gauging the flavour symmetry in the SM results in gauge anomalies which get cancelled in their setup by introducing one additional fermionic partner for each quark. These fermions couple to S_u and S_d , thereby communicating the breaking of the flavour symmetry to the SM fermions. They acquire masses proportional to the flavon vevs and may be integrated out at leading order. This results in an effective Yukawa coupling of the form

$$Y_u \sim \frac{M}{\langle S_u \rangle} \quad \text{and} \quad Y_d \sim \frac{M}{\langle S_d \rangle}, \quad (5.1)$$

where M is an additional mass scale. This scale is introduced into the model by hand and is associated to the breaking of the flavour symmetry. From this effective Yukawa coupling one can easily see that the additional fermions feature an inverse hierarchy, i.e. the top partner has lowest mass. Thus, indirect flavour bounds of the light quarks (e.g. from $K - \bar{K}$ mixing) can be naturally fulfilled in this framework.

The effects on flavour observables are controlled by the flavour symmetry breaking scale M in this model. It may well be as low as the TeV-scale which allows for interesting new physics, mainly from $t - t'$ mixing and flavour gauge bosons. Most of the flavour effects decouple for large values of M , however, the mixing of the right-handed fermions is not directly related to M . Thus some residual effects may be visible in flavour precision observables.

In their setup, Grinstein et al. have solely focused on the quark sector. However, their idea has been extended to $SU(5)$ [139], left-right symmetry [140, 141] and supersymmetric theories [142]. In addition, Feldmann gave an outline on how to extend the idea to a PS GUT in the Appendix of his $SU(5)$ realisation [139]. Picking up this idea we show in this chapter how a GRV-like setup can be realised in a PS-symmetric theory.

5.2. Model Setup

The GUT symmetry considered in this model is the PS symmetry as defined in (1.18). This reduces the maximal flavour symmetry to $SU(3)_I \times SU(3)_{II}$ for the complete SM fermion sector¹ as discussed in Section 2.4.1. The full gauge symmetry assumed in this chapter is thus given by

$$\mathcal{G} = \underbrace{\left(SU(4) \times SU(2) \times SU(2)' \right)}_{\text{Pati-Salam}} \times \underbrace{\left(SU(3)_I \times SU(3)_{II} \right)}_{\text{flavour}} \times Z_2. \quad (5.2)$$

¹Note that the $SU(3)^3$ flavour symmetry considered by Grinstein et al. was only the symmetry of the quark sector.

We emphasise that the Z_2 symmetry now acts on both the GUT and the flavour sector. It is realised such that a general representation R is transformed into \tilde{R} as

$$R = (\varrho_c, \varrho, \varrho')(\varrho_I, \varrho_{II}) \xrightarrow{Z_2} \tilde{R} = (\bar{\varrho}_c, \varrho', \varrho)(\bar{\varrho}_{II}, \bar{\varrho}_I), \quad (5.3)$$

where we use the shorthand notation $(SU(4), SU(2), SU(2)')(SU(3)_I, SU(3)_{II})$ and $\bar{\varrho}$ denotes the complex conjugate of the representation ϱ . As we only introduce (pseudo-) real representations of $SU(2) \times SU(2)'$ we have dropped the complex conjugation of the corresponding representations in \tilde{R} . We anticipate that the Z_2 symmetry will not change the chirality of the fields relating \tilde{R}_L with R_R .

In contrast to the models discussed in the previous chapters we do not impose supersymmetry in our considerations.

Particle Content

The left- and right-handed SM fermions q_L and q_R are embedded in the $(\mathbf{4}, \mathbf{2}, \mathbf{1})(\mathbf{3}, \mathbf{1})$ and $(\mathbf{4}, \mathbf{1}, \mathbf{2})(\mathbf{1}, \mathbf{3})$ representations of PS and flavour, respectively. Instead of q_L we list \bar{q}_L in our spectrum² as it is the Z_2 partner of q_R and is in line with the convention for the SM Yukawa term (cf. (1.2b)). The SM Higgs doublet h is embedded in the usual $(\mathbf{1}, \mathbf{2}, \mathbf{2})(\mathbf{1}, \mathbf{1})$ which is similar to the models considered above but restricted to flavour singlet Higgs fields only. This effectively realises a two Higgs doublet model (2HDM).

In order to implement the setup of Grinstein et al, we have to include the additional fermionic fields $\bar{\Omega}_L$ and Ω_R . These are similar to the SM fermion fields but transform solely under $SU(2)'$ and have different flavour quantum numbers. However, including only these fields is not sufficient as they do not form a pair under the Z_2 symmetry. Hence, we must additionally introduce their fermionic Z_2 partners Ξ_R and $\bar{\Xi}_L$.

We introduce two flavour symmetry breaking flavons³ $S(\mathbf{1}, \mathbf{1}, \mathbf{1})(\bar{\mathbf{3}}, \mathbf{3})$ and $T'(\mathbf{1}, \mathbf{1}, \mathbf{3})(\bar{\mathbf{3}}, \mathbf{3})$. In addition, we have to include $T(\mathbf{1}, \mathbf{3}, \mathbf{1})(\bar{\mathbf{3}}, \mathbf{3})$ which together with T' forms a pair under Z_2 . Transforming as a triplet of $SU(2)$, T must not break the flavour symmetry at a high scale. The reason for including flavons that transform non-trivially under PS will be discussed later on and is related to the fact that no flavour mixing is possible as long as PS remains unbroken.

Besides the fields introduced above we have to add fields differentiating the lepton and quark sector. As discussed in Section 2.3 this can be achieved by generating a Majorana mass for the right-handed neutrinos. Hence, we include the PS breaking pair Φ and Φ' , similar to the previous chapters. To stay within a renormalisable framework we additionally introduce the fermionic fields $\bar{\Theta}_L$ and Θ_R as well as the scalar fields S_ν and S'_ν .

The complete particle content of the model is summarised in Table 5.1 together with their transformation properties under the imposed PS and flavour symmetry. Adopting the standard left-right convention for Yukawa and mass terms, i.e. $\bar{\psi}_L \psi_R$, throughout, we

²This is different, though consistent, to the embedding used so far where we have considered $\Psi_L \sim q_L$ and $\Psi_R \sim \bar{q}_R$.

³We use the terminus of flavons for scalar fields transforming non-trivially under the flavour symmetry and imprinting the flavour structure of the fermion sector by their vevs. Thus we distinguish them from spurions, used in a MFV analysis.

5. Gauged Flavour Symmetry

	$SU(4) \times SU(2) \times SU(2)'$	$SU(3)_I \times SU(3)_{II}$
$\bar{q}_L \oplus q_R$	$(\bar{\mathbf{4}}, \mathbf{2}, \mathbf{1}) \oplus (\mathbf{4}, \mathbf{1}, \mathbf{2})$	$(\bar{\mathbf{3}}, \mathbf{1}) \oplus (\mathbf{1}, \mathbf{3})$
h	$(\mathbf{1}, \mathbf{2}, \mathbf{2})$	$(\mathbf{1}, \mathbf{1})$
$\bar{\Xi}_L \oplus \Omega_R$	$(\bar{\mathbf{4}}, \mathbf{2}, \mathbf{1}) \oplus (\mathbf{4}, \mathbf{1}, \mathbf{2})$	$(\mathbf{1}, \bar{\mathbf{3}}) \oplus (\mathbf{3}, \mathbf{1})$
$\bar{\Omega}_L \oplus \Xi_R$	$(\bar{\mathbf{4}}, \mathbf{1}, \mathbf{2}) \oplus (\mathbf{4}, \mathbf{2}, \mathbf{1})$	$(\mathbf{1}, \bar{\mathbf{3}}) \oplus (\mathbf{3}, \mathbf{1})$
$T \oplus T'$	$(\mathbf{1}, \mathbf{3}, \mathbf{1}) \oplus (\mathbf{1}, \mathbf{1}, \mathbf{3})$	$(\bar{\mathbf{3}}, \mathbf{3}) \oplus (\bar{\mathbf{3}}, \mathbf{3})$
S	$(\mathbf{1}, \mathbf{1}, \mathbf{1})$	$(\bar{\mathbf{3}}, \mathbf{3})$
$\bar{\Theta}_L \oplus \Theta_R$	$(\mathbf{1}, \mathbf{1}, \mathbf{1}) \oplus (\mathbf{1}, \mathbf{1}, \mathbf{1})$	$(\bar{\mathbf{3}}, \mathbf{8}) \oplus (\mathbf{8}, \mathbf{3})$
$\Phi \oplus \Phi'$	$(\mathbf{4}, \mathbf{2}, \mathbf{1}) \oplus (\bar{\mathbf{4}}, \mathbf{1}, \mathbf{2})$	$(\mathbf{8}, \mathbf{1}) \oplus (\mathbf{1}, \mathbf{8})$
$S_\nu \oplus S'_\nu$	$(\mathbf{1}, \mathbf{1}, \mathbf{1}) \oplus (\mathbf{1}, \mathbf{1}, \mathbf{1})$	$(\mathbf{6}, \mathbf{1}) \oplus (\mathbf{1}, \bar{\mathbf{6}})$

Table 5.1.: The particle content of the theory with imposed PS and flavour symmetry. Left- and right-handed fermions $\psi_{L,R}$ are denoted by subscripts L and R , respectively.

list the Dirac adjoint $\bar{\psi}_L$ rather than the left-handed field ψ_L . Here, we do not show the fields necessary to break the PS symmetry as they are except for $\Phi^{(\prime)}$ not relevant for our discussions. A PS breaking setup similar to the models discussed as class E in Chapter 3 is conceivable where we may even introduce SUSY at some high scale.

Lagrangian

We split the Lagrangian in two parts, a general piece $\mathcal{L}_{\text{Yuk}}^0$ and a part containing only couplings relevant for the neutrino sector, $\mathcal{L}_{\text{Yuk}}^\nu$;

$$\mathcal{L}_{\text{Yuk}} = \mathcal{L}_{\text{Yuk}}^0 + \mathcal{L}_{\text{Yuk}}^\nu. \quad (5.4)$$

This is in line with our approach of treating the lepton sector only qualitatively. From the fields given in Table 5.1 we can deduce the most general renormalisable Yukawa Lagrangian, invariant under the full symmetry \mathcal{G} :

$$\begin{aligned} \mathcal{L}_{\text{Yuk}}^0 = & \lambda \bar{q}_L h \Omega_R + \bar{\Omega}_L (\kappa_S S + \kappa_T T') \Omega_R + M \bar{\Omega}_L q_R + \text{h.c.} \\ & + \lambda \bar{\Xi}_L h q_R + \bar{\Xi}_L (\kappa_S S + \kappa_T T) \Xi_R + M \bar{q}_L \Xi_R + \text{h.c.} \end{aligned} \quad (5.5a)$$

$$\begin{aligned} \mathcal{L}_{\text{Yuk}}^\nu \sim & \bar{\Theta}_L \Phi' \Omega_R + \bar{\Theta}_L S_\nu \bar{\Theta}_L + \bar{\Theta}_L S^\dagger \Theta_R + \text{h.c.} \\ & + \bar{\Xi}_L \Phi \Theta_R + \Theta_R S'_\nu \Theta_R + \text{h.c.} \end{aligned} \quad (5.5b)$$

As the Z_2 symmetry relates the terms of the first and second line, the general Yukawa Lagrangian $\mathcal{L}_{\text{Yuk}}^0$ depends on only four independent parameters; three dimensionless couplings λ , κ_S , κ_T and one mass scale M . By redefining the phases of the fermions we can choose λ and M to be real and positive. As in our considerations κ_S and κ_T appear only in combination with the flavons which generally acquire complex vevs, their phases can be kept arbitrary

at this point. For the neutrino Lagrangian $\mathcal{L}_{\text{Yuk}}^\nu$ we do not introduce explicit couplings as we are only interested in the qualitative structure. Generally, the Z_2 symmetry would also relate various couplings in $\mathcal{L}_{\text{Yuk}}^\nu$.

VEV Structure

The flavour structure of the SM fermions originates from vevs of the flavon fields S and T' . One of the two flavons would suffice to break the flavour symmetry completely. However, phenomenologically we need to generate a difference between the up and the down-type flavour sector. Hence, we need at least two vevs coupling differently to the up and down sector. This is not possible if we include solely a pair of two singlets or triplets as these can always be combined to a single vev. Different $SU(2)'$ representations are also not possible as we want to preserve the structure of the Yukawa Lagrangian. Including both S and T' , their vevs combine to two mass matrices that differ in the up and the down sector. Therefore, both have to get a similar vev and none may dominate over the other. The $SU(2)$ triplet T must not get a vev at the flavour breaking scale as it would break the electroweak symmetry. Nevertheless, a vev at or below the electroweak scale is allowed. One may even argue that the scalar potential induces a vev of the order $\langle T \rangle \sim v^2/M$ due to a possible mixing with the SM Higgs doublets. Phenomenologically, such a vev is rather constrained by electroweak precision observables as it breaks custodial symmetry and thus modifies the ρ -parameter (see e.g. [143, 144]). As it is negligible with respect to S and T' , it does not significantly contribute to the flavour structure and we omit it in the following.

We align the vev of T' along the τ_3 direction of $SU(2)'$. To make the mass scale explicit⁴, we split off the M -dependence from S and T' . Thus, we propose the following parametrisation of the vev structure for the charged Yukawa sector:

$$\kappa_S \langle S \rangle = s M, \quad \kappa_T \langle T' \rangle = \begin{pmatrix} t' & 0 \\ 0 & -t' \end{pmatrix} M \quad \text{and} \quad \langle T \rangle \equiv 0, \quad (5.6)$$

where t' and s are defined as dimensionless 3×3 matrices in flavour space. We note that we do not aim for the construction of a scalar potential able to generate these vevs. Rather, we assume phenomenologically interesting vev structures and postpone studies concerning scalar potentials to later projects.

As we are aiming for a double see-saw mechanism to generate the light neutrino masses, we assign vevs of different scales to the scalar fields Φ' and S_ν . Again, we make the mass scale explicit and parametrise the vevs for the neutrino Majorana mass terms by

$$\langle \Phi' \rangle = \Lambda \varphi \quad \text{and} \quad \langle S'_\nu \rangle \sim \langle S_\nu \rangle = \Lambda' s_\nu, \quad (5.7)$$

where we introduce the new mass scales Λ and Λ' as well as the flavour tensor structures φ and s_ν .

Gauge Boson Mass

The mass of the flavour gauge bosons can be derived from the kinetic terms of the flavour breaking fields. Therefore, they are in general proportional to the mass scale of the vevs.

⁴Still there is an internal hierarchy in the vevs of S and T'

5. Gauged Flavour Symmetry

Their masses are in general at a very high scale as we already need to break the flavour symmetry while generating masses for the right-handed neutrinos. If a remaining part of the symmetry is preserved, some of the flavour gauge bosons may have masses in the TeV range. As we do not specify the vev structure of S_ν , S'_ν and Φ' we stick to the general case and assume that all of the masses are related to either Λ or Λ' , depending on the explicit realisation of the lepton sector (cf. Section 5.4). In the setup presented here, all flavour gauge bosons have masses of order Λ' and are not relevant for a phenomenological study. We note that this qualitatively differs from the original idea presented by Grinstein et al.

As we invoke the PS gauge symmetry, we comment briefly on the masses of the corresponding gauge bosons, especially the W'^{\pm} and Z' . We do not specify at which scale $SU(4)$ or $SU(2)'$ are broken. However, both breaking scales are bounded from below by the vev of Φ' as it breaks PS completely (cf. Section 3.1). Thus their masses are at least of order Λ .

Gauge Anomalies

In the ansatz of Grinstein et al, the additionally introduced fermions naturally cancel the gauge anomalies arising when gauging the flavour symmetry. As we have to introduce two additional fermionic partners for each SM fermion this is no longer guaranteed in our setup⁵. The first pair (say $\bar{\Xi}_L$ and Ω_R) cancels the anomaly while the second pair ($\bar{\Omega}_L$ and Ξ_R) introduces a new one. However, these remaining anomalies can be absorbed as we also introduce new fermionic degrees of freedom ($\bar{\Theta}_L$ and Θ_R) in the neutrino sector. In particular, this partly fixes the neutrino sector as we will show in Section 5.4.

Scales of the Model

In the model setup presented here we introduce multiple mass scales. These are themselves only partially constrained. However, the overall ordering of the scales is fixed by the model. In addition to the hierarchies of the mass scales, the vevs of the flavons s and t' themselves feature internal hierarchies.

We find that the additional flavour effects decouple for large values of the flavour scale M . Moreover, we assume our model to be consistent with current experiments even when we lower M down to a few TeV. In this energy regime bounds from flavour precision observables as well as the non-observation of additional states become relevant. We do not deduce explicit bounds on M as they would require a global analysis which is beyond the scope of this work. In the following we simply assume M to be of the order of a few TeV.

The scales Λ and Λ' are related to the generation of neutrino masses. They are bounded from below by the largest eigenvalue of s and t and should themselves feature a hierarchy, $\Lambda \ll \Lambda'$. As the Majorana mass term is only invariant under the SM gauge group and not under PS, Λ' is bounded from above by the GUT scale. However, we do not fix the GUT scale or any aspect of PS breaking in the first place. Various realisations have been discussed in Chapter 3. Here, we only assume our theory to be realised well below the Planck scale. Hence, this is the maximally allowed scale.

As discussed before, the flavour gauge bosons masses M_A are in general of the order Λ' . The additional PS gauge bosons are bounded from below by the scale Λ and may reach up to

⁵We note that the assumed Z_2 symmetry guarantees the cancellation of PS but not flavour gauge anomalies.

the GUT-scale, depending on the explicit realisation of the PS symmetry breaking which we do not specify here.

We propose the hierarchy of scales depicted in Figure 5.1 where numerical values are only given as a rough reference and should not be taken at face value.

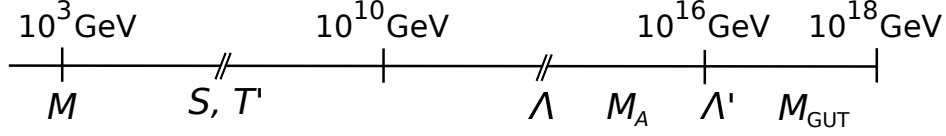


Figure 5.1.: Visualisation of the scales of the model (Numerical values for illustrative purposes only).

Strictly speaking, the flavour sector deduced in this chapter receives threshold corrections due to the multiple scale structure. However, we neglect these effects as we do not aim for a full top-down description of the model which would explain the patterns of the flavon vevs. For simplicity, we perform our scan using flavour parameters (e.g. fermion masses) fixed at the Z boson mass scale.

5.3. Quark Flavour Sector

The effective quark flavour structure of the Lagrangian given in (5.5) can be calculated by diagonalising the quark mass matrix. The full mass matrix is 9×9 dimensional as the three SM quarks mix with their heavy partners. As it is mainly dominated by the masses of the heavy partners, we may formally integrate them out in order to get a first impression of the flavour sector of the theory. Afterwards, we perform the explicit diagonalisation of the 9×9 mass matrix as expansion in the flavour breaking mass scale M . Having calculated these transformation, we apply them to the gauge kinetic sector and calculate explicitly the effective low-energy flavour sector. We note that the calculations here apply equally to the charged lepton sector.

5.3.1. Approximate Flavour Structure

If we assume that the masses of Ω and Ξ dominate the mass matrix, the diagonalisation is equivalent to integrating out those heavy degrees of freedom. This assumption is fulfilled if we assume that the eigenvalues of s and t are large, i.e. $s \sim t \gg 1$. We explicitly integrate out the fields Ω and Ξ by solving their equations of motion (dropping the kinetic part);

$$\frac{\partial \mathcal{L}_{\text{Yuk}}}{\partial \Omega_R} \stackrel{!}{=} 0 \quad \text{and} \quad \frac{\partial \mathcal{L}_{\text{Yuk}}}{\partial \Xi_R} \stackrel{!}{=} 0. \quad (5.8)$$

Substituting the resulting expressions back into the Lagrangian we find

$$\begin{aligned} \mathcal{L}_{\text{Yuk}}^{\text{eff}} = & -\lambda h_u^0 \bar{q}_L^u [t_u^{-1} + s^{-1}] q_R^u + h.c. \\ & -\lambda h_d^0 \bar{q}_L^d [t_d^{-1} + s^{-1}] q_R^d + h.c. , \end{aligned} \quad (5.9)$$

5. Gauged Flavour Symmetry

where we define the 3×3 matrices

$$t_u \equiv s + t' \quad \text{and} \quad t_d \equiv s - t'. \quad (5.10)$$

The effective Yukawa couplings correspond to the standard Yukawa couplings of a 2HDM and can easily be read off from the effective Lagrangian,

$$Y_{u,d} = -\lambda [t_{u,d}^{-1} + s^{-1}]. \quad (5.11)$$

In general, we would now need to invert this equation to fix the values of the flavon vevs s and t' . However, as (5.11) represents a set of coupled matrix equations this is nontrivial and it is not reasonable to give an analytic expression as it is lengthy and we do not learn anything from presenting it. Hence, we solve this equation only numerically for given matrices $Y_{u,d}$. Here it is important to note that we have to allow for a right-handed misalignment U_{CKM} in the SM Yukawa matrices (cf. Section 2.1.2). This mixing is physical in our setup as the right-handed quarks couple to the charged $SU(2)'$ gauge bosons. Although these are not directly observable due to the heavy $SU(2)'$ gauge bosons, the mixing influences the low energy observables as we encounter right-handed quarks coupling to the $SU(2)$ gauge bosons (cf. (5.42c) and (5.42e)). We describe the method used to obtain numerical results for s and t' in Appendix C.2.

One important feature already arising at this stage is the existence of multiple solutions for s and t' . This can be seen explicitly in the one generation case. Here, it is possible to analytically solve (5.11) for s and t' which are now complex numbers. For the first generation we find⁶

$$s = \frac{-8\lambda}{3y_u + 3y_d \mp 3\sqrt{(y_u - y_d)^2 + \frac{4}{9}y_u y_d}}, \quad (5.12a)$$

$$t_u = \frac{-8\lambda}{5y_u - 3y_d \pm 3\sqrt{(y_u - y_d)^2 + \frac{4}{9}y_u y_d}}, \quad (5.12b)$$

$$t_d = \frac{-8\lambda}{5y_d - 3y_u \pm 3\sqrt{(y_u - y_d)^2 + \frac{4}{9}y_u y_d}}. \quad (5.12c)$$

From these discussions we can conclude that all effects of the flavour sector are determined by the SM Yukawa matrices (up to a finite ambiguity), allowing for an additional right-handed misalignment U_{CKM} . However, the model differs from MFV as the Yukawa matrices are related to the flavon vevs (spurions) in an intricate way.

5.3.2. Diagonalising the Mass Matrix

In the previous section, we have calculated the effective Yukawa matrices based on the assumption $s, t' \gg 1$. This assumption is not valid for the third generation as $y_t \sim 1$ which results in sizeable corrections for parameters related to it. Hence, we now diagonalise the full 9×9 mass matrix \mathcal{M} as expansion in the flavour breaking scale M .

⁶We choose to present t_u and t_d instead of t' as it allows for a symmetric notation.

Starting from the general Lagrangian (5.5) we assign vevs to the flavour symmetry breaking fields S and T' as well as the Higgs bidoublet h . This gives rise to the effective quark Lagrangian⁷

$$\begin{aligned} \mathcal{L}_{\text{mass}} = & \frac{1}{\sqrt{2}} \lambda v_u \bar{q}_L^u \Omega_R^u + M \bar{\Omega}_L^u t_u \Omega_R^u + M \bar{\Omega}_L^u q_R^u + \text{h.c.} \\ & + \frac{1}{\sqrt{2}} \lambda v_u \bar{\Xi}_L^u q_R^u + M \bar{\Xi}_L^u s \Xi_R^u + M \bar{q}_L^u \Xi_R^u + \text{h.c.} \\ & + (u \leftrightarrow d). \end{aligned} \quad (5.13)$$

(1) Diagonalising s

Making use of our freedom to choose a basis of the $SU(3)_I \times SU(3)_{II}$ flavour symmetry we can diagonalise one of the two flavon vevs. Here, we choose to diagonalise s which we denote by \hat{s} . This choice of basis is valid for both, the up and the down sector of the model, as they are correlated by the PS symmetry. For definiteness, we focus on the up sector in the rest of this section. Similar results arise for the down sector and the corresponding expressions can be obtained by replacing u with d . For the basis transformations it will be useful to write the mass matrix explicitly. Therefore, we define vectors containing the left- and right-handed fermions

$$\bar{\Psi}_{L(1)}^u \equiv (\bar{q}_L^u, \bar{\Omega}_L^u, \bar{\Xi}_L^u) \quad \text{and} \quad \Psi_{R(1)}^u \equiv (q_R^u, \Omega_R^u, \Xi_R^u). \quad (5.14)$$

Using these, we can write the 9×9 mass matrix in compact form as

$$\mathcal{M}_{(1)}^u = \begin{pmatrix} 0 & \mathbb{1} \lambda \epsilon_u & \mathbb{1} \\ \mathbb{1} & t_u & 0 \\ \mathbb{1} \lambda \epsilon_u & 0 & \hat{s} \end{pmatrix} M, \quad (5.15)$$

where each block corresponds to a 3×3 matrix and we defined the expansion parameter

$$\epsilon_{u,d} \equiv \frac{v_{u,d}}{\sqrt{2} M} \ll 1, \quad \text{fulfilling} \quad \epsilon_u^2 + \epsilon_d^2 = \epsilon^2 = \frac{v^2}{2M}. \quad (5.16)$$

(2) Diagonalising t_u

We now change into a basis in which t_u becomes diagonal. This can be achieved by applying two unitary 3×3 matrices U_u and V_u , such that

$$\hat{t}_u = V_u t_u U_u^\dagger. \quad (5.17)$$

As we do not want to alter the leading order blocks of the mass matrix we choose the transformation to be

$$\bar{\Psi}_{L(2)}^u \equiv \bar{\Psi}_{L(1)}^u \text{diag}(\mathbb{1}, V_u^\dagger, \mathbb{1}), \quad \Psi_{R(2)}^u \equiv \text{diag}(V_u, U_u, \mathbb{1}) \Psi_{R(1)}^u. \quad (5.18)$$

⁷For the moment we neglect the effect on the lepton sector and any breaking of $SU(4)$. A discussion of the leptons will follow in Section 5.4.

5. Gauged Flavour Symmetry

This transformations leads to the mass matrix

$$\mathcal{M}_{(2)}^u = \begin{pmatrix} 0 & U_u^\dagger \lambda \epsilon_u & \mathbb{1} \\ \mathbb{1} & \hat{t}_u & 0 \\ V_u^\dagger \lambda \epsilon_u & 0 & \hat{s} \end{pmatrix} M. \quad (5.19)$$

We note that by construction the unitary rotations U_u and V_u reappear at order ϵ_u only. It is furthermore important to realise that these unitary matrices are now isospin-dependent and differ for the up and down sector.

(3) Diagonalising $\mathcal{M}_{(2)}^u$ for $\epsilon_u = 0$

If we go to the limiting case of ϵ going to zero, the three generations decouple completely. Thus, the 9×9 matrix becomes block diagonal in generation space and we can decompose it into three 3×3 blocks, one for each generation i . These can be diagonalised by two independent rotations. We may generalise this rotation to the three dimensional case by defining the diagonal 3×3 matrices

$$\hat{c}_x = \text{diag}(c_x^1, c_x^2, c_x^3) \quad \text{and} \quad \hat{s}_x = \text{diag}(s_x^1, s_x^2, s_x^3), \quad (5.20)$$

where x is either s or t_u and the (co-)sines are defined as

$$c_s^i = \frac{\hat{s}_i}{\sqrt{1 + \hat{s}_i^2}}, \quad s_s^i = \frac{1}{\sqrt{1 + \hat{s}_i^2}}, \quad c_{t_u}^i = \frac{\hat{t}_u^i}{\sqrt{1 + \hat{t}_u^{i2}}}, \quad s_{t_u}^i = \frac{1}{\sqrt{1 + \hat{t}_u^{i2}}}. \quad (5.21)$$

This leads in a straightforward way to the diagonalisation of $\mathcal{M}_{(2)}^u$ for $\epsilon_u = 0$ by going to the basis

$$\bar{\Psi}_{L(3)}^u \equiv \bar{\Psi}_{L(2)}^u \begin{pmatrix} \hat{c}_s & 0 & \hat{s}_s \\ 0 & \mathbb{1} & 0 \\ -\hat{s}_s & 0 & \hat{c}_s \end{pmatrix}, \quad \Psi_{R(3)}^u \equiv \begin{pmatrix} \hat{c}_{t_u} & -\hat{s}_{t_u} & 0 \\ \hat{s}_{t_u} & \hat{c}_{t_u} & 0 \\ 0 & 0 & \mathbb{1} \end{pmatrix} \Psi_{R(2)}^u. \quad (5.22)$$

The full mass matrix including terms proportional to ϵ_u takes the form

$$\mathcal{M}_{(3)}^u = \begin{pmatrix} (-\hat{s}_s V_u^\dagger \hat{c}_{t_u} - \hat{c}_s U_u^\dagger \hat{s}_{t_u}) \lambda \epsilon_u & (-\hat{s}_s V_u^\dagger \hat{s}_{t_u} + \hat{c}_s U_u^\dagger \hat{c}_{t_u}) \lambda \epsilon_u & 0 \\ 0 & \hat{s}_{t_u}^{-1} & 0 \\ (\hat{c}_s V_u^\dagger \hat{c}_{t_u} - \hat{s}_s U_u^\dagger \hat{s}_{t_u}) \lambda \epsilon_u & (\hat{c}_s V_u^\dagger \hat{s}_{t_u} + \hat{s}_s U_u^\dagger \hat{c}_{t_u}) \lambda \epsilon_u & \hat{s}_s^{-1} \end{pmatrix} M. \quad (5.23)$$

(4) Block-diagonalising $\mathcal{M}_{(3)}^u$ up to order ϵ_u^2

For simplicity, we reparametrise the mass matrix (5.23) to

$$\mathcal{M}_{(3)}^u = \begin{pmatrix} a_u \epsilon_u & b_u \epsilon_u & 0 \\ 0 & \hat{e}_u & 0 \\ c_u \epsilon_u & d_u \epsilon_u & \hat{f} \end{pmatrix} M, \quad (5.24)$$

where a_u, b_u, c_u and d_u are general 3×3 matrices whereas \hat{e}_u and \hat{f} are diagonal and positive definite. We note that \hat{f} is identical for the up and the down sector as we set $\langle T \rangle = 0$.

For the one generation case, where $a_u \dots f$ are just complex numbers, we can diagonalise the mass matrix by a bi-unitary transformation parametrised by complex three dimensional rotations. These rotation can generally be generated by a series of three rotations about a single axis. For technical reasons we choose to express each of these as a truncated series in the small rotation angles which are proportional to powers of ϵ . We calculate the mixing angles from the expressions which result when keeping terms up to the quadratic one. This can be extended to three generations by considering 3×3 matrices as generalised “rotation angles”. Such a rotation block-diagonalises the mass matrix to a given order. The generalised rotation matrices can be written as

$$\mathcal{R}_{12}(\xi) = \begin{pmatrix} \mathbb{1} - \frac{1}{2} \xi \xi^\dagger & -\xi & 0 \\ \xi^\dagger & \mathbb{1} - \frac{1}{2} \xi^\dagger \xi & 0 \\ 0 & 0 & \mathbb{1} \end{pmatrix}, \quad (5.25)$$

where we have chosen $(\alpha, \beta) = (1, 2)$ for definiteness. We block-diagonalise $\mathcal{M}_{(3)}^u$ up to order ϵ_u^3 which results in the following series of basis transformations

$$\bar{\Psi}_{L(4)}^u \equiv \bar{\Psi}_{L(3)}^u [\mathcal{R}_{12}(\xi_{12}^u)]^\dagger [\mathcal{R}_{23}(\xi_{23}^u)]^\dagger [\mathcal{R}_{13}(\xi_{13}^u)]^\dagger, \quad (5.26a)$$

$$\Psi_{R(4)}^u \equiv [\mathcal{R}_{12}(\zeta_{12}^u)] [\mathcal{R}_{23}(\zeta_{23}^u)] [\mathcal{R}_{13}(\zeta_{13}^u)] \Psi_{R(3)}^u, \quad (5.26b)$$

with generalised “rotation angles”. We calculate them in terms of the parameters of (5.24) to be

$$\xi_{12}^u = b_u \hat{e}_u^{-1} \epsilon_u, \quad [\xi_{23}^u]_{ij} = \frac{-\hat{e}_u^i d_u^{\dagger ij}}{\hat{e}_u^{i2} - \hat{f}_j^2} \epsilon_u, \quad \xi_{13}^u = a_u c_u^\dagger \hat{f}^{-2} \epsilon_u^2, \quad (5.27a)$$

$$\zeta_{12}^u = a_u^\dagger b_u \hat{e}_u^{-2} \epsilon_u^2, \quad [\zeta_{23}^u]_{ij} = \frac{-d_u^{\dagger ij} \hat{f}_j}{\hat{e}_u^{i2} - \hat{f}_j^2} \epsilon_u, \quad \zeta_{13}^u = c_u^\dagger \hat{f}^{-1} \epsilon_u, \quad (5.27b)$$

where $\xi_{\alpha\beta}^u$ and $\zeta_{\alpha\beta}^u$ are 3×3 matrices. Applying the basis transformation to the mass matrix we end up with

$$\mathcal{M}_{(4)}^u = \begin{pmatrix} (a_u + \mathcal{O}(\epsilon_u^2)) \frac{1}{\sqrt{2}} v_u & 0 & 0 \\ 0 & (\hat{e}_u + \mathcal{O}(\epsilon_u^2)) M & 0 \\ 0 & 0 & (\hat{f} + \mathcal{O}(\epsilon_u^2)) M \end{pmatrix} + \mathcal{O}(\epsilon_u^3) M, \quad (5.28)$$

where for simplicity we only show the leading terms of the diagonal elements. We note that \hat{e}_u and \hat{f} are already diagonal⁸ while a_u is a general 3×3 matrix.

(5) The Approximate Mass Basis

For the given order in ϵ we arrived at a setup similar to the SM where we can identify the non-diagonal up Yukawa matrix by a_u ;

$$Y_u \approx a_u = (-\hat{s}_s V_u^\dagger \hat{c}_{t_u} - \hat{c}_s U_u^\dagger \hat{s}_{t_u}) \lambda. \quad (5.29)$$

⁸The new misalignment from $\mathcal{O}(\epsilon_u^2)$ corrections can be neglected.

5. Gauged Flavour Symmetry

Hence, we may apply the standard diagonalisation procedure of the SM. To diagonalise a_u we introduce the bi-unitary transformation

$$\hat{Y}_u = \mathcal{U}_u a_u \mathcal{V}_u^\dagger. \quad (5.30)$$

The approximate mass basis is given by

$$\bar{\Psi}_{L(5)}^u \equiv \bar{\Psi}_{L(4)}^u \text{diag}(\mathcal{V}_u^\dagger, \mathbb{1}, \mathbb{1}), \quad \Psi_{R(5)}^u \equiv \text{diag}(\mathcal{U}_u, \mathbb{1}, \mathbb{1}) \Psi_{R(4)}^u. \quad (5.31)$$

We note that the expression for Y_u reduces to (5.11) in the case of $s, t_u \gg 1$;

$$\begin{aligned} Y_u \hat{=} a_u V_u &= -\lambda \left(\frac{1}{\sqrt{1+\hat{s}^2}} V_u^\dagger \frac{\hat{t}_u}{\sqrt{1+\hat{t}_u^2}} + \frac{\hat{s}}{\sqrt{1+\hat{s}^2}} U_u^\dagger \frac{1}{\sqrt{1+\hat{t}_u^2}} \right) V_u \\ &\xrightarrow{s, t_u \gg 1} -\lambda \left(\frac{1}{\hat{s}} + U_u^\dagger \frac{1}{\hat{t}_u} V_u \right) = -\lambda (\hat{s}^{-1} + t_u^{-1}). \end{aligned} \quad (5.32)$$

We conclude this section by reminding that a similar sequence of basis transformations is applicable to the down sector if one replaces the index u by d .

5.3.3. Gauge Kinetic Terms

Having diagonalised the mass matrix we apply the resulting transformations to the gauge kinetic terms. This is important as only the mass eigenstates are observable in experiments. We are mainly interested in the flavour sector and therefore consider only the gauge kinetic terms corresponding to $SU(2) \times SU(2)'$ as the $SU(4)$ part is flavour blind. To be able to use the formalism developed above, we again write the relevant gauge kinetic sector by means of the left- and right-handed vectors Ψ_L and Ψ_R ;

$$\begin{aligned} \mathcal{L}^{\text{kin}} \supset & \bar{\Psi}_{L(1)} \left(g \vec{W} \vec{\tau} \right) \mathcal{K}_{L(1)} \Psi_{L(1)} & + \bar{\Psi}_{R(1)} \left(g \vec{W} \vec{\tau} \right) \mathcal{K}_{R(1)} \Psi_{R(1)} \\ & + \bar{\Psi}_{L(1)} \left(g \vec{W}' \vec{\tau} \right) \mathcal{K}'_{L(1)} \Psi_{L(1)} & + \bar{\Psi}_{R(1)} \left(g \vec{W}' \vec{\tau} \right) \mathcal{K}'_{R(1)} \Psi_{R(1)} \\ & + \bar{\Psi}_{L(1)} \left(\frac{1}{2} g_{B-L} Q_{B-L} \vec{B}_{B-L} \right) \Psi_{L(1)} & + \bar{\Psi}_{R(1)} \left(\frac{1}{2} g_{B-L} Q_{B-L} \vec{B}_{B-L} \right) \Psi_{R(1)}, \end{aligned} \quad (5.33)$$

where Q_{B-L} is the difference of baryon and lepton number (cf. Section 3.1). The complete $SU(2) \times SU(2)'$ structure is encoded in the \mathcal{K} matrices,

$$\mathcal{K}_{L(1)} = \begin{pmatrix} \mathbb{1} & 0 & 0 \\ 0 & 0 & 0 \\ 0 & 0 & \mathbb{1} \end{pmatrix}, \quad \mathcal{K}_{R(1)} = \begin{pmatrix} 0 & 0 & 0 \\ 0 & 0 & 0 \\ 0 & 0 & \mathbb{1} \end{pmatrix}, \quad (5.34a)$$

$$\mathcal{K}'_{L(1)} = \begin{pmatrix} 0 & 0 & 0 \\ 0 & \mathbb{1} & 0 \\ 0 & 0 & 0 \end{pmatrix}, \quad \mathcal{K}'_{R(1)} = \begin{pmatrix} \mathbb{1} & 0 & 0 \\ 0 & \mathbb{1} & 0 \\ 0 & 0 & 0 \end{pmatrix}. \quad (5.34b)$$

Here, we especially emphasise that the $SU(2)$ gauge bosons couple to both left- and right-handed fermions. Likewise, the $SU(2)'$ gauge bosons couple to both chiralities.

While breaking $SU(2)' \times U(1)_{B-L} \rightarrow U(1)_Y$ the neutral bosons $W'^{(3)}$ and B_{B-L} mix, resulting in a massless B_Y and a massive Z' . This mixing is closely related to the electroweak symmetry breaking in the SM. The charged part of the $SU(2)'$ gauge bosons W'^{\pm} are defined similarly to the SM W^{\pm} bosons and also get masses from the $SU(2)'$ breaking. Thus we can rewrite the gauge kinetic terms in the $SU(2)'$ broken phase as

$$\begin{aligned}
 \mathcal{L}^{\text{kin}} \supset & \bar{\Psi}_{L(1)} \left(g \vec{W} \vec{\tau} \right) \mathcal{K}_{L(1)} \Psi_{L(1)} + \bar{\Psi}_{R(1)} \left(g \vec{W} \vec{\tau} \right) \mathcal{K}_{R(1)} \Psi_{R(1)} \\
 & + \bar{\Psi}_{L(1)} \left(g s'_W \tau^3 \mathcal{K}'_{L(1)} + \frac{1}{2} g_{B-L} c'_W Q_{B-L} \right) \mathcal{B}_Y \Psi_{L(1)} \\
 & + \bar{\Psi}_{R(1)} \left(g s'_W \tau^3 \mathcal{K}'_{R(1)} + \frac{1}{2} g_{B-L} c'_W Q_{B-L} \right) \mathcal{B}_Y \Psi_{R(1)} \\
 & + \bar{\Psi}_{L(1)} \left(g W'^{\pm} (\tau^1 \pm i \tau^2) \right) \mathcal{K}'_{L(1)} \Psi_{L(1)} \\
 & + \bar{\Psi}_{R(1)} \left(g W'^{\pm} (\tau^1 \pm i \tau^2) \right) \mathcal{K}'_{R(1)} \Psi_{R(1)} \\
 & + \bar{\Psi}_{L(1)} \left(g c'_W \tau^3 \mathcal{K}'_{L(1)} - \frac{1}{2} g_{B-L} s'_W Q_{B-L} \right) \mathcal{Z}' \Psi_{L(1)} \\
 & + \bar{\Psi}_{R(1)} \left(g c'_W \tau^3 \mathcal{K}'_{R(1)} - \frac{1}{2} g_{B-L} s'_W Q_{B-L} \right) \mathcal{Z}' \Psi_{R(1)}, \tag{5.35}
 \end{aligned}$$

where we identify $g s'_W = g_{B-L} c'_W \equiv g'$.

As discussed before, the W'^{\pm} and Z' gauge bosons of $SU(2)'$ are irrelevant for low-energy flavour effects. Thus, we do not discuss these terms further and focus on the first three lines of (5.35) in the following. For the low-energy flavour sector we further have to perform the electroweak symmetry breaking. After electroweak symmetry breaking and using the standard relation $g s_W = g' c_W = e$ the relevant kinetic Lagrangian is given by

$$\begin{aligned}
 \mathcal{L}^{\text{kin}} \supset & \bar{\Psi}_{L(1)} \left(g W^{\pm} (\tau^1 \pm i \tau^2) \right) \mathcal{K}_{L(1)} \Psi_{L(1)} \\
 & + \bar{\Psi}_{R(1)} \left(g W^{\pm} (\tau^1 \pm i \tau^2) \right) \mathcal{K}_{R(1)} \Psi_{R(1)} \\
 & + \bar{\Psi}_{L(1)} \frac{g}{c_W} \left(c_W^2 \tau^3 \mathcal{K}_{L(1)} - s_W^2 \tau^3 \mathcal{K}'_{L(1)} - \frac{1}{2} s_W^2 Q_{B-L} \right) \mathcal{Z} \Psi_{L(1)} \\
 & + \bar{\Psi}_{R(1)} \frac{g}{c_W} \left(c_W^2 \tau^3 \mathcal{K}_{R(1)} - s_W^2 \tau^3 \mathcal{K}'_{R(1)} - \frac{1}{2} s_W^2 Q_{B-L} \right) \mathcal{Z} \Psi_{R(1)} \\
 & + \bar{\Psi}_{L(1)} e \left(\tau^3 \left(\mathcal{K}_{L(1)} + \mathcal{K}'_{L(1)} \right) + \frac{1}{2} Q_{B-L} \right) \mathcal{A} \Psi_{L(1)} \\
 & + \bar{\Psi}_{R(1)} e \left(\tau^3 \left(\underbrace{\mathcal{K}_{R(1)} + \mathcal{K}'_{R(1)}}_{\equiv 1} \right) + \frac{1}{2} Q_{B-L} \right) \mathcal{A} \Psi_{R(1)}. \tag{5.36}
 \end{aligned}$$

5. Gauged Flavour Symmetry

For the sake of readability we explicitly split the charged part into its isospin components. Moreover, we separate the ‘‘SM-like’’ terms from the specific additional contributions present in the model. We obtain

$$\begin{aligned}
\mathcal{L}^{\text{kin}} \supset & \quad g \bar{\Psi}_{L(1)}^u \left(\mathbb{1} - \mathcal{J}_{L(1)}^+ \right) \mathcal{W}^+ \Psi_{L(1)}^d + \text{h.c.} \\
& + g \bar{\Psi}_{R(1)}^u \left(0 + \mathcal{J}_{R(1)}^+ \right) \mathcal{W}^+ \Psi_{R(1)}^d + \text{h.c.} \\
& + \frac{g}{c_W} \bar{\Psi}_{L(1)} \left((\tau^3 - s_W^2 Q_e) \mathbb{1} - \tau^3 \mathcal{J}_{L(1)}^0 \right) \not{Z} \Psi_{L(1)} \\
& + \frac{g}{c_W} \bar{\Psi}_{R(1)} \left(-s_W^2 Q_e \mathbb{1} + \tau^3 \mathcal{J}_{R(1)}^0 \right) \not{Z} \Psi_{R(1)} \\
& + e Q_e \left(\bar{\Psi}_{L(1)} \not{A} \Psi_{L(1)} + \bar{\Psi}_{R(1)} \not{A} \Psi_{R(1)} \right) .
\end{aligned} \tag{5.37}$$

To be able to write the Lagrangian in such a short-hand notation we make use of the fact that each fermion solely transforms under either $SU(2)$ or $SU(2)'$. This results in a relation similar to the Gell-Mann Nishijima formula [145, 146] where τ^3 is understood to act on both $SU(2)$ and $SU(2)'$;

$$Q_e = \frac{1}{2} Q_{B-L} + \tau^3. \tag{5.38}$$

In addition we have defined

$$\mathcal{J}_{L(1)}^+ \equiv \mathcal{K}'_{L(1)} = \left(\mathcal{J}_{L(1)}^- \right)^\dagger, \quad \mathcal{J}_{L(1)}^0 \equiv \mathcal{K}'_{L(1)}, \tag{5.39a}$$

$$\mathcal{J}_{R(1)}^+ \equiv \mathcal{K}'_{R(1)} = \left(\mathcal{J}_{R(1)}^- \right)^\dagger, \quad \mathcal{J}_{R(1)}^0 \equiv \mathcal{K}'_{R(1)}, \tag{5.39b}$$

which correspond to the additional contributions. For the neutral sector these are the only matrices transforming non-trivially under basis transformations. From the last line in (5.37) we can read off, that the coupling to the photon is diagonal and proportional to the corresponding electric charge in all sub-spaces. Thus, we reproduce the observation that the $U(1)_{\text{em}}$ remains unbroken.

Due to the isospin structure of the charged and neutral couplings, $\mathcal{J}_{L,R}^\pm$ and $\mathcal{J}_{L,R}^0$ transform with up- as well as down-type transformations. We drop the indices u and d for simplicity as $\mathcal{J}_{L,R}^0$ does not mix up- and down-type transformations. However, we note that the contribution for the up and down sector differs in sign as we explicitly split off the τ^3 matrix in (5.37). For $\mathcal{J}_{L,R}^+$ we make the transformations explicit. The corresponding $\mathcal{J}_{L,R}^-$ can then be deduced by Hermitian conjugation of $\mathcal{J}_{L,R}^+$.

Approximate Mass Basis

After applying all basis transformations defined in the previous section we get the following expressions for the flavour-dependent gauge couplings

$$\mathcal{J}_{L(5)}^+ = \begin{pmatrix} \mathcal{V}_u \left(\frac{1}{2} (\xi_{12}^u \xi_{12}^{u\dagger} + \xi_{12}^d \xi_{12}^{d\dagger}) \right) \mathcal{V}_d^\dagger & -\mathcal{V}_u \xi_{12}^d & \mathcal{V}_u \left(\xi_{13}^u - \xi_{13}^d - \xi_{12}^d \xi_{23}^d \right) \\ -\xi_{12}^{u\dagger} \mathcal{V}_d^\dagger & \mathbb{1} - \xi_{12}^{u\dagger} \xi_{12}^d + \xi_{23}^u \xi_{23}^{d\dagger} & \xi_{23}^u \\ \left(-\xi_{13}^{u\dagger} + \xi_{13}^{d\dagger} - \xi_{23}^{u\dagger} \xi_{12}^u \right) \mathcal{V}_d^\dagger & \xi_{23}^{d\dagger} & \frac{1}{2} (\xi_{23}^{u\dagger} \xi_{23}^u + \xi_{23}^{d\dagger} \xi_{23}^d) \end{pmatrix} + \mathcal{O}(\epsilon^3), \quad (5.40a)$$

$$\mathcal{J}_{R(5)}^+ = \begin{pmatrix} \mathcal{U}_u \xi_{13}^u \xi_{13}^{d\dagger} \mathcal{U}_d^\dagger & \mathcal{U}_u \xi_{13}^u \xi_{23}^{d\dagger} & -\mathcal{U}_u \xi_{13}^u \\ \xi_{23}^u \xi_{13}^{d\dagger} \mathcal{U}_d^\dagger & \xi_{23}^u \xi_{23}^{d\dagger} & -\xi_{23}^u \\ -\xi_{13}^{d\dagger} \mathcal{U}_d^\dagger & -\xi_{23}^{d\dagger} & \mathbb{1} - \frac{1}{2} (\xi_{13}^{u\dagger} \xi_{13}^u + \xi_{23}^{u\dagger} \xi_{23}^u + \xi_{13}^{d\dagger} \xi_{13}^d + \xi_{23}^{d\dagger} \xi_{23}^d) \end{pmatrix} + \mathcal{O}(\epsilon^3), \quad (5.40b)$$

$$\mathcal{J}_{L(5)}^0 = \begin{pmatrix} \mathcal{V} \xi_{12} \xi_{12}^\dagger \mathcal{V}^\dagger & -\mathcal{V} \xi_{12} & -\mathcal{V} \xi_{12} \xi_{23} \\ -\xi_{12}^\dagger \mathcal{V}^\dagger & \mathbb{1} - \xi_{12}^\dagger \xi_{12} - \xi_{23} \xi_{23}^\dagger & \xi_{23} \\ -\xi_{23}^\dagger \xi_{12}^\dagger \mathcal{V}^\dagger & \xi_{23}^\dagger & \xi_{23}^\dagger \xi_{23} \end{pmatrix} + \mathcal{O}(\epsilon^3), \quad (5.40c)$$

$$\mathcal{J}_{R(5)}^0 = \begin{pmatrix} \mathcal{U} \xi_{13} \xi_{13}^\dagger \mathcal{U}^\dagger & \mathcal{U} \xi_{13} \xi_{23}^\dagger & -\mathcal{U} \xi_{13} \\ \xi_{23} \xi_{13}^\dagger \mathcal{U}^\dagger & \xi_{23} \xi_{23}^\dagger & -\xi_{23} \\ -\xi_{13}^\dagger \mathcal{U}^\dagger & -\xi_{23}^\dagger & \mathbb{1} - \xi_{13}^\dagger \xi_{13} + \xi_{23}^\dagger \xi_{23} \end{pmatrix} + \mathcal{O}(\epsilon^3). \quad (5.40d)$$

We now reinsert these matrices into the gauge kinetic couplings. As we are mainly interested in the couplings of the SM quarks $q_{L,R(5)}$ we present only the terms of the first 3×3 blocks here. As motivated above, we give the gauge kinetic Lagrangian in the form,

$$\begin{aligned} \mathcal{L}^{\text{kin}} \supset & g \bar{q}_{L(5)}^u (V_{\text{CKM}} - \Delta V_{\text{CKM}}) \mathcal{W}^+ q_{L(5)}^d \\ & + g \bar{q}_{R(5)}^u V'_{\text{CKM}} \mathcal{W}^+ q_{R(5)}^d + \text{h.c.} \\ & + \frac{g}{c_W} \bar{q}_{L(5)} \left((\tau^3 - s_W^2 Q_e) \mathbb{1} - \tau^3 \Delta g_{Z\bar{q}_L q_L} \right) \cancel{Z} q_{L(5)} \\ & + \frac{g}{c_W} \bar{q}_{R(5)} \left(-s_W^2 Q_e \mathbb{1} + \tau^3 \Delta g_{Z\bar{q}_R q_R} \right) \cancel{Z} q_{R(5)}, \end{aligned} \quad (5.41)$$

where we define the extra flavour effects as ΔV_{CKM} , V'_{CKM} , $\Delta g_{Z\bar{q}_L q_L}$ and $\Delta g_{Z\bar{q}_R q_R}$. Making use of the definitions given in (5.27), we identify the low-energy flavour parameter to be parametrised by

$$V_{\text{CKM}} = \mathcal{V}_u \mathcal{V}_d^\dagger, \quad (5.42a)$$

$$\Delta V_{\text{CKM}} = \frac{1}{2} \mathcal{V}_u \left(b_u \hat{e}_u^{-2} b_u^\dagger + b_d \hat{e}_d^{-2} b_d^\dagger \right) \mathcal{V}_d^\dagger \epsilon^2 + \mathcal{O}(\epsilon^3), \quad (5.42b)$$

$$V'_{\text{CKM}} = \mathcal{U}_u c_u^\dagger \hat{f}^{-2} c_d \mathcal{U}_d^\dagger \epsilon^2 + \mathcal{O}(\epsilon^3), \quad (5.42c)$$

$$\Delta g_{Z\bar{q}_L q_L} = \mathcal{V} b \hat{e}^{-2} b^\dagger \mathcal{V}^\dagger \epsilon^2 + \mathcal{O}(\epsilon^3), \quad (5.42d)$$

$$\Delta g_{Z\bar{q}_R q_R} = \mathcal{U} c^\dagger \hat{f}^{-2} c \mathcal{U}^\dagger \epsilon^2 + \mathcal{O}(\epsilon^3). \quad (5.42e)$$

We note that the effective CKM matrix is no longer unitary, as it receives a correction ΔV_{CKM} , proportional to ϵ^2 .

5.3.4. Higgs Coupling

From the Lagrangian (5.5) we can read off that there is no direct coupling of the Higgs boson to a pair of SM quarks. Similar to the quark masses, this coupling is generated effectively by the heavy quark partners. Thus, it is no longer guaranteed that the Higgs-quark-quark coupling $g_{h\bar{q}q}$ is proportional to the quark masses and diagonal among the generations. The coupling can be deduced by either integrating out the heavy fermions or by explicitly applying the basis transformations defined above to the Higgs couplings. We find, that the correction to the quark masses and the Higgs-quark-quark coupling is of order ϵ^2 and differs by a combinatorial factor of three.

Such an effect can be understood by explicitly studying the leading order correction. The diagrams responsible for this correction are depicted in Figure 5.2. Both lead to an effective coupling of three Higgs bosons to the SM quarks. They provide a correction to the quark masses if all Higgs fields acquire their vev. Furthermore, if only two of them are set to their vev, the diagrams contribute to the Higgs-quark-quark coupling. As there are three possible choices, this contribution picks up the combinatorial factor of three. This effect also occurs in the SM when considering generally all possible dimension six operators [147].

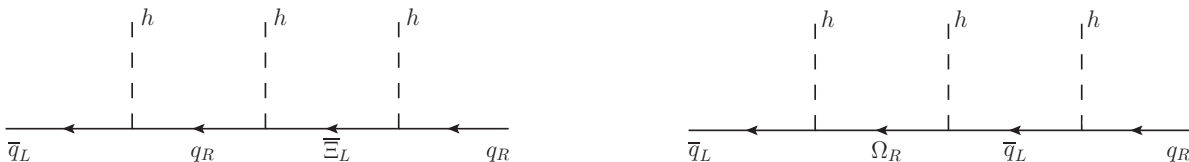


Figure 5.2.: Leading order correction to the quark masses and the Higgs-quark-quark coupling.

We make the effect explicit by calculating the ϵ^2 -correction of the effective Yukawa coupling⁹

$$Y \approx a - \frac{1}{2} (b \hat{e}^{-2} b^\dagger a + a c^\dagger f^{-2} c) \epsilon^2, \quad (5.43)$$

and for the Higgs-quark-quark coupling

$$g_{h\bar{q}q} \approx \mathcal{V} \left[a - \frac{3}{2} (b \hat{e}^{-2} b^\dagger a + a c^\dagger f^{-2} c) \epsilon^2 \right] \mathcal{U}^\dagger. \quad (5.44)$$

In contrast to the Yukawa coupling, we explicitly give the Higgs-quark-quark coupling in the mass basis. We note that the corrections to both Y and $g_{h\bar{q}q}$ are not aligned with the leading order piece. Thus, \mathcal{U} and \mathcal{V}^\dagger will not diagonalise $g_{h\bar{q}q}$ although we may choose them such that they diagonalise Y to arbitrary order in ϵ . Moreover, if we compare (5.43) with (5.44), we anticipate that the diagonal $g_{h\bar{q}q}$ couplings are reduced compared to their SM value. Numerically, we explicitly find such an effect in our scan over model parameters, where we exemplarily show the Higgs-top coupling in Figure 5.7(a).

⁹As the effect is equivalent in the up- and down-sector, we omit the subscripts u and d here.

5.4. Lepton Sector

Having discussed the quark sector in quite some detail we now focus on the lepton sector of the model. Here, we only give an overview of possible extensions of the quark Lagrangian which are compatible with realistic neutrino observables. Although we have already stated the operators generating the Majorana mass structure in (5.5b), we show which alternative setups are feasible and briefly discuss their features in this section. In the end we recapitulate the results obtained for the explicit lepton sector chosen in Table 5.1.

As we have seen in the previous models and also more generally in Section 2.3.1, we may generate a phenomenologically viable structure of neutrino masses and mixing by introducing heavy right-handed Majorana fermions. In the setup discussed here we actually have three flavour triplets of SM neutral fermions at our disposal; the SM neutrino partner q_R^ν as well as its heavy partners Ω_R^ν and $\bar{\Omega}_L^\nu$. All of these may get a large Majorana mass and are allowed to mix. We note that the neutrino components of \bar{q}_L , $\bar{\Xi}_L$ and Ξ_R are merely singlets in the SM broken phase and may thus only get Majorana masses of order the electroweak scale. We start with an effective ansatz, where we consider mass terms for each of these “heavy neutrinos” separately. Although this is not the most general setup, we restrict ourselves to it as we do not intend to give an exhaustive picture. Having identified one particularly promising effective mass term we discuss two dynamical realisations of it. The first introduces appropriate scalar fields while the second generates the corresponding mass term effectively via some GRV-like mechanism.

5.4.1. Effective Ansatz

For the effective neutrino mass matrix it is sufficient to study the up-type component of the Lagrangian (5.5). Additionally, we add mass terms for the three SM Singlets q_R^ν , Ω_R^ν and $\bar{\Omega}_L^\nu$. After electroweak symmetry breaking, we can write the effective Lagrangian as

$$\begin{aligned} \mathcal{L}_\nu^{\text{eff}} = & \lambda v_u \bar{q}_L^\nu \Omega_R^\nu + M \bar{\Omega}_L^\nu t_u \Omega_R^\nu + M \bar{\Omega}_L^\nu q_R^\nu + \text{h.c.} \\ & + \lambda v_u \bar{\Xi}_L^\nu q_R^\nu + M \bar{\Xi}_L^\nu s \Xi_R^\nu + M \bar{q}_L^\nu \Xi_R^\nu + \text{h.c.} \\ & + \frac{\Lambda}{2} q_R^\nu x_\nu q_R^\nu + \frac{\Lambda}{2} \Omega_R^\nu x_\Omega \Omega_R^\nu + \frac{\Lambda}{2} \bar{\Omega}_L^\nu x'_\Omega \bar{\Omega}_L^\nu, \end{aligned} \quad (5.45)$$

where the x_i are arbitrary 3×3 matrices and Λ is some large see-saw mass scale. For a hierarchical mass structure we can formally integrate out the heavy degrees of freedom one by one. We now study the effective SM neutrino mass matrix resulting from (5.45) with only one non-vanishing x_i .

$\mathbf{x}_\nu \neq \mathbf{0}$

This setup would be the natural first guess. It reflects the known see-saw ansatz of neutrino mass generation. However, in our setup the Dirac part of the neutrino mass matrix features large hierarchies as it is related to the up-quark mass matrix. Calculating the effective neutrino mass matrix explicitly we obtain

$$m_\nu^{\text{eff}} \sim \frac{M^2 \epsilon^2}{\Lambda} (s^{-1} + t_u^{-1}) x_\nu^{-1} (s^{-1} + t_u^{-1})^T. \quad (5.46)$$

5. Gauged Flavour Symmetry

The term $(s^{-1} + t_u^{-1})$ contains a strong hierarchy as it corresponds to the up-type Yukawa matrix (cf. (5.11)). Thus, the matrix x_ν has to cancel the hierarchy in the quark sector twice in order to generate neutrino masses with only a mild hierarchy.

$\mathbf{x}_\Omega \neq \mathbf{0}$

Another ansatz is to take the neutrino part of Ω_R as see-saw partner of the SM neutrino. This is motivated by the observation that it has a non-hierarchical Dirac coupling to \bar{q}_L^ν . Therefore, a usual type I see-saw leads to the well known effective mass for \bar{q}_L^ν . However, there are also other couplings of \bar{q}_L^ν and Ω_R^ν which result in additional contributions to the effective mass. A full calculation leads to

$$m_\nu^{\text{eff}} \sim \frac{M^2 \epsilon^2}{\Lambda} (1 + s^{-1} t_u) x_\Omega^{-1} (1 + s^{-1} t_u)^T . \quad (5.47)$$

We expect only a mild hierarchy in $(s^{-1} t_u)$ as the quark sector is strongly aligned and both s and t_u feature similar hierarchies. Numerically, we also find that its hierarchy is small ($\lesssim 100$) for realistic values of s and t_u .

$\mathbf{x}'_\Omega \neq \mathbf{0}$

The third possible case is discussed for reasons of completeness only; it has neither a good motivation nor does it generate an interesting effective neutrino mass. As $\bar{\Omega}_L^\nu$ does not directly couple to \bar{q}_L^ν , its effect on the neutrino mass are of second order. $\bar{\Omega}_L^\nu$ has a Dirac coupling to q_R^ν and Ω_R^ν and thus induces a see-saw mechanism including those. After integrating out $\bar{\Omega}_L^\nu$ as well as $\bar{\Xi}_L^\nu$ and Ξ_R^ν , we obtain a mass structure where no entry is clearly dominating the matrix. Only if we assume the special case of a mild hierarchy between M and Λ ($\Lambda \epsilon \ll M \ll \Lambda$) we are able to integrate out Ω_R^ν . The effective neutrino mass results in

$$m_\nu^{\text{eff}} \sim \epsilon^2 \Lambda t_u^{-1} x'_\Omega (t_u^{-1})^T , \quad (5.48)$$

which again gives reasonable neutrino masses only for a large scale M (small ϵ) and a strong hierarchy in x'_Ω .

$\mathbf{x}_\Omega \sim \mathbf{x}'_\Omega \neq \mathbf{0}$

For future reference, we additionally consider the case where x_Ω and x'_Ω are non-vanishing and of similar size. In this case we have two separate see-saw masses in place; one involving \bar{q}_L^ν and Ω_R^ν , and a second one involving q_R^ν and $\bar{\Omega}_L^\nu$. This leads to effective Majorana masses for \bar{q}_L^ν and q_R^ν which are negligible compared to their corresponding Dirac coupling. This coupling is generated by integrating out the pair $\bar{\Xi}_L, \Xi_R$ and is given by

$$m_\nu^{\text{D,eff}} \sim M \epsilon s^{-1} . \quad (5.49)$$

Such a neutrino mass is phenomenologically not acceptable as it is of similar size and hierarchy as the quark masses.

From these general discussions we conclude that the model should feature a Majorana mass term for Ω_R^ν alone. In the following, show how such a setup can be realised.

5.4.2. Single Scalar extension

As the effective Majorana operator of Ω_R^ν introduced in (5.45) is of dimensions three¹⁰ we can interpret x_Ω as vev of a scalar field X_Ω . This scalar has to transform non-trivially under PS, thus breaking the symmetry completely. Looking at the PS group structure of the Majorana operator of Ω_R we find that there is only a single representation that is able to generate a Majorana mass. As we have to project out the neutrino components, only the symmetric part in both $SU(4)$ and $SU(2)'$ may contribute. The flavour quantum numbers are also determined as the Majorana mass term must be symmetric in Ω_R . Thus X_Ω has to transform as $(\overline{\mathbf{10}}, \mathbf{1}, \mathbf{3})(\overline{\mathbf{6}}, \mathbf{1})$. For the sake of Z_2 symmetry we have to additionally introduce the partner X'_Ω transforming as $(\mathbf{10}, \mathbf{3}, \mathbf{1})(\mathbf{1}, \mathbf{6})$ which must not get a vev as it would break $SU(2)$.

Although such a setup is phenomenologically valid it does not resolve the issue of gauge anomaly cancellation as only scalar fields are introduced. Thus, we will not discuss this realisation in more detail here. We note that such a setup may be useful when considering a supersymmetric extension of the model, as in this case all superfields contribute to the gauge anomalies.

5.4.3. GRV-like extension

Instead of introducing the Majorana mass term for Ω_R^ν directly through a vev of a scalar field we may also generate it similarly to the Yukawa term by introducing additional fermions. This has the advantage that these fermions contribute to the flavour gauge anomaly and may cancel it if chosen appropriately. The general structure of such a setup is

$$\mathcal{L}_{\text{Maj}} \sim \overline{\Theta}_L \Phi' \Omega_R + \frac{1}{2} \overline{\Theta}_L S_\nu \overline{\Theta}_L, \quad (5.50)$$

where Φ' and S_ν are additional scalar fields and $\overline{\Theta}_L$ is the newly introduced heavy fermion. Both scalars get a vev

$$\langle \Phi' \rangle = \Lambda \varphi \quad \text{and} \quad \langle S_\nu \rangle = \Lambda' s_\nu \quad (5.51)$$

at different scales $\Lambda \ll \Lambda'$ which both are large ($\gg M \hat{s}$). This ansatz results in the effective Majorana mass parameter

$$x_\Omega \sim \frac{\Lambda^2}{\Lambda'} \varphi^T s_\nu^{-1} \varphi \quad (5.52)$$

for Ω_R^ν in (5.45). Thus, the setup effectively generates a double see-saw as described in Section 2.3.2. So far we have not specified the transformation properties of $\overline{\Theta}_L$, Φ' and S_ν . Here, several options are possible of which we will discuss three in more detail. From these we find one that appears particularly interesting and therefore realise it in our model setup presented above. We note that different representations introduce different invariant structures and φ as well as s_ν need not be matrices in complete flavour space. We will neglect any indices and contractions for reasons of readability in the following Lagrangians.

¹⁰As we consider a non-SUSY setup, terms up to dimension 4 are renormalisable.

5. Gauged Flavour Symmetry

(I) Φ' transforming as PS Singlet

The first possibility we discuss is that Φ' transforms as a PS singlet. In such a case, $\bar{\Theta}_L$ transforms as $(\bar{\mathbf{4}}, \mathbf{1}, \mathbf{2})(\mathbf{1}, \mathbf{3})$, where the transformations under flavour are chosen such that $\bar{\Theta}_L$ cancels the flavour gauge anomaly. Thus, it is similar to the quark fields and their partner. The representation of $\bar{\Theta}_L$ also fixes the transformation of S_ν and Φ' completely. Moreover, we have to introduce their Z_2 partners as we do not want to break Z_2 explicitly. The resulting additional particle content of the neutral lepton sector is given in Table 5.2.

	$SU(4) \times SU(2) \times SU(2)'$	$SU(3)_I \times SU(3)_{II}$
$\bar{\Theta}_L \oplus \Theta_R$	$(\bar{\mathbf{4}}, \mathbf{1}, \mathbf{2}) \oplus (\mathbf{4}, \mathbf{2}, \mathbf{1})$	$(\mathbf{1}, \mathbf{3}) \oplus (\bar{\mathbf{3}}, \mathbf{1})$
$\Phi \oplus \Phi'$	$(\mathbf{1}, \mathbf{1}, \mathbf{1}) \oplus (\mathbf{1}, \mathbf{1}, \mathbf{1})$	$(\mathbf{3}, \mathbf{3}) \oplus (\bar{\mathbf{3}}, \bar{\mathbf{3}})$
$S_\nu \oplus S'_\nu$	$(\mathbf{10}, \mathbf{1}, \mathbf{3}) \oplus (\bar{\mathbf{10}}, \mathbf{3}, \mathbf{1})$	$(\mathbf{1}, \bar{\mathbf{6}}) \oplus (\mathbf{6}, \mathbf{1})$

Table 5.2.: Additional particle content for the lepton sector with transformation properties in case I.

This setup introduces the Majorana mass term for Ω_R as well as a coupling of the Z_2 partners where S'_ν must not get a vev. In addition, the coupling $\bar{\Xi}_L \Theta_R \Phi$ is allowed which might contribute dangerously to the quark and lepton mass matrix as it extends the fermion mass matrix to a 12×12 structure. Concerning the vev of S_ν we find that only the neutral component may get a non-vanishing vev and thus only the additional neutral fermion gets massive. This leaves us with a “complete” generation of massless, charged fermions. Although this is not a problem as such, we would have to introduce additional fields and new terms in the Lagrangian to make these massless fields heavy. This is against our principle of simplicity and thus we do not consider this setup any further.

(II) $\bar{\Theta}_L$ as PS Singlet

As only a SM neutral component of $\bar{\Theta}_L$ may get a Majorana mass through its coupling to S_ν we now consider $\bar{\Theta}_L$ to transform as a PS singlet. This implies that the PS structure has to be implemented in Φ' in order to generate a PS invariant term. We have already encountered a PS scalar transforming as $(\bar{\mathbf{4}}, \mathbf{1}, \mathbf{2})$ in Chapter 3 where we introduced the corresponding superfield to break PS completely. We have also seen that its vev may well be in the range of 10^{12} GeV and higher. Thus it perfectly qualifies here. However, requiring $\bar{\Theta}_L$ to transform as PS singlet does not fix its flavour structure and the one of Φ' . Again we have more than one possibility. In order to cancel the flavour gauge anomaly we need to introduce eight fermions transforming as anti-triplet under $SU(3)_I$ as well as their Z_2 partners. Thus, we chose $\bar{\Theta}_L$ to transform either as $(\mathbf{8}, \mathbf{3})$ or $(\bar{\mathbf{3}}, \mathbf{8})$ under flavour.

Case IIA: We start our discussion with the case that $\bar{\Theta}_L$ transforms as $(\mathbf{8}, \mathbf{3})$. Having fixed the PS transformation of Φ' and the flavour transformation of $\bar{\Theta}_L$ we can deduce all other transformations, leading to the particle content given in Table 5.3.

	$SU(4) \times SU(2) \times SU(2)'$	$SU(3)_I \times SU(3)_{II}$
$\bar{\Theta}_L \oplus \Theta_R$	$(\mathbf{1}, \mathbf{1}, \mathbf{1}) \oplus (\mathbf{1}, \mathbf{1}, \mathbf{1})$	$(\mathbf{8}, \mathbf{3}) \oplus (\bar{\mathbf{3}}, \mathbf{8})$
$\Phi \oplus \Phi'$	$(\mathbf{4}, \mathbf{2}, \mathbf{1}) \oplus (\bar{\mathbf{4}}, \mathbf{1}, \mathbf{2})$	$(\mathbf{3}, \mathbf{3}) \oplus (\bar{\mathbf{3}}, \bar{\mathbf{3}})$
$S_\nu \oplus S'_\nu$	$(\mathbf{1}, \mathbf{1}, \mathbf{1}) \oplus (\mathbf{1}, \mathbf{1}, \mathbf{1})$	$(\mathbf{1}, \bar{\mathbf{6}}) \oplus (\mathbf{6}, \mathbf{1})$

Table 5.3.: Additional particle content for the lepton sector with transformation properties in case IIA.

This field content introduces additional terms in the Lagrangian, which are given by

$$\begin{aligned} \mathcal{L} \supset & \bar{\Theta}_L \Phi' \Omega_R + \bar{\Theta}_L S_\nu \bar{\Theta}_L + \bar{\Omega}_L \Phi'^* \Theta_R + \bar{\Theta}_L S^* \Theta_R \\ & + \bar{\Xi}_L \Phi \Theta_R + \Theta_R S'_\nu \Theta_R + \bar{\Theta}_L \Phi^* \Xi_R. \end{aligned} \quad (5.53)$$

Here, the Dirac mass term $\langle \Phi' \rangle^* \bar{\Omega}_L \Theta_R$ is of special interest as it generates a large mass for $\bar{\Omega}_L$ and thus a large value $x_{\Omega'}$. If S'_ν acquires a vev similar to S_ν , we obtain a symmetric setup generating a Majorana mass for Ω_R as well as $\bar{\Omega}_L$. If S'_ν does not acquire a vev, $\bar{\Omega}_L$ is still heavy due to the Dirac coupling and results in a mass structure similar to the one containing $x_{\Omega'}$. Thus, this setup always generates an effective Lagrangian similar to (5.45) with $x_\Omega \sim x_{\Omega'} \neq 0$ which is phenomenologically excluded. However, by imposing an additional symmetry forbidding the aforementioned Dirac term and demanding S'_ν to receiving a large vev, the setup generates an effective light neutrino mass matrix compatible to experimental data. As we do not intend to introduce additional symmetries we do not study such a setup in detail here.

Case IIB: The second possibility is to consider a setup in which $\bar{\Theta}_L$ transforms as $(\bar{\mathbf{3}}, \mathbf{8})$. Again, this fixes all other representations leading to the field content shown in Table 5.4.

	$SU(4) \times SU(2) \times SU(2)'$	$SU(3)_I \times SU(3)_{II}$
$\bar{\Theta}_L \oplus \Theta_R$	$(\mathbf{1}, \mathbf{1}, \mathbf{1}) \oplus (\mathbf{1}, \mathbf{1}, \mathbf{1})$	$(\bar{\mathbf{3}}, \mathbf{8}) \oplus (\mathbf{8}, \mathbf{3})$
$\Phi \oplus \Phi'$	$(\mathbf{4}, \mathbf{2}, \mathbf{1}) \oplus (\bar{\mathbf{4}}, \mathbf{1}, \mathbf{2})$	$(\mathbf{8}, \mathbf{1}) \oplus (\mathbf{1}, \mathbf{8})$
$S_\nu \oplus S'_\nu$	$(\mathbf{1}, \mathbf{1}, \mathbf{1}) \oplus (\mathbf{1}, \mathbf{1}, \mathbf{1})$	$(\mathbf{6}, \mathbf{1}) \oplus (\mathbf{1}, \bar{\mathbf{6}})$

Table 5.4.: Additional particle content for the lepton sector with transformation properties in case IIB.

This field content does not allow for the problematic Dirac couplings of the setup before. Thus, the additional terms in the Lagrangian are reduced to

$$\begin{aligned} \mathcal{L} \supset & \bar{\Theta}_L \Phi' \Omega_R + \bar{\Theta}_L S_\nu \bar{\Theta}_L + \bar{\Theta}_L S^* \Theta_R \\ & + \bar{\Xi}_L \Phi \Theta_R + \Theta_R S'_\nu \Theta_R, \end{aligned} \quad (5.54)$$

5. Gauged Flavour Symmetry

where Φ again must not get a vev. If S'_ν does not get a vev, Θ_R does not receive a large mass in the first place. However, it forms a Dirac mass term with $\bar{\Theta}_L$ and thus gets massive. In addition, this coupling generates a dangerous Dirac coupling between \bar{q}_L^ν and q_R^ν of the form $M^2 \Lambda^{-1} \epsilon (s + t_u) \varphi^{-1}$ which dominates the mass matrix. Thus, such a setup is phenomenologically not reasonable.

Nevertheless, if S'_ν acquires a vev of similar size as S_ν , Θ_R is rendered heavy and the Dirac coupling is suppressed. In this case, the flavour symmetry is broken completely at the large scale Λ' . Such a setup reproduces the effective Lagrangian (5.45) for the case $x_\Omega \neq 0$ and thus generates a phenomenologically reasonable neutrino mass in the eV-range without internal hierarchies.

5.4.4. Resulting Lepton Sector

To sum up, in order to generate a viable lepton sector we introduce one additional fermion $\bar{\Theta}_L$ transforming as $(\mathbf{1}, \mathbf{1}, \mathbf{1})(\bar{\mathbf{3}}, \mathbf{8})$ as well as the two scalar fields Φ' and S_ν . Furthermore, we need to include their partners to be consistent with the Z_2 symmetry. The two PS singlets S_ν and S'_ν receive a vev of the scale Λ' whereas Φ' acquires a vev at a lower but still high scale Λ (cf. (5.7)). These additional fields lead to the setup already given in the Lagrangian (5.5b) and the fields displayed in Table 5.1.

However, we do not aim for an explicit construction of the full lepton sector which would require a detailed discussion of the breaking of $SU(4)$. Hence, we keep our presentation of the neutrino sector at a qualitative level. The complete leptonic Lagrangian we consider is given by

$$\begin{aligned} \mathcal{L}_{\text{Yuk}}^{\text{lepton}} \sim & \bar{q}_L H \Omega_R + \bar{\Omega}_L (S + T') \Omega_R + M \bar{\Omega}_L q_R \\ & + \bar{\Xi}_L H q_R + \bar{\Xi}_L (S + T) \Xi_R + M \bar{q}_L \Xi_R \\ & + \bar{\Theta}_L \Phi' \Omega_R + \bar{\Theta}_L S_\nu \bar{\Theta}_L + \bar{\Theta}_L S^\dagger \Theta_R \\ & + \bar{\Xi}_L \Phi \Theta_R + \Theta_R S'_\nu \Theta_R + \text{h.c.} , \end{aligned} \quad (5.55)$$

where we have neglected all couplings which we assume to be of order one. Moreover, we implicitly consider only the leptonic components of the fields.

This Lagrangian generates the effective neutrino mass matrix

$$m_\nu^{\text{eff}} \sim \frac{\Lambda' v_u^2}{\Lambda^2 \varphi^2} (1 + s^{-1} t_u) s_\nu (1 + s^{-1} t_u)^T . \quad (5.56)$$

We note that φ^2 has no flavour structure as Φ' transforms solely under $SU(3)_{II}$ while ν_L transforms under $SU(3)_I$. It is important to notice, that the mixing in the neutrino sector is not fixed by the quark sector. It is rather determined by the symmetry structure of the vev s_ν and may thus qualitatively deviate from the CKM matrix.

Moreover, the leptonic Lagrangian (5.55) leads to a mass matrix for the charged leptons which is equal to the one of the down-type quarks at the GUT scale, $Y_e \sim Y_d$. This is a reasonable first approximation. In addition, we may induce deviations from this equality if we allow the flavon fields S and T' to transform non-trivially under $SU(4)$. The $SU(4)$ group

structure of the terms $\bar{\Omega}_L (S + T') \Omega_R$ and $\bar{\Xi}_L (S + T) \Xi_R$ also allows S and T' to transform as **15**. This will not alter the quark sector but introduces a factor of -3 for the lepton sector, as the generator breaking $SU(4)$ is given by $T^{15} \sim \text{diag}(1, 1, 1, -3)$. Such a setup is similar to the ansatz of Georgi and Jarlskog [104]. Thus, if only one of the two flavons transforms as **15**, we introduce a relative factor in (5.11), which will create a deviation from the aforementioned equivalence; e.g. for $T' (\mathbf{15}, \mathbf{1}, \mathbf{3})(\bar{\mathbf{3}}, \mathbf{3})$ we get

$$Y_e \sim (s + 3t')^{-1} + s^{-1}. \quad (5.57)$$

Another ansatz is to split either S or T' in two parts, one transforming trivially and one transforming as **15**. This would generate even more variations in the lepton Yukawa matrices as we may arbitrarily split the flavon vevs; e.g. for $S' (\mathbf{1}, \mathbf{1}, \mathbf{1})(\bar{\mathbf{3}}, \mathbf{3})$ and $S'' (\mathbf{15}, \mathbf{1}, \mathbf{1})(\bar{\mathbf{3}}, \mathbf{3})$ we get

$$Y_e \sim ((s_1 - 3s_{15}) - t')^{-1} + (s_1 - 3s_{15})^{-1}, \text{ with } s_1 + s_{15} \equiv s. \quad (5.58)$$

To conclude, although we have not constructed the lepton sector in detail we find that in general the model is capable of a phenomenologically allowed lepton sector.

5.5. Phenomenology of the Quark Sector

In the previous sections we have presented the setup of the model and calculated analytically the resulting effects on flavour parameters. However, we are not able to solve the derived Yukawa matrices (5.30) for s and t analytically. Thus, we are not able to parametrise the effects by the known flavour parameters (m_i and V_{ij}). Nevertheless, it is possible to invert the approximate formula given in (5.11) numerically. Here, we encounter the technical complication that multiple solutions exist; two for each generation. Starting from a left-right symmetric theory we cannot rotate the right-handed up and down sector separately. Hence, we have to introduce the additional mixing matrix U_{CKM} which parametrises the coupling of the W'^{\pm} bosons to the quarks. Furthermore, the enlarged symmetry introduces additional physical phases in the Yukawa sector.

Experimentally we have no information on U_{CKM} nor do we know the solution which provides an appropriate description of nature. Therefore, we choose to scan over these degrees of freedom. In this section, we explain how this scan is performed and present the resulting flavour effects.

5.5.1. Setup of the Scan

In principle the scan should be performed over the complete set of model parameters, namely s , t' , λ , $\tan\beta$ and M . However, as s and t' feature large hierarchies a direct scan over these is not feasible. Thus we use an alternative ansatz and scan over ‘‘adapted flavour parameters’’ which we define in the following.

Adapted Flavour Parameters

We start our considerations with the quark masses and mixing angles as fitted in the SM framework [15]. In addition we add mixing angles and phases for the unknown matrix U_{CKM} which describes the mixing of the right-handed quarks. With this input we calculate an explicit realisation for Y_u and Y_d in an arbitrary basis. For a given pair of Yukawa matrices it is possible to invert (5.11) numerically and thus derive s and t' (see Appendix C.2). These are however only approximate and we expect sizeable corrections for the third generation. Nevertheless, for given values of s and t' we can explicitly diagonalise the 9×9 mass matrix and calculate the derived 3×3 Yukawa matrices. Comparing these with the input we find that the mass and mixing angles related to the third generation are systematically too small. Therefore, we adjust the input parameters such that the derived 3×3 Yukawa matrices match the ones obtained within the SM. In the following we denote these adjusted input parameters as adapted flavour parameters and define ranges over which we perform the scan.

Performing the Scan

Having defined the adapted flavour parameters we set the stage to perform a systematic scan over possible flavour effects. We do not claim this scan to be exhaustive as the setup may systematically exclude allowed regions of the parameter space. Nevertheless, it provides an insight into the essential flavour effects of this model. The scan itself is performed using the following steps:

1. Randomly generate a point in the space of adapted flavour parameters as well as for λ , $\tan \beta$ and M . The allowed ranges are given in Appendix C.3.
2. Calculate s and t' by inverting (5.11) using the procedure described in Appendix C.2.
3. Insert the so calculated s and t' as well as λ , $\tan \beta$ and M into the full 9×9 dimensional mass matrix and diagonalise it explicitly.
4. Deduce the effective Yukawa parameters (m_i and V_{ij}).
5. Compare these with the experimentally allowed 3σ ranges¹¹ and save the point $(s, t', \lambda, \tan \beta, M)$ in case of agreement.

Following these steps, we have scanned the model parameters in the ranges $\lambda \in [1, 3]$, $\tan \beta \in [1, 15]$ and $M \in [700, 2500]$ GeV. The scanned ranges of the adapted flavour parameters as well as the explicit Yukawa matrices used for the scan are discussed in Appendix C.3. The allowed ranges for the effective Yukawa parameters are given in Table 5.5 and Table 5.6.

We have generated roughly 3,000 points using the full range of adapted parameters. However, as scanning the full parameter space of the right-handed rotations is quite inefficient, we have also performed a scan where we have limited the right-handed rotations to be small ($\Theta_R^i \lesssim 1.5^\circ$). This results in 30,000 additional points which differ qualitatively from

¹¹We take the masses at $m_i = m_i(M_Z)$ and the experimental values for the individual CKM entries V_{ij} (not those obtained from additionally demanding unitarity).

the full scan only for V'_{CKM} , i.e. in the coupling of the right-handed quarks to the SM gauge bosons. To enhance the statistics, we use the combination of both for all plots except for those containing V'_{CKM} where we use only the set of 3,000 points.

Covering the Parameter Space

We intend to vary the adapted flavour parameters in a wide range such that the model explores the complete range of experimentally allowed Yukawa parameters. This is possible for most of the parameters, however, not all of them are distributed equally over the allowed range. Especially the absolute values of the CKM elements $|V_{tb}|$, $|V_{ts}|$, $|V_{cs}|$ and $|V_{cd}|$ are more constrained in our setup. This can be traced back to fact that the direct bounds for these CKM elements are relatively weak while the correction ΔV_{CKM} (related to non-unitarity) is small. If we instead compare the covered range to the CKM elements as deduced from the fit of the SM Wolfenstein parameters [15], we generate many points outside of the 3σ region. In particular, we find that our $|V_{tb}|$ is typically smaller. The experimental bounds we impose for the individual CKM elements as well as the ranges deduced from the SM fit and the ranges covered by our scan are given in Table 5.5.

The masses all cover the full allowed range. Yet we find that especially the charm mass tends to lower values. For the light quark masses we also see a deficit (although not as pronounced as for m_c) for the largest values of the allowed ranges. We interpret these effects as relics of our scan as the setup generally lowers the mass eigenvalues. The allowed ranges for the masses as well as model parameters are given in Table 5.6.

An additional relic of our scan is the fact that λ does not cover the full allowed range but rather peaks around $\lambda = 2$, which is the point we used to determine the ranges for the adapted parameters. As we are mainly interested in this part of the parameter space we do not expand our scan. Concerning $\tan\beta$ and M , we find that they are equally distributed throughout the full allowed range.

5.5.2. Effects on the Flavour Parameter

Having checked that we are able to generate the flavour parameters of the SM we now turn to possible effects on additional flavour observables provided by the scan discussed above.

Dependence on the Scale M

In the definition of the flavour breaking vevs (5.6) we have explicitly factored out the dependence on the mass scale M . This is motivated by the observation, that the explicit M -dependence of the approximate Yukawa relation (5.11) can thereby be cancelled. Thus, we expect no explicit dependence on M in $a \dots f$ arising when diagonalising the mass matrix. However, there may still be an implicit M -dependence due to effects hidden in the determination of s and t . As (5.11) is a good approximation for the first two generations (where $y_u, y_d \ll 1$ and thus $s, t \gg 1$) we expect no further M -dependence here. For the third generation, we have explicitly checked for a possible additional M -dependence using the scan. As a result, we find no additional dependence on M in any of the quantities; at least above a certain threshold of roughly 1 TeV. This allows us to make the dependence on the scale M explicit throughout the model and especially in all corrections.

5. Gauged Flavour Symmetry

	$ V_{ud} $	$ V_{us} $	$ V_{ub} $
experiment	0.9736 - 0.9749	0.2229 - 0.2277	0.0027 - 0.0056
unitarity	0.9739 - 0.9747	0.2235 - 0.2272	0.0031 - 0.0040
covered	0.9737 - 0.9748	0.2231 - 0.2277	0.0027 - 0.0056
	$ V_{cd} $	$ V_{cs} $	$ V_{cb} $
experiment	0.2010 - 0.2490	0.9380 - 1.0340	0.0372 - 0.0450
unitarity	0.2234 - 0.2271	0.9730 - 0.9739	0.0378 - 0.0450
covered	0.2229 - 0.2276	0.9727 - 0.9741	0.0372 - 0.0450
	$ V_{td} $	$ V_{ts} $	$ V_{tb} $
experiment	0.0066 - 0.0102	0.0319 - 0.0481	0.9250 - 1.1170
unitarity	0.0079 - 0.0099	0.0372 - 0.0438	0.9990 - 0.9993
covered	0.0066 - 0.0102	0.0355 - 0.0447	0.9711 - 0.9992

Table 5.5.: Coverage of the allowed range of flavour parameters. The first line corresponds to the direct experimental limits we impose for the scan; the second line is the allowed range deduced from the SM fit to the Wolfenstein parameters and the last line corresponds to the range covered by our scan.

m_u	0.5 – 2.9 MeV	m_d	1.2 – 4.8 MeV	λ	1.5 – 2.5
m_c	0.53 – 0.71 GeV	m_s	30 – 78 MeV	$\tan \beta$	1 – 15
m_t	162 – 180 GeV	m_b	2.78 – 2.96 GeV	M	750 – 2500 GeV

Table 5.6.: Ranges for the quark masses and the model parameters covered by our scan.

The effects on the flavour parameters are usually proportional to $\epsilon^2 \propto M^{-2}$ (cf. (5.42)). As we know the M -dependence theoretically, we may limit ourselves to an arbitrary mass band, which we choose to be $M \in [1, 1.2]$ TeV, for some of the further studies which reduces our set to $\sim 3,500$ points. This clarifies the dependence on the other parameters of the scan as it reduces the spread due to the variation of M . The values obtained for this mass band may afterwards be used to extrapolate the effects to larger values of M using the explicit M -dependence. On the contrary, we can also use the explicit M -dependence to rescale all generated points to a single mass scale. We make use of this rescaling in the discussion of V'_{CKM} later in this section in order to increase the statistics for the small mass band.

Masses of the Additional Fermions

The masses of the heavy up-type quark partners can be read off from the diagonalised mass matrix (5.28). A similar expression can be deduced for the down-type quark partners by interchanging u with d . As we have explicitly factored out the flavour mass scale M it is

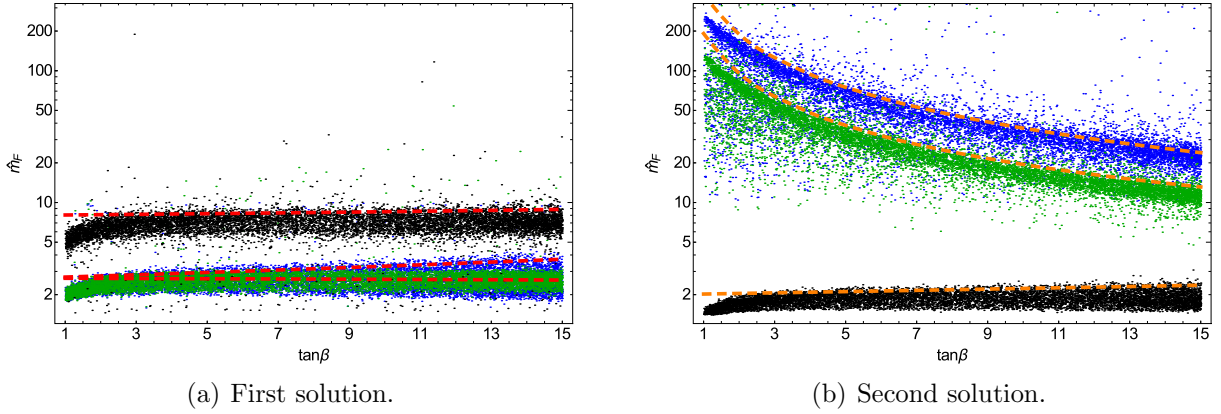


Figure 5.3.: Mass ratios \hat{m}_F of the lightest additional fermionic partners with respect to $\tan\beta$. The plots show the masses of the first bottom partner in blue, the first top partner in black and the second top and bottom partners in green. The two solutions of (5.12) are given for each mass ratio as dashed lines in red (a) and orange (b), respectively.

reasonable to consider only the mass ratio

$$\hat{m}_F = \frac{m_F}{M}. \quad (5.59)$$

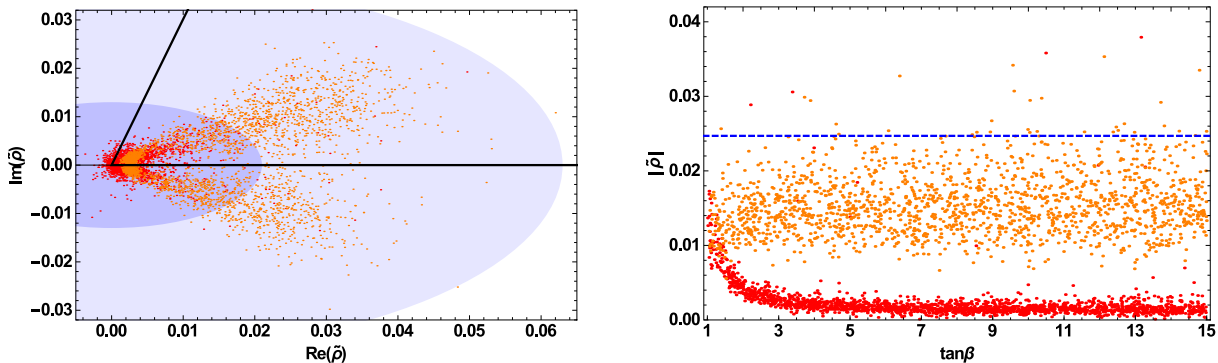
As \hat{f} does not depend on isospin, we can directly infer that one set of heavy up-type partners equals one set of down-type partners in mass (later on denoted by U'' and D'' , where U (D) are any of the up-type (down-type) quarks). This we find verified by the scan where these masses are equal at the sub-percentage level. They split up if we include a vev for the $SU(2)$ -breaking fields T , $\langle T \rangle \neq 0$, whereby their difference is proportional to $\langle T \rangle$.

However, we find two distinct bands of solutions for each of these mass ratios. These are expected¹² as we have already encountered two solutions while inverting the approximate Yukawa relation for one generation (cf. (5.12)). We note that due to the 2HDM character y_u and y_d are $\tan\beta$ -dependent in this formula. The resulting $\tan\beta$ -dependence of the heavy fermion masses calculated from the one generation case fits the results of the scan reasonably well as illustrated in Figure 5.3. Here, we have plotted the mass ratios \hat{m}_F of the four lightest fermion partners (b' , t' , b'' and t'') against $\tan\beta$. For clarity we have separate the two possible solutions; the mass ratios of t'' and b'' are shown in green (as both equal in mass), the one of b' in blue and that of t' in black. Additionally, we have plotted the $\tan\beta$ -dependence of the mass ratios deduced from (5.12) where we used the SM Yukawa couplings and $\lambda = 2$ as fixed input. In doing so, we introduce a colour coding for this and the following plots such that masses belonging theoretically to the first (second) solution of (5.12) are given in red (orange).

From the plot we can conclude, that the mass ratios of the additional fermions may be of order one and thus, their masses can be in the TeV-range. However, depending on the

¹²In general, we would expect 8 distinct solutions, however, the effects for each generation are dominated by their “own” multiplicity.

5. Gauged Flavour Symmetry



(a) Zooming in on the lower edge of the standard unitarity triangle. The blue shaded region corresponds to the 1σ and 3σ ellipse of $\bar{\rho}$ and $\bar{\eta}$.

(b) Absolute value of the non-unitarity measure $|\tilde{\rho}|$ with respect to $\tan\beta$ in the mass band $M \in [1, 1.2]$ TeV. The dashed blue line indicates the corresponding 1σ error on $|\bar{\rho} + i\bar{\eta}|$ in the SM.

Figure 5.4.: Non-unitarity of the CKM matrix. In red (orange) we present the non-unitarity measure $\tilde{\rho}$ for the first (second) solution of (5.12) for the third generation.

solution nature chooses we may expect either a set of three quark partners (b' , t'' and b'') within a small mass range or solely the top partner t' to appear in experiments. Thus, the two solutions qualitatively differ in their predictions which we also see in the following discussions.

Non-Unitarity of V_{CKM}

Due to the additional ϵ^2 -dependent contribution ΔV_{CKM} to the CKM matrix the coupling of the W^\pm bosons to the quarks is no longer unitary. This non-unitarity can be quantified by studying the unitarity triangles constructed from the CKM matrix. For explicitness we limit the discussion to the “standard unitarity triangle” here. We have obtained similar results with similar or even smaller effects for the other possible triangles.

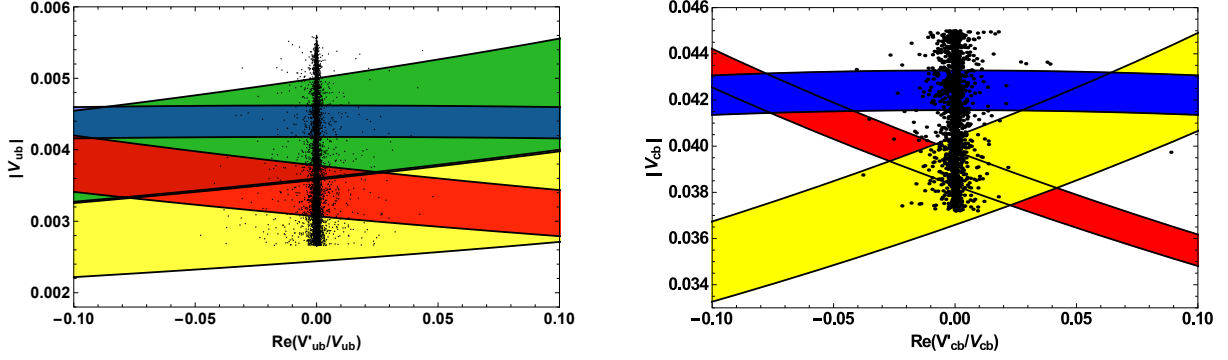
Generically we do not expect large deviations from the SM here as we have limited the scan points to lay within the uncertainty of the absolute values of the CKM matrix elements. This is a simplified assumption as right-handed couplings would influence the determination of the CKM elements from experimental measurement. To give a complete picture we would have to redo the determination of the CKM elements in the presence of additional couplings of right-handed quarks (V'_{CKM}) and without the assumption of unitarity. However, such an explicit fit is beyond the scope of this thesis.

To quantify the non-unitarity in the “standard” unitarity triangle we define the complex quantity

$$\tilde{\rho} = \frac{V_{ub}V_{ud}^* + V_{cb}V_{cd}^* + V_{tb}V_{td}^*}{V_{cb}V_{cd}^*}, \quad (5.60)$$

which is a nil test in the SM.

In Figure 5.4 we show the lower edge of the triangle for the complete set of scan points. In addition, we present the $\tan\beta$ -dependence of the non-unitarity (the absolute value $|\tilde{\rho}|$) where we limit the given points to lie in the mass band $M \in [1, 1.2]$ TeV for the sake of



(a) Influence of couplings of right-handed quarks on the determination of V_{ub} . The bands show different measurements; blue: inclusive decays, red: $B \rightarrow \pi l \nu$, yellow: $B \rightarrow \rho l \nu$, green: $B \rightarrow \tau \nu$. The possible values deduced in the scan are shown in black.

(b) Influence of couplings of right-handed quarks on the determination of V_{cb} . The bands show different measurements; blue: inclusive decays, red: $B \rightarrow D^* l \nu$, yellow: $B \rightarrow D l \nu$. The possible values deduced in the scan are shown in black.

Figure 5.5.: Influence of V'_{CKM} on the determination of V_{CKM} [148]. Using the explicit M -dependence, the possible values of the scan have been scaled to a reference scale of $M = 1 \text{ TeV}$.

clarity. Again, we separate the points belonging to the different solutions, using the colour code introduced above. We compare these effects with the 1σ and 3σ uncertainty on the SM Wolfenstein parameters $\bar{\rho}$ and $\bar{\eta}$, which determine the upper edge of the SM unitarity triangle. As expected, we observe that the non-unitarity is compatible with the SM uncertainties. Moreover, we again find that the effect depends crucially on the type of solution. This is particularly apparent in the $\tan \beta$ -dependence of $|\bar{\rho}|$ (cf. Figure 5.4(b)). Here, the second solution (orange) is basically independent of $\tan \beta$ whereas the first (red) is of similar size for $\tan \beta = 1$ and practically vanishes for $\tan \beta \gtrsim 3$. Thus, the effect may be absent even for small values of the flavour breaking mass scale M . Taking a look at the lower edge of the unitarity triangle we find that the real part of $\bar{\rho}$ is generically positive (cf. Figure 5.4(a)). This indicates that the effect is dominated by the reduction of V_{tb} which shortens the right side of the triangle.

Right-Handed Coupling V'_{CKM}

In the setup introduced above, the right-handed SM fermions couple to the SM W^\pm bosons due to their mixing with Ξ_R . The coupling strength is parametrised by V'_{CKM} and is given in (5.42c). From the formula we can read off that the coupling is proportional to ϵ^2 which is also confirmed in our scan. Such a right-handed coupling is of great interest as it influences the determination of the CKM elements in the SM; in particular in view of the tension between the inclusive and exclusive determination of V_{ub} and V_{cb} . The additional couplings V'_{ub} and V'_{cb} may reduce this tension as the inclusive decay is proportional to $|V_{xb}|^2 + |V'_{xb}|^2$, whereas the exclusive decays are proportional to either¹³ of $|V_{xb} \pm V'_{xb}|^2$ [149]. However, it

¹³Depending on whether the decay is mediated by axial or vector currents.

5. Gauged Flavour Symmetry

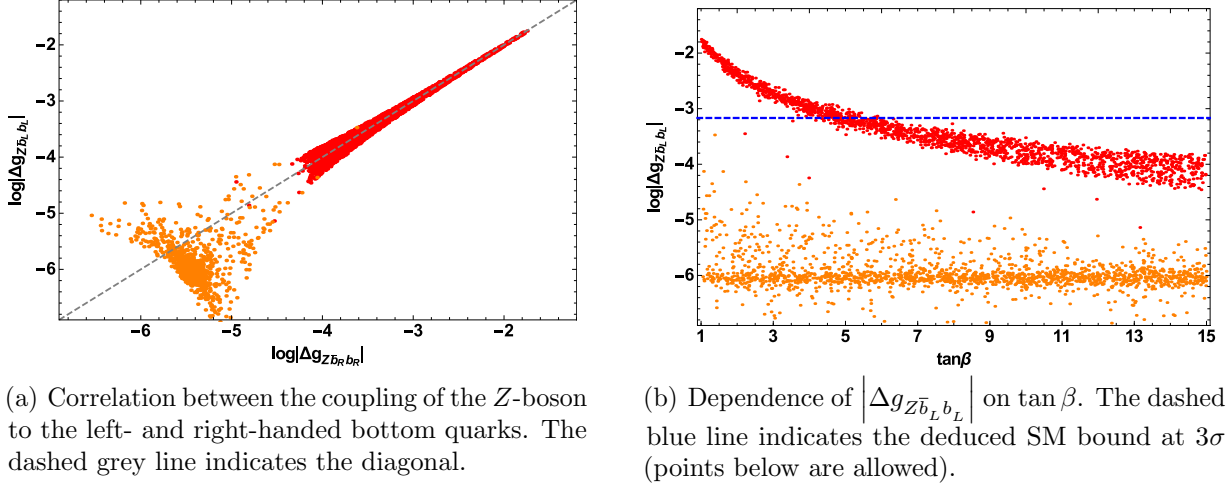


Figure 5.6.: Correction of the Z -boson coupling to the b quarks. In red (orange) we show the points belonging to the first (second) solution for the mass band $M \in [1, 1.2]$ TeV.

has also been shown that V'_{CKM} cannot simultaneously explain all measurements [148–151]. Still, the scan may show which measurements are “theoretically preferred” in our setup.

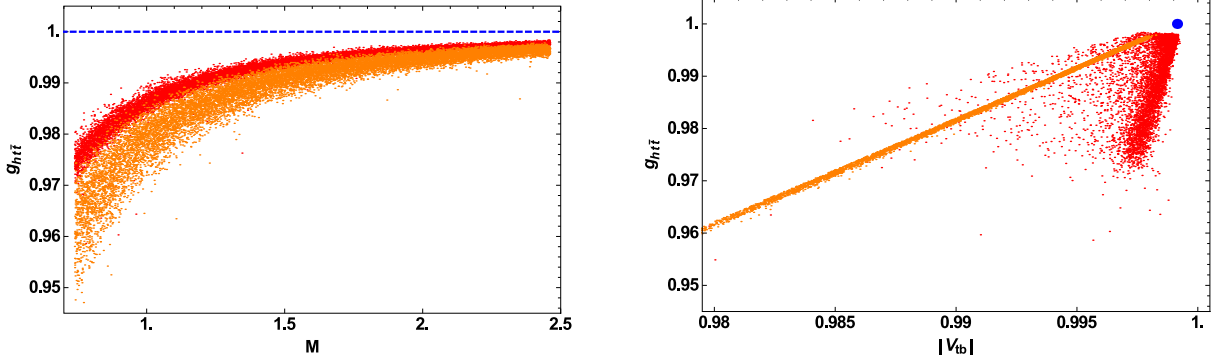
Using the scan, we have checked for such effects but find no conclusive answer. In Figure 5.5 we have plotted the current 1σ measurements of V_{ub} and V_{cb} depending on an additional right-handed coupling [148]. Additionally, we show points generated in the scan scaled to a reference mass scale $M = 1$ TeV. We find that the relative contributions of V'_{CKM} are at the percent level at most and that the scan shows no preference for any of the measurements. Additionally, we do not see any correlation between V'_{ub} and V'_{cb} .

Anomalous Z Couplings

Besides the effects mentioned so far we obtain a modification of the coupling between the Z -boson and the quarks. Similarly to the effects discussed above, we find the largest deviation in the top quark coupling. However, the experimental constraints are quite weak here as the Z -boson cannot decay into a pair of top quarks. Thus we focus on the coupling of the bottom quarks to the Z -boson where the correction is still sizeable. This decay is kinematically allowed and has been measured precisely at LEP2 to $\Gamma(Z \rightarrow b\bar{b}) \approx (375.87 \pm 0.17)$ MeV [15]. In this decay, the coupling of the right- as well as left-handed b -quarks is involved. Looking at the correlation between both we find that for large values the corrections equal each other (cf. Figure 5.6(a)). Thus, we can use the simplifying assumption that the variation on both is equal. Assuming furthermore that the correction to the coupling is within the experimental uncertainty, we may limit the couplings to

$$|\Delta g_{Z\bar{b}_L b_L}| \sim |\Delta g_{Z\bar{b}_R b_R}| \lesssim 6.8 \times 10^{-4} \quad @ 3\sigma. \quad (5.61)$$

This bound reduces the number of allowed points generated in the scan by roughly 10 percent. The excluded points all belong to the first solution of (5.12). Moreover, they are proportional to ϵ^2 and show a correlation in $\tan\beta$. For larger values of either $\tan\beta$ or M , the effects



(a) Dependence of the modified Higgs-top-top coupling as a function of M . The SM expectation is shown as dashed blue line. The direct error is larger than the plotted range.

(b) Correlation between the Higgs-top-top coupling with respect to $|V_{tb}|$. The SM point is given in blue. The errors on both quantities are larger than the plotted ranges.

Figure 5.7.: Correction of the Higgs-top-top coupling. In red (orange) we show the points belonging to the first (second) solution.

decreases and thus the bound is fulfilled more often. In Figure 5.6 we show the correlation between the left- and right-handed corrections as well as the $\tan\beta$ -dependence for the aforementioned mass band $M \in [1, 1.2]$ TeV. In the right plot we find that for the first solution we are able to exclude roughly all model point for $\tan\beta \lesssim 4$.

Anomalous Higgs Couplings

The Higgs coupling to the top-quark $g_{h\bar{t}t}$ may receive sizeable corrections in our setup (cf. Section 5.3.4). However, already for the b quark as well as all lighter quarks this effect is negligible. As the effect is due to corrections of order ϵ^2 it reduces drastically for increasing M . For small values of M , the effect is of the order of a few percent (see Figure 5.7(a)). However, experimentally the Higgs-top-top coupling is only poorly known and has roughly 30 percent uncertainty [152, 153]. Thus, this correction will rather be important for precision observables, where the top and the Higgs occur in loops so that indirect constraints apply.

In addition, we find a correlation of $g_{h\bar{t}t}$ to V_{tb} which may be of phenomenological interest as the top quark decays nearly instantaneously into a bottom quark and a W boson. Depending on the two solutions, V_{tb} either shows the same M -dependence (orange) or is rather independent of M (red) (see Figure 5.7(b)). Such a correlation may enlarge the effect on e.g. associated Higgs production $gg \rightarrow \bar{t}tH$ which would be reduced in our setup.

Next to the reduction of the coupling $g_{h\bar{q}q}$ we find a flavour changing coupling of the Higgs. These may be relevant for flavour changing neutral currents. Here, the bounds for light quarks are already quite severe (which may be relevant although naturally suppressed in our setup) and those for the heavy quarks will become stricter over time. Thus, a careful study of the FCNC effects including the Z boson couplings would be interesting but is beyond the scope of this thesis.

5.6. Comments on a Supersymmetric Extension

So far we have limited ourselves to the non-supersymmetric setup. This has the advantage that we can directly deduce low-energy flavour observables without specifying the soft-SUSY breaking sector. However, without SUSY we are left with the naturalness problem (cf. Section 1.2). In the model presented in this chapter the situation is even worse as we introduce multiple scales featuring large hierarchies. Thus, we have presented an effective analysis rather than a conclusive top-down picture of the model. The task of constructing a complete top-down model is left for future studies and should involve the introduction of SUSY at some largish scale. Technically, the implementation of SUSY is straight forward and can be achieved by promoting each field to a superfield and rewriting the Lagrangian in terms of a superpotential. However, there are two subtleties in doing so which we want to mention here.

Anomaly cancellation

Simply promoting each field to a superfield reintroduces gauge anomalies in the model. This is due to the fermionic partners introduced for each of the scalar fields in Table 5.1 which will contribute to the anomalies. Thus, the fields that in the non-SUSY setup belong to the scalar sector have to have a vanishing contribution to the anomaly for each factor of the gauge group¹⁴. This is not the case in the setup proposed above as gauge anomalies in the flavour sector remain.

One possible solution to this issue would be the introduction of a “partner” for each of the scalar fields, thereby directly cancelling the anomaly by hand. In such a setup additional couplings would arise which could be forbidden by global symmetries, similar to the previous chapter. Another strategy would be to reconsider the lepton sector of the theory. In the non-SUSY case we have chosen the additional fields for the lepton sector such that they cancel the gauge anomaly of the quark sector. This construction strongly limited our choices. However, in the SUSY setup it is not as simple as in the non-SUSY case to find a suitable lepton sector.

D-Term flatness

A second problem arising in the simplest supersymmetric extension is D-term flatness. Taking into account all fields which acquire vevs, we have to ensure that the D-terms of all gauge vector fields vanish. Thus, we have to introduce vevs of similar hierarchy which may cancel the D-term contribution of each other. The simplest ansatz would be to include additional superfields receiving a similar vev in the conjugated representation. This is in line with cancelling the gauge anomalies. Operators leading to experimentally problematic couplings may again be forbidden by introducing a global symmetry.

Although we have outlined the principle steps needed to introduce SUSY, we will not discuss such a setup in any detail here. This is due to the fact that we do not expect any new insights in the model as we are no longer able to directly deduce flavour effects.

¹⁴Note that mixed anomalies do not occur in a gauge symmetry without explicit $U(1)$ factors (cf. Appendix C.1).

5.7. Summary

In this chapter we have presented a model of a gauged $SU(3)_I \times SU(3)_{II}$ flavour symmetry within a Pati-Salam Grand Unified Theory, where the Yukawa matrices are generated by flavon vevs which occupy the lower end of the energy spectrum (reaching down to the TeV-range). We have introduced two flavons acquiring hierarchical vev structures at similar scales. The breaking of the flavour symmetry is mediated to the SM fermions by additionally introduced fermionic fields. These new fermions couple to the flavons and acquire masses proportional to their vevs. The lightest of each of these fermions is of the order of the “flavour breaking” scale M which is introduced into the theory by hand and may well be in the TeV-range. We have focused on a non-supersymmetric realisation and limited ourselves to renormalisable operators of the Lagrangian. Concerning the phenomenological discussion of the model we have concentrated on the quark sector as it features the most stringent bounds.

The model presented here provides a new ansatz of implementing flavour as it reproduces the SM flavour sector from matrices that vastly differ from the SM Yukawa matrices. It is thus different from the ansatz of Minimal Flavour Violation which is often implemented in flavour models beyond the Standard Model. In our setup, we also encounter only small effects in the flavour sector. These are determined by the SM Yukawa matrices (up to right-handed rotations which have only minor effects on the low energy observables) which imprint their structure on the model by fixing the form of the flavon vevs in an intricate way. However, the effects do not depend linearly on the Yukawa matrices as it would be the case in MFV. Still, the model is able to reproduce the SM flavour sector from 21 dimensionless parameters and one mass scale without being in conflict with current flavour data. In addition, it gives rise to interesting non-standard effects which could be observable in future experiments.

Setting up the model we have followed the idea of Grinstein, Redi and Villadoro. However, the phenomenology of the model is significantly different due to the more constrained framework of a GUT symmetry. The flavour gauge bosons are of no phenomenological interest as they receive masses far above the TeV scale. The embedding of the SM Higgs in PS uplifts the setup to a two Higgs doublet model. In addition, we double the extra fermionic fields introduced in the setup of the quark sector. Thus, they do not cancel the flavour gauge anomalies. However, additional fermionic fields are required for the construction of a viable lepton sector, which in turn solves the issue of flavour gauge anomalies. As we need to distinguish the up-type from the down-type sector we need to introduce a flavon transforming non-trivially under $SU(2)'$. Moreover, the Z_2 symmetry requires a further coupling of the quarks to the PS singlet flavon field. This complicates the simple relation between the flavon vevs and the SM Yukawa matrices found by Grinstein et al. In addition, this setup leads to an ambiguity in the determination of the flavon vevs where we find two solutions for each generation. For this reason, we explicitly calculate the transformation to the mass basis as an expansion in the flavour scale M . This enables us to express the effects on the flavour couplings in this expansion. However, we are not able to parametrise the flavon vevs by SM quantities. Thus, we have alternatively performed a scan over the parameter space of the model in a specific (though well defined) manner. With this scan, we are able to cover most of the experimentally allowed ranges of the quark masses and CKM matrix elements.

5. Gauged Flavour Symmetry

From the scan we can conclude that the effects on the flavour parameters are generically small and compatible with the SM expectations. This smallness is due to the general setup of the scan, as we only allow for parameter points which are consistent with the absolute values of V_{CKM} . As the Yukawa matrices of the quark sector are strongly aligned, the low energy flavour phenomenology is dominated by flavour diagonal effects. This may be generally different in the lepton sector where the mixing angles of the PMNS matrix are much larger. Thus, a more detailed study of the lepton sector would be very interesting.

Although most effects are small, we find observables which allow to exclude some regions of the parameter space. An example for such an effect is the coupling of the Z -boson to a pair of bottom quarks. This coupling is incompatible with the measured branching fraction $\Gamma(Z \rightarrow \bar{b}b)$ for scan points belonging to the first solution with small $\tan\beta$ and moderated mass scale M . As the additional fermions are allowed to have masses in the TeV-range, they may be detectable in the next run of the LHC or future experiments. Here, we find a clear discrimination in the aforementioned ambiguity. Depending on the solution nature chooses we may expect either one or three lightest new fermionic partners with nearly degenerate mass. Of special interest is also the influence of V'_{CKM} (the coupling of the W bosons to the right-handed quarks) on the determination of V_{ub} and V_{cb} as there is a tension between different experimental measurements. However, we find no conclusive solution to this state of affairs as the effects are only at the percent level and no set of measurements is preferred by our model.

In addition, we find that the scan is consistent with the explicit M -dependence given in the parametrisation of the flavour effects. Thus, all effects on the flavour observables vanish quadratically when increasing M . As the effects on most of the flavour observables are beyond the scope of current experiments a global analysis would be needed to be able to favour or exclude large regions of the parameter space.

Besides the discussion of the quark sector we have also sketched possible realisations of lepton flavour in this chapter as the PS symmetry connects both sectors. We have limited ourselves to a qualitative discussion of the lepton sector. Making use of a Majorana structure for the right-handed neutrinos allows us to generate masses and mixing patterns which differ from the quark sector. Due to the additionally introduced fermionic partners we identified nine SM neutral fermions which are able to play the role of the right-handed neutrino. Hence, we have discussed several possibilities of generating a viable neutrino flavour sector. For the realisation of the model presented in this chapter we have chosen a setup in which one set of the right-handed neutrino partners gets a mass at some large scale (above $\sim 10^{10}$ GeV) which in turn generates the masses and mixing of the light SM neutrinos. In addition we have commented on variations of the setup which allow for corrections of the lepton mass structure. However, this already requires a complete breaking of the flavour symmetry at this scale and thus effects of flavour gauge bosons are far beyond experimental reach.

Chapter 6

Conclusions & Outlook

In this thesis we have addressed the question of embedding a theory of flavour in the framework of Pati-Salam symmetric Grand Unified Theories. This we have realised by constructing three individual model setups which deal with different aspects of model building. A detailed summary on each of the models can be found at the end of the corresponding chapters.

Throughout this thesis we have shown that a rich variety of setups beyond the Standard Model (SM) are possible which might help to understand the flavour sector and possible further unification of particle interactions better. Especially if we give up the constraint of single scale unification we found plenty of setups featuring intermediate mass scales with phenomenologically interesting consequences (Chapter 3). Examples include scenarios with additional coloured particles in the TeV range, Majorana mass scales in the range of $10^{12} - 10^{14}$ GeV and/or complete unification near or at the Planck scale.

In the classes of models presented in Chapter 3 we have not been interested in an explicit realisation of the flavour sector but have rather studied the unification behaviour of setups in which multiple fields may occur in three copies, just like the SM fermions. This multiplicity is motivated by the additional study presented in this thesis on the possibility of additional fields which themselves carry flavour structure. Here, we have especially considered the case that the electroweak symmetry breaking Higgs of the SM appears in three copies (Chapter 3) which may transform non-trivially under the flavour gauge group (Chapter 4).

We have gauged the flavour symmetry in models constructed in Chapter 4 and Chapter 5 in order to break it spontaneously by vacuum expectation values (vev) of scalar fields, the so-called flavons. In Chapter 4 these flavon vevs are located at high energies (near the Planck scale) and in Chapter 5 at the lower end (TeV range). For both setups we have been able to qualitatively reproduce the observed masses and mixing structures. In Chapter 5 we have presented a more quantitative analysis, where we have considered possible effects on the low-energy (SM) flavour parameters.

In the first of these setups (Chapter 4) we have constructed the flavour sector according to an idea originally presented by Froggatt and Nielsen. The second model (Chapter 5) we have based on a work of Grinstein, Redi and Villadoro (GRV). Both of these setups have already been studied in the literature for various extensions of the SM but not in a setup as the one chosen here. In contrast to the already existing models we have studied in Chapter 4 the implication of considering SM Higgs fields transforming as a flavour triplet which has motivated us to allow for non-fundamental representations of the flavons. In the model

6. Conclusions & Outlook

presented in Chapter 5, we have presented an explicit realisation in a PS-symmetric theory which so far was only sketched in the literature. The variations needed to realise such a setup significantly change the low-energy effects of the model. Here, especially the effects due to the imposed Z_2 symmetry are qualitatively different as they introduce couplings of the right-handed SM fermions to the weak gauge bosons.

Generally we have kept our considerations on a rather qualitative level. This has allowed us to consider large model classes as we have only fixed the general framework for the models. Hence, we have studied general features and possible effects rather than explicitly studying a single model in great detail.

A possible next step would be to study any of the models presented in Chapter 3 and Chapter 4 in more detail, i.e. fix the free parameters for a single model and explicitly deduce the low-energy effects. Alternatively one could perform scans over parts of the parameter space similar to the scan performed in Chapter 5, which would also be reasonable only for a single setup. Such scans may allow to constrain the various parameter spaces to general robust predictions. For this purpose it is important to perform a global fit, as various observables which are possibly unrelated in the SM may yield constraints on a single parameter. Such an global analysis is also very interesting for the GRV-type model presented in Chapter 5, where we have already generated the corrections to the low-energy parameters. However, as the current experimental data does not allow for conclusive predictions yet, we did not aim for such an analysis in this thesis.

Another issue which was raised throughout this thesis is the general possibility of generating vevs from scalar potentials featuring non-fundamental representations. This is needed in Chapter 4 where the vevs of multiple fields should feature different hierarchies as well as in Chapter 5 where each vev should have a hierarchical pattern imprinted in its matrix structure. For both setups it is important to study which general vev structures can be achieved in the corresponding setup.

Moreover, we have presented models motivating for an enlarged SM Higgs sector in this thesis. In order to explicitly deduce low-energy effects in any of these models it is crucial to understand such a sector in more detail. Again, the aspect of generating the electroweak breaking vev in the presence of a flavour symmetry is essential for the construction of flavour models, especially in Chapter 4.

Throughout this thesis we have shown that especially for the flavour sector GUT models are not able to make robust and conclusive statements when considering non-minimal models, i.e. dropping the assumption of a single scale unification and allowing for scalar fields transforming in non-fundamental representations. We have been able to generate a rich variety of intermediate scales and flavour aspects already for setups based on few simple assumptions. Thus, it will be very challenging to exclude substantial classes of models. Still, one should keep in mind that these simple assumptions already by construction satisfy the severe bounds coming from SM phenomenology. These are largely dominated by quark flavour physics and electroweak precision observables. Thus, measurements from different sectors of the SM may shed some light on possible routes beyond the SM. As the measurement of neutrino masses itself is an effect not predicted by the SM, it will be essential to gain a

better understanding of this sector. Also lepton flavour violation might be very important as it is extremely suppressed in the SM but predicted by multiple models beyond the SM. To conclude, GUTs may help to answer the question of the origin of flavour but in order to achieve this one needs to find significant deviations from the SM predictions by future experiments.

Appendix

Appendix A

Unification Model

A.1. Model Naming Scheme

The global naming convention is laid out at the end of Section 3.1. For all configurations of type g we use a numerical naming scheme. The numbers follow an internal numbering given by the structure of our Mathematica file. This file is available from the author upon request.

Table A.1 displays the connection between the multiplicities of the different fields present below the Planck scale and the names of the models discussed in more detail in this thesis.

	name	$\#h$	$\#F$	$\#\Phi^{(\prime)}$	$\#\Sigma$	$\#E$	$\#T^{(\prime)}$
SUSY models:	Em	0	0	1	1	0	0
	Fm	0	0	1	0	0	1
	Es/Fs	1	1	1	1	1	1
	Ee/Fe	3	3	3	3	1	1
	F189	1	3	1	1	1	1
	Bm/Cm	0	0	1	1	0	1
	Bs/Cs	1	1	1	1	1	1
	Be/Ce	3	3	1	1	1	1
	B199	3	3	1	3	0	1
	C211	3	3	3	3	0	1
Non-SUSY models:	E289	3	3	1	1	0	0
	F213	1	3	3	3	1	1
	B53	1	3	1	1	3	1
	C45	1	1	3	3	1	1

Table A.1.: Particle content and multiplicities for the models discussed in this thesis.

A.2. Mass Matrices

In Chapter 3, we have constructed the maximally allowed renormalisable superpotential that follows from the field content given in Table 3.1. The superpotential is given by (3.3). From this superpotential, we have calculated the minimisation conditions to be able to deduce the full mass matrix of the setup. This we have used to assign the fields present in the spectrum to the sub-unification scales relevant for gauge coupling unification. The results are listed in Table 3.2. In this Appendix, we present the mass matrices for each of the unbroken (with respect to the SM) field components and give the explicit mass eigenvalues. These we calculate by inserting the minimisation conditions (3.7) into the Lagrangian (3.4) and setting all fields to their ground states. Hence, the masses generally depend on the vevs of the symmetry breaking fields, which set the scales of the model.

Mass of the octet

The mass of the colour octet contained in Σ is determined by the minimisation conditions. It is given by

$$\mathcal{M}(\Sigma_8) = \frac{l_{\Sigma\Phi} v_{\Phi}^2}{v_{\Sigma}} + 4l_{\Sigma} v_{\Sigma}. \quad (\text{A.1})$$

In class F, the mass of the octet is solely given by its bilinear mass term m_{Σ} .

Mass of E

As already mentioned in Section 3.4.1, the superfield E does not receive any mass contribution from the symmetry breaking. Thus, the mass of its components is solely determined by the bilinear superpotential term:

$$\mathcal{M}(E) = m_E. \quad (\text{A.2})$$

Mass of the bitriplet with $|Y| = 1/6$

The superfields Φ and $\bar{\Phi}$ contain a bitriplet with hypercharge $Y = \pm 1/6$. Similar triplets are contained in the superfield E but do not mix, as there is no coupling between the two. The mass of the bitriplets coming from Φ and $\bar{\Phi}$ can be determined to

$$\mathcal{M}\left(\left(\mathbf{3}/\bar{\mathbf{3}}, \mathbf{2}\right)_{\pm 1/6}\right) = \frac{1}{3} (3l_{T\Phi} v_T + 4l_{\Sigma\Phi} v_{\Sigma}). \quad (\text{A.3})$$

In class E (F), the first (second) term is absent.

Mass of the triplet with $|Y| = 2/3$

A set of triplets with hypercharge $Y = \pm 2/3$ is contained in the superfields Φ and $\bar{\Phi}$ as well as in Σ . These triplets mix as they have identical SM representations. The resulting

(symmetric) mass matrix is given by

$$\mathcal{M}^2\left((\mathbf{3}/\bar{\mathbf{3}}, \mathbf{2})_{\pm 2/3}\right) = \quad (\text{A.4})$$

$$\begin{pmatrix} \frac{1}{2} g_4^2 v_\Phi^2 + \frac{4}{9} l_{\Sigma\Phi}^2 v_X^2 & -\frac{1}{2} g_4^2 v_\Phi^2 & \frac{-i(3g_4^2 v_\Sigma^2 + 2v_X^2)v_\Phi^2}{3\sqrt{3}v_\Sigma} & \frac{i}{\sqrt{3}} g_4^2 v_\Phi v_\Sigma \\ \star & \frac{1}{2} g_4^2 v_\Phi^2 + \frac{4}{9} l_{\Sigma\Phi}^2 v_X^2 & \frac{i}{\sqrt{3}} g_4^2 v_\Phi v_\Sigma & \frac{-i(3g_4^2 v_\Sigma^2 + 2v_X^2)v_\Phi^2}{3\sqrt{3}v_\Sigma} \\ \star & \star & \frac{1}{3} \left(\frac{v_\Phi^2}{v_\Sigma^2} l_{\Sigma\Phi}^2 v_X^2 + 2g_4^2 v_\Sigma^2 \right) & -\frac{2}{3} g_4^2 v_\Sigma^2 \\ \star & \star & \star & \frac{1}{3} \left(\frac{v_\Phi^2}{v_\Sigma^2} l_{\Sigma\Phi}^2 v_X^2 + 2g_4^2 v_\Sigma^2 \right) \end{pmatrix},$$

where we have defined

$$v_X^2 = (3v_\Phi^2 + 4v_\Sigma^2). \quad (\text{A.5})$$

In class F, the mixing between the components of Φ and Σ vanishes and thus the mass matrix splits into two 2×2 blocks. The mass eigenvalues are given by

$$\frac{1}{\sqrt{3}} \left(0, g_4 v_X, \frac{v_\Phi}{v_\Sigma} v_X, \frac{v_\Phi}{v_\Sigma} v_X \right). \quad (\text{A.6})$$

The eigenvalue 0 corresponds to the six charged Goldstone bosons, which get ‘‘eaten up’’ by the heavy $SU(4)$ gauge bosons.

Mass of the triplet with $|\mathbf{Y}| = \pm 1/3$

Another set of colour triplets is contained in the superfields Φ and $\bar{\Phi}$ as well as F . These have a hypercharge of $Y = \pm 1/3$. Their mass matrix can be calculated to

$$\mathcal{M}^2\left((\mathbf{3}/\bar{\mathbf{3}}, \mathbf{1})_{\pm 1/3}\right) = \quad (\text{A.7})$$

$$\begin{pmatrix} 2l_{F\Phi}^2 v_\Phi^2 + \frac{4}{9} (2l_{\Sigma\Phi} v_\Sigma + 3l_{T\Phi} v_T)^2 & \frac{-\sqrt{2}}{3} v_\Phi (3l_{F\Phi} m_F + 4l_{F\bar{\Phi}} l_{\Sigma\Phi} v_\Sigma + l_{F\bar{\Phi}} l_{T\Phi} v_T) \\ \star & m_F^2 + 2l_{F\bar{\Phi}}^2 v_\Phi^2 \end{pmatrix}.$$

In the case that m_F is small with respect to the vevs, the approximate eigenvalues are given by

$$\left(m_F - \frac{3l_{F\Phi} l_{F\bar{\Phi}} v_\Phi^2}{2l_{\Sigma\Phi} v_\Sigma + 3l_{T\Phi} v_T}, \frac{4}{3} l_{\Sigma\Phi} v_\Sigma + 2l_{T\Phi} v_T \right). \quad (\text{A.8})$$

Mass of T

Similar to the colour octet, the mass of the $SU(2)$ triplet T is determined by the minimisation conditions. It can be calculated to be

$$\mathcal{M}(T) = \frac{l_{T\Phi} v_\Phi^2}{v_T}. \quad (\text{A.9})$$

In class E (vanishing v_T), it is proportional to its bilinear mass parameter m_T .

A. Unification Model

Mass of the Higgs bidoublet

The mass matrix of the MSSM Higgs bidoublet h has already been discussed in Section 3.4.2. For completeness, we present the mass matrix only.

$$\mathcal{M}^2 \left((\mathbf{1}, \mathbf{2})_{\pm 1/2} \right) = \begin{pmatrix} m_h^2 + l_{h\Phi}^2 v_\Phi^2 & (l_{T\Phi} v_T - m_h) l_{h\Phi} v_\Phi \\ (l_{T\Phi} v_T - m_h) l_{h\Phi} v_\Phi & l_{h\Phi}^2 v_\Phi^2 + l_{T\Phi}^2 v_T^2 \end{pmatrix}. \quad (\text{A.10})$$

Mass of the Singlets with $|\mathbf{Y}| = 1$

The fields Φ' and $\bar{\Phi}'$ as well as T' contain singlets under $SU(3) \times SU(2)$ with hypercharge $Y = \pm 1$. Their 8×8 mass matrix can be split in 2×2 blocks. The remaining 4×4 structure is given by

$$\mathcal{M}^2 \left((\mathbf{1}, \mathbf{1})_{\pm 1} \right) = \begin{pmatrix} \mathcal{M}_{v_\Phi}^2 & 0 & i g_{2'}^2 v_\Phi v_T \mathcal{M}_1 & -i\sqrt{2} l_{T\Phi}^2 (v_\Phi^2 + 2v_T^2) \frac{v_\Phi}{v_T} \mathbb{1} \\ \star & \mathcal{M}_{v_\Phi}^2 & i\sqrt{2} l_{T\Phi}^2 (v_\Phi^2 + 2v_T^2) \frac{v_\Phi}{v_T} \mathbb{1} & i g_{2'}^2 v_\Phi v_T \mathcal{M}_1 \\ \star & \star & \mathcal{M}_{v_T}^2 & 0 \\ \star & \star & \star & \mathcal{M}_{v_T}^2 \end{pmatrix}, \quad (\text{A.11})$$

where we have defined the 2×2 matrices

$$\mathcal{M}_{v_\Phi}^2 = \begin{pmatrix} \frac{1}{2} g_{2'}^2 v_\Phi^2 + 2l_{T\Phi}^2 (v_\Phi^2 + v_T^2) & -\frac{1}{2} g_{2'}^2 v_\Phi^2 \\ -\frac{1}{2} g_{2'}^2 v_\Phi^2 & \frac{1}{2} g_{2'}^2 v_\Phi^2 + 2l_{T\Phi}^2 (v_\Phi^2 + v_T^2) \end{pmatrix}, \quad (\text{A.12})$$

$$\mathcal{M}_{v_T}^2 = \begin{pmatrix} \frac{1}{2} g_{2'}^2 v_T^2 + l_{T\Phi}^2 \left(2v_\Phi^2 + \frac{v_\Phi^4}{v_T^2} \right) & -g_{2'}^2 v_T^2 \\ -g_{2'}^2 v_T^2 & \frac{1}{2} g_{2'}^2 v_T^2 + l_{T\Phi}^2 \left(2v_\Phi^2 + \frac{v_\Phi^4}{v_T^2} \right) \end{pmatrix}, \quad (\text{A.13})$$

$$\mathcal{M}_1 = \begin{pmatrix} 1 & -1 \\ -1 & 1 \end{pmatrix}. \quad (\text{A.14})$$

In class E, the off-diagonal 2×2 blocks vanish. In addition, the mass matrix of the singlets formally belonging to T (lower 4×4 block) is diagonal and determined by their bilinear mass term m_T only. The general mass eigenvalues of (A.11) are given by

$$\left(0, 0, g_{2'} \sqrt{v_\Phi^2 + 2v_T^2}, l_{T\Phi} \frac{(v_\Phi^2 + 2v_T^2)}{v_T}, l_{T\Phi} \frac{(v_\Phi^2 + 2v_T^2)}{v_T}, l_{T\Phi} \frac{(v_\Phi^2 + 2v_T^2)}{v_T} \right). \quad (\text{A.15})$$

The vanishing eigenvalues are two of the Goldstone bosons of $SU(2)'$, which get “eaten up” by the heavy gauge bosons.

Masses of the Singlets

As already mentioned in the main part of this thesis, the mass matrix of the SM singlets is very complicated. It is at least 6×6 dimensional, as we find a singlet component in T' , Σ , Φ' and $\overline{\Phi}'$ as well as the two explicitly included singlets S_{27} and S_{78} . As it is of no relevance for the running of the gauge couplings, we have not considered it in detail. Nevertheless, we have deduced a qualitative dependence of the masses on the vevs numerically as given in Table 3.2. In addition, we have verified that two neutral Goldstone bosons, one related to $SU(4)$ and one to $SU(2)'$, are contained in the singlet mass matrix.

A.3. Vacuum Expectation Values and Mass Scales

In the first part of Chapter 3 we calculate the superpotential and the masses of all superfields. Therefore we use the vevs as natural scales. Since in this part, the fields related to these vevs are more important than the symmetry breaking associated to the vevs, we label the vevs by their corresponding field.

In the second part, we are primarily interested in the various scales relevant for the running of the gauge couplings. Hence, we switch our notation to the mass scales. These are labelled by a subscript that indicates the symmetry which is broken at this stage. Nevertheless, these are of course related to the vevs discussed above. As the vevs are associated with different breakings, these relations depend on the individual class. We show these relations explicitly in Table A.2.

vev	class A	class B	class C	class D	class E	class F
v_Σ	M_{PS}	M_{PS}	M_{QL}	M_{PS}	M_{PS}	—
v_T	M_{PS}	M_{LR}	M_{PS}	M_{PS}	—	M_{PS}
v_Φ	M_{PS}	$M_{\text{U}(1)}$	$M_{\text{U}(1)}$	$M_{\text{U}(1)}$	M_{LR}	M_{LR}
$\frac{v_\Phi^2}{v_\Sigma + v_T}$	M_{PS}	M_{IND}	M_{IND}	M_{IND}	M_{IND}	M_{IND}

Table A.2.: Relations between the vevs and the symmetry breaking mass scales for the different classes. The subscript indicate the symmetry which is broken at this scale (PS: Pati-Salam, LR: left-right, QL: quark-lepton or U(1): remaining U(1) factors) or refers to the induced (see-saw) scale (M_{IND}).

A.4. Beta-Function Coefficients

As stated in (3.14), the running of the gauge couplings can be described to leading logarithmic order by

$$\frac{1}{\alpha_i(\mu_2)} = \frac{1}{\alpha_i(\mu_1)} - \frac{b_i}{2\pi} \ln\left(\frac{\mu_2}{\mu_1}\right). \quad (\text{A.16})$$

A. Unification Model

field	PS	LR	SM	$\tilde{b}_Y^{\mathfrak{R}}$	$\tilde{b}_{B-L}^{\mathfrak{R}}$	$\tilde{b}_2^{\mathfrak{R}}$	$\tilde{b}_3^{\mathfrak{R}}$	$\tilde{b}_4^{\mathfrak{R}}$	
h	$(\mathbf{1}, \mathbf{2}, \mathbf{2})$	$(\mathbf{1}, \mathbf{2}, \mathbf{2})_0$	$(\mathbf{1}, \mathbf{2})_{\frac{1}{2}}$	$\frac{1}{2}$	0	$\frac{1}{2}$	0	0	
			$(\mathbf{1}, \mathbf{2})_{-\frac{1}{2}}$	$\frac{1}{2}$		$\frac{1}{2}$	0		
F	$(\mathbf{6}, \mathbf{1}, \mathbf{1})$	$(\mathbf{3}, \mathbf{1}, \mathbf{1})_{\frac{2}{3}}$	$(\mathbf{3}, \mathbf{1})_{\frac{1}{3}}$	$\frac{1}{3}$	$\frac{4}{3}$	0	$\frac{1}{2}$	1	
		$(\bar{\mathbf{3}}, \mathbf{1}, \mathbf{1})_{-\frac{2}{3}}$	$(\bar{\mathbf{3}}, \mathbf{1})_{-\frac{1}{3}}$	$\frac{1}{3}$	$\frac{4}{3}$	0	$\frac{1}{2}$		
Φ'	$(\mathbf{4}, \mathbf{1}, \mathbf{2})$	$(\mathbf{3}, \mathbf{1}, \mathbf{2})_{-\frac{1}{3}}$	$(\mathbf{3}, \mathbf{1})_{\frac{1}{3}}$	$\frac{1}{3}$	$\frac{2}{3}$	0	$\frac{1}{2}$	1	
			$(\mathbf{3}, \mathbf{1})_{-\frac{2}{3}}$	$\frac{4}{3}$		0	$\frac{1}{2}$		
		$(\mathbf{1}, \mathbf{1}, \mathbf{2})_1$	$(\mathbf{1}, \mathbf{1})_1$	1	2	0	0	0	
			$(\mathbf{1}, \mathbf{1})_0$	0		0	0	0	
$\bar{\Phi}'$	$(\bar{\mathbf{4}}, \mathbf{1}, \mathbf{2})$	$(\bar{\mathbf{3}}, \mathbf{1}, \mathbf{2})_{\frac{1}{3}}$	$(\bar{\mathbf{3}}, \mathbf{1})_{\frac{2}{3}}$	$\frac{4}{3}$	$\frac{2}{3}$	0	$\frac{1}{2}$	1	
			$(\bar{\mathbf{3}}, \mathbf{1})_{-\frac{1}{3}}$	$\frac{1}{3}$		0	$\frac{1}{2}$		
		$(\mathbf{1}, \mathbf{1}, \mathbf{2})_{-1}$	$(\mathbf{1}, \mathbf{1})_0$	0	2	0	0	0	
			$(\mathbf{1}, \mathbf{1})_{-1}$	1		0	0	0	
Φ	$(\mathbf{4}, \mathbf{2}, \mathbf{1})$	$(\mathbf{3}, \mathbf{2}, \mathbf{1})_{-\frac{1}{3}}$	$(\mathbf{3}, \mathbf{2})_{-\frac{1}{6}}$	$\frac{1}{6}$	$\frac{2}{3}$	$\frac{3}{2}$	1	1	
		$(\mathbf{1}, \mathbf{2}, \mathbf{1})_1$	$(\mathbf{1}, \mathbf{2})_{\frac{1}{2}}$	$\frac{1}{2}$	2	$\frac{1}{2}$	0		
$\bar{\Phi}$	$(\bar{\mathbf{4}}, \mathbf{2}, \mathbf{1})$	$(\bar{\mathbf{3}}, \mathbf{2}, \mathbf{1})_{\frac{1}{3}}$	$(\bar{\mathbf{3}}, \mathbf{2})_{\frac{1}{6}}$	$\frac{1}{6}$	$\frac{2}{3}$	$\frac{3}{2}$	1	1	
		$(\mathbf{1}, \mathbf{2}, \mathbf{1})_{-1}$	$(\mathbf{1}, \mathbf{2})_{-\frac{1}{2}}$	$\frac{1}{2}$	2	$\frac{1}{2}$	0		
Σ	$(\mathbf{15}, \mathbf{1}, \mathbf{1})$	$(\mathbf{8}, \mathbf{1}, \mathbf{1})_0$	$(\mathbf{8}, \mathbf{1})_0$	0	0	0	3	4	
		$(\mathbf{3}, \mathbf{1}, \mathbf{1})_{-\frac{4}{3}}$	$(\mathbf{3}, \mathbf{1})_{-\frac{2}{3}}$	$\frac{4}{3}$	$\frac{16}{3}$	0	$\frac{1}{2}$		
		$(\bar{\mathbf{3}}, \mathbf{1}, \mathbf{1})_{\frac{4}{3}}$	$(\bar{\mathbf{3}}, \mathbf{1})_{\frac{2}{3}}$	$\frac{4}{3}$	$\frac{16}{3}$	0	$\frac{1}{2}$		
		$(\mathbf{1}, \mathbf{1}, \mathbf{1})_0$	$(\mathbf{1}, \mathbf{1})_0$	0	0	0	0		
E	$(\mathbf{6}, \mathbf{2}, \mathbf{2})$	$(\mathbf{3}, \mathbf{2}, \mathbf{2})_{\frac{2}{3}}$	$(\mathbf{3}, \mathbf{2})_{\frac{5}{6}}$	$\frac{25}{6}$	$\frac{16}{3}$	$\frac{3}{2}$	1	4	
			$(\mathbf{3}, \mathbf{2})_{\frac{1}{6}}$	$\frac{1}{6}$		$\frac{3}{2}$	1		
		$(\bar{\mathbf{3}}, \mathbf{2}, \mathbf{2})_{-\frac{2}{3}}$	$(\bar{\mathbf{3}}, \mathbf{2})_{-\frac{1}{6}}$	$\frac{1}{6}$	$\frac{16}{3}$	$\frac{3}{2}$	1		
			$(\bar{\mathbf{3}}, \mathbf{2})_{-\frac{5}{6}}$	$\frac{25}{6}$		$\frac{3}{2}$	1		
T'	$(\mathbf{1}, \mathbf{1}, \mathbf{3})$	$(\mathbf{1}, \mathbf{1}, \mathbf{3})_0$	$(\mathbf{1}, \mathbf{1})_1$	0	0	0	0	0	
			$(\mathbf{1}, \mathbf{1})_0$	0	0	0	0	0	
			$(\mathbf{1}, \mathbf{1})_{-1}$	0	0	0	0	0	
T	$(\mathbf{1}, \mathbf{3}, \mathbf{1})$	$(\mathbf{1}, \mathbf{3}, \mathbf{1})_0$	$(\mathbf{1}, \mathbf{3})_0$	0	0	2	0	0	

Table A.3.: Complete particle content considered in Chapter 3. Additionally we list their representations under PS ($SU(4), SU(2), SU(2)'$), LR ($SU(3)_c, SU(2), SU(2)'$) $_{U(1)_{B-L}}$ and the SM ($SU(3)_c, SU(2)_w$) $_{U(1)_Y}$ as well as their contributions $\tilde{b}_i^{\mathfrak{R}}$ to the beta functions for all intermediate gauge couplings.

The coefficient b_i can be calculated from the representation of the fields contributing at the given mass scale [117]. Each field contributes with $\tilde{b}_i^{\mathfrak{R}}$ to the i th gauge coupling. For a given set of gauge groups $SU(N)$ with $N \geq 2$, the contribution of a field with representation $\mathfrak{R} = (\mathbf{R}_1, \dots, \mathbf{R}_n)$ to the running coefficient is given by

$$\tilde{b}_i^{\mathfrak{R}} = C(\mathbf{R}_i) \prod_{k \neq i} d(\mathbf{R}_k). \quad (\text{A.17})$$

where $d(\mathbf{R}_i)$ is the dimension and $C(\mathbf{R}_i)$ the Dynkin index of the representation \mathbf{R}_i . This index can be calculated using the representing matrices T_R^a

$$\text{tr } T_R^a T_R^b = C(\mathbf{R}) \delta^{ab}, \quad (\text{A.18})$$

with the convention $C(\mathbf{N}) = \frac{1}{2}$ for fundamental representations \mathbf{N} . For a $U(1)$ the contribution is up to a consistent rescaling:

$$\tilde{b}_{U(1)}^{\mathfrak{R}} = Q_{U(1)}^2 \prod_k d(\mathbf{I}_k). \quad (\text{A.19})$$

Table A.3 displays the contributions $\tilde{b}_i^{\mathfrak{R}}$ of each field as well as its complete decomposition with respect to the subgroups of the PS symmetry. So far the considerations do not depend on whether we are in a supersymmetric or non-supersymmetric framework. However, the full contribution b_i of a field does, as a superfield has both, fermionic and scalar components. For the non-supersymmetric case, we have to divide the contributions into scalar and fermionic parts:

$$b_i^{\text{SM}} = \frac{2}{3} \sum_{\mathfrak{R}_{\text{ferm.}}} \tilde{b}_i^{\mathfrak{R}} + \frac{1}{3} \sum_{\mathfrak{R}_{\text{scalar}}} \tilde{b}_i^{\mathfrak{R}} - \frac{11}{3} C_2(G_i), \quad (\text{A.20})$$

where the last part originates from the gauge bosons. Here, $C_2(\mathbf{G}_i)$ is the quadratic Casimir operator which for the adjoint representation results in $C_2(\mathbf{G}_i) = \dim(\mathbf{G}_i)$.

In the supersymmetric case this formula simplifies, as there exist a superpartner for each scalar/fermionic field. Hence, we do not have to split the sum in such a way and (A.20) simplifies to

$$b_i^{\text{SUSY}} = \sum_{\mathfrak{R}} \tilde{b}_i^{\mathfrak{R}} - 3 C_2(G_i). \quad (\text{A.21})$$

Low-Energy Flavour Model

B.1. Tensor Products of $SU(3)$

In Chapter 4 we need to construct $SU(3)$ invariant structures containing non-fundamental representations. Here we discuss how these can be generated.

Each representation of $SU(3)$ can be expressed as tensor containing upper and lower indices which run from $1 \dots 3$. The lower (upper) indices transform like in (anti-) fundamental representation, respectively. The basic invariant structures of $SU(3)$ are δ_i^j , ϵ_{ijk} and ϵ^{ijk} . Thus, we can construct any invariant combination of representations by combining the indices of the representation with the basic invariant structures. As long as we compute solely invariants of triplets this is almost trivial. In this case we can split up each of these products in combinations of two or three representations, as each field has a single index and all have to be contracted by the basic structures listed above. Thus, only three combinations are possible; $\delta_i^j \phi^i \phi'_j$, $\epsilon_{ijk} \phi^i \phi'^j \phi''^k$ and $\epsilon^{ijk} \phi_i \phi'_j \phi''_k$. However, we have to consider all possible permutations, which in our case may be done by hand.

If we consider larger representations, finding all possible contractions is no longer trivial, as these generally do not decompose into trivial structures. It is still possible to generate invariant structures by simply combining upper and lower indices, yet these are usually not linearly independent. Thus, we have to introduce a formalism which generates a set of linearly independent invariants for general products of $SU(3)$. Here, we only briefly introduce such a formalism and exemplarily give one invariant structure. A more detailed discussion can be found in [D], where we made use of this formalism to generate the invariants of our models given there. The formalism is based on Young Tableaux and “bird tracks” and a detail derivation can be found in [154].

Each operator in the Yukawa sector of the models considered in Chapter 4 consist of a product of three triplets with various flavon fields. Thus, it is useful to first calculate the decomposition of this product This can then later on be combined with the flavons to form an $SU(3)$ singlet. We calculate the product by generating the allowed Young-Tableaux, where each box is assigned to one of the indices. From the resulting Young-Tableaux, we then

B. Low-Energy Flavour Model

deduce which indices have to be (anti-) symmetrised. Following this procedure we find

$$\mathbf{3}_i \otimes \mathbf{3}_j \otimes \mathbf{3}_k = \mathbf{10}_{lmn} \oplus \mathbf{8}_m^l \oplus \mathbf{8}_m^l \oplus \mathbf{1} = \quad (\text{B.1a})$$

$$\left[\frac{1}{6} (\delta_l^i \delta_m^j \delta_n^k + \delta_l^j \delta_m^k \delta_n^i + \delta_l^k \delta_m^i \delta_n^j + \delta_l^i \delta_m^k \delta_n^j + \delta_l^j \delta_m^i \delta_n^k + \delta_l^k \delta_m^j \delta_n^i) \right. \quad (\text{B.1b})$$

$$\left. + \frac{1}{2} (\delta_m^i \epsilon^{jkl} + \delta_m^j \epsilon^{ikl}) \right. \quad (\text{B.1c})$$

$$\left. + \frac{1}{2} (\delta_m^i \epsilon^{kjl} + \delta_m^k \epsilon^{ijl}) \right. \quad (\text{B.1d})$$

$$\left. + \epsilon^{ijk} \right] \mathbf{3}_i \mathbf{3}_j \mathbf{3}_k . \quad (\text{B.1e})$$

Using this tensor product reduction, we may now calculate the invariant structures by calculating the reduction for the product of the additional flavons. In this reduction we then need to consider the singlet, octet and decuplet parts only. Exemplarily, we discuss the product of a decuplet with an anti-decuplet, which is relevant to the leading correction (4.17). Again we first construct the allowed Young-Tableaux and then (anti-) symmetrise the corresponding indices. Here, we find

$$\mathbf{10}_{ijk} \otimes \overline{\mathbf{10}}^{lmn} = \mathbf{8}_a^b \oplus \mathbf{1} \oplus \dots \quad (\text{B.2a})$$

$$\left[\delta_l^i \delta_m^j \delta_a^k \delta_n^b \right. \quad (\text{B.2b})$$

$$\left. + \delta_l^i \delta_m^j \delta_n^k + \dots \right] \mathbf{10}_{ijk} \otimes \overline{\mathbf{10}}^{lmn} . \quad (\text{B.2c})$$

Using (B.1) and (B.2) we can easily construct the invariant combinations of the product $\mathbf{3} \times \mathbf{3} \times \mathbf{3} \times \mathbf{10} \times \overline{\mathbf{10}}$. Here, we find three independent structures. This framework can be extended to an arbitrary product of representations. As the explicit notation is tedious and lengthy, we will not present the details here.

B.2. From $U(1)$ to Z_N

In order to set up a phenomenologically viable model of flavour, we introduce a global $U(1)$ symmetry in Section 4.2. However, a broken global symmetry results in massless Goldstone bosons which are in general phenomenologically excluded. Thus, they have to be removed from the low energy spectrum. A possible strategy is to gauge the $U(1)$, in which case the Goldstone mode gets “eaten up” by the gauge boson. Another possibility is to consider only a Z_N subgroup of the global $U(1)$. This is possible as long as the $U(1)$ is introduced to forbid phenomenologically problematic operators. The procedure to achieve such a reduction is discussed in the following.

The constraints on the Lagrangian arising from a Z_N and $U(1)$ symmetry are different. Imposing only Z_N , higher order operators (more fields) are reintroduced into the theory again. This is due to the fact that a Z_N symmetry is cyclic in contrast to a $U(1)$. However, in most cases it is sufficient to implement a Z_N , as the models are only considered to a particular order. Higher order terms are generally suppressed and thus phenomenologically not relevant.

Finding an appropriate N

There is no universal way of reducing a given $U(1)$ symmetry to an appropriate Z_N subgroup, especially as the latter depends on the order to which we require the Lagrangian to be identical. Thus, we present the generic way we use to reduce possible $U(1)$ symmetries in Chapter 4. For a given N , it is easy to deduce the corresponding Z_N charges and afterwards test whether the resulting theory is identical up to a certain order. Given a set of $U(1)$ charges $Q_{U(1)}$, we first need to normalise these to integer values. For each field ϕ , we can then calculate the corresponding Z_N charge by

$$Q_{Z_N} = \text{mod}(Q_{U(1)}, N) . \quad (\text{B.3})$$

Thus, we start from an “educated guess” for N and test whether the allowed operators result in an equivalent description of the considered observables (which in the model above are the Yukawa matrices). A good “educated guess” is to chose N such, that it exceeds the sum of the maximal $U(1)$ charge of all forbidden operators by one;

$$N \geq \max_{O \in \{\text{forbidden}\}} \left| \sum Q_{U(1)} \right| + 1 . \quad (\text{B.4})$$

However, one may also reconsider the original $U(1)$ charges assigned to the fields, as Z_N generally allows for more field combinations in the Lagrangian. As there is no unique way of assigning the charges in the first place, we will not consider this ansatz any further.

Reducing Z_N to $Z_n \times Z_m$

Having identified a suitable N and assigned the appropriate charges we may split the symmetry into its $Z_m \times Z_n$ factors. This is possible for each N which can be written as $N = n \times m$ with n and m coprime, i.e. having no common prime factor. The charges can be calculated following

$$0 \rightarrow (0, 0), \quad 1 \rightarrow \left(\left[\frac{n}{2} \right], \left[\frac{m}{2} \right] \right), \quad (\text{B.5})$$

$$q \rightarrow \left(\text{mod} \left(q \left[\frac{n}{2} \right], n \right), \text{mod} \left(q \left[\frac{m}{2} \right], m \right) \right), \quad N - 1 \rightarrow \left(\left[\frac{n}{2} \right], \left[\frac{m}{2} \right] \right), \quad (\text{B.6})$$

where $\lfloor x \rfloor$ ($\lceil x \rceil$) denote the floor (ceiling) function. We note that the charge assignment is not unique. Using this algorithm, we may reduce the order of the Z_N symmetry to a “lowest” possible value. On the other hand, this increases the number of symmetry factors. As both representations are equivalent, it depends on the personal choice which representation is used.

Low-Energy Flavour Symmetry Breaking

C.1. Gauge Anomalies

A gauge anomaly is a pure quantum phenomenon. It arises if the leading order theory is invariant under gauge transformations while loop corrections are not. Thus, the symmetry is broken by higher order corrections, which are always present in a quantum theory. The SM itself is free of gauge anomalies. However, if we consider extensions of the SM or gauge additional flavour symmetry groups we have to be aware of those.

Formally, an anomaly can be calculated by evaluating the one loop Feynman diagram of three gauge bosons with chiral fermions¹ running in the loop. As it depends only on the representations \mathfrak{R} of the fermions, it can be defined for each gauge factor by

$$\text{tr} (\{T_R^a, T_R^b\} T_R^c) = A(R) d^{abc}, \quad (\text{C.1})$$

where $A(R)$ is the contribution to the gauge anomaly of representation R (of a single gauge factor). The anomaly contribution of the fundamental representation R^f is defined to be $A(R^f) = 1$. For the theory to be anomaly free we have to demand

$$\sum_{R_i} A(R_i) \equiv 0, \quad (\text{C.2})$$

for each gauge group factor. From (C.1) one can conclude that gauge anomalies only arise for $SU(N)$ with $N \geq 3$ and $SO(6)$ (which indeed is equivalent to $SU(4)$).

Calculating Anomalies

Using the definition of the gauge anomalies as well as basic aspects of group theory one can easily prove the following basic properties of anomalies for $SU(N)$ (c.f. [108]),

$$A(\bar{R}) = -A(R), \quad (\text{C.3a})$$

$$A(R_1 \oplus R_2) = A(R_1) + A(R_2), \quad (\text{C.3b})$$

$$A(R_1 \otimes R_2) = \dim(R_1)A(R_2) + \dim(R_2)A(R_1). \quad (\text{C.3c})$$

¹We note that in supersymmetric theories the fermionic partners of the scalar fields also contribute to the gauge anomaly.

C. Low-Energy Flavour Symmetry Breaking

These properties and the fact that each representation of $SU(N)$ can be constructed from products of the fundamental representations enable us to iteratively calculate the anomaly of an arbitrary representation. Alternatively, one can calculate the anomaly contribution explicitly by using the defining equation (C.1). We note that the first line in (C.3) implies that each real representation does not contribute to the anomaly. Hence, one could avoid anomalies by only considering vector representations such as $D \oplus \bar{D}$.

Mixed Anomalies

For multiple group factors, the defining equation (C.1) can be generalised. In the generalised setup, each of the T_a^D may belong to an arbitrary group factor. Thus we can conclude, that a nontrivial anomaly can only occur for 0, 2, 3 non-abelian generators. The number of abelian generators is arbitrary. Thus, mixed anomalies occur only between abelian (usually $U(1)$) and one non-abelian groups. Mixed anomalies between two non-abelian groups are not possible. Hence, there is no mixed anomaly in PS as long as we do not consider a $U(1)_F$ flavour group.

Anomalies of $SU(3)$ and $SU(4)$

In this thesis we only need the anomalies of non-trivial representations of $SU(3)$ and $SU(4)$. Hence, we have listed the anomalies of the smallest representations of those in Table C.1.

SU(3)							SU(4)				
R	3	6	8	10	15	15'	R	4	6	10	15
$A(R)$	1	7	0	27	14	77	$A(R)$	1	0	8	0

Table C.1.: Anomaly contribution of the lowest dimensional representations of $SU(3)$ and $SU(4)$.

C.2. Calculation of S and T

As already discussed in Chapter 5, it is a not-trivial task to invert the relation between the flavour breaking vevs s & t' and the Yukawa matrices Y_u & Y_d . In this Appendix, we present a procedure for calculating s and t' numerically for a given set of Y_u and Y_d .

Inverting the approximate relation²

To start with, we develop an algorithm to deduce an analytic function for calculating s and t' for a given set of $Y_{u,d}$. Unfortunately, the so derived formula can only be evaluated numerically. We start from the approximate relations (5.11) in the full three generation case,

$$Y_u = (s + t')^{-1} + s^{-1}, \quad (\text{C.4a})$$

$$Y_d = (s - t')^{-1} + s^{-1}. \quad (\text{C.4b})$$

Defining

$$H \equiv s^{-1} t', \quad (\text{C.5})$$

we obtain

$$Y_u s = (\mathbf{1} + H)^{-1} + \mathbf{1}, \quad (\text{C.6a})$$

$$Y_d s = (\mathbf{1} - H)^{-1} + \mathbf{1}. \quad (\text{C.6b})$$

Multiplying the second line with the inverse of the first, we are able to get rid of the s -dependence;

$$G \equiv Y_d Y_u^{-1} = [(\mathbf{1} - H)^{-1} + \mathbf{1}] [(\mathbf{1} + H)^{-1} + \mathbf{1}]^{-1}. \quad (\text{C.7})$$

We now assume G to be a triangular matrix. This can always be achieved by applying a suitable similarity transformation. For this particular case, also H has to have a triangular form, as this property is conserved by the operations performed in (C.7). This allows us to solve this equation explicitly for the six elements parametrising H . Thus, we are able to give a solution for $H(G)$ in the special case of a triangular shape. However, $Y_d Y_u^{-1}$ is usually not given in triangular form. Therefore, we need to generalise this result for generic forms of G . For this purpose we expand the function $H(G)$ as a series in G . Due to the Cayley-Hamilton theorem this series stops after the quadratic term³ (for a detailed discussion see e.g. [155, 156]). Hence, we use the ansatz

$$H(G) = a \mathbf{1} + b G + c G^2, \quad (\text{C.8})$$

to express $H(G)$ in a basis independent way. Here, the coefficients a , b , and c depend only on the traces of G , G^2 and G^3 , and are thus basis independent. We can solve this ansatz for

²This part is based on a discussion with Th. Feldmann and largely worked out by him.

³In general one can conclude from the theorem that, for each $n \times n$ matrix M , M^n can be expressed by a polynomial $\sum_{i < n} x_i M^i$, where the x_i depend solely on the traces of powers of M up to order M^n

C. Low-Energy Flavour Symmetry Breaking

a , b and c in the special case of G having a triangular form. As these coefficients are basis independent, we are able to calculate H for any form of $G = Y_d Y_u^{-1}$.

So far, we are able to perform all of the calculations analytically. However, evaluating also the resulting equation for H analytically is not reasonable. Thus we content ourselves with the numerical evaluation. Having determined the numerical matrix H , we can use (C.6a) to calculate s ;

$$s = Y_u^{-1} ((\mathbb{1} + H)^{-1} + \mathbb{1}) . \quad (\text{C.9})$$

This allows us to calculate t' using (C.5);

$$t' = s H . \quad (\text{C.10})$$

Thus, we are able to calculate numerical expressions for s and t' for a given set of Yukawa matrices Y_u and Y_d .

Accounting for effects of the third generation

The calculation presented above is based on the validity of the approximate formula (5.11) and thus on the assumption $s, t' \ll 1$. This is not the case for the third generation, as $y_t \sim 1$. Hence, we expect sizeable corrections for all parameters related to the third generation. On the other hand, for a numerically given set s and t' we are able to exactly calculate the effective Yukawa couplings by diagonalising the explicit 9×9 mass matrix (5.15). Thus, we can explicitly determine the mismatch between the input Yukawa matrices $Y_{u,d}^{\text{in}}$ and the derived effective Yukawa matrices $Y_{u,d}^{\text{eff}}$. Here, we find that the resulting parameters of the third generation are generally too small. Thus, we may correct for this effect by altering $Y_{u,d}^{\text{in}}$. However, in Section 5.5 we chose a slightly different approach and scan the parameter space using the so-called ‘‘adapted flavour parameters’’.

C.3. Scan over Flavour Parameter

As described in Section 5.5 we scan over the ‘‘adapted flavour parameters’’ in order to deduce the effects on the low-energy flavour observables in our setup. In this Appendix, we give some details on the explicit realisation of the scan.

Generally, we have varied the ‘‘adapted flavour parameters’’ in the 3σ -range of their corresponding SM flavour parameters ($@M_Z$) as given in [157]. With respect to the parameters featuring large variations, we have enlarged the range (making use of our experiences from fitting to the SM values). The resulting ranges are given in Table C.2. From these we calculate the Yukawa matrices in the following explicit definition;

$$Y_u = \sqrt{1 + \frac{1}{\tan^2 \beta}} \frac{\sqrt{2}}{246 \text{ GeV}} \text{diag} (e^{i\delta_1}, e^{i\delta_2}, e^{i\delta_3}) \times \text{diag} (m_u, m_c, m_t) \quad (\text{C.11a})$$

$$Y_d = \sqrt{1 + \tan^2 \beta} \frac{\sqrt{2}}{246 \text{ GeV}} U^L \times \text{diag} (m_d, m_s, m_b) \times U^R, \quad (\text{C.11b})$$

where we define

$$U^L = \text{diag}(e^{i\delta_4}, e^{i\delta_5}, e^{i\delta_6}) \times V(\theta_{12}^L, \theta_{23}^L, \theta_{13}^L, \delta) \times \text{diag}(e^{i\delta_7}, e^{i\delta_8}, e^{i\delta_9}) \quad (\text{C.12a})$$

$$U^R = V(\theta_{12}^R, \theta_{23}^R, \theta_{13}^R, \delta_{13}) \times \text{diag}(e^{i\delta_{10}}, e^{i\delta_{11}}, e^{i\delta_{12}}) \quad (\text{C.12b})$$

In this explicit realisation, we allow for more phases δ_i as there are physical phases in the model. However, this is consistent, as we scan all these phases over their full range $[0, 2\pi]$.

m_u [MeV]	m_c [GeV]	m_t [GeV]	m_d [MeV]	m_s [MeV]	m_b [GeV]
0.5 - 2.9	0.53 - 0.71	162 - 288	1.2 - 4.8	30 - 78	2.78 - 4.44
	θ_{12}^L [°]	θ_{23}^L [°]	θ_{13}^L [°]	δ	
	12.89 - 13.19	1.54 - 2.56	0.101 - 0.280	-1.2 - 3.6	
	θ_{12}^R [°]	θ_{23}^R [°]	θ_{13}^R [°]	$\delta_{1..13}^R$	
full	0 - 90	0 - 90	0 - 90	0 - 2π	
reduced	0 - 1.6	0 - 1.6	0 - 1.6	0 - 2π	
	$\tan \beta$	ϵ^{-1}	λ		
	1 - 15	3 - 10	1.5 - 3		

Table C.2.: Ranges for the ‘‘Adapted Flavour Parameters’’ over which the scan is performed.

Bibliography

- [1] Georgi H. and Glashow S. *Unity of All Elementary Particle Forces*. Phys.Rev.Lett. **32**, (1974), 438–441.
- [2] Fritzsch H. and Minkowski P. *Unified Interactions of Leptons and Hadrons*. Annals Phys. **93**, (1975), 193–266.
- [3] Cleveland B., Daily T., Davis J. Raymond, Distel J.R., Lande K. et al. *Measurement of the solar electron neutrino flux with the Homestake chlorine detector*. Astrophys.J. **496**, (1998), 505–526.
- [4] Fukuda Y. et al. [Super-Kamiokande Collaboration]. *Measurements of the solar neutrino flux from Super-Kamiokande's first 300 days*. Phys.Rev.Lett. **81**, (1998), 1158–1162. arXiv:hep-ex/9805021.
- [5] Ahmad Q. et al. [SNO Collaboration]. *Direct evidence for neutrino flavor transformation from neutral current interactions in the Sudbury Neutrino Observatory*. Phys.Rev.Lett. **89**, (2002), 011301. arXiv:nucl-ex/0204008.
- [6] Pati J.C. and Salam A. *Unified Lepton-Hadron Symmetry and a Gauge Theory of the Basic Interactions*. Phys.Rev. **D8**, (1973), 1240–1251.
- [7] Pati J.C. and Salam A. *Lepton Number as the Fourth Color*. Phys.Rev. **D10**, (1974), 275–289.
- [8] Wess J. and Zumino B. *A Lagrangian Model Invariant Under Supergauge Transformations*. Phys.Lett. **B49**, (1974), 52.
- [9] Dimopoulos S., Raby S. and Wilczek F. *Supersymmetry and the Scale of Unification*. Phys.Rev. **D24**, (1981), 1681–1683.
- [10] Ibanez L.E. and Ross G.G. *Low-Energy Predictions in Supersymmetric Grand Unified Theories*. Phys.Lett. **B105**, (1981), 439.
- [11] Grinstein B., Redi M. and Villadoro G. *Low Scale Flavor Gauge Symmetries*. JHEP **1011**, (2010), 067. arXiv:1009.2049.
- [12] Cheng T. and Li L. *Gauge Theory of Elementary Particle Physics* .
- [13] Novaes S. *Standard model: An Introduction* arXiv:hep-ph/0001283.

Bibliography

- [14] Donoghue J., Golowich E. and Holstein B.R. *Dynamics of the standard model*. Camb.Monogr.Part.Phys.Nucl.Phys.Cosmol. **2**, (1992), 1–540.
- [15] Olive K. et al. [Particle Data Group]. *Review of Particle Physics*. Chin.Phys. **C38**, (2014), 090001. Online updates: <http://pdg.lbl.gov>.
- [16] Wilson K.G. *Confinement of Quarks*. Phys.Rev. **D10**, (1974), 2445–2459.
- [17] Huang K. *Quarks, Leptons & Gauge Fields*. World Scientific, 1992.
- [18] Guralnik G., Hagen C. and Kibble T. *Global Conservation Laws and Massless Particles*. Phys.Rev.Lett. **13**, (1964), 585–587.
- [19] Englert F. and Brout R. *Broken Symmetry and the Mass of Gauge Vector Mesons*. Phys.Rev.Lett. **13**, (1964), 321–323.
- [20] Higgs P.W. *Spontaneous Symmetry Breakdown without Massless Bosons*. Phys.Rev. **145**, (1966), 1156–1163.
- [21] Aad G. et al. [ATLAS]. *Observation of a new particle in the search for the Standard Model Higgs boson with the ATLAS detector at the LHC*. Phys.Lett. **B716**, (2012), 1–29. arXiv:1207.7214.
- [22] Chatrchyan S. et al. [CMS]. *Observation of a new boson at a mass of 125 GeV with the CMS experiment at the LHC*. Phys.Lett. **B716**, (2012), 30–61. arXiv:1207.7235.
- [23] Baak M. et al. [Gfitter Group]. *The global electroweak fit at NNLO and prospects for the LHC and ILC*. Eur.Phys.J. **C74**, (2014), 3046. arXiv:1407.3792.
- [24] Ramond P. *Journeys Beyond the Standard Model*. Frontiers in physics. Westview Press, 2004.
- [25] Ellis J. *Outstanding questions: Physics beyond the Standard Model*. Phil.Trans.Roy.Soc.Lond. **A370**, (2012), 818–830.
- [26] Quigg C. *Beyond the standard model in many directions* 57–118. arXiv:hep-ph/0404228.
- [27] Gross D.J. and Wilczek F. *Ultraviolet Behavior of Nonabelian Gauge Theories*. Phys.Rev.Lett. **30**, (1973), 1343–1346.
- [28] Georgi H., Quinn H.R. and Weinberg S. *Hierarchy of Interactions in Unified Gauge Theories*. Phys.Rev.Lett. **33**, (1974), 451–454.
- [29] Langacker P. and Luo M.x. *Implications of precision electroweak experiments for M_t , ρ_0 , $\sin^2 \theta_W$ and grand unification*. Phys.Rev. **D44**, (1991), 817–822.
- [30] Ross G.G. and Roberts R. *Minimal supersymmetric unification predictions*. Nucl.Phys. **B377**, (1992), 571–592.

- [31] Nilles H.P. *Supersymmetry, Supergravity and Particle Physics*. Phys.Rept. **110**, (1984), 1–162.
- [32] Haber H.E. and Kane G.L. *The Search for Supersymmetry: Probing Physics Beyond the Standard Model*. Phys.Rept. **117**, (1985), 75–263.
- [33] Martin S.P. *A Supersymmetry primer*. Adv.Ser.Direct.High Energy Phys. **21**, (2010), 1–153. arXiv:hep-ph/9709356.
- [34] Aitchison I.J. *Supersymmetry and the MSSM: An Elementary introduction* arXiv:hep-ph/0505105.
- [35] Dimopoulos S. and Georgi H. *Softly Broken Supersymmetry and SU(5)*. Nucl.Phys. **B193**, (1981), 150.
- [36] Gunion J.F., Haber H.E., Kane G.L. and Dawson S. *The Higgs Hunter’s Guide*. Front.Phys. **80**, (2000), 1–448.
- [37] Branco G., Ferreira P., Lavoura L., Rebelo M., Sher M. et al. *Theory and phenomenology of two-Higgs-doublet models*. Phys.Rept. **516**, (2012), 1–102. arXiv:1106.0034.
- [38] Grisaru M.T., Siegel W. and Rocek M. *Improved Methods for Supergraphs*. Nucl.Phys. **B159**, (1979), 429.
- [39] Bechtle P., Bringmann T., Desch K., Dreiner H., Hamer M. et al. *Constrained Supersymmetry after two years of LHC data: a global view with Fittino*. JHEP **1206**, (2012), 098. arXiv:1204.4199.
- [40] Khachatryan V. et al. [CMS]. *Search for supersymmetry using razor variables in events with b-tagged jets in pp collisions at $\sqrt{s} = 8$ TeV*. Phys.Rev. **D91**, (2015), 052018. Online updates: <https://twiki.cern.ch/twiki/bin/view/CMSPublic/PhysicsResultsSUS>, arXiv:1502.00300.
- [41] Aad G. et al. [ATLAS]. *Search for new phenomena in events with a photon and missing transverse momentum in pp collisions at $\sqrt{s} = 8$ TeV with the ATLAS detector*. Phys.Rev. **D91** (1), (2015), 012008. Online updates: <https://twiki.cern.ch/twiki/bin/view/AtlasPublic/SupersymmetryPublicResults>, arXiv:1411.1559.
- [42] Slansky R. *Group Theory for Unified Model Building*. Phys.Rept. **79**, (1981), 1–128.
- [43] Raby S. *SUSY GUT Model Building*. Eur.Phys.J. **C59**, (2009), 223–247. arXiv:0807.4921.
- [44] Nishino H. et al. [Super-Kamiokande Collaboration]. *Search for Proton Decay via $p \rightarrow e^+\pi^0$ and $p \rightarrow \mu^+\pi^0$ in a Large Water Cherenkov Detector*. Phys.Rev.Lett. **102**, (2009), 141801. arXiv:0903.0676.

Bibliography

- [45] Abe K. et al. [Super-Kamiokande Collaboration]. *Search for proton decay via $p \rightarrow \nu\nu K^+$ using 260 kiloton-year data of Super-Kamiokande*. Phys.Rev. **D90** (7), (2014), 072005. arXiv:1408.1195.
- [46] Green M.B. and Schwarz J.H. *Anomaly Cancellation in Supersymmetric D=10 Gauge Theory and Superstring Theory*. Phys.Lett. **B149**, (1984), 117–122.
- [47] Green M.B., Schwarz J. and Witten E. *SUPERSTRING THEORY. VOL. 1: INTRODUCTION*. Cambridge Monogr.Math.Phys. .
- [48] Hewett J.L. and Rizzo T.G. *Low-Energy Phenomenology of Superstring Inspired E(6) Models*. Phys.Rept. **183**, (1989), 193.
- [49] Gross D.J., Harvey J.A., Martinec E.J. and Rohm R. *The Heterotic String*. Phys.Rev.Lett. **54**, (1985), 502–505.
- [50] Adler S.L. *Further thoughts on supersymmetric E(8) as a family and grand unification theory* arXiv:hep-ph/0401212.
- [51] King S. *Neutrino mass models*. Rept.Prog.Phys. **67**, (2004), 107–158. arXiv:hep-ph/0310204.
- [52] Babu K. *TASI Lectures on Flavor Physics* 49–123. arXiv:0910.2948.
- [53] Chew G., Gell-Mann M. and Rosenfeld A. *STRONGLY INTERACTING PARTICLES*. Sci.Am. **210N2**, (1964), 74.
- [54] Gell-Mann M. *The Eightfold Way: A Theory of strong interaction symmetry* .
- [55] Ne’eman Y. *Derivation of strong interactions from a gauge invariance*. Nucl.Phys. **26**, (1961), 222–229.
- [56] Gell-Mann M. *Symmetries of baryons and mesons*. Phys.Rev. **125**, (1962), 1067–1084.
- [57] Cabibbo N. *Unitary Symmetry and Leptonic Decays*. Phys.Rev.Lett. **10**, (1963), 531–533.
- [58] Kobayashi M. and Maskawa T. *CP Violation in the Renormalizable Theory of Weak Interaction*. Prog.Theor.Phys. **49**, (1973), 652–657.
- [59] Pontecorvo B. *Mesonium and anti-mesonium*. Sov.Phys.JETP **6**, (1957), 429.
- [60] Pontecorvo B. *Neutrino Experiments and the Problem of Conservation of Leptonic Charge*. Sov.Phys.JETP **26**, (1968), 984–988.
- [61] Maki Z., Nakagawa M. and Sakata S. *Remarks on the unified model of elementary particles*. Prog.Theor.Phys. **28**, (1962), 870–880.
- [62] Wolfenstein L. *Parametrization of the Kobayashi-Maskawa Matrix*. Phys.Rev.Lett. **51**, (1983), 1945.

- [63] Bona M. et al. [UTfit Collaboration]. *The Unitarity Triangle Fit in the Standard Model and Hadronic Parameters from Lattice QCD: A Reappraisal after the Measurements of Delta $m(s)$ and $BR(B \text{ to } \tau \nu(\tau))$* . JHEP **0610**, (2006), 081. arXiv:hep-ph/0606167.
- [64] Charles J. et al. [CKMfitter Group]. *CP violation and the CKM matrix: Assessing the impact of the asymmetric B factories*. Eur.Phys.J. **C41**, (2005), 1–131. arXiv:hep-ph/0406184.
- [65] Ade P. et al. [Planck]. *Planck 2013 results. XVI. Cosmological parameters*. Astron.Astrophys. **571**, (2014), A16. arXiv:1303.5076.
- [66] Bahcall J.N. *Solving the mystery of the missing neutrinos* arXiv:physics/0406040.
- [67] Pontecorvo B. *Inverse beta processes and nonconservation of lepton charge*. Sov.Phys.JETP **7**, (1958), 172–173.
- [68] Gribov V. and Pontecorvo B. *Neutrino astronomy and lepton charge*. Phys.Lett. **B28**, (1969), 493.
- [69] Fukuda Y. et al. [Kamiokande Collaboration]. *Solar neutrino data covering solar cycle 22*. Phys.Rev.Lett. **77**, (1996), 1683–1686.
- [70] Abdurashitov J. et al. [SAGE Collaboration]. *Solar neutrino flux measurements by the Soviet-American Gallium Experiment (SAGE) for half the 22 year solar cycle*. J.Exp.Theor.Phys. **95**, (2002), 181–193. arXiv:astro-ph/0204245.
- [71] Gavrin V. [SAGE Collaboration]. *Measurement of the solar neutrino capture rate in SAGE and the value of the pp-neutrino flux at the earth*. Nucl.Phys.Proc.Suppl. **138**, (2005), 87–90.
- [72] Cribier M. [GALLEX Collaboration]. *Results of the whole GALLEX experiment*. Nucl.Phys.Proc.Suppl. **70**, (1999), 284–291.
- [73] Ahmed S. et al. [SNO Collaboration]. *Measurement of the total active B-8 solar neutrino flux at the Sudbury Neutrino Observatory with enhanced neutral current sensitivity*. Phys.Rev.Lett. **92**, (2004), 181301. arXiv:nucl-ex/0309004.
- [74] Fukuda Y. et al. [Super-Kamiokande Collaboration]. *Evidence for oscillation of atmospheric neutrinos*. Phys.Rev.Lett. **81**, (1998), 1562–1567. arXiv:hep-ex/9807003.
- [75] An F. et al. [DAYA-BAY Collaboration]. *Observation of electron-antineutrino disappearance at Daya Bay*. Phys.Rev.Lett. **108**, (2012), 171803. arXiv:1203.1669.
- [76] Ahn J. et al. [RENO collaboration]. *Observation of Reactor Electron Antineutrino Disappearance in the RENO Experiment*. Phys.Rev.Lett. **108**, (2012), 191802. arXiv:1204.0626.

Bibliography

- [77] Abe Y. et al. [DOUBLE-CHOOZ Collaboration]. *Indication for the disappearance of reactor electron antineutrinos in the Double Chooz experiment*. Phys.Rev.Lett. **108**, (2012), 131801. arXiv:1112.6353.
- [78] Arnaboldi C. et al. [CUORE Collaboration]. *CUORE: A Cryogenic underground observatory for rare events*. Nucl.Instrum.Meth. **A518**, (2004), 775–798. arXiv:hep-ex/0212053.
- [79] Auger M. et al. [EXO Collaboration]. *Search for Neutrinoless Double-Beta Decay in ^{136}Xe with EXO-200*. Phys.Rev.Lett. **109**, (2012), 032505. arXiv:1205.5608.
- [80] Agostini M. et al. [GERDA Collaboration]. *Results on Neutrinoless Double- β Decay of ^{76}Ge from Phase I of the GERDA Experiment*. Phys.Rev.Lett. **111** (12), (2013), 122503. arXiv:1307.4720.
- [81] Gaitskell R. et al. [Majorana Collaboration]. *The Majorana zero neutrino double beta decay experiment* arXiv:nucl-ex/0311013.
- [82] Osipowicz A. et al. [KATRIN Collaboration]. *KATRIN: A Next generation tritium beta decay experiment with sub-eV sensitivity for the electron neutrino mass. Letter of intent* arXiv:hep-ex/0109033.
- [83] Gonzalez-Garcia M., Maltoni M., Salvado J. and Schwetz T. *Global fit to three neutrino mixing: critical look at present precision*. JHEP **1212**, (2012), 123. arXiv:1209.3023.
- [84] Capozzi F., Fogli G., Lisi E., Marrone A., Montanino D. et al. *Status of three-neutrino oscillation parameters, circa 2013*. Phys.Rev. **D89** (9), (2014), 093018. arXiv:1312.2878.
- [85] Forero D., Tortola M. and Valle J. *Neutrino oscillations refitted*. Phys.Rev. **D90** (9), (2014), 093006. arXiv:1405.7540.
- [86] Messier M. *Review of neutrino oscillations experiments*. eConf **C060409**, (2006), 018. arXiv:hep-ex/0606013.
- [87] King S.F. and Luhn C. *Neutrino Mass and Mixing with Discrete Symmetry*. Rept.Prog.Phys. **76**, (2013), 056201. arXiv:1301.1340.
- [88] Minkowski P. *μ to e gamma at a Rate of One Out of 1-Billion Muon Decays?*. Phys.Lett. **B67**, (1977), 421.
- [89] Yanagida T. *HORIZONTAL SYMMETRY AND MASSES OF NEUTRINOS*. Conf.Proc. **C7902131**, (1979), 95–99.
- [90] Gell-Mann M., Ramond P. and Slansky R. *Complex Spinors and Unified Theories*. Conf.Proc. **C790927**, (1979), 315–321. arXiv:1306.4669.
- [91] Lindner M., Schmidt M.A. and Smirnov A.Y. *Screening of Dirac flavor structure in the seesaw and neutrino mixing*. JHEP **0507**, (2005), 048. arXiv:hep-ph/0505067.

- [92] Hagedorn C., Schmidt M.A. and Smirnov A.Y. *Lepton Mixing and Cancellation of the Dirac Mass Hierarchy in $SO(10)$ GUTs with Flavor Symmetries $T(7)$ and $\Sigma(81)$* . Phys.Rev. **D79**, (2009), 036002. arXiv:0811.2955.
- [93] King S. *Atmospheric and solar neutrinos with a heavy singlet*. Phys.Lett. **B439**, (1998), 350–356. arXiv:hep-ph/9806440.
- [94] Davidson S. and King S. *Bimaximal neutrino mixing in the MSSM with a single right-handed neutrino*. Phys.Lett. **B445**, (1998), 191–198. arXiv:hep-ph/9808296.
- [95] King S. *Atmospheric and solar neutrinos from single right-handed neutrino dominance and $U(1)$ family symmetry*. Nucl.Phys. **B562**, (1999), 57–77. arXiv:hep-ph/9904210.
- [96] King S. *Large mixing angle MSW and atmospheric neutrinos from single right-handed neutrino dominance and $U(1)$ family symmetry*. Nucl.Phys. **B576**, (2000), 85–105. arXiv:hep-ph/9912492.
- [97] King S. *Constructing the large mixing angle MNS matrix in seesaw models with right-handed neutrino dominance*. JHEP **0209**, (2002), 011. arXiv:hep-ph/0204360.
- [98] King S.F., Merle A., Morisi S., Shimizu Y. and Tanimoto M. *Neutrino Mass and Mixing: from Theory to Experiment*. New J.Phys. **16**, (2014), 045018. arXiv:1402.4271.
- [99] Schwarz J.H. *Superstring Theory*. Phys.Rept. **89**, (1982), 223–322.
- [100] Aharony O., Gubser S.S., Maldacena J.M., Ooguri H. and Oz Y. *Large N field theories, string theory and gravity*. Phys.Rept. **323**, (2000), 183–386. arXiv:hep-th/9905111.
- [101] Ibanez L.E. and Uranga A.M. *String theory and particle physics: An introduction to string phenomenology* .
- [102] Hall L.J., Rattazzi R. and Sarid U. *The Top quark mass in supersymmetric $SO(10)$ unification*. Phys.Rev. **D50**, (1994), 7048–7065. arXiv:hep-ph/9306309.
- [103] Carena M., Olechowski M., Pokorski S. and Wagner C. *Electroweak symmetry breaking and bottom - top Yukawa unification*. Nucl.Phys. **B426**, (1994), 269–300. arXiv:hep-ph/9402253.
- [104] Georgi H. and Jarlskog C. *A New Lepton - Quark Mass Relation in a Unified Theory*. Phys.Lett. **B86**, (1979), 297–300.
- [105] Antusch S., Gross C., Maurer V. and Sluka C. *$\theta^P MNS_{13} = \theta_C/\sqrt{2}$ from GUTs*. Nucl.Phys. **B866**, (2013), 255–269. arXiv:1205.1051.
- [106] King S. *Tri-bimaximal-Cabibbo Mixing*. Phys.Lett. **B718**, (2012), 136–142. arXiv:1205.0506.
- [107] Aulakh C.S., Bajc B., Melfo A., Rasin A. and Senjanovic G. *$SO(10)$ theory of R -parity and neutrino mass*. Nucl.Phys. **B597**, (2001), 89–109. arXiv:hep-ph/0004031.

Bibliography

- [108] Georgi H. *Lie Algebras in Particle Physics. From Isospin to Unified Theories.* Front.Phys. **54**, (1982), 1–255.
- [109] Aulakh C.S., Bajc B., Melfo A., Rasin A. and Senjanovic G. *Intermediate scales in supersymmetric GUTs: The Survival of the fittest.* Phys.Lett. **B460**, (1999), 325–332. arXiv:hep-ph/9904352.
- [110] Aulakh C.S., Benakli K. and Senjanovic G. *Reconciling supersymmetry and left-right symmetry.* Phys.Rev.Lett. **79**, (1997), 2188–2191. arXiv:hep-ph/9703434.
- [111] Aulakh C.S., Melfo A. and Senjanovic G. *Minimal supersymmetric left-right model.* Phys.Rev. **D57**, (1998), 4174–4178. arXiv:hep-ph/9707256.
- [112] Ellis J.R., Gunion J., Haber H.E., Roszkowski L. and Zwirner F. *Higgs Bosons in a Nonminimal Supersymmetric Model.* Phys.Rev. **D39**, (1989), 844.
- [113] Nilles H.P., Srednicki M. and Wyler D. *Weak Interaction Breakdown Induced by Supergravity.* Phys.Lett. **B120**, (1983), 346.
- [114] Kilian W. and Reuter J. *Unification without doublet-triplet splitting.* Phys.Lett. **B642**, (2006), 81–84. arXiv:hep-ph/0606277.
- [115] Howl R. and King S. *Planck scale unification in a supersymmetric standard model.* Phys.Lett. **B652**, (2007), 331–337. arXiv:0705.0301.
- [116] Mohapatra R.N. and Senjanovic G. *Neutrino Mass and Spontaneous Parity Violation.* Phys.Rev.Lett. **44**, (1980), 912.
- [117] Jones D. *The Two Loop beta Function for a $G(1) \times G(2)$ Gauge Theory.* Phys.Rev. **D25**, (1982), 581.
- [118] Chowdhury D. and Eberhardt O. *Global fits of the two-loop renormalized Two-Higgs-Doublet model with soft Z_2 breaking* arXiv:1503.08216.
- [119] Froggatt C. and Nielsen H.B. *Hierarchy of Quark Masses, Cabibbo Angles and CP Violation.* Nucl.Phys. **B147**, (1979), 277.
- [120] King S. and Ross G.G. *Fermion masses and mixing angles from $SU(3)$ family symmetry.* Phys.Lett. **B520**, (2001), 243–253. arXiv:hep-ph/0108112.
- [121] King S. and Ross G.G. *Fermion masses and mixing angles from $SU(3)$ family symmetry and unification.* Phys.Lett. **B574**, (2003), 239–252. arXiv:hep-ph/0307190.
- [122] de Medeiros Varzielas I. and Ross G.G. *$SU(3)$ family symmetry and neutrino bi-tri-maximal mixing.* Nucl.Phys. **B733**, (2006), 31–47. arXiv:hep-ph/0507176.
- [123] King S.F. and Malinsky M. *Towards a Complete Theory of Fermion Masses and Mixings with $SO(3)$ Family Symmetry and 5-D $SO(10)$ Unification.* JHEP **0611**, (2006), 071. arXiv:hep-ph/0608021.

- [124] Antusch S. and King S.F. *From hierarchical to partially degenerate neutrinos via type II upgrade of type I seesaw models*. Nucl.Phys. **B705**, (2005), 239–268. arXiv:hep-ph/0402121.
- [125] King S. *Predicting neutrino parameters from $SO(3)$ family symmetry and quark-lepton unification*. JHEP **0508**, (2005), 105. arXiv:hep-ph/0506297.
- [126] Lee T. *A Theory of Spontaneous T Violation*. Phys.Rev. **D8**, (1973), 1226–1239.
- [127] Weinberg S. *Gauge Theory of CP Violation*. Phys.Rev.Lett. **37**, (1976), 657.
- [128] Grossman Y. *Phenomenology of models with more than two Higgs doublets*. Nucl.Phys. **B426**, (1994), 355–384. arXiv:hep-ph/9401311.
- [129] Keus V., King S.F. and Moretti S. *Three-Higgs-doublet models: symmetries, potentials and Higgs boson masses*. JHEP **1401**, (2014), 052. arXiv:1310.8253.
- [130] Ivanov I. and Vdovin E. *Classification of finite reparametrization symmetry groups in the three-Higgs-doublet model*. Eur.Phys.J. **C73** (2), (2013), 2309. arXiv:1210.6553.
- [131] Aranda A., Bonilla C. and Diaz-Cruz J.L. *Three generations of Higgses and the cyclic groups*. Phys.Lett. **B717**, (2012), 248–251. arXiv:1204.5558.
- [132] King S., Moretti S. and Nevzorov R. *Exceptional supersymmetric standard model*. Phys.Lett. **B634**, (2006), 278–284. arXiv:hep-ph/0511256.
- [133] Roberts R., Romanino A., Ross G.G. and Velasco-Sevilla L. *Precision test of a fermion mass texture*. Nucl.Phys. **B615**, (2001), 358–384. arXiv:hep-ph/0104088.
- [134] Altarelli G. and Feruglio F. *Discrete Flavor Symmetries and Models of Neutrino Mixing*. Rev.Mod.Phys. **82**, (2010), 2701–2729. arXiv:1002.0211.
- [135] Altarelli G. and Feruglio F. *Tri-bimaximal neutrino mixing, $A(4)$ and the modular symmetry*. Nucl.Phys. **B741**, (2006), 215–235. arXiv:hep-ph/0512103.
- [136] Ciuchini M., Degrossi G., Gambino P. and Giudice G. *Next-to-leading QCD corrections to $B \rightarrow X(s)$ gamma in supersymmetry*. Nucl.Phys. **B534**, (1998), 3–20. arXiv:hep-ph/9806308.
- [137] Buras A., Gambino P., Gorbahn M., Jager S. and Silvestrini L. *Universal unitarity triangle and physics beyond the standard model*. Phys.Lett. **B500**, (2001), 161–167. arXiv:hep-ph/0007085.
- [138] D’Ambrosio G., Giudice G., Isidori G. and Strumia A. *Minimal flavor violation: An Effective field theory approach*. Nucl.Phys. **B645**, (2002), 155–187. arXiv:hep-ph/0207036.
- [139] Feldmann T. *See-Saw Masses for Quarks and Leptons in $SU(5)$* . JHEP **1104**, (2011), 043. arXiv:1010.2116.

- [140] Guadagnoli D., Mohapatra R.N. and Sung I. *Gauged Flavor Group with Left-Right Symmetry*. JHEP **1104**, (2011), 093. arXiv:1103.4170.
- [141] Mohapatra R.N. *Gauged Flavor, Supersymmetry and Grand Unification*. AIP Conf.Proc. **1467**, (2012), 7–14. arXiv:1205.6190.
- [142] Krnjaic G. and Stolarski D. *Gauging the Way to MFV*. JHEP **1304**, (2013), 064. arXiv:1212.4860.
- [143] Melfo A., Nemevsek M., Nesti F., Senjanovic G. and Zhang Y. *Type II Seesaw at LHC: The Roadmap*. Phys.Rev. **D85**, (2012), 055018. arXiv:1108.4416.
- [144] Aoki M., Kanemura S. and Yagyu K. *Testing the Higgs triplet model with the mass difference at the LHC*. Phys.Rev. **D85**, (2012), 055007. arXiv:1110.4625.
- [145] Nakano T. and Nishijima K. *Charge Independence for V-particles*. Prog.Theor.Phys. **10**, (1953), 581–582.
- [146] Gell-Mann M. *The interpretation of the new particles as displaced charge multiplets*. Nuovo Cim. **4** (S2), (1956), 848–866.
- [147] Buchmuller W. and Wyler D. *Effective Lagrangian Analysis of New Interactions and Flavor Conservation*. Nucl.Phys. **B268**, (1986), 621–653.
- [148] Crivellin A. and Pokorski S. *Can the differences in the determinations of V_{ub} and V_{cb} be explained by New Physics?* Phys.Rev.Lett. **114** (1), (2015), 011802. arXiv:1407.1320.
- [149] Buras A.J., Gemmler K. and Isidori G. *Quark flavour mixing with right-handed currents: an effective theory approach*. Nucl.Phys. **B843**, (2011), 107–142. arXiv:1007.1993.
- [150] Crivellin A. *Effects of right-handed charged currents on the determinations of $-V_{ub}$ — and $-V_{cb}$ —*. Phys.Rev. **D81**, (2010), 031301. arXiv:0907.2461.
- [151] Feldmann T., Müller B. and van Dyk D. *Analyzing $b \rightarrow u$ transitions in semileptonic $\bar{B}_s \rightarrow K^{*+}(\rightarrow K\pi)\ell^- \bar{\nu}_\ell$ decays* arXiv:1503.09063.
- [152] López-Val D., Plehn T. and Rauch M. *Measuring Extended Higgs Sectors as a Consistent Free Couplings Model*. JHEP **1310**, (2013), 134. arXiv:1308.1979.
- [153] Giardino P.P., Kannike K., Masina I., Raidal M. and Strumia A. *The universal Higgs fit*. JHEP **1405**, (2014), 046. arXiv:1303.3570.
- [154] Cvitanovic P. *Group theory: Birdtracks, Lie's and exceptional groups* .
- [155] Zhang F. *Matrix Theory: Basic Results and Techniques*. Universitext (1979). Springer, 1999.
- [156] Petersen P. *Linear Algebra*. Undergraduate Texts in Mathematics. Springer, 2012.
- [157] Bora K. *Updated values of running quark and lepton masses at GUT scale in SM, 2HDM and MSSM*. J.Phys. **2**, (2012), 2013. arXiv:1206.5909.

Danksagung

Diese Arbeit wäre ohne die Unterstützung, die ich von vielen Seiten erhalten habe, nicht möglich gewesen. Daher möchte ich hier die Gelegenheit nutzen, um “Danke” zu sagen.

Der Dank gebührt in erster Linie meiner Familie, die mich zu jeder Zeit vollstens unterstützt und immer an mich geglaubt hat. Des Weiteren gilt der Dank meiner Freundin Teresa, die gerade während der finalen Phase stark auf mich verzichten musste. Auch Sie hat mich immer tatkräftigst unterstützt und mir häufig Mut zugesprochen.

Auch möchte ich meinem Betreuer Prof. Dr. W. Kilian danken, der mir ermöglichte diese interessante Arbeit zu schreiben. Zusätzlich danke ich Prof. Dr. Th. Feldmann für die gemeinsame Arbeit am letzten Projekt. Beide standen mir zu jederzeit bereit, um meine Fragen zu beantworten und ihr Wissen mit mir zu teilen.

Ein ganz besonderer Dank gilt Christoph, der unermüdlich diese Arbeit Korrektur gelesen hat. Auch haben mir die vielen Diskussionen während meiner Doktorandenphase sehr weiter geholfen. Dies gilt auch für Karsten, der mir am Anfang meiner Doktorandenzeit einen tieferen Einblick in die Gruppentheorie sowie in Supersymmetrie ermöglicht hat. Zusätzlich möchte ich Susanne und Sven für das finale Korrekturlesen der Arbeit danken.

Mein Dank geht des Weiteren an alle derzeitigen und ehemaligen Mitarbeiter der Theoretischen Teilchenphysik I für das hervorragende Arbeitsklima. Zusätzlich geht der Dank an alle Freunde, Kommilitonen und insbesondere meine WG, die das Studium in Siegen zu einem wahren Vergnügen gemacht haben.

List of publications

The main results of Part II have been published in

- [A] F. Hartmann, W. Kilian and K. Schnitter, “Multiple Scales in Pati-Salam Unification Models,” *JHEP* **1405**, 064 (2014).
- [B] F. Hartmann and W. Kilian, “Flavour Models with Three Higgs Generations,” *Eur. Phys. J. C* **74**, 3055 (2014).
- [C] Th. Feldmann, F. Hartmann, Ch. Luhn and W. Kilian, “Combining Pati-Salam and Flavour Symmetries”, arXiv:1506.00782, (2015).
- [D] F. Hartmann, “Flavour and Higgs in Pati-Salam Models”, Masterarbeit, (2011).